To the Graduate Council:
I am submitting herewith a dissertation written by John McAlister entitled "On Structured Models of Coordinating Systems." I have examined the final paper copy of this dissertation for form and content and recommend that it be accepted in partial fulfillment of the requirements for the degree of Doctor of Philosophy, with a major in Mathematics.

Dr. Tadele A. Mengesha, Major Professor

We have read this dissertation
and recommend its acceptance:

Tadele A. Mengesha

Nina H. Fefferman

Ioannis Sgouralis

Simon Levin

Accepted for the Council:

Marieke Van Puymbroeck

Vice Provost and Dean of the Graduate School

To the Graduate Council:
I am submitting herewith a dissertation written by John McAlister entitled "On Structured Models of Coordinating Systems." I have examined the final electronic copy of this dissertation for form and content and recommend that it be accepted in partial fulfillment of the requirements for the degree of Doctor of Philosophy, with a major in Mathematics.

Dr. Tadele A. Mengesha, Major Professor

We have read this dissertation
and recommend its acceptance:

Tadele A. Mengesha

Nina H. Fefferman

Ioannis Sgouralis

Simon Levin

Accepted for the Council:

Marieke Van Puymbroeck

Vice Provost and Dean of the Graduate School

(Original signatures are on file with official student records.)

On Structured Models of Coordinating Systems

A Dissertation Presented for the

Doctor of Philosophy

Degree

The University of Tennessee, Knoxville

John McAlister

May 2026

To my parents, who raised me to be curious and patient

Acknowledgements

I would most like to thank the members of my doctoral committee, Dr. Nina H. Fefferman, Dr. Tadele A. Mengesha, Dr. Ioannis Sgouralis, and Dr. Simon A. Levin for reading and commenting on this work. In particular I would like to thank Dr. Fefferman and Dr. Mengesha, my doctoral advisors, for their constant help throughout my time at the University of Tennessee.

In addition to my doctoral committee, there are many other people who deserve thanks for their contribution to this dissertation. I would like to thank the staff at the National Institute for Modeling Biological Systems for all of their support throughout my time at the institute. Much of the computation that was crucial for this entire dissertation was performed with the NIMBioS cluster computer with the help of Graham Darryberry. All of the travel that I was able to do to share this research and to learn about related research was thanks to the help of Kristen Mecke and Sherri Dugger. Additionally I want to thank the staff members of the mathematics department at the University of Tennessee, most notably Pam Armentrout, who helped me constantly throughout my time in the department.

I would like to thank everyone who commented on the papers that make up this dissertation, including the past and present members of the Fefferman lab: Courtney Schreiner, Amber Young, Dr. Matt Hassenjager, Dr. Belal Hossain, Dr. David Flaherty, Dr. Maggie Sullens, Dr. Kimberlyn Roosa, Dr. Matt Young, Dr. Justin Wright, Dr. Matthew Silk, Dr. Alex Pritchard, Dr. Anna Sisk and Dr. Kelly Buch. Others who have commented on this work include the anonymous referees and editors who have improved the manuscripts that appear as chapters 2 and 5 in this dissertation.

In Addition to those who contributed to the work enclosed, there are many more people who deserve thanks as they played a large role in supporting me during the writing of this dissertation. I would like to thank my mother and father, Lori and Lawrence McAlister for making it possible for me to pursue this dream and for raising me to value curiosity and determination, the two main ingredients of this dissertation. I would like to thank my sister and brother-in-law, Dr. Anne McAlister and Andy Taylor for being great examples of what it is to be a student and an academic. I would like to thank my brother and sister-in-law, Ryan McAlister and Molly Power for their unrelenting support and encouragement. I would also like to thank my wonderful girlfriend, Sydney Fagan, who has been there for me through all the long nights and early mornings of writing and of research. I am deeply grateful for her ability to make me laugh when I was feeling discouraged and her willingness to listen to me ramble about some of the ideas in this dissertation before they were fully formed.

Finally I want to acknowledge all of my friends in the math department that made this experience enjoyable: Jack Haight, George Babus, Lane Rogers, Tushar, Shannon Hall, Caden Farley, and especially Nathan Burns with whom I discussed most of the ideas enclosed in this dissertation over drinks at Clancy's Tavern on Gay street every Tuesday night for the past 3 years.

There are many more people deserving of my thanks and acknowledgment, but should I list them all, I would exceed the page limit on this document before I wrote a single word about my research. To those people and to everyone I've listed: thank you.

"No man is an Iland, intire of it selfe; every man is a peece of the Continent, a part of the maine"

-John Donne in *Meditation XVII* from *Devotions upon Emergent Occasions*

Abstract

Coordination is a fundamental game theoretic process that can be used to describe a wide range of interactions from language formation and political polarization to signaling mechanics and the evolution of cooperative behavior. Underpinning all of it is the simple idea that a player is better off using the same strategy as the players around it. Modeling this simple type of interaction can lead to a rich diversity of behaviors, but it also brings with it a range of challenges. Different models can treat these challenges differently, but every modeling decision that is made to overcome one challenge reveals another. In this work I present four models of coordinating systems: A simulation model, a discrete time dual model, an ODE model, and a non-local diffusion model. Each modeling method allows us to use a different set of mathematical tools to interpret and make predictions about the behavior of coordinating systems, and in this way, each model addresses a different set of modeling challenges. Of course, no model perfectly addresses every challenge, but when taken together, we can gain a better understanding of coordinating systems as a whole.

Table of Contents

List of Tables

List of Figures

Chapter 1

Introduction

Gallia est omnis divisa in partes tres

Julius Caesar

Commentarii de Bello Gallico

1.1 The Study of Coordination

In his account of his campaign in Gaul, Julius Caesar starts by describing the differences among the people groups living in the region at the time. The three different people groups differed in language, customs, and culture and yet the three groups lived adjacent to one another in what would later become France. Although any two people would have benefited from speaking a common language, the relational structure of the region meant that three distinct languages persisted. At the time, no one would have thought to consider the ways that these groups coordinated their languages, institutions, and laws, through mathematics. Indeed Caesar lived 1,980 years too early to see the first paper describing game theory as a topic of its own (von Neumann, 1928) and 2,000 years too early to see the first textbook on the topic (von Neumann and Morgenstern, 1944). However, decision makers have had the choice to coordinate with one another since the evolution of the first animals with decision-making capabilities. Even before the brain was used to integrate and react, natural selection has shaped the ways that individuals have coordinated and interacted without

complex cognition on the part of the individual. It is the purpose of this thesis to detail the ways that these coordination processes have been described mathematically, to explain the barriers that limit our mathematical understanding of coordination, and to present new work, by my collaborators and myself, which advances our understanding of coordination in settings with explicit relational structure. I do not claim to give a mechanistic explanation for the differences between the people groups in Gaul around the time of 50 B.C.E., but I do seek to elucidate the requirements on general relational structures which can lead stable configurations with many different strategies. Much of the text of this dissertation, including whole chapters, are taken directly from my papers, which are published or are currently under peer review (McAlister and Fefferman, 2025; McAlister et al., 2025).

In general, a coordination game is any game theoretic interaction in which two players will receive a higher payoff if they pick the same strategy than they would if they picked different strategies. Consider a payoff matrix, for a symmetric game, $A = [[a_{ij}]]$, where $a_{i,j}$ is the payoff of a player playing strategy i against a player playing strategy j. The coordination game, when considered as a two-player game is quite simple. Any payoff matrix

$$\begin{bmatrix} a & b \\ c & d \end{bmatrix} \tag{1.1}$$

where $a > c$ and $d > b$ describes a coordination game.

The main way that we understand games of this nature is through best response and Nash equilibria, named after John Nash, who described these concepts in general in his dissertation in 1950. That work was published in the Annals of Mathematics a year later (Nash, 1951). In order to discuss these concepts we introduce the following notation. For a game with n players from the set V who each have a choice of strategies from the set C_v, a strategy profile $u \in \prod_{v \in V} C_v$ is a mapping from players to strategies. u_v is the strategy that player v plays in u and u_{-v} is the strategy that all the players other than v play in u. The payoff of player v, playing a strategy $c \in C$ against some u_{-v}, is given as $w_v(c, u_{-v})$. It is not standard to use V as the set of players nor was it the habit of Nash to use w to mean

payoff, however, I make these choices to maximize consistency throughout this dissertation. We say that player v, playing strategy $s \in C_v$, is playing a pure strategy best response to u if their payoff satisfies $w_v(s, u_{-v}) \geq w_v(c, u_{-v})$ for all $c \in C_v$. There may be multiple best responses to u_{-v}, so we call the set of pure strategy best response $BR_v(u)$. Instead of playing a pure strategy, one may also consider the mixed strategy concept, which is a probability distribution over the pure strategies. If a player has m pure strategies, the mixed strategies live in the $m-1$ simplex, Δ^{m-1}, and we can define the mixed strategy best response in the same way. For a player v, the mixed strategy $s \in \Delta^{m-1}$ is a best response to u_{-v} if and only if $w_v(s, u_{-v}) \geq w_v(c, u_{-v})$ for all $c \in \Delta^{m-1}$. The set of mixed strategy best responses to u is called $br_v(u)$, and note that, for games with linear payoff matrices, $BR_v(u) \subset br_v(u)$. With these definitions, we can say that a strategy profile u is a Nash equilibrium if and only if $u_v \in br_v(u)$ for all $v \in V$. The pure strategy Nash equilibrium is defined exactly as you would expect: $u_v \in BR_v(u)$ for all $v \in V$. It is the famous result of Nash that for any *zero sum* game with a finite number of players and a finite number of strategies, there is at least one mixed-strategy Nash equilibrium (Nash, 1950).

Coordination games are not zero-sum games, so we cannot use Nash's theorem to prove the existence of a Nash equilibrium. However, in the two-player case (and in the n player case as we will see later) it is easy to find examples of Nash Equilibria. In the two-player case with the payoff matrix (1.1), the strategy profiles $(1, 1)$ and $(2, 2)$ are both obviously Nash equilibria. It is an easy calculus exercise to find that there is also a mixed strategy equilibrium where both players play strategy 1 with probability $p = \frac{d-c}{a+d-b-c}$. Having entirely characterized the solutions to the general two-player coordination game, we say that it is entirely understood (Maschler et al., 2013).

The next set of innovations in the study of coordination came when economists started to consider the multiplayer coordination game. Thinking first of the case where there are only two strategies present, Kandori, Milath and Rob put forward a conceptualization of the multiplayer game wherein every player selects another player uniformly randomly and plays the two person game against them (Kandori et al., 1993). Kandori et al. considered dynamic games where players would randomly and rarely update their strategies to take on the best

response of the current strategy profile, and, under this framework they were able to show that for a two strategy coordination game, such a system will always converge to a Nash equilibrium, even in the critical case where $a = d > b = c$ (Kandori and Rob, 1995). Around the same time, a different group was studying these kinds of games through a different lens. Rather than thinking of a single player changing its strategy as a rare event, if every player takes on their best response at the same time, the system will exhibit at least one cyclically stable strategy, which is a set of strategy profiles, each of which is the best response to another (Gilboa and Matsui, 1991). This solution concept, along with other solution concepts which were becoming more popular at the time (e.g., Evolutionary Stable Strategy (ESS) (Smith, 1982)), made it easier to talk about multiplayer games dynamically. Foster and Young (1990) had also set the backdrop for some of these innovations by formalizing the way that evolutionary games behaved under stochastic dynamics.

One important note about the work of Kandori Milath and Rob is that, through the evolutionary concept, the system will converge to the risk dominant Nash equilibrium (i.e. the Nash equilibrium for which the loss from another player deviating is minimized). This equilibrium may be different from the social optimum or the efficient equilibrium in which players maximize the sum of the payoffs across all the players. Much work was done to describe how to change coordination problems like this to favor the efficient equilibrium. Robson and Vega-Redando (1995) found that by changing the way players were paired up in each of the pairwise interactions, the efficient equilibrium could be selected by the system. Likewise, Oechssler (1997) found that breaking the group of players into smaller groups which rarely exchange players, the system tends towards the efficient equilibrium.

In both the studies by Oeshssler and by Robson and Vega-Redondo, we see that the way that individuals interact with one another has a strong effect on the outcome of coordinating systems. Around the same time, Glenn Ellison was investigating this very question. If individuals are not paired up to interact randomly, but are given an explicit relational structure, we get a *structured coordination game*. Ellison (1993) extended the results of Kandori Milath and Rob and considered what would happen in the case in which, instead of the players interacted uniformly (which has now become known as the unstructured

coordination game), they interacted with their nearest neighbors in a line, circle, or lattice. In each case, when there are only two strategies available, and players experience ϵ-noise during the evolutionary process, the system converges to the risk dominant Nash equilibrium. The critical contribution was that Ellison was able to describe the rate of convergence for these systems based on the structure of the players. He was able to do this because each of the structures he considered were highly symmetric. In this way, the state space is reducible, and the resulting Markov chain becomes tractable.

In the following years, more studies about how the relational structure determines the coordination process were published (e.g. Ely (2002); Oechssler (1999)), and work on the structured coordination game continued. As more and more models of coordination processes were written, the definition of a coordination game had to be changed to allow for more flexibility. We currently use the definition that a two-player coordination game is an interaction which satisfies the bandwagon property. This bandwagon property, described by Kandori and Rob (1998), is a generalization of the previous characterization. A game satisfies the bandwagon property if $C(s)$ is the support of a possibly mixed strategy s (i.e. the set of all pure strategies expressed at a non-zero probability), then $BR_v(s) \subseteq C(s)$ for all $v \in V$ and $s \in C$. This definition works when the game is symmetric, and each player has the same strategy set. In the multiplayer case, the weak bandwagon property was coined by Cui and Shi (2022) stating that, if $C(u)$ is the support of a strategy profile $u \in \prod_{v \in V} \Delta^{m-1}$, then $BR_v(u) \subseteq C(u)$ for all $v \in V$ and any strategy profile u.

At the same time, Ellison was also working on generalizations of his results. He described a general evolutionary process with noise as an ordered triple containing a state space, a Markov transition matrix on the state space, P, and a family of Markov transition matrices $P(\epsilon)$ so that $P(0) = P$. For an appropriate evolutionary process described as above, he showed in his Radius-Coradius theorem that if Ω is a subset of the state space, $R(\Omega)$ is the number of mutations required to leave the basin of attraction of Ω, and $CR(\Omega)$ is the maximum mutation distance from a point in the state space to Ω, then Ω contains the long run stochastically stable set of the process if $R(\Omega) > CR(\Omega)$ (Ellison, 2000). This result also quantified the time to convergence to Ω from anywhere in the state space.

With these results, models of coordination games and other games on graphs became very popular at the beginning of the century. The early results specific to the coordination games before 2010 are well covered in the review by Weidenholzer (2010). However, by 2010, little more could be said about general graphs, *analytically* than could be said a decade before. In the unstructured case, it was well known that a $\frac{1}{2}$-dominant strategy (a strategy which is the pure strategy best response to a strategy profile where it is played half the time) is the unique long run equilibrium of a coordination process. On a lattice or a "circular city" the same thing was known to be true but little more could be said about relational structures which were less symmetric or entirely random. During that same decade continued advances in evolutionary game dynamics (more general than the coordination game) on structured populations expanded and were made more flexible and robust (Nowak, 2006; Nowak et al., 2010) but there was still no result which determined the equilibria of a game for a general relational structure.

By 2010, economists and evolutionary game theorists had an easy problem to state: *Given a graph G, what are the equilibrium states of that graph for a dynamic coordination game?* I will not answer this question in its entirety in this thesis. Despite how easy the question is to state, arriving at an analytical answer, in general, if it is possible, will be exceedingly difficult. This question has not been posed only by economists and game theorists. Indeed many areas of math, science, and engineering have asked this question under different names. The social scientists and statistical physicists have called this question "Opinion Dynamics" (Degroot, 1974; Friedkin and Johnsen, 1990; Zha et al., 2020) where their Nash equilibria are called "stable domains" as in Bierwirth and Lenger (2025). The political scientists call nearly the same question "polarization" (Waugh et al., 2009; Levin et al., 2021), and the network scientists give it the name "community detection" (Clauset et al., 2004; Blondel et al., 2008; Li et al., 2024). Even in ecology, the question of coexistence of competing species in structured models shares similarities to the coordination game (Coletti and de Lima, 2025). Each of these fields tackles a very similar problem through different approaches and with different mathematical techniques.

Among the game theorists, some progress has been made in the general setting since 2010. Building on work from Morris (2000) that describes the requirements on the game that are necessary for a strategy to spread across an infinite number of players depending on the relational structure, recent analytical work has focused on the case where there are only two strategies present and (in general) one dominates the other. Paarporn et al. (2021) examine when coordination systems are invasible by discordant behaviors and describe the trade off between security against widespread attacks and security against localized attacks in terms of the relational structure. Arditti et al. (2024) were able to show necessary and sufficient conditions for the stability of the consensus equilibrium under an evolutionary process with asynchronous update. Both of these results represent exciting steps forward in understanding coordination processes, but they both still rely heavily on the assumption that there are only two strategies and that individuals update asynchronously. Moreover, they both focus on the trivial consensus equilibrium and say little about the non-consensus equilibria. Apt et al. (2017) makes some progress by characterizing the fitness landscape using finite improvement paths through the state space and puts bounds on the cost of moving from non-consensus to consensus equilibria. Moreover, they and Cai and Daskalakis (2011) characterize the algorithmic complexity of finding non-consensus equilibria and least cost paths from non-consensus to consensus equilibria.

To say anything more about the form of non-consensus equilibria, others, including researchers from the fields of physics, network science, and political science, have turned to simulation to make progress on this question (Buskens and Snijders, 2016; Tomassini and Pestelacci, 2010). These simulation studies are useful in describing the general relationship between graph characteristics and the existence of non-consensus equilibria or convergence to efficient equilibria, but they do little to tease apart the direct relationship between structure and equilibrium. For my part, I begin this dissertation in chapter 2 with a simulation study focusing on the critical neutral case, which is sometimes called the pure-coordination case. This work forms the basis for our understanding of the coordination game in the neutral case and reveals some interesting results in its own right, but it does not achieve the goal of being able to determine the shape of non-trivial equilibria from the shape of the network. There

remains a gap in the theory when it comes to describing the neutral game with unlimited pure strategies in general domains.

At this point, it is reasonable to ask why anyone would care about the relationship between structure and coordination. It has proven hard to tease apart analytically, and it is provably difficult algorithmically, so why should we care? The coordination game on graphs, especially the neutral case, provides us with a way of thinking about community detection from the bottom up instead of from the top down. There has been much work in the past two decades about graph partitioning and community detection (e.g. Newman (2006); Clauset et al. (2004); McDiarmid and Skerman (2020); Brandes et al. (2006)) with applications from computer networks to population ecology. In general, these graph partitioning problems are $\mathcal{NP}$-Complete and require knowledge of the global setting of the graph. I, as well as Jackson and Storms (2025) and others describe the equilibrium states of coordination processes as strategic communities that are the result of partitioning. Because the agents in these coordination processes do not need global information about the system, this conception of locally driven community detection may be able to distribute the computational load when attempting to partition large graphs. It is also interesting because of the implications in the application areas from economic, social sciences, and political science. Understanding the ways that relational structure impacts coordination processes can tell us something about how groups form on every level of organization.

Another reason that this problem is interesting to consider is because of the unique challenges it poses. The challenges are unique because they require a mixture of a local and global approach. Previous authors have relied on reductions of the state space so that global information about the system is practically equivalent to the local information an agent has. This means that the problem can be studied as a global problem rather than a collection of coupled local problems. For instance, in Ellison (1993), the reduction to the line or the circular cities means that the state space is small, the only individuals making decisions are those at the boundaries of the strategic communities, and the positions of those boundaries are exactly equivalent to the location of the system in the state space. That is, knowing the boundaries gives you all the information you need to describe the system entirely. This

is not the case when the domain cannot be reduced and there are many strategies present. Understanding the boundaries of the strategic communities does not encapsulate all of the necessary information to describe the position in the state space, so there is little hope of using only a global description of the boundary to describe the problem fully.

The other major issue in studying the structured coordination game through dynamic game theory is the fact that the standard ways to understand the game (i.e., myopic best response) rely on an argmax function, which is highly irregular and not suitable for the standard tools of applied analysis and dynamical systems.

In addition to the challenges of using the myopic best response operator and building a payoff function which captures local and global information, any model of a complex system would ideally be numerically fast to solve and analytically tractable to understand. As such, in the pursuit of understanding coordinating systems, we need to build a model which overcomes each of these challenges. However, any attempt to overcome one challenge results in the failure to overcome another. Indeed, any modeling decision we make to study coordinating systems will be imperfect. This is the main conflict in modeling complex systems and it is the main reason why this dissertation is built on a diversity of models. Although no model will treat every challenge exactly, each model is built with a particular challenge in mind so that we can understand coordinating systems in general by comparing the behavior of several different models.

The conflict between local and global information is the main issue that I treat in chapter 3. In this chapter, I examine the assumptions required on the system to simplify the game state to only local information (i.e. boundary information) and, under these conditions, describe what can be said about the relationship between structure and coordination equilibrium. By separating the equilibrium results from the dynamic results, I circumvent some of the issues that arise from simplifying the problem in the way we desire.

The conflict of intractable dynamics in time is the main issue I treat in the chapter 4. Here I examine a system of ODEs whose behavior models a mixed strategy concept of the coordination game, and investigate the connections between the two systems. In particular,

I examine the connection between the stable equilibria in each system as a way of describing stability criteria in general settings.

Lastly, in Chapter 5, I consider both issues by describing a modified game in the continuous domain that relies on the machinery of nonlinear nonlocal diffusion. This machinery, which bridges the gap between global information and local behavior, provides a new and exciting way for coordination behavior in structured settings to be studied. I conclude by comparing each of these models (as well as the simulation study) to gain a better understanding of coordinating systems and by giving some conjectures that are left untreated in Chapter 6. However, first, I continue the introduction by giving preliminary results about the structured coordination game.

1.2 The Foundational Model and Preliminaries

Consider a graph $G(V, E)$. We will consider each vertex as a player in the game (and now, you see why we call the set of players V throughout this manuscript). Consider also a set of strategies C which is most naturally thought of as a set of colors which each vertex may take on (and the second mysterious set name is resolved). In this way, any strategy profile, $u \in C^{|V|}$ can be thought of as a graph coloring. A strategy profile describes a correspondence between players and strategies, so to reference the strategy that a player v is using in a strategy profile u, we write u_v.

For a general game on a graph with a payoff matrix A, we must consider each pure strategy in C as a standard basis element from $\mathbb{R}^m$ where m is the number of strategies. In this way, the pairwise payoff for a player playing $\hat{e}_i$ against an opponent $\hat{e}_j$ is given as $(\hat{e}_i)^\intercal A \hat{e}_j$. Thus, for general games on graphs, the fitness of a single player, v, is the sum (or equivalently the average) of the pairwise payoffs they receive from each of their neighbors in the neighborhood $\Gamma(v)$. For the pure coordination game (also called the neutral option coordination game), $A = I_m$ and so we can reduce the payoff function a great deal. For each

vertex, the payoff of a strategy profile is given as

$$w_v(u) = \big|\{w \in \Gamma(v); u_w = u_v\}\big|. \tag{1.2}$$

In the case where we want to talk about the payoff for v playing a strategy different from the one described by u, we write $w_v(c|u) = |\{w \in \Gamma(v); u_w = c\}|$. This, and the following analytical results, can be found, nearly identically, in my publication McAlister and Fefferman (2025).

Similar to a coordination game, an Anti-coordination game is a game where, if all of the payoffs were multiplied by -1, it would satisfy the bandwagon property. As such, when $A = -I$, we have an anti-coordination game and can make a similar reduction. In this case, it is easy to see that any proper coloring of a graph (Foulds, 1992) is a Nash equilibrium of the Anti-coordination game. The Anti-coordination game is not a focus of this thesis, but it will be mentioned occasionally, and so the definition is supplied here.

Using the payoff function (1.2), it is easy to see that for any strategy profile u, we compute the best response as

$$BR_v(u) = \underset{i \in C}{\operatorname{argmax}}\, w(i|u) \tag{1.3}$$

. As with everyone who has studied the coordination game in the past, we will consider it as a dynamic game, and initially, we will consider it through the best response replication dynamic. In discrete time steps, if every player takes on a best response to the previous strategy profile, we get a new strategy profile, and in this way, we describe a non-deterministic dynamical system

$$u_v(t+1) \in BR_v(u(t)) \; \forall v \in V. \tag{1.4}$$

This is non-deterministic because $BR_v(u)$ is not necessarily a single strategy. In the case of pure coordination, ties occur frequently. We cannot include a tie-breaking order as in Nisan et al. (2011) because it would violate the assumption that every strategy is equivalent. Instead, we use a "ε-inertia" assumption and say that switching strategies has a payoff cost of ε, so if $u_v(t) \in BR_v(u(t))$ then $u_v(t+1) = u_v(t)$. However, if $u_v(t) \notin BR_v(u(t))$ then $u_v(t)$

is selected from $BR_v(u)$ uniformly randomly. Note that the ε of switching strategies can be made so small that for any finite graph, if switching strategies can improve the fitness of a player by any amount, it will overcome the cost of switching.

Having defined the dynamical system (1.4), we can give two (rather obvious) facts about the system:

Proposition 1.1. *A strategy profile is a Nash equilibrium of the game played on $G(V, E)$ with payoff as in (1.2) if and only if it is an equilibrium point in the dynamical system (1.4).*

Proposition 1.2. *Every graph admits a pure strategy Nash equilibrium to the game with payoff as in (1.2). In particular, every graph admits the consensus equilibrium*

These results follow directly from the definition of Nash equilibrium, and so they are presented without proof here.

When discussing the pure coordination game in which no strategy provides a different intrinsic fitness benefit than another, it is clear that any relabeling of the strategies leaves the strategy profile unchanged. Because fitness only depends on whether two strategies are alike or not, if the players playing strategy i all take on strategy j and the players playing strategy j all take on strategy i, the game state is identical. That means we have some redundancy that can be alleviated by considering strategy profiles as vertex partitions. The correspondence between strategy profiles and vertex partitions is quite natural. For a strategy profile u which includes strategies $1, 2, ..., m$, we let the corresponding vertex partition $Q = \{q^1, q^2, ..., q^m\}$ where $q^i = \{v \in V, u_v = i\}$. We call this correspondence Φ and write for a partition Q corresponding to a strategy profile u. $Q = \Phi u$. For a partition $Q = \{q^1, ..., q^m\}$ each part is called a *strategic community* or *cluster*. If $\mathcal{Q}(\mathcal{V})$ is the set of all partitions of V, then note that $\Phi : C^{|V|} \to \mathcal{Q}(V)$ is surjective but not injective exactly because of the redundancy discussed above. In this way we let Φ define an equivalence relation on $C^{|V|}$, we say $u_a \sim_\Phi u_b$ if $\Phi u_a = \Phi u_b$.

It may be helpful in some cases to describe a strategy profile as a partition from $\mathcal{Q}(V)$ but it may also be helpful to describe is as a strategy profile directly. When this is the case we consider the set $\mathcal{A}$ which is the set of equivalence classes of $C^{|V|}$ under the equivalence

$\sim_\Phi$. In these instances, we will refer to a strategy profile u as an element of $\mathcal{A}$, because describing results as properties of every strategy profile in $A \in \mathcal{A}$ does little to increase precision but does a great deal to decrease clarity. (If this notion makes you uncomfortable, consider how comfortable you are when I say let $f \in L^p(\mathbb{R})$).

Having defined the correspondence. We introduce some definitions that we will use frequently. They are taken directly from McAlister and Fefferman (2025).

Definition 1.1 (Equilibrium Partition)**.** *An equilibrium partition is a partition which corresponds to an equivalence class of strategy profiles which are Nash Equilibria.*

Definition 1.2 (Indecomposable)**.** *If the only equilibrium partition of a graph is the trivial partition, that graph is said to be Indecomposable. Naturally, if non-trivial equilibrium partitions exist, the graph is said to be decomposable.*

Naturally, if $u_0 \in \mathcal{A}$ is the consensus equilibrium (i.e., it is one of the consensus equilibria in the equivalence class $A \in \mathcal{A}$), then $\Phi(u_0) = \{V\}$ is the trivial partition. For this reason, sometimes the consensus equilibrium is also considered the trivial equilibrium.

As described in section 1.1, the main goal of this dissertation is to describe the effect of structure on coordination in a very general setting where symmetric reduction is often impossible. However, before we begin that journey, we present two simple results for well behaved graphs that we may refer back to. Again, these are taken directly from McAlister and Fefferman (2025).

Theorem 1.1. *K_n is indecomposable.*

Proof. Suppose, by way of contradiction, there is an equilibrium strategy profile u^* with $d \geq 2$ clusters, $q^1, ..., q^m$. Because every pair of vertices shares an edge,

$$w_v(i|u) = \begin{cases} |q^i| & u_v = i \\ |q^i| - 1 & u_v \neq i \end{cases} \tag{1.5}$$

so the fitness of a vertex is directly associated with the size of the cluster of which it is a part. Consider a vertex $v_1 \in q^1$. Because it is at equilibrium,

$$w_{v_1}(1|u^*) = \max_{c \in C}\{w_{v_1}(c|u^*)\} =: a.$$

Therefore, $|q^1| = a + 1$. Moreover, if v_1 played a different strategy, 2, its fitness would be $w_{v_1}(c_2|u^*) \leq a$ so $|q^2| \leq a$. Now consider a separate vertex, $v_2 \in q^2$. $w_{v_2}(2|u^*) = |q^2| - 1 \leq a - 1$ by equation (1.5). However, $w_{v_2}(1|u^*) = a + 1$. Thus $u^*_{v_2} = 2 \notin \text{argmax}_{c \in C}\{w_{v_2}(c|u^*)\}$, so u^* is not an equilibrium. □

Theorem 1.2. *$K_{n,m}$ admits an equilibrium partition with d parts if and only if $d|n$ and $d|m$.*

Proof. Consider the complete bipartite graph $K_{n,m}$ which has parts E^n and E^m, with n and m vertices, respectively.

$\Longleftarrow$ Let d be a common divisor of m and n. It is sufficient to construct an equilibrium strategy profile with d strategies. Partition the vertices of E^m so that there are m/d vertices using each strategy. Likewise, partition the vertices of E^n so that there are n/d vertices using each strategy. Consider $v \in E^m$. Notice, because it shares an edge with every vertex in E^n, its fitness is certainly

$$w_v(c|u) = \frac{n}{d} \quad \forall\, c \in C \tag{1.6}$$

Therefore, it is certainly playing a best response. The same can be said for every vertex in E^n. Thus, we have constructed an equilibrium strategy profile with d clusters, and so the corresponding partition is an equilibrium partition.

$\Longrightarrow$ Suppose, by way of contradiction and without loss of generality, that d is not a divisor of m. Suppose further that u^* is an equilibrium strategy profile with d clusters. d does not divide m, so $\exists$ strategies r and s such that $|q^r \cap E^m| > |q^s \cap E^m|$. If u^* is at equilibrium, it must follow that $q^s \cap E^n = \emptyset$. It then follows that $q^s \cap E^m = \emptyset$. If q^s is empty, then there are not d clusters in u^*. This contradiction proves that, if there is an equilibrium strategy profile in $K_{n,m}$, the number of clusters must be a common divisor of n and m. □

Corollary 1.1. *$K_{n,m}$ is indecomposable if and only if n and m are coprime.*

The results in both theorems 1.1 and 1.2 depend heavily on the structure of the graph. For this reason, we cannot extrapolate these techniques to draw general conclusions about the system. This is the goal of the remainder of this dissertation: to derive analytical results for the relationship between the structure of the player space and the types of equilibria which can exist.

Chapter 2

Structured Coordination through Simulation

2.1 Introduction

Seeking to start answering the question of how relational structure impacts coordination dynamics, we have examined the structured coordination game, in which every strategy is neutral, on general graphs, through simulation. This entire chapter is taken directly from my 2025 publication entitled Insights into the Structured Coordination Game with Neutral Options through Simulation McAlister and Fefferman (2025). Some sections of the original publication have been moved to elsewhere in this dissertation. Much of the introduction and analytical results have already been discussed in chapter 1. The conjectures that appear at the end of the original publication have been moved to the end of the dissertation in chapter 6. The rest of the paper is reproduced nearly identically here, except for some slight changes in wording and notation when appropriate.

The main issue discussed here is that little is known about equilibrium partitions, especially non-trivial equilibrium partitions, analytically. To gain a better intuition for the system, we first do a numerical treatment of the problem to get a better sense of just how common or how rare non-trivial equilibrium partitions are. In doing so, we will

solidify the ways in which we discuss the coordination game through vertex partitioning, as well as develop a better understanding of the way the system behaves in general. By establishing new ways to discuss this system, we get closer to a more complete theoretical understanding of coordinated behavior and thereby enhance relevance to application areas such as the evolution of cooperation, spatial distributions of language and convention, and local conventions among cooperating groups.

In section 2.2, we present a catalogue of all of the Nash equilibria of the game, which we call equilibrium partitions, for groups no larger than 7. In section 2.3, we use a larger simulation, sweeping over many graphs on greater numbers of vertices, to understand trends between features of the graphs like edge density, diameter, centralization, etc., and features of the partitions they admit. Finally, in section 2.4, we offer some discussion of the results. However, we begin by describing, in more detail, some of the particulars of the vertex partitioning approach.

Recalling definition 1.1, we can make two propositions which will aid in our numerical understanding of the system.

Proposition 2.1. *If $Q = \{q^c\}_{c\in C}$ is an equilibrium partition of a connected graph of order at least 2, then $|q^c| \neq 1$ for any $c \in C$.*

The proof of proposition 2.1 is trivial.

Proposition 2.2. *If $Q = \{q^c\}_{c\in C}$ is an equilibrium partition and the subgraph spanned by q^i is disconnected, then, if $q^i_1, ..., q^i_n$ are the connected components of q^i, $\tilde{Q} = \{q^c\}_{c\neq i} \cup \{q^i_j\}_{j=1}^n$ is also an equilibrium partition.*

Before we give the proof, we present some notation for simplicity. Let ∂q^c be the set of those vertices in q^c which have neighbors which are not in q^c. Moreover, let $\overline{\partial q^c}$ be those vertices not in q^c which have neighbors in q^c.

Proof. Let $u \in \mathcal{A}$ be an equilibrium partition and let $P = \Phi u$. Write $P = \{p^i\}_{i=1}^m$ and, without loss of generality, say the subgraph spanned by p^1 is disconnected. We will show that refining the partition so that every part corresponds to a connected subgraph results in

an equilibrium partition. It will be no loss of generality to suppose the original equilibrium partition has only 1 disconnected part, so p^i corresponds to a connected subgraph for $i > 1$. Refine the partition to $\tilde{P} = \{p_1^1, ..., p_n^1\} \cup \{p^i\}_{i=2}^m$ and consider the corresponding strategy profile $\tilde{u} = \Phi^{-1}\tilde{P}$ (Note that $\Phi^{-1} : \mathcal{C} \to \mathcal{A}$ is injective because of the way the equivalence classes are defined on $\mathcal{A}$). The new parts, $p_1^1, ..., p_n^1$, correspond to new strategies which were not previously present in the original strategy profile. Any vertex $v \in p^i \setminus \overline{\partial p^1}$ for $i > 1$ will be unaffected by this refinement, so we need only consider those vertices in p^1 and $\overline{\partial p^1}$.

First, we will consider a vertex $v \in p^c \cap \partial p^1$. Observe that $w_v(c|\tilde{u}) = w_v(c|u) =\geq w_v(1|u)$. Trivially, $p_i^1 \subset p^1$ for all i, so $|p_i^1 \cap \Gamma(v)| \leq |p^1 \cap \Gamma(v)|$ for all i. This means, if $(1, i)$ is the strategy corresponding to p_i^1, then $w_v((1, i)|\tilde{u}) \leq w_v(1|u) \leq w_v(c|\tilde{u})$ for all i. Of course, it is still true that $w_v(c|\tilde{u}) \geq w_v(s|\tilde{u})$ for any $s \neq 1$ because these vertices are unchanged from the original Nash equilibrium. Thus v is playing its best response in $\tilde{u}$.

Now we consider those vertices $v \in p^1 \setminus \partial p^1$. Notice that under the refinement, $v \in p_i^1 \setminus \partial p_i^1$ because the refinement only separates the connected components of the subgraph spanned by p^1. Of course, those vertices which only neighbor other vertices using the same strategy are using their best response. This continues to be true under the refinement.

Lastly, we consider those vertices $v \in \partial p^1$ which, under the refinement, are in ∂p_i^1 for some i. $\Gamma(v) \cap p^1 = \Gamma(v) \cap P_i^1$ because the refinement did not break any connected components of p^1 into separate parts. Thus, $w_v(1|u) = w_v((1, i)|\tilde{u})$. Because v was playing a best response with respect to u, $w_v(1|u) \geq w_v(c|u) = w_v(c|\tilde{u})$ and because p_i^1 and p_j^1 have no neighboring vertices for any $i \neq j$, $w_v((1, j)|\tilde{u}) = 0$ for any $i \neq j$. Therefore, $w_v((1, i)|\tilde{u}) \geq w_v(c|\tilde{u})$ for any $c > 1$ or $c = (1, 1), ...(1, n)$. Thus, v is playing a best response under the refinement.

Therefore, under the refinement, every vertex is still using a best response strategy, so $\tilde{u}$ is a Nash equilibrium, and the refinement $\tilde{P} = \Phi\tilde{u}$ is an equilibrium partition. □

With this understanding, we can classify equilibria by assuming that every strategic community is connected. Therefore, when we classify equilibria, we ignore any equilibria with disconnected strategic communities. This supposition means that we can entirely describe an equilibrium partition by its cut set. This will be helpful in section 2.2. The same thing is

not true during the transient dynamics of the coordination process. Strategic communities cannot be separated as easily without changing the time dynamics of the system. This complication is discussed more in chapter 3. We will continue in our goal to solidify our intuition for the system by cataloging all the equilibrium partitions for small graphs.

2.2 Catalogue

In order to start working towards more robust analytical results later in this dissertation, we start by presenting a catalogue of all the equilibrium partitions on small graphs. We will see that, for the smallest graphs, non-trivial partitions are rare, but even by $n = 6$, less than half of connected graphs are indecomposable (and note obviously that all disconnected graphs are decomposable simply by partitioning connected components). This catalogue demonstrates that indecomposability depends highly on the exact structure of the graph, and to support the conjecture that indecomposability will become asymptotically rare in Erdős-Rényi random graphs ($\Gamma_{n,N(n)}$) (Erdős and Rényi, 1959) as $n \to \infty$.

Although it is very easy to make an exhaustive list of equilibrium partitions on graphs with no more than 5 vertices using only the results from section 2.1, when the number of graphs to consider grows, we resort to computer assisted exhaustive search. First, note that it is a very easy computation to check if a partition is an equilibrium partition. For a graph with n vertices, the operation runs in $\mathcal{O}(n^2)$, but we consider only small n, so this step is practically trivial. With an easily available catalogue of connected graphs of order at most seven, it is a nearly trivial task to consider every possible vertex partition. For ease of computation, we can disregard any partition which has a part of size 1 by proposition 2.1. With far fewer than Bell's number, the number of partitions of n distinguishable elements, $B(n)$, (Bóna, 2017) of partitions to check for each graph of order n, the exhaustive search can be completed very quickly.

The biggest complication is making sure that each partition is unique up to isomorphism; this is a non-trivial step, but it can be done, albeit inelegantly, by relying on algorithms to detect graph isomorphisms.

There are three ways by which two partitions of the same graph might be isomorphic. The first, and easier to detect, is the case in which the parts of the partitions are simply relabeled (Tab.2.1 row 1). We can exclude many of these isomorphisms by relabeling early in the algorithm without much difficulty.

The next way for two partitions of the same graph to be isomorphic is by way of graphical symmetry(Tab. 2.1 row 2). To tackle this problem, we need only find an injection, Λ, from the set of labeled partitions of labeled graphs to the set of labeled graphs. We do this through graph expansion. By adding a number of pendant vertices of each vertex in the original graph corresponding to the part of the partition to which it belongs (i.e., if $P = \{q_i\}_{i=1}^{n}$, then $v \in q_i$ is given i pendant vertices), we have such an injection. If partitions are isomorphic by way of graphical symmetry, then they will be expanded to labeled graphs which are isomorphic. $P_1 \simeq P_2 \Rightarrow \Lambda(P_1) \sim \Lambda(P_2)$. More specifically, the labeled graphs will be isomorphic to one another, so as unlabeled graphs, they are identical. Moreover, because this expansion is injective, if two expanded graphs are identical (or the two labeled graphs are isomorphic) to one another, it is certain that the corresponding graph partitions are isomorphic. $\Lambda(P_1) \sim \Lambda(P_2) \Rightarrow P_1 \simeq P_2$. There are existing efficient algorithms to detect isomorphisms between labeled graphs, so we take advantage of these to efficiently detect isomorphisms between graph partitions.

The final way two partitions might be isomorphic is through a combination of graphical symmetry and relabeling (Tab. 2.1 row 3). In this case, because we deal with very small partitions, we can simply check for isomorphism through graphical symmetry for every possible relabeling. Note that it is far more efficient to initially only test the partitions which are distinct up to relabeling, then add in the relabeled versions of the partitions to test in this third case, than it is to run the algorithm without any removal.

In the very worst case, the algorithm to detect partition isomorphisms has complexity $n!$ times the complexity of the graph isomorphism detection algorithm ($2^{\mathcal{O}(\log(n)^3)}$) Helfgott et al. (2017) but through use of proposition 2.1 and early removal of relabeled partitions, we can get this below $\lfloor \frac{n}{2} \rfloor ! 2^{\mathcal{O}(\log(4n)^3)}$, which is more than sufficient for the size of graphs we will

Table 2.1: An example of the three different ways two labeled partitions of labeled graphs can be isomorphic to one another and the "vector view," which is simply how the computer stores the partition information. The first row shows two partitions which are isomorphic by way of relabeling. The second row shows two partitions which are isomorphic by way of graphical symmetry. The third row shows two partitions which are isomorphic by way of both graphical symmetry and relabeling.

Type	Partition Diagram	Vector View
Isomorphic by way of relabeling	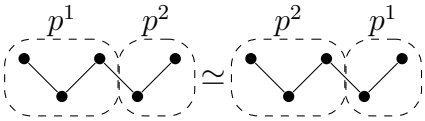	$[1,1,1,2,2] \simeq [2,2,2,1,1]$
Isomorphic by way of symmetry	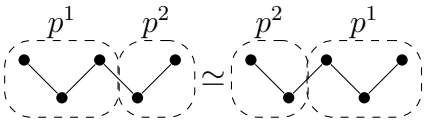	$[1,1,1,2,2] \simeq [2,2,1,1,1]$
Isomorphic by way of symmetry and relabeling	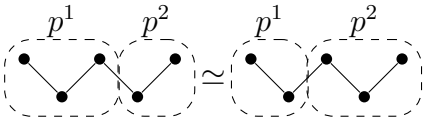	$[1,1,1,2,2] \simeq [1,1,2,2,2]$

catalogue. Notice the replacement of n with $4n$ is due to the fact that our injection adds up to $\lfloor \frac{n}{2} \rfloor n$ vertices to the graph.

The only remaining complication is whether we include disconnected parts in our partitions. For our purposes, because of proposition 2.2, we will only consider those partitions with connected parts. Therefore, we discard any partitions with disconnected parts and do not include them in our catalogue. The refinement of such a partition, wherein every part has a connected spanning subgraph, will certainly be included.

Having resolved both of these complications, we can examine every graph with at most 7 vertices and do an exhaustive search of all equilibrium partitions. In the following subsections, the results of the search are presented.

2.2.1 n=1

Finding equilibrium partitions in K_1 is trivial (Fig. 2.1).

Figure 2.1: The only equilibrium partition in K_1 is obviously the trivial partition. There is no further investigation required.

2.2.2 n=2

Finding equilibrium partitions in K_2 is also made trivial by proposition 2.1 (Fig.2.2).

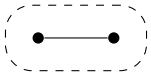

Figure 2.2: The only equilibrium in K_2 is the trivial partition

2.2.3 n=3

There are only two connected, non-isomorphic graphs of order 3, and the only equilibrium partition admitted by either is, again, the trivial partition (Fig. 2.3). This is also immediate from proposition 2.1.

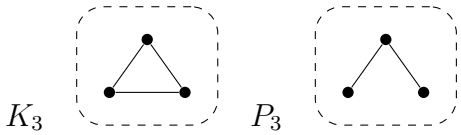

Figure 2.3: The only equilibrium in K_3 and P_3 is the trivial partition

2.2.4 n=4

There are 6 connected, non-isomorphic graphs of order 4. Four of them are indecomposable (Fig. 2.4). By proposition 2.1, any candidate equilibrium partition must have two parts, each with two vertices. With this fact, there are very few potential partitions to consider, and each can be ruled out using the definition of equilibrium.

The remaining two connected graphs have non-trivial equilibrium partitions. In addition to the trivial partition, they each have only one non-trivial partition (Fig. 2.5). Notice that,

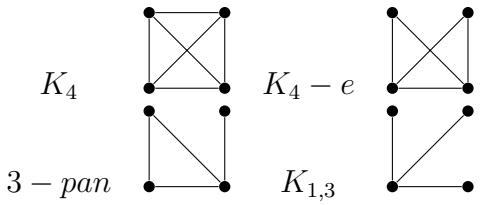

Figure 2.4: The indecomposable connected graphs on four vertices

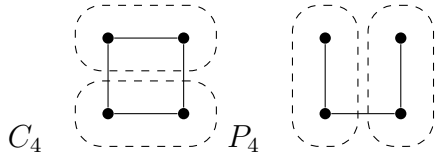

Figure 2.5: The two connected graphs on four vertices which are decomposable.

if the vertices of C_4 are labeled, there are two distinct equilibrium partitions. However, they are clearly isomorphic to one another and so only count as one equilibrium partition.

2.2.5 n=5

There are 21 connected non-isomorphic graphs of order 5. It is easy to see that every equilibrium on these graphs has either one or two clusters, again by proposition 2.1. This leaves only 11 candidate partitions to consider for each connected graph. Of the 21 connected graphs, 13 of them are indecomposable (Fig. 2.6).

The remaining 8 are decomposable. Each obviously admits the trivial partition, as well as a unique non-trivial partition, up to isomorphism. Each non-trivial equilibrium partition is pictured in figure 2.7.

2.2.6 n=6

There are 112 non-isomorphic connected graphs on 6 vertices (Cvetković and Petrić, 1984). Finding each of these partitions by hand is inefficient, so we relied solely on the computer exhaustive search. The partitions are displayed visually in the online resource 1. The results of this search showed that 48 of the connected graphs on 6 vertices are indecomposable (Fig. B.1). The remaining 64 connected graphs are decomposable. Of

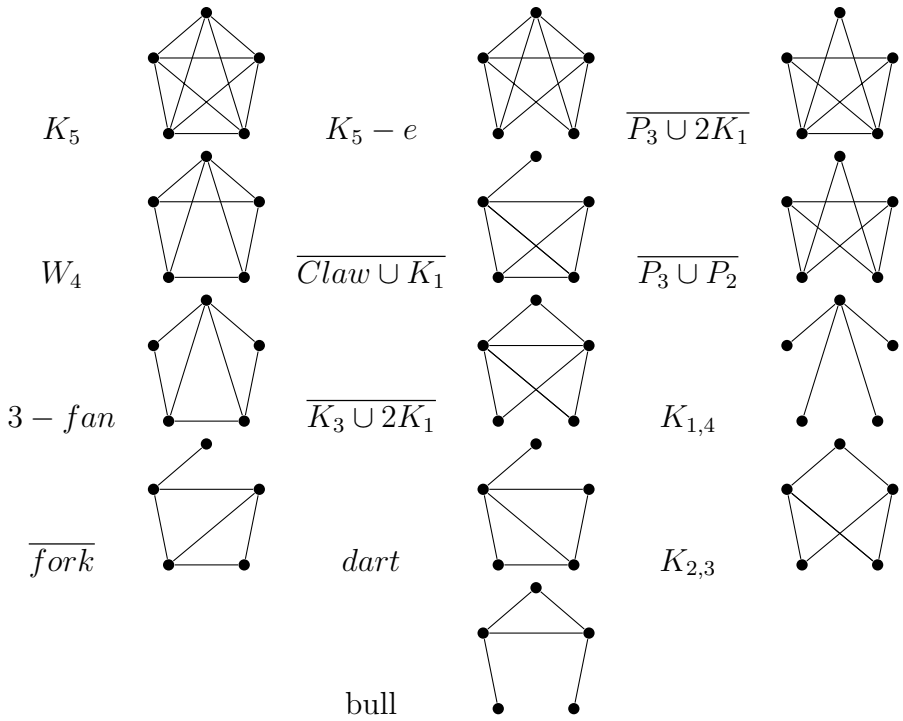

Figure 2.6: Every indecomposable connected graph on 5 vertices.

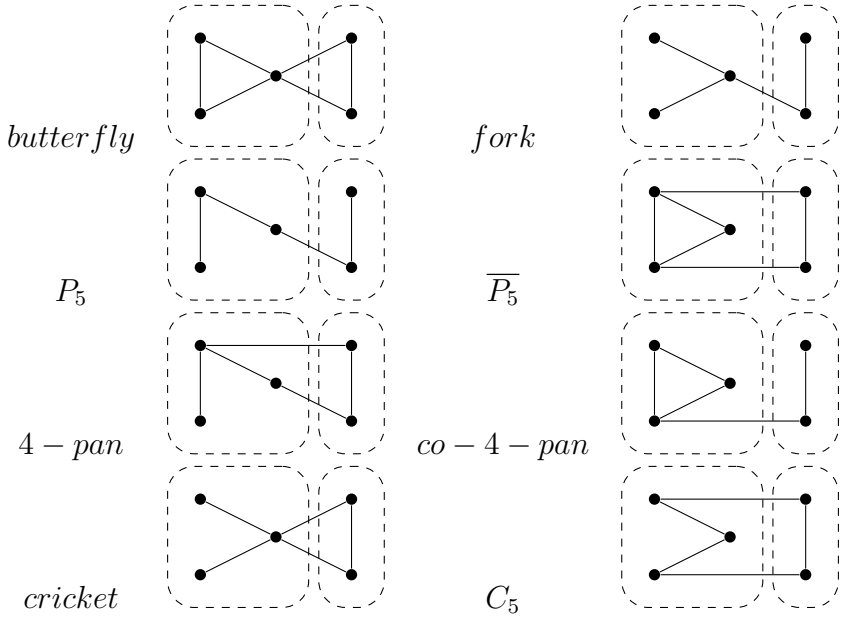

Figure 2.7: All of the decomposable graphs of order 5 with their non-trivial equilibrium partitions shown. Each has only one non-trivial equilibrium partition up to relabeling.

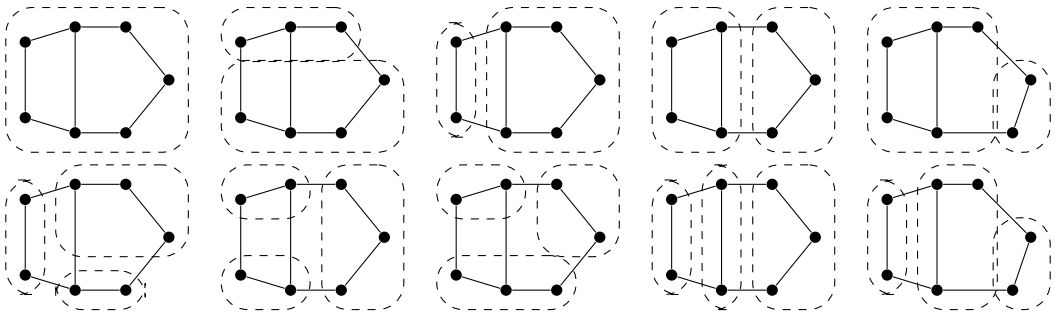

Figure 2.8: The ten distinct equilibrium partitions of the graph X_{38}, which is graph #445 in the graph atlas. This is the only graph among those catalogued which admits ten distinct equilibrium partitions.

these, 43 have unique non-trivial equilibria. They are pictured in Figure B.2. 13 of them have exactly two non-trivial equilibrium partitions up to isomorphism (Fig. B.3), six have exactly three non-trivial equilibrium partitions, up to isomorohism (Fig. B.4), and the remaining two have exactly four non-trivial equilibrium partitions (Fig. B.5).

2.2.7 n=7

As inefficient as the visual examination method is for graphs of order 6, it is even less feasible for graphs of order 7. Therefore, we rely on the exhaustive search to gain insight into these partitions. For the obvious reason, we will not present a figure presenting all of them, either here or in the appendix, but the code to construct the catalogue of partitions is available here (McAlister, 2024). Of the 853 graphs of order 7, 319 are indecomposable, 291 have a unique non-trivial equilibrium partition. All others have multiple non-trivial equilibrium partitions, including a single graph with ten distinct equilibrium partitions (Fig. 2.8).

2.2.8 Catalogue Summary

In total, there are 996 connected graphs on at most 7 vertices, and so there are 996 trivial equilibrium partitions. There are 597 graphs which admit non-trivial equilibrium partitions. The majority of these (350) have exactly 1 non-trivial equilibrium, 141 have two non-trivial

Table 2.2: A table showing the number of connected graphs which admit n different equilibrium partitions for n from 1 to 10, up to isomorphism. Among graphs of size less than or equal to seven, there are no graphs which admit more than 10 different partitions.

	number of graphs with n partitions									
Graph size	1	2	3	4	5	6	7	8	9	10
1	1	0	0	0	0	0	0	0	0	0
2	1	0	0	0	0	0	0	0	0	0
3	2	0	0	0	0	0	0	0	0	0
4	4	2	0	0	0	0	0	0	0	0
5	13	8	0	0	0	0	0	0	0	0
6	48	43	13	6	2	0	0	0	0	0
7	319	297	128	56	25	15	8	3	1	1
Total	399	350	141	62	27	15	8	3	1	1

equilibria, 62 have three non-trivial equilibria, and 55 have four or more non-trivial equilibria. This data is separated by graph size in Table 2.2.

Examining all 2083 partitions, we find that 996 of them are trivial (clearly because there are 996 different graphs in the catalogue), 897 have 2 parts, and 190 have three parts. We know this is the upper limit for graphs this small by proposition 2.1. This data is separated by graph size in table 2.3

Table 2.3: A table showing the number of distinct partitions with n clusters for each graph size from 1 to 6 vertices.

	number of partitions with n parts					
Graph Size	1		2		3	
1	1	100%	0	0%	0	0%
2	1	100%	0	0%	0	0%
3	2	100%	0	0%	0	0%
4	6	75%	2	25%	0	0%
5	21	72%	8	27%	0	0%
6	112	54%	79	38%	16	8%
7	853	46%	808	44%	174	9%
Total	996	48%	897	43%	190	9%

A crucial observation is that indecomposability becomes less common as graph order increases. We cannot yet rigorously extend this observation past $n = 7$, but, through visual examination of the catalogue, we can observe that indecomposability depends greatly on

the particular topology of the graph and is clearly less common when the edge number of a graph decreases. We will revisit this observation in Section 2.4 to formulate some conjectures about indecomposability in infinitely large $\Gamma_{n,N(n)}$ graphs.

2.3 Simulation

Having a complete catalogue of equilibria is helpful for small graphs where the equilibria are easy to draw. However, it becomes unhelpful and unreasonably time-intensive to make a catalogue for larger graphs. Instead, we turn to simulation in order to find equilibria. Because of the growth of Bell's numbers, we no longer simply check all partitions in search of equilibrium partitions; instead, we search for equilibrium partitions by considering the initial value problem (1.4). By producing random initial conditions, we can run the myopic best response process until the strategy profile ends in an equilibrium. Using this strategy, there are several things to consider: The first is that solutions may terminate in cyclical behavior where $u(t+n) = u(t)$ for all $t > T$ and $n > 1$. These states are interesting and worth studying, but they are not equilibrium partitions. Additionally, we must contend with the basins of stability of different equilibria. It may be the case that a graph admits several equilibrium partitions, but the basin of stability for one equilibrium is so large that it is unlikely for randomly generated initial data to result in a solution that tends towards a different equilibrium.

In order to discuss the basin of stability for a graph, we introduce the notation $\phi : \mathcal{P}(\mathcal{Q}_G) \to [0,1]$, where $\mathcal{Q}_G$ is the set of vertex partitions of G, $\mathcal{P}(\mathcal{Q}_G)$ is the power set of $\mathcal{Q}_G$, and $\phi((Q_i)_{i=1}^n)$ is the probability that, given a random initial strategy profile, the IVP will converge to the sequence $(Q_i)_{i=1}^n$. In the case that we are interested in the convergence to a partition Q, we write $\phi(Q)$. This means that $\sum_{(Q_i)\in\mathcal{P}(\mathcal{Q})} \phi((Q_i)) \leq 1$ (with equality when a graph G does not admit any non-convergent solutions). Moreover, if Q^0 is the trivial partition (which corresponds to the consensus equilibrium) and G is finite, then $\phi(Q_G^0) = 1 \implies G$ is indecomposable. This relationship is not true in the case that G is infinite because we must contend with events of measure zero. Note that the converse is not true even when G

is finite because, by definition, a graph may be indecomposable but still admit cycling (e.g. $K_{1,n}$).

2.3.1 Basins of Stability for Consensus Equilibria

In the first of two simulations, we attempt to understand the size of the basin of stability of the trivial equilibrium, $\phi(Q^0)$, in many different graphs. Using the Erdős-Rényi (ER) algorithm to generate 10,000 random graphs with various sizes and edge densities, we produced solutions from 500 randomly selected initial strategy profiles and recorded the limiting behavior of the solution. In total, approximately 5 million solutions were attempted, and their limits were measured. The initial strategy profiles were generated by randomly sampling from a set of n strategies n times, where n is the number of vertices in the graph. It is important to note that the basins of stability in this sense are not exactly partitions of the state space but rather partitions of unity over the state space. Because of the stochastic tie-breaking, basins of stability overlap. Therefore, when we measure the relative size of a basin of stability, it is not just the cardinality of a subset of the state space divided by the size of the state space itself. Instead, it is a weighted average over the entire state space of the probability that that state will evolve to the equilibrium in question.

The main result of this simulation was the apparent increase in $\phi(Q^0)$ with the increase in connectivity of the graph (Fig.2.9). Something equally interesting but more subtle is that when recorded against edge density, the data is highly stratified by graph order. If instead the data is measured against mean degree, this stratification is no longer apparent. This is consistent with the fact that the Nash equilibrium is a highly local property. The property of being in equilibrium depends only on those vertices with which a vertex shares an edge and does not depend directly on the order of the graph itself.

Included in this simulation are only those ER graphs that were connected. We can say certainly that the probability that a disconnected graph arrives at the consensus equilibrium is bounded above by $\frac{1}{2}$. This is because, even if each connected component will surely evolve to a consensus equilibrium of its own, the likelihood of each connected component evolving

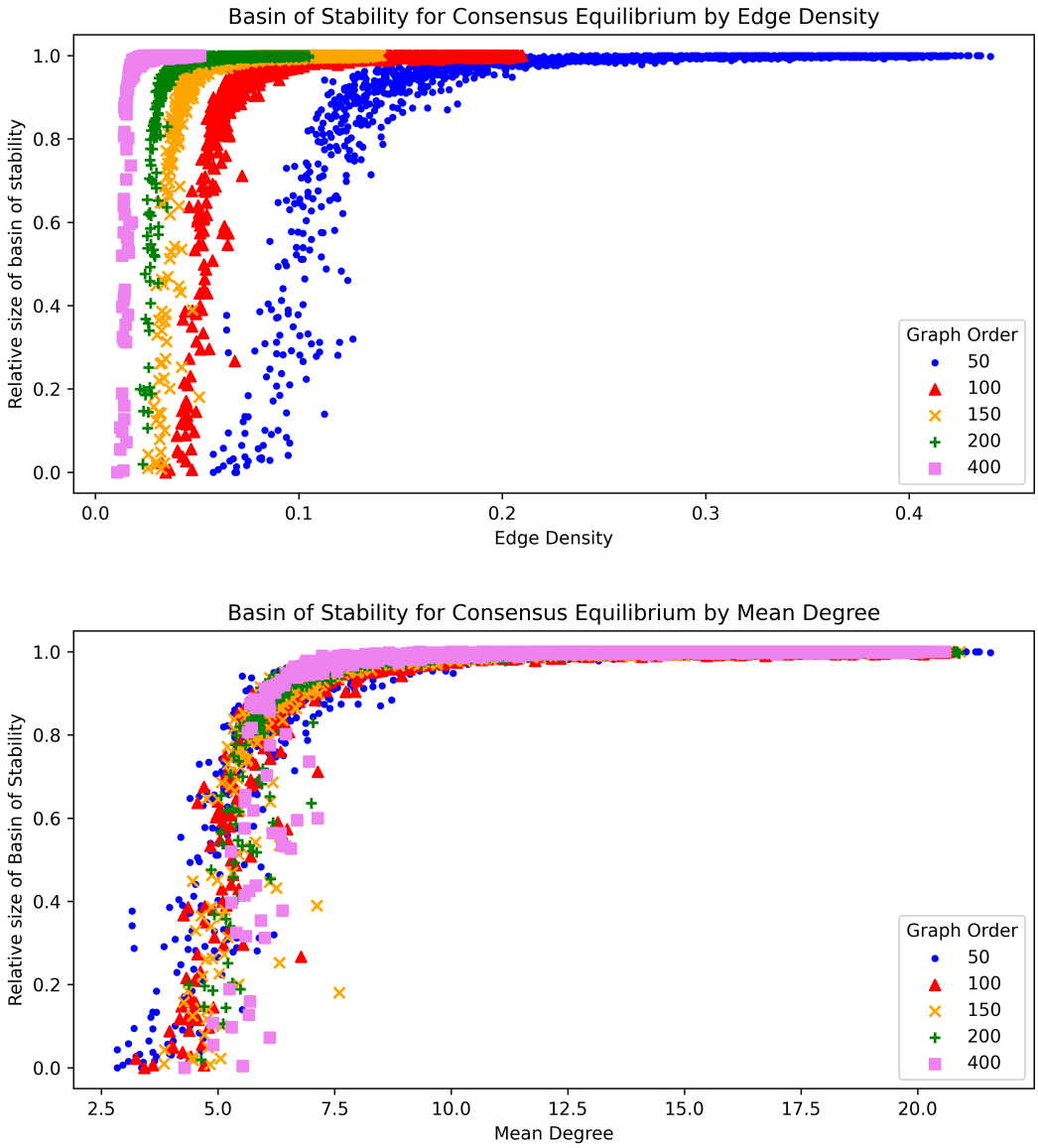

Figure 2.9: Top: A scatter plot showing every random graph with edge density on the x-axis and relative proportion of the time the consensus equilibrium was reached on the y-axis. **Bottom:** A similar scatter plot with mean degree on the x-axis instead of edge density. Both plots show the clear trend that the probability of arriving at the consensus equilibrium increases as "connectivity" (in whatever sense we consider) increases.

to the same consensus equilibrium is less than 1. Indeed, if there are r connected components in the graph G, even if every connected component will certainly evolve to a consensus, when the initial conditions are given uniformly randomly, the probability of converging to a global

consensus is only $\phi(Q^0) = \frac{1}{r^{c-1}}$, where c is the number of strategies present in the initial condition. In every non-degenerate case, where $r > 1$, this probability is less than $\frac{1}{2}$.

$\phi(Q^0)$ does seem to be related to the probability of being connected in the ER graph given by the recursive expression

$$\mathbb{P}(\Gamma_{n,p} \in \mathcal{C}) = 1 - \sum_{i=1}^{n-1} \mathbb{P}(\Gamma_{i,p} \in \mathcal{C}) \binom{n-1}{i-1} (1-p)^{i(n-i)} \tag{2.1}$$

where $\Gamma_{n,p}$ is the random ER graph with parameters n and p (p is the probability that any two vertices share an edge), and $\mathcal{C}$ is the set of all graphs which are connected. When $\Gamma_{n,p}$ with the same parameters is very likely to be connected, then we observe that $\phi(Q^0)$ is close to 1 (Fig. 2.10). We consider this relationship further in section 2.4.

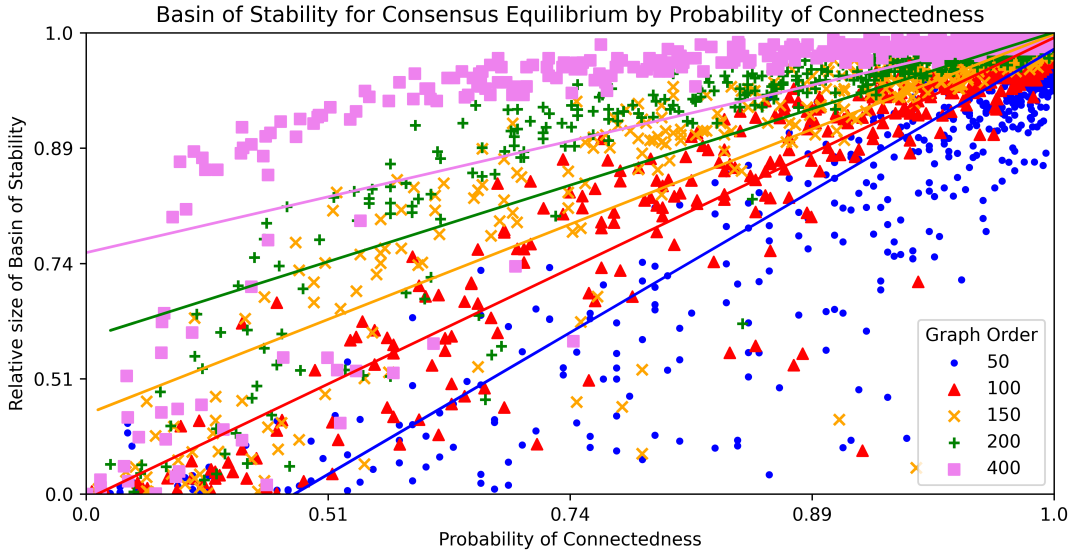

Figure 2.10: A scatter plot showing the relative size of the basin of stability as it is related to the probability of connectedness, shown on exponentially transformed axes. Trend lines are included for each series ($n = 50, 100, 150, 200, 400$ from bottom to top), not because we hypothesize that this relationship is linear, but in order to demonstrate that this relationship is supported even though certain parts of the data are more dense than others.

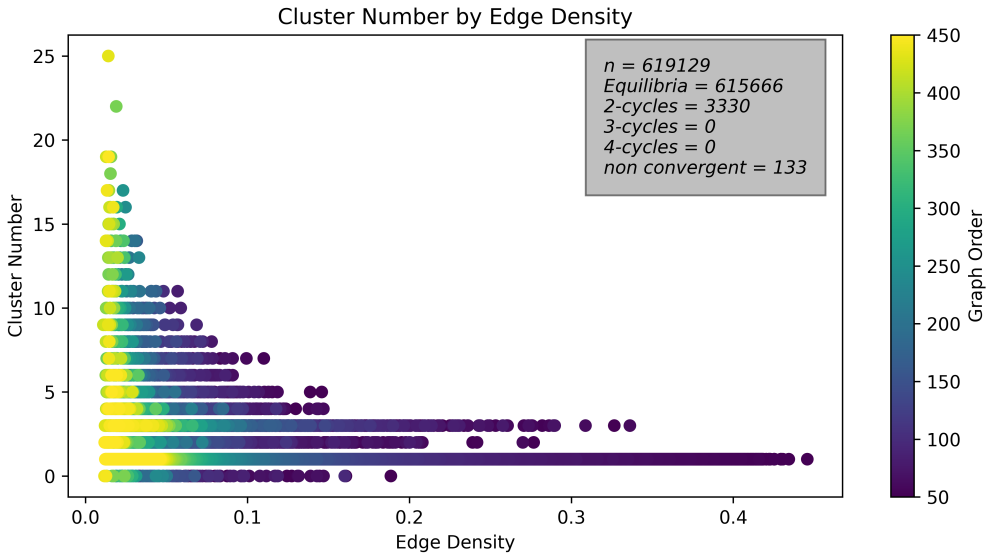

Figure 2.11: A scatter plot of cluster number (which is the number of distinct strategies present at equilibrium) as it relates to the edge density of the graph. This plot also shows that of the 619,129 IVPs that were simulated, 614,666 of them ended in an equilibrium, 3330 ended in a 2-cycle, and 113 did not converge by the end of the simulation. There were no 3-cycles or 4-cycles observed across either of the simulations. Any point with a cluster number of 0 corresponds to a solution that did not converge.

2.3.2 Broader Simulations

The basin of stability simulation tells us about how the graphical structure can promote or suppress consensus equilibrium, but it tells us less about particular solutions to the IVP and their limits. In order to understand the limit of the IVP a little better, we generated 1 million Erdős-Rényi random graphs, discarded the disconnected graphs, and found solutions to the IVP with randomly generated initial data (generated in the same way as in the previous simulation) to give us a (lower resolution) picture of a wider range of graphs. In particular, this simulation demonstrates better how graph size affects a broader range of limiting behaviors.

Cluster number is the number of strategies present at equilibrium, or in the language of partitions, it is simply the number of parts to the equilibrium partition. When plotted against edge density of the graph by which the equilibrium was admitted, we see a story consistent with that of the basin of stability simulation (Fig. 2.11). When edge density increases,

the number of strategies present at equilibrium tends towards 1 (which corresponds to the consensus equilibrium). Additionally, this simulation shows a little more about how this interaction looks on the *graph order*$\times$ *mean degree* plane (which is a transformation of the parameter space for the ER graph random variable $\Gamma_{n,p}$) (Fig. 2.12).

When visualized on the *graph order*$\times$ *mean degree* plane, the non-trivial dynamics seem only to occur near the frontier where it becomes exceedingly unlikely for an ER graph to be connected. A foundational result of the study of random graphs is the asymptotic probability of connectedness (Karoński, 1982). For the purpose of visualizing the results, we have superimposed level sets of the approximated probability of connectedness by way of the sharp threshold functions found in Erdős and Rényi (1959) and Erdős and Rényi (1960). It is clear that these level sets divide the plane into regions with qualitatively different behavior. We examine the results of the simulation through the lens of connectedness probability further in section 2.4.

The other notable result from this simulation is that, although 2-cycles were relatively common, three and four cycles were entirely absent. Among all the IVPs across both simulations, there was never an n-cycle for $n > 2$. (Although, among the 133 solutions that did not converge to a recognized equilibrium before the simulation timed out, there was a common behavior that mimicked a 4-cycle, which is further discussed with the related conjecture about n-cycles in section 6.3.)

2.4 Discussion

Here, we have introduced the structured coordination game with neutral options, and we have seen that the dynamics are categorically different from the dynamics of the structured coordination game when one strategy may dominate the other in terms of payoff or risk avoidance, and so cannot be studied in the same way. When noise enters the system through stochastic tie-breaking rather than through random mutation, as in Kandori et al. (1993); Ellison (1993); Weidenholzer (2010), we cannot use the radius and coradius of absorbing sets to find long-run equilibrium as in Ellison (1993). However, we conjecture

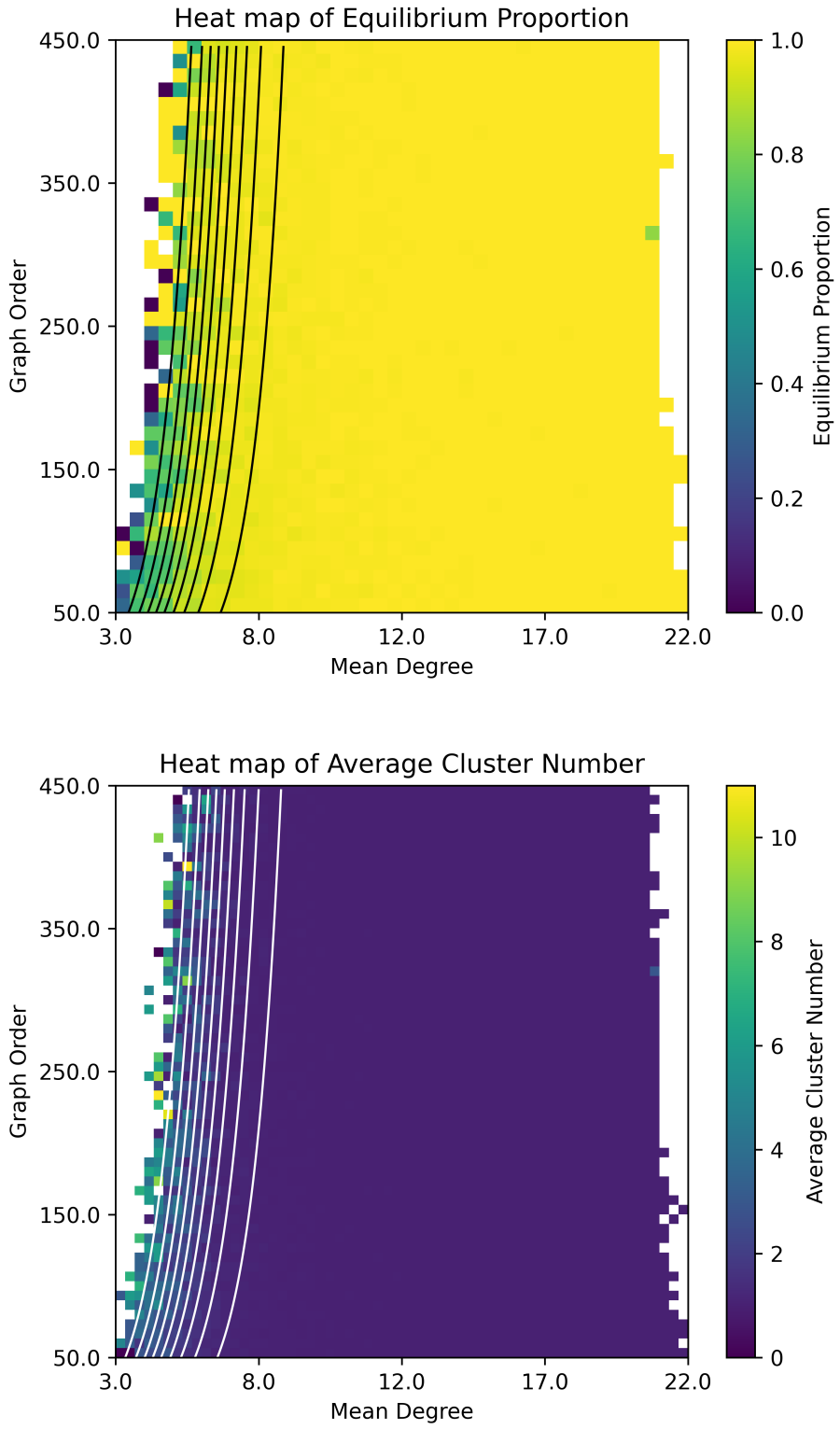

Figure 2.12: Top: a heat map showing the frequency of converging to an equilibrium for each combination of graph order and mean degree. **Bottom:** a heat map showing the average cluster number for each choice of graph order and mean degree. On both images are superimposed level curves of the asymptotic probability of connectedness ranging from $p = 0.1$ to $p = 0.9$. The white cells are regions where no connected graph was generated.

that, asymptotically, many of the same results (adapted to ignore payoff/risk dominance) remain in place. That is, in general, we can expect the system to converge to a consensus equilibrium even if other equilibria are present.

The main result is that higher connectivity of the network promotes convergence to the consensus equilibrium. This is not an altogether surprising result. It is, however, critically different from the conclusions of Buskens and Snijders (2016) that network density does not have an effect on the likelihood of converging to a homogeneous state. These differences can be explained both by the differences in graph order being observed in the studies and by the fact that, in the non-neutral case, differences in payoff mean that converging to a non-consensus equilibrium is already rare, even at low edge densities. The graphs considered herein were, in general, nearly amodular with high probability (Campigotto et al., 2013). However, near the parameter space where $\Gamma_{n,p}$ is not likely to be connected, the expected modularity increases with high probability to above 0.4 (McDiarmid and Skerman, 2020). Thus, as in Buskens and Snijders (2016), we observe that higher modularity is associated with non-trivial equilibria (which they call persistence of heterogeneous behavior).

These results have filled a crucial hole in the previous analytical and numerical treatments of this game by considering the critical case in which there are many strategies available, but no strategy dominates any other strategy in any sense. In this critical case, we see rich and beautiful dynamics. The study of this critical case may be helpful in understanding the evolution and fixation of local conventions in social settings. In a biological context, the results here seem to suggest that when cooperative behaviors offer no intrinsic fitness benefit (i.e., the benefit depends strictly on the number of associates engaging in the same behavior), well connected groups should almost always reach a consensus. A crucial observation, which suggests an area of future study, is that ER graphs are often not good examples of social networks because of factors like preferential attachment (Newman, 2003). An important future direction of this study will be to repeat these simulations with different types of random graphs to see which results are general and which results are particular to ER graphs

This simulation approach has helped lay the groundwork for an exciting body of analytical work to come. With a complete catalogue of equilibria for small graphs, as well as extensive simulated results in Erdős-Rényi graphs, we now have robust evidence to support our three main conjectures: 1) the existence of a threshold function for indecomposability which is close to $\binom{n}{2} - cn$, 2) the existence of a threshold function for the relative size of the basin of stability of the consensus equilibrium which is close to $\frac{1}{2}n \log n$, and 3) the impossibility of n-cycles in this system for $n > 2$. These results represent the first steps towards understanding coordination under myopic best response in this critical case, which in turn will improve our understanding of many processes, from the selection of conventions among coworkers in an office to spatial distribution of language and culture, and how these may change with increasing interconnectedness.

Chapter 3

Structured Coordination through Minimal Subgraphs

3.1 Introduction

Having discussed the numerical properties of equilibrium partitions, we continue on to the larger goal, which is to increase our analytical understanding of the system. These partitions are vertex partitions, which are useful for community detection, so before we begin our discussion of their analytical properties, we begin by comparing these partitions to other community detection type partitions.

The most famous community detection partitioning method is the maximum modularity partition, which, unsurprisingly, seeks to find the partition P which maximizes the quantity

$$Q(P) = \frac{1}{2m} \sum_{v,w \in V^2} \left[W_{v,w} - \frac{d_v d_w}{2m} \right] \delta(c_v, c_w)$$

Where W is the adjacency matrix, d_v is the degree of v and $\delta(c_v, c_w)$ is a function which returns 1 if v and w are in the same part in P and 0 otherwise (Clauset et al., 2004).

Typically, when network scientists are discussing community detection, they are describing methods which find or approximate maximum modularity partitions. Finding such a

partition is known to be $\mathcal{NP}$-complete (Brandes et al., 2006) and so for very large graphs, approximation methods must be used. For any partition, this quantity must range from $\frac{-1}{2}$ to 1, and if the trivial partition (consensus partition) is the maximum modularity partition, then the graph is called "amodular."

In a heuristic way, the modularity partitions and the equilibrium partitions have a great deal of overlap, and indeed, many partitions which are maximum modularity partitions are also equilibrium partitions. However, there are examples of maximum modularity partitions which are not equilibrium partitions, and there are examples of equilibrium partitions which are not maximum modularity partitions (Fig. 3.1).

Although they are not identical, these types of partitions tell us something similar. In a modularity partition, every part is more connected internally than it is externally. In an equilibrium partition, each vertex is more connected to its strategic community than to any other strategic community. In this way, both give us an idea of communities which are highly connected internally and sparsely connected externally.

Translating between the modularity partition and the equilibrium partition is difficult because modularity is determined from a global view, considering what proportion of the edges are contained inside a part to the expectation by random chance. In contrast, equilibrium partitions are determined by individual vertex characteristics, which depend only on the immediate neighborhood of the vertex. For this reason, one can generate rather pathological equilibrium partitions on amodular graphs. In each of these examples, however, the equilibrium partition is associated to a non-strict Nash equilibrium, leading to the conjecture in section 6.3 that an amodular graph cannot have an equilibrium partition associated to a strict Nash equilibrium.

The other important kind of vertex partition with which our partitioning method shares great similarity is the min-cut partition. This vertex partition is the partition which requires the fewest number of edges that connect vertices in different parts of the partition.

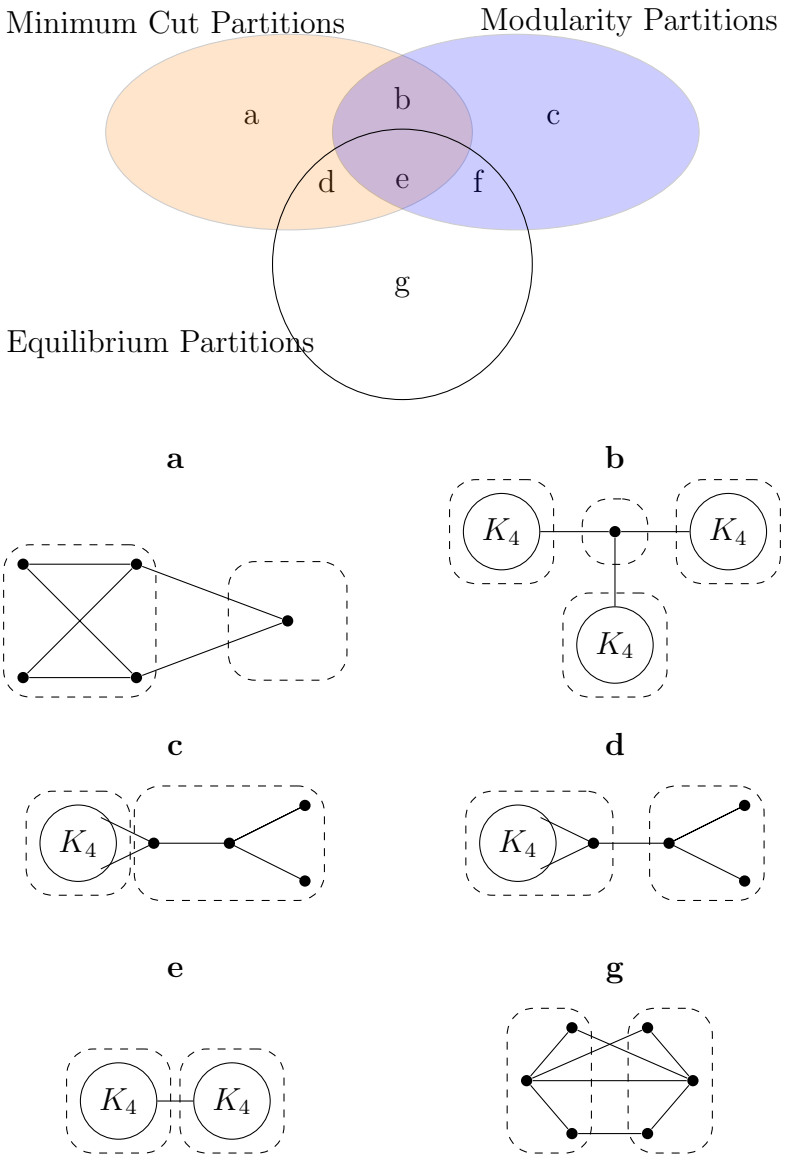

Figure 3.1: Top A Venn diagram showing Minimum Cut Partitions, Modularity Partitions, and Equilibrium Partitions. **Bottom** In each of the 6 panels below the Venn diagram is an example (if one is known) of a partition which falls into each region of the Venn diagram. Clusters in the partitions are marked out by dashed lines. For the region f, no example is given here, although there is no reason to suspect this region is empty.

Let W be the adjacency matrix for the graph G, which has m edges. The minimum edge cut partition is the partition into $|C|$ parts which minimizes the quantity $E(u)$.

$$E(u) = \sum_{v,w} W_{vw}(1 - \delta(u_v u_w)) = 2m - \sum_{v,w} W_{vw}\delta(u_v, u_w) \tag{3.1}$$

Note that a minimum cut partition requires exactly $|C|$ parts. Otherwise, the minimum cut partition would always be the trivial partition. The mincut partition and the equilibrium partition are closely related, but again, one does not imply the other. In this instance, however, we can describe the overlap of the two kinds of partitions. Every mincut partition which does not have a part of size 1 is an equilibrium partition, but the converse is not true.

Lemma 3.1 (Mincut partitions with no parts of size 1 are equilibrium partitions)**.** *Every Minimum Cut Partition with all clusters having size* > 1 *corresponds to an equilibrium partition.*

Proof. Suppose that $P = \{P^c\}_{c\in C}$ is a minimum cut partition of $G(V, E)$ with adjacency matrix W. Let $u \in \Phi^{-1}P$ and suppose u is not a Nash equilibrium (and thus no element of $\Phi^{-1}P$ is a Nash equilibrium). Therefore $\exists v^\star \in V$ which is using strategy $r \in C$ for which $w_{v^\star}(r|u) < w_\star v(s|u) \iff |\Gamma(v^\star) \cap P^r| < |\Gamma(v^\star) \cap P^s|$ for some $s \in C$. Let $\hat{u}$ be a new strategy profile where $\hat{u}_w = u_w$ for all $w \neq v^\star$ and $\hat{u}_{v^\star} = s$. Call the corresponding partition $\hat{P}$. Note that $\hat{P}$ is still a partition with the same number of clusters because removing a vertex from any cluster does not leave it empty, by assumption. We can easily compute that

$$\begin{aligned} E(P) - E(\hat{P}) &= -\sum_v \sum_w W_{vw}\delta(P_v, P_w) + \sum_v \sum_w W_{vw}\delta(\hat{P}_v, \hat{P}_w) \\ &= -\sum_{v\neq v^\star} \left[\sum_{w\neq v^\star} W_{vw}\delta(P_w, P_v) + W_{vv^\star}\delta(P_{v^\star}, P_v) \right] - \sum_{w\neq v_\star} W_{v^\star w}\delta(P_{v^\star}, P_w) \\ &\quad + \sum_{v\neq v^\star} \left[\sum_{w\neq v^\star} W_{vw}\delta(\hat{P}_w, \hat{P}_v) + W_{vv^\star}\delta(\hat{P}_{v^\star}, \hat{P}_v) \right] + \sum_{w\neq v^\star} W_{v^\star w}\delta(\hat{P}_{v^\star}, \hat{P}_w) \end{aligned} \tag{3.2}$$

Because $v_\star$ is the only vertex which has changed strategy in the new strategy profile, and because of the symmetry of the adjacency matrix and the Kronecker delta function, this

reduces to

$$\begin{aligned} E(P) - E(\hat{P}) &= -2 \sum_{v \neq v^\star} W_{vv^\star} \delta(P_v, P_{v^\star}) + 2 \sum_{v \neq v^\star} W_{vv^\star} \delta(\hat{P}_v, \hat{P}_{v^\star}) \\ &= -2|\Gamma(v^\star) \cap P^r| + 2|\Gamma(v^\star) \cap P^s| \end{aligned} \tag{3.3}$$

which is clearly positive. Thus, P was not a minimum cut partition. This contradiction proves the result. □

Thus, we have shown that if a partition is a mincut partition, we can instantly tell if it is an equilibrium partition or not. The converse is not true. There are many equilibrium partitions which may or may not be mincut partitions, and the reason for this has to do with the difference between local and global maximization. In order to explain this, we must first introduce the idea of potential games.

A potential game, first described by Monderer and Shapley (1996) is game for which there is a potential function $\mathcal{W}$ so that for all v

$$\mathcal{W}(r, u_{-v}) - \mathcal{W}(s, u_{-v}) = w_v(r|u_{-v}) - w_v(s|u_{-v}). \tag{3.4}$$

In plain English this means that there is a single function which can describe the change in payoff from a unilateral change in strategy from any player. More specifically, equation (3.4) describes an exact potential function. Other kinds of potential function exist (Lã et al., 2016) and are useful, but for the coordination game, the exact potential function will suffice. The most important point about the potential function is that if players sequentially change their strategies to improve their own payoff, they form a sequence of strategy profiles which will certainly lead to a Nash equilibrium. These paths (called finite improvement paths) imply that, for continuous strategy spaces, Nash equilibria are local maxima of the potential function. For games with discrete strategies, Nash equilibria can still be said to locally maximize the potential function, as long as the correct definition of "locally" is supplied. With this definition, the connection between the two partitions can be made clear.

Lemma 3.2. $-\frac{1}{2}E(\Phi u)$ *from* (3.1) *is a potential function for the pure coordination game played on the graph* G *with adjacency matrix* W

Proof. Let $u = (r, u_{-v})$ and $u' = (s, u_{-v})$, For notation let $\mathcal{P} = \Phi u$ and $\mathcal{P}' = \Phi(u')$ So we can say that $v \in P^r$ in $\mathcal{P}$, and in $v \in P'^s$ in $\mathcal{P}'$. Now consider $E(u) - E(u')$. By the same computation as in lemma 3.1 we know that

$$E(\Phi u) - E(\Phi u') = 2|\Gamma(v) \cap P^s| - 2|\Gamma(v) \cap P^r| = 2(w_v(s|u_{-1}) - w_v(r|u_{-1})$$

It is immediate therefore that $\frac{-1}{2}E(\Phi u) - \frac{-1}{2}E(\Phi u') = w_v(r|u_{-v}) - w_v(s|u_{-v})$. This result did not depend on our choice of v, and thus we know that $-\frac{1}{2}E(\Phi u)$ is a potential function for the pure strategy coordination game. □

With this connection, we can better describe the relationship between these two partitions. The mincut partition minimizes $E(P)$ and thus maximizes $-\frac{1}{2}E(P)$ across all partitions into $|C|$ parts. The equilibrium partition corresponds to Nash equilibria of the game, which are found at local maxima of a potential function like $-\frac{1}{2}E(\Phi u)$. While the meaning of "local maxima" in this discrete setting remains unclear, we can now put into words how these partitions are related. The mincut maximizes the potential function globally, given a constraint on the number of parts in the partition. The equilibrium partition maximizes the potential function locally.

The notion of locality we need is defined by the unilateral decisions each player (vertex) can make. From a strategy profile u, each of the n players in that strategy profile can change their strategy to one of $|C| - 1$ different strategies which means that there are $n(|C| - 1)$ strategy profiles that are only 1 unilateral decision away from u. Any two strategy profiles can be connected by a chain of unilateral decisions by a finite number of players, and so we can use the unit of "single strategic changes" to put a metric on the space of strategy profiles. More specifically, let X be the space of strategy profiles and let $d(x, y)$ be a metric on X equal to the minimum number of single strategic changes necessary to get from strategy x to strategy y. If we think of every strategy profile in X as a vertex on a graph where two

vertices are connected by an edge if they are a single strategic change away from one another, then the metric is exactly the graph distance between vertices x and y. Call this metric space $(X, d(\cdot,\cdot))$. A Nash equilibrium is any strategy profile $u \in X$ so that $\mathcal{W}(u) \geq \mathcal{W}(x)$ for all $x \in \Gamma(u) := \{y \in X, d(y,u) \leq 1\}$.

Because $\mathcal{W} = -\frac{1}{2}E(\Phi(u))$ is an exact potential function and thus when two strategy profiles are in the same equivalence class under $\sim_\Phi$ they must have the same value of $\mathcal{W}$, we define a similar notion of locality for the set of equivalence classes $\mathcal{A}$. Two equivalence classes $A, B \in \mathcal{A}$ are adjacent to one another if any two strategy profiles $a \in A, b \in B$ are adjacent to one another in $(X, d(\cdot,\cdot))$. Therefore, in the same way, we have a metric on the set $\mathcal{A}$. We will call this metric space $(\mathcal{A}, \tilde{D}(\cdot,\cdot))$. Moreover, we know that $u \in \mathcal{A}$ is an equilibrium partition if $\mathcal{W}(u) \geq \mathcal{W}(x)$ for all $x \in \Gamma(u) := \{y \in \mathcal{A}; \tilde{D}(y,u) \leq 1\}$.

Although this reframing allows us to unite the ideas of mincut partitions and equilibrium partitions very naturally, the metric space $(\mathcal{A}, \tilde{D})$ is of little use without understanding its structure. Moreover, the space $(\mathcal{A}, \tilde{D})$ does not much improve the way that we can understand the system geometrically. As with most questions about the coordination game, we cannot, at present, describe the structure of the metric space in general nor can we give a general geometric interpretation. However, we can give a geometric interpretation for a certain subset of graphs, and on that subset, we can describe a quasimetric space for which our understanding of locality can be understood from only the partition boundaries. For the remainder of this chapter, we will discuss planar graphs with simple duals (i.e., planar 3-edge connected graphs). In section 3.2, we will describe a new quasimetric space with some of the same properties as $(\mathcal{A}, \tilde{D})$ on this set of graphs which allows us to describe equilibrium partitions through a single minimization problem rather than many coupled maximization problems. From this, we arrive at an equilibrium result but we cannot derive any results about the game dynamics in general for reasons discussed later in the chapter. Only in the case that there are only two strategies can we use our dual understanding of the problem in the dynamic sense. In section 3.3, we will make the natural extension from the planar graph setting to the 2D continuous space setting. Here we will describe results for both equilibria and system dynamics, which mirror the results in the discrete setting.

3.2 Discrete Player Spaces

A planar graph can be described as a plane graph, which is an embedding of the graph into the plane. This embedding will have no two edges intersecting, and the edges will partition the plane into different connected regions called faces. For a planar graph G, the dual graph G^* is the graph where each face of the plane graph of G is represented as a vertex and two vertices in G^* are connected by an edge if the two faces they represent are separated by a single edge in the plane graph of G. In general, the dual of a planar graph G need not be a simple graph. For the present discussion, we will limit ourselves to planar graphs with simple duals, (i.e., those graphs which planar and 3-edge connected (Foulds, 1992)). More complete information about dual graphs and their properties can be found in most graph theory textbooks like Nishizeki and Chiba (1988) or Bóna (2017).

The reason that the dual is important to the question at hand is that a partition of the graph G corresponds to a subgraph of the dual G^*. The subgraph object is more intuitive for imagining local perturbations, and it also makes the connection to the continuous player space extension much more clear.

3.2.1 Partitions and Subgraphs in the Dual

For a particular embedding of the planar 3-edge-connected graph G, every partition in $\mathcal{Q}_G$ corresponds to a subgraph in G^* this correspondence, which we call Ψ is not an injection, however, because a partition P with disconnected parts and the refinement of P where each connected component of a part becomes its own part (as described in proposition 2.2) are mapped to the same subgraph. If we constrain our domain only to those vertex partitions with connected parts, which we call $\mathcal{QC}_G$, then we have injectivity from $\mathcal{QC}_G$ to the set of subgraphs of G^*, which we call $\mathcal{S}_{G^*}$. If C_P is the cutset for a partition $P \in \mathcal{QC}$, then ΨP is the subgraph of G^* which is spanned by the edges of G^* associated to C_P in G. We can describe the structure of any subgraph in the image of Ψ.

Lemma 3.3 (Image of Ψ)**.** *$\Psi : \mathcal{QC}_G \to \mathcal{S}_{G^*}$ is injective and, for any partition $P \in \mathcal{QC}_G$, ΨP is the union of simple cycles in G^* (i.e., it is a bridge-free subgraph of G^*).*

Proof. The relationship between partitions and subgraphs of the dual is uniquely defined by the cut set of the partition. Let C_P be the cut set of a partition P with connected components. Every edge of G corresponds to exactly one edge in G^*. This correspondence is due to the construction of the dual graph: an edge separating two faces results in an edge connecting the two vertices representing those two faces in the dual. Because of this, when ΨP is defined as the subgraph of G^* spanned by the edges in G^* associated to C_P in G, we know that Ψ is injective. If two partitions with connected components had identical cutsets they would be the same partition. If $\Psi P = \Psi Q$ then the cutsets of P and Q must be identical and therefore $P = Q$.

Having established the injectivity of Ψ, we can show now that ΨP is the union of simple cycles. Consider any part P^i in P. We know P^i is connected. The edges that connect a vertex in P^i to a vertex outside of p form a minimal separator for P^i and thus a minimal cutset which divides the graph G into exactly two components, P^i and $G - P^i$. It is a standard result, which can be found in chapter 4 of Godsil and Royle (2001), that a minimal cutset of a planar graph corresponds bijectively to a simple cycle in G^* given a choice of embedding. Therefore, the cutset for the partition P, which is the union of minimal separators for each of the connected components of each part in P, corresponds to the union of simple cycles. Thus ΨP is the union of simple cycles in G^*. □

Notice that because the correspondence between edges in an embedding of G and edges in G^* is bijective, if we limit the range to subgraphs of G^* which are bridge-free (i.e., the union of simple cycles), then Ψ is bijective.

Corollary 3.1. *If G is a planar 3-edge-connected graph with dual G^*, then any subgraph of G^* which is bridge-free is mapped to by a partition of G.*

If we let $\mathcal{SC}_{G^*}$ be the space of subgraphs of G^* which are simple cycles than $\Psi : \mathcal{Q}_G \to \mathcal{SC}_{G^*}$ is a bijection. The space $\mathcal{SC}_{G^*}$ is crucially and unfortunately not the cycle space of G^* because the union of two cycles may not be a cycle itself.

We now have an association between our set of strategy profiles $\mathcal{A}_G$ and the class of subgraphs $\mathcal{SC}_{G^*}$ by $\Psi \circ \Phi$ However, this is not a bijection because, although $\Phi : \mathcal{A}_G \to \mathcal{Q}_G$

is bijective, $\Psi : \mathcal{Q}_G \to \mathcal{SC}_{G^*}$ is not. Recall that for Ψ to be a bijection, we must restrict the domain to $\mathcal{QC}_G$. The preimage of $\mathcal{QC}_G$ under Φ is a strict subset of $\mathcal{A}$. Moreover, $\Phi^{-1}\mathcal{QC}_G$ may not be a metric space with respect to the metric $\tilde{D}$.

This means that in order to find equilibrium partitions using this dual approach we must now resolve the following two related questions: Can we still interpret the meaning of the potential function $\mathcal{W}$ in the space $\mathcal{SC}_{G^*}$ and is there a metric, or quasi-metric, we can put on the space $\mathcal{SC}_{G^*}$ so that local maxima of the potential function in $\mathcal{SC}_{G^*}$ can still be associated with Nash equilibria?

3.2.2 Equilibrium Results

Our first goal, translating the potential function so that it makes sense in $\mathcal{SC}_{G^*}$ is simple because we can construct a function $\mathcal{V}$ so that $\mathcal{W}(u) = \mathcal{V}(\Psi \circ \Phi u)$ for all $u \in \mathcal{A}$. This task is made very simple by the simplicity of $\mathcal{V}$.

Lemma 3.4. *Let $\mathcal{V}(s) = \frac{-1}{2} size(s)$ where $size(s)$ is the number of edges in the subgraph s. With this construction, $\mathcal{W}(u) = \mathcal{V}(\Psi \circ \Phi u)$ for all $u \in \mathcal{A}$*

Proof. For a partition $P \in \mathcal{Q}_G$, $E(P) = 2m - \sum_{v,w} W_{v,w}\delta(P_v, P_w)$. $\delta(P_v, P_w)$ returns a 1 if v and w are in the same part of the partition and 0 otherwise, so naturally $E(P)$ enumerates the cutset of the partition P. Because every cut edge in P is an edge in the subgraph $\Psi P \subset G^*$, it is clear that $E(P) = size(\Phi P)$ for all $P \in \mathcal{Q}_G$. Therefore, for any $u \in \mathcal{A}$,

$$\mathcal{V}(\Psi \circ \Phi u) = \frac{-1}{2} size(\Psi \circ \Phi u) = \frac{-1}{2} E(\Phi u) = \mathcal{W}(u)$$

□

The corollary of this will also be helpful

Corollary 3.2. *If $u, u' \in \mathcal{A}$ and $\Psi \circ \Phi u = \Psi \circ \Phi u' = s$ then $\mathcal{W}(u) = \mathcal{W}(u')$.*

This means that, in order to find a Nash equilibria, we are in search of subgraphs of G^* which maximize $\mathcal{V}(s)$ locally. Equivalently, we are in search of subgraphs which minimize

$size(s)$, and thus we can say that Nash equilibria correspond to the local minimizers of size in the subgraph space of the dual so long as we can provide the correct understanding of "local."

Finding the correct sense of locality is a far greater challenge exactly because of the lack of a well-defined inverse for Ψ. Even if we restrict the domain only to $\Phi^{-1}\mathcal{QC}_G$ and use the metric $\tilde{D}$ on this restricted domain together with the bijection $\Psi \circ \Phi : \Phi^{-1}(\mathcal{QC}_G) \to \mathcal{SC}_{G^*}$, it is not certain whether local maxima of $\mathcal{V}(s)$ are still Nash equilibria because the strategy profiles associated to the local maxima of $\mathcal{V}$ in $\mathcal{SC}_{G^*}$ may not be local maxima of $\mathcal{W}$ in $\mathcal{A}$. We can say something about the relative sizes of the subgraphs associated to strategy profiles in the vicinity of a Nash equilibrium.

Theorem 3.1 (Relative Sizes of subgraphs near Nash equilibria)**.** *if G is a 3-edge-connected graph with dual G^* and u is a Nash equilibrium then $size(\Psi \circ \Phi u) \leq size(\Psi \circ \Phi u')$ for all $u' \in \Gamma(u)$.*

Proof. The result is direct from lemmas 3.2,3.3, and 3.4. □

This result is interesting, but does not accomplish the goal of being able to describe Nash equilibria purely in the dual sense. In order to do that we need to resolve the second issue, which is finding a metric on $\mathcal{SC}_{G^*}$, so that we can describe what a local maximum is with the goal of constructing the metric carefully enough so that local maxima of $\mathcal{V}(s)$ correspond to Nash equilibria in $\mathcal{A}$.

To do this, we will, again, imagine all of the elements of $\mathcal{SC}_{G^*}$ so that they are vertices in a graph, and we will define adjacency on that graph so that graph distance becomes an appropriate metric for $\mathcal{SC}_{G^*}$. The goal is to have a metric space so that local maxima of $\mathcal{V}(s)$ in $\mathcal{SC}_{G^*}$ correspond to Nash equilibria in some way. In order to do this, we must first introduce two definitions.

Definition 3.1 (Departure Vertex)**.** *For a face f of the planar graph G^*, and a subgraph $s \in \mathcal{SC}_{G^*}$, a vertex v adjacent to the face f is a departure vertex of f if s includes v and at least one edge adjacent to v and not incident to the face f. (e.g., Fig. 3.2)*

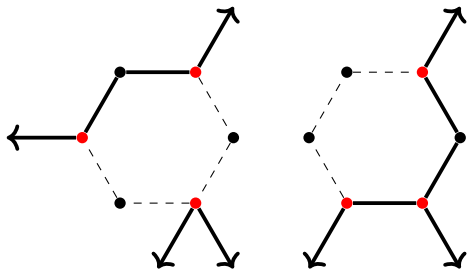

Figure 3.2: For a particular face, the departure vertices of that face are the vertices included in the subgraph with at least one adjacent edge not incident to the face included in the subgraph. The examples of departure vertices are highlighted in red where the dashed lines are edges of the graph which are not included in the subgraph.

Definition 3.2 (Single Face Rewiring (SFR))**.** *For a simple planar graph G^* and a subgraph $s \in \mathcal{SC}_{G^*}$, a Single Face Rewiring from s to r is a resampling of edges from G^* so that, for one face f of G^**

1. *Any edge not incident to the face f which was in s is still in r after the SFR.*
2. *Edges incident to f in G^* are included in r in any way so that all departure vertices of f in s are still departure vertices of f in r.*
3. *Edges incident to f cannot be added in such a way that would create a bridge in r.*
4. *If two departure vertices were connected by a path along f in s, but are not connected by a path along f in r, then they must be entirely disconnected in r.*

Although the definition of the Single Face Rewiring sounds complicated the idea is rather simple. A SFR takes a subgraph in $\mathcal{SC}_{G^*}$ and perturbs it to a subgraph which is nearly identical to the original subgraph except that the edges incident to a face f may have changed. There are several examples of SFRs in figure 3.3.

We will use SFRs to describe the distance between two subgraphs in $\mathcal{SC}_{G^*}$. In order to do this we must first prove that $\mathcal{SC}_{G^*}$ is closed under SFR.

Lemma 3.5. *For a simple planar graph G^*, $\mathcal{SC}_{G^*}$ is closed under SFR.*

Proof. Let $s \in \mathcal{SC}_{G^*}$ and select the face f of G^*. s is therefore bridge-free. If we perform a Single Face Rewiring of s on the face f, we can start by removing all of the edges of s which

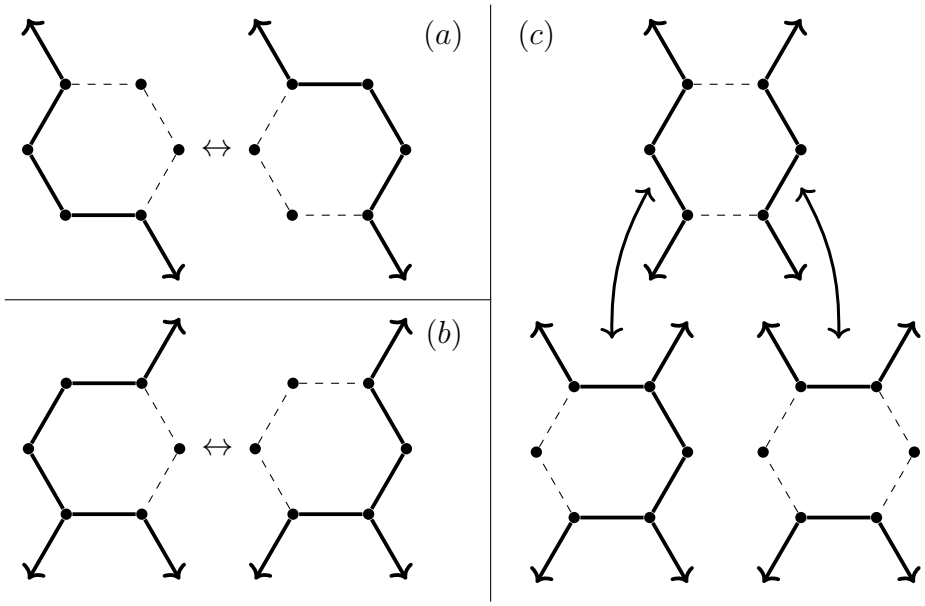

Figure 3.3: Three examples of single face rewirings. (**a**) shows a simple SFR, taking the opposite route between the two departure vertices of the face. (**b**) shows a more complicated SFR, which shows the path around the face changing while still containing each of the three departure vertices of the face. (**c**) shows the complicated case in which the face is incident to two distinct sub-paths. It depends on the connectivity of the rest of the graph which of these steps, indicated by the two headed arrows, is a valid SFR.

are incident to f in G^*. What remains is a subgraph which is not necessarily bridge-free because there may be vertices of degree 1. If such a vertex exists, it is a departure vertex of f. To complete the SFR, we add in new edges from G^* selected from those edges incident to f. In order for the SFR to be valid, each departure vertex must be adjacent to at least one edge incident to f, meaning that each departure vertex has degree at least 2. Moreover, the addition of edges incident to f cannot create a bridge, and so there cannot be any vertices adjacent to the face f with degree 1. Thus, the rewiring results in a subgraph with no bridges and where all vertices have degree at least 2. We are certain that such a graph is the union of simple cycles and thus the new subgraph is bridge-free. □

Now it would be convenient to construct the metric space in the typical way by assuming that a subgraph in $\mathcal{SC}_{G^*}$ is a vertex in a graph and two vertices share an edge if one subgraph can be made into the other through one SFR. Unfortunately SFRs are not necessarily symmetric. Because of the rules about connectivity when doing the rewiring, there are non-reversible SFRs. Because of this, the best that we can hope for is a quasi-metric space. To construct this space, still imagine every element of $\mathcal{SC}_{G^*}$ as a vertex in a graph with directed edges from one subgraph to another if the first subgraph can be changed into another by a single SFR. Naturally, we define the quasimetric, $D_{G^*}(\cdot,\cdot)$, as the shortest path distance through the resulting directed graph. Note that it is equivalent to the minimum number of SFRs to get from one subgraph to another. Because it is not symmetric we will note specifically that $D_{G^*}(s,r)$ is the number of SFRs required to go from s to r. Now we can consider the quasimetric space $(\mathcal{SC}_{G^*}, D_{G^*})$.

Now that we have constructed the quasimetric, we can give a little more intuition into the structure of the space by examining an example.

Example 3.1. *Starting from a bridge-free subgraph of the graph G, each face can be rewired methodically to result in any other subgraph in $\mathcal{SC}_G$. Figure 3.4 is an illustrative example of how one "moves around" in the quasimetric space. Although the figure does not demonstrate such an example, not every SFR is reversible, which is why it defines a quasimetric and not a simple metric.*

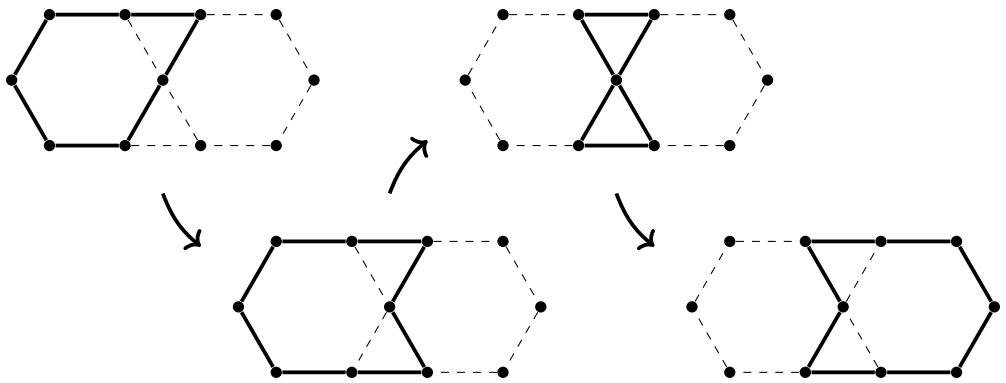

Figure 3.4: A sequence of three SFRs transforming one subgraph into another. The edges of the graph G are dashed if they are not included in the subgraph at a particular step. Each step represents a single face rewiring of one of the 5 faces of the planar graph.

Although the space does not have a proper metric, the quasimetric still allows us to describe neighborhoods about a subgraph in $\mathcal{SC}_{G^*}$. In order to do this we define $\Gamma_{G^*}(s) := \{r \in \mathcal{SC}_{G^*}; D_{G^*}(s,r) \leq 1\}$. These neighborhoods will allow us to give an appropriate notion of "locality." We have constructed this quasimetric so that it shares similarities with the metric space $(\mathcal{A}, \tilde{D})$. This way subgraphs which minimize size locally in $(\mathcal{SC}_{G^*}, D_{G^*})$ will be related to those $u \in A$ that maximize $\mathcal{W}$ locally. Although we would hope for a way to say if s is a local size minimizer in $(\mathcal{SC}_{G^*}, D_{G^*})$ then any $u \in \Phi^{-1} \circ \Psi^{-1} s$ is a Nash equilibrium, this is not necessarily true. However, we can say something slightly less powerful. In order to arrive there, we first describe the following lemma.

Lemma 3.6. *If $u \in \mathcal{A}$ has $\Phi u \in \mathcal{QC}_G$ and $\tilde{D}(u,u') = 1$ in $\mathcal{A}$ for some u', then $D_{G^*}(\Psi \circ \Phi u, \Psi \circ \Phi u') = 1$ in $\mathcal{SC}_{G^*}$.*

Proof. Consider the difference between u and u' in $\mathcal{A}$. The single strategic change involves only one vertex in G, leaving the part of the partition it was in previously and joining a new part of the partition. First consider $\Psi \circ \Phi u$. Let f be the face in G^* which corresponds to the vertex v in G. In the single strategic change, only v changes its strategy. Every other player remains unchanged. That means for $P = \Phi u$ and $P' = \Phi u'$, $\delta(P_w, P_y) = \delta(P'_w, P'_y)$ for every $w, y \in V \setminus \{v\}$. Each of these edges (w,y) corresponds to exactly one edge which is not incident to f in G^*. Therefore, every edge which is not incident to f in G^* and is present in

$\Psi \circ \Phi u$ is also present in $\Psi \circ \Phi u'$. Likewise, every edge which is not incident to f in G^* and is not present in $\Psi \circ \Phi u$ is also not present in $\Psi \circ \Phi u'$.

Because G is assumed to be planar and 3-edge-connected, every face is adjacent to at least 3 vertices. In the dual, this means that every vertex is adjacent to at least 3 faces. We can use this face to show that every departure vertex of f in $\Psi \circ \Phi u$ will also be a departure vertex in $\Psi \circ \Phi u'$. If x is a departure vertex of f in $\Psi \circ \Phi u$, then it is adjacent to f and adjacent to at least one edge in $\Psi \circ \Phi u$ which is not incident to the face f. This edge, e^*, connects two faces f_1 and f_2 that are not f. Because it is present in $\Psi \circ \Phi u$, e^* corresponds to an edge of the cutset in Φu, meaning that the vertices in G which correspond to the faces f_1 and f_2 in G^* are not in the same part of the partition. That means these vertices are not playing the same strategy in u. Because these vertices are not v, they will also not be playing the same strategy as one another in u', and thus e^* will still be present in $\Psi \circ \Phi u'$. Thus, x is still a departure vertex.

To show that there are no bridges in $\Psi \circ \Phi u'$, we need only use lemma 3.3.

Finally, we must show that if two departure vertices of f, which were connected by a path incident to f in $\Psi \circ \Phi u$ and are no longer connected by a path incident to f in $\Psi \circ \Phi u'$, then they are entirely disconnected. Assume that two vertices a and b in G^* are connected by a path incident to f in $\Psi \circ \Phi u$ but not in $\Psi \circ \Phi u'$. This means that there are at least two non-adjacent edges incident to f in G^* that are not present in $\Psi \circ \Phi u'$. More specifically, there are two paths from a to b incident to f, and there is at least one edge incident to f that is not present in $\Psi \circ \Phi u'$ from each of those two paths.

This means that for any strategy profile in the preimage, $\Phi^{-1} \circ \Psi^{-1}(\Psi \circ \Phi u')$. there are two vertices x, y adjacent to v that are using the same strategy as v in u'. Because x and y did not change their strategy from u to u', it must also be true that they were using the same strategy in u. Because we assumed that $\Psi u \in \mathcal{QC}_G$, we know that all parts of the partition are connected and thus x and y are connected by a path of vertices using the same strategy. When v changes its strategy to take on the same strategy as x and y in u', there is now necessarily a cycle starting and ending at v of vertices using the same strategy in u'.

From here, we rely on the planar properties of G and G^*. The cycle of vertices in the same strategic community starting and ending at v forms a Jordan curve in the plane. In the dual, that same Jordan curve starts and ends in the face f and intersects every edge corresponding to the edges of G, which defined the curve. The Jordan curve theorem tells us that the plane is separated into two parts: an "inside" and an "outside."

Observe that on any path from a to b in G^* incident to f, one of the edges must be absent from $\Psi \circ \Phi u'$ and correspond to an edge of G that defined the Jordan curve. This means that the Jordan curve intersects both paths from a to b incident to f. Importantly, it must intersect both paths exactly once because the cycle in J included only two edges incident to v, and so the Jordan curve can intersect only the two corresponding edges of G^*. This implies that a and b cannot both be "inside" and the cannot both be "outside." One must be inside, and one must be outside.

By construction, every edge of G^* that the Jordan curve intersects is *not* included in $\Psi \circ \Phi u'$. Because any path from a to b in G must cross the Jordan curve, it is certain that a and b are disconnected in $\Psi \circ \Phi u'$.

This means that if u and u' are a single strategic change away from one another. Then $\Psi \circ \Phi u$ can be made into $\Psi \circ \Phi u'$ by a resampling of the edges which satisfies points (1-4) of the definition of SFR. Therefore $D(\Psi \circ \Phi u, \Psi \circ \Phi u') = 1$ in $\mathcal{SG}_{G^*}$. □

With this lemma, it is possible to show the main result of this section.

Theorem 3.2. *If $s \in \mathcal{SC}_{G^*}$ satisfies*

$$size(s) \leq size(r) \quad \forall r \in \Gamma_{G^*}(s)$$

then there is a $u \in \Phi^{-1}\Psi^{-1}s$ so that u is an equilibrium. Moreover, this u will satisfy $\Phi u \in \mathcal{QC}_G$.

Proof. By Lemma 3.6 we know that if $u \in \Phi^{-1}\mathcal{QC}_G$ and $\tilde{D}(u, u') \leq 1$ in $\mathcal{A}$ then $D_{G^*}(\Psi \circ \Phi u, \Psi \circ \Phi u') \leq 1$. This means that for $u \in \Phi^{-1}\mathcal{QC}_G$, $\Psi \circ \Phi(\Gamma(u)) \subseteq \Gamma_{G^*}(\Psi \circ \Phi u)$. Equivalently $\Gamma(u) \subset \Phi^{-1} \circ \Psi^{-1}(\Gamma_{G^*}(\Psi \circ \Phi u)$ for $u \in \Phi^{-1}\mathcal{QC}_G$. We can complete the first part of the proof

by noting that by lemma 3.4 and corollary 3.2 if $\mathcal{V}(\Psi \circ \Phi u) \geq \mathcal{V}(s)$ for all $s \in \Gamma_{G^*}(\Psi \circ \Phi u)$ then

$$\mathcal{W}(u) \geq \mathcal{W}(u') \quad \forall u' \in \Phi^{-1} \circ \Psi^{-1}(\Gamma_{G^*}(\Psi \circ \Phi u)).$$

Putting these together this means that if $u \in \Phi^{-1}\mathcal{QC}_G$ and $\mathcal{V}(\Psi \circ \Phi u) \geq \mathcal{V}(s)$ for all $s \in \Gamma_{G^*}(\Psi \circ \Phi u)$, then $\mathcal{W}(u) \geq \mathcal{W}(u')$ for all $u' \in \Gamma(u)$. Lastly, recall that for every $s \in \mathcal{SC}_{G^*}$ there is a $u \in \Phi^{-1} \circ \Psi^{-1}s$ such that $\Phi u \in \mathcal{QC}_G$. This implies that if s minimizes size in the neighborhood Γ_{G^*} then there is a $u \in \Phi^{-1} \circ \Psi^{-1}s$ with $\Phi u \in \mathcal{QC}_G$ that satisfies $\mathcal{W}(u) \geq \mathcal{W}(u')$ for all $u' \in \Gamma(u)$. This completes the proof. □

This is the strongest statement that we can make from an equilibrium standpoint. As described before, it is untrue to say that the image of a local size minimizer in $(\mathcal{SC}_{G^*}, \delta)$ is a Nash equilibrium in $\mathcal{A}$ because lemma 3.6 only holds true for those strategy profiles where the strategic communities are connected. This fact limits our ability to use this theorem and prevents us, in most cases, from being able to use the dual concept to address the game dynamically in the dual. However, there are several modifications that can be made to the game that allow the dual dynamics to become tractable.

3.2.3 Barriers to Dynamic Results

The main issue with using the dual concept is that, in order for us to be able to gain any insight about the game, we need to restrict the domain of strategy profiles so that $\Psi \circ \Phi$ is a bijection. Doing this clearly limits the game dynamics. Moreover, considering the game dynamics in the dual cannot easily be done in the synchronous setting because performing more than one SFR at a time is ill-defined. This is because if one SFR disconnects several components and a second reconnects those components, the outcome is not well defined

The mixture of local and global information is the key element that makes this game difficult to study analytically. In the dual, the global information about the connectivity of the system required in order to "move around" in the subgraph space prevents us from describing flows in a simple way and makes the prospect of using it to describe the game with synchronous update impossible.

There is, however, a reduction of the game, which has been taken by many other scholars studying this system. Which allows for the dynamics in the dual to be made entirely clear. We will reduce the game to the case where there are only two strategies. This removes the need for global connectivity information in the dual because, with only two strategies, the cut set of the partition fully describes the strategy profile regardless of whether each strategic community is connected. We describe this more exactly in the following subsection.

3.2.4 Dynamics with Only Two Strategies

When there are only two strategies, the strategy profile u is entirely determined by the cutset of the partition Φu. Let $\mathcal{Y}_G$ be the set of strategy profiles on G with only two strategies available. Of course for every strategy profile, there is exactly one other strategy profile which is equivalent under $\sim_\Phi$, which is the strategy profile where every player has their strategy filled from one to the other. Call the set of equivalence classes under $\sim_\Phi$ $\mathcal{B} = \mathcal{Y}/S_2$. We can give $\mathcal{Y}$ and $\mathcal{B}$ the same metrics as $\mathcal{X}$ and $\mathcal{A}$ previously because they are constructed in the same manner.

In order to use this metric space correctly, we must first describe two spaces in detail. The first is the cutspace of the graph G, which we represent at $T(G)$. In a connected graph, a set of edges $E' \subset E$ which, if removed from G, results in two disjoint and disconnected parts of the graph, is called a cut. The cutspace is the vector space of all of the cuts of the graph G over the field $\mathbb{Z}_2$ (when two cuts are added, any edge of G which is in exactly one of the cuts is included in the sum and all other edges are excluded).

Similarly, in a connected graph G, the cyclespace, $C(G)$, is the set of all of the subgraphs of G where every vertex has odd degree. This again is a vector space over the same field, and addition is defined in the same way.

The reason why we introduce these spaces is to note that they are dual to one another. It is a standard result that for a planar graph G with a dual G^*, there is an isomorphism, Υ, between $T(G)$ and $C(G^*)$. That isomorphism can be described in exactly the same way that Ψ was described. Every edge of G corresponds exactly to one edge in G^*, and so if

$t \in T(G)$ then $\Upsilon(t)$ is the subgraph spanned by all of the edges corresponding to edges in T. That is to say, if P is the partition with cutset $t \in T(G)$, then $\Upsilon(t) = \Psi(P)$. (Foulds, 1992; Nishizeki and Chiba, 1988; Gross and Jay, 2005)

It is also important to point out the existence of a bijection Λ between $\mathcal{B}_G$ and $T(G)$. At its simplest, for a strategy profile $u \in \mathcal{B}_G$, Λu is the cutset of Φu.

Lemma 3.7. *$\Lambda : \mathcal{B}_G \to T(G)$ defined as Λu is the cutset of Φu is a bijection*

Proof. It is clear that Φ is an injection because $\mathcal{B}_G$ are equivalence classes under $\sim_\Phi$. If we limit the range of Φ to only partitions with two parts, then it is a bijection. Thus, we need only note that a partition into two parts is uniquely determined by its cutset.

Assume two partitions into two parts, P and Q, are different. Without loss of generality, say there exists a pair of vertices v, w which are in the same part in P and in different parts in Q. If this does not happen, P and Q were identical. Consider the shortest path from v to w. The sequence of vertices can be labeled from v to w in order by which part they belong to, and when two adjacent vertices are not in the same part, they must have a cut edge between them. Let C_P be the cutset of the partition P and let C_Q be the cutset of the partition Q. The path from v to w must have an even number of edges included in C_P. This is because either every vertex in the path is in the same part as v and w or, whenever the path enters the opposite part, it must exit before it reaches w. The same path must have an odd number of edges included in C_Q because the path must leave the part that v is in at least once, and if it enters it again, it must depart before it arrives at w.

We have shown, therefore, that if two partitions of a connected graph into two parts are not the same, then their cutsets cannot be the same. Moreover, every cut in $T(G)$, by definition, divides the vertices of G into two disjoint sets, which can naturally be expressed as a partition. Therefore Λ is both injective and surjective from $\mathcal{B}_G$ to $T(G)$. □

What we have shown is that Λ is a bijection between $\mathcal{B}_G$ and $T(G)$ defined by Λu is the cutset of Φu. Υ is also a bijection from $T(G)$ to $C(G^*)$ defined so that Υt is the subgraph of G^* which is spanned by the edges corresponding edges of G in the cut t. Ψ maps partitions of G to subgraphs of G^* by ΨP is the subgraph of G^* spanned by the edges corresponding

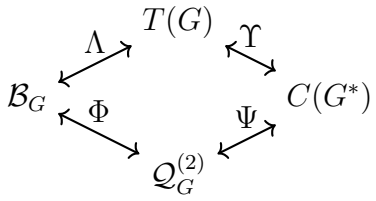

Figure 3.5: A diagram of the relationships between the spaces discussed in this section. $\mathcal{B}_G$ is the set of strategy profiles with two strategies on the graph G (mod strategic permutations). $T(G)$ is the cutspace of the graph G. $\mathcal{Q}_G^{(2)}$ is the set of vertex partitions with two parts. $C(G^*)$ is cyclespace of the dual graph G^* Λ is the bijection from lemma 3.7, Φ is the bijection described in chapter 1, Ψ is a mapping from partitions to subgraphs of G^* and Υ is the isomorphism from cutspace to cyclespace from Hartvigsen and Mardon (1994).

to the edges of G in the cutset of P. The following result shows that Ψ is equivalent to $\Upsilon \circ \Lambda \circ \Phi^{-1}$.

Lemma 3.8. $\Psi : \mathcal{Q}_G^{(2)} \to C(G^*)$ *is equivalent to* $\Upsilon \circ \Lambda \circ \Phi^{-1}$

Proof. Let P be a partition in $\mathcal{Q}_G^{(2)}$ and observe that $\Lambda \circ \Phi^{-1} P$ is exactly the cutset of $\Phi\Phi^{-1}P$ Because Φ is a bijection from $\mathcal{B}_G$ to $\mathcal{Q}_G^{(2)}$ we know that $\Lambda \circ \Phi^{-1} P$ is the cutset of P.

Observe now that $\Upsilon \circ \Lambda \circ \Phi^{-1} P$ is the subgraph of G^* spanned by the edges in G^* corresponding to the edges of G in $\Lambda \circ \Phi^{-1} P$. These edges are exactly the cut set of P and so $\Upsilon \circ \Lambda \circ \Phi^{-1} P$ is the subgraph of G^* which is spanned by the edges corresponding to the edges of G in the cutset of P. This is exactly the definition of ΨP

This means that $\Psi P = \Upsilon \circ \Lambda \circ \Phi^{-1} P$ for all $P \in \mathcal{Q}_G^{(2)}$. □

This means that the dual relationship we have been talking about, $\Psi \circ \Phi$ is a bijection from the metric space strategy profiles $\mathcal{B}_G$ to the cyclespace of the dual $C(G^*)$, which is a vector space. Each of the sets and spaces mentioned here are described in figure 3.5.

We will again put a metric on the cycle space based on the Single Face Rewirings from before. For the cycle space, however, the definition is easier.

Definition 3.3 (Cycle Single Face Rewiring)**.** *A Cycle Single Face Rewiring (CSFR) from* s *to* r*, where* $s, r \in C(G^*)$ *is a resampling of the edges of* G^* *so that for exactly one face* f *of* G^*

1. *Every edge not incident to the face f which is in s is still in r and every edge not incident to f which is missing from s is still missing from r.*

2. *Every edge incident to f which was in s is not in r and every edge incident to f which was not in s is in r.*

This definition is equivalent to saying that if C_f is the cycle in G^* that encloses only the face f, then s and r are a CSFR away from one another iff $r = s + C_f$ for some face $f \in G^*$. Now we can talk about the metric vector space $(C(G^*), D)$ in the same way as before by considering every element of $C(G^*)$ as the vertex of a graph and having vertices be connected by an edge if they are one CSFR away from one another. Because the $C(G^*)$ is a vector space over the field $\mathbb{Z}_2$, we know that $r = s + C_f \iff s = r + C_f$, so every edge is bidirectional. This means the norm D can be thought of as the graph distance from one element of $C(G^*)$ to another.

Theorem 3.3. *$\Psi \circ \Phi : \mathcal{B}_G \to C(G^*)$ is an isometry.*

Proof. If u and u' are adjacent in $(\mathcal{B}_G, \tilde{D})$, then there is a single vertex v which changed their strategy. Without loss of generality, we can say they changed from strategy 1 to strategy 2. This means that the cutset of the partitions Φu and $\Phi u'$ differ only on edges adjacent to the vertex v. Indeed if an edge, adjacent to v, was present in the cut set of Φu then it is not present in the cut set of $\Phi u'$, because there are only two strategies. If v was originally playing a different strategy from w and changed strategies, then v must now be playing the same strategy as w. The same logic can tell us that if an edge adjacent to v is not in the cutset of Φu then it must be in the cutset of $\Phi u'$.

This means that $\Psi \circ \Phi u$ and $\Psi \circ \Phi u'$ differ only on the edges incident to the face v in G^* which corresponds to the vertex v in G. Moreover, every edge incident to the face f was either present in $\Psi \circ \Phi u$ and not in $\Psi \circ \Phi u'$ or not present in $\Psi \circ \Phi u$ and present in $\Psi \circ \Phi u'$. The easier way to say this is that $\Psi \circ \Phi u - \Psi \circ \Phi u' = C_f$. Thus there is an edge in $(C(G), D)$ from $\Psi \circ \Phi u$ to $\Psi \circ \Phi u'$).

In the other direction, we can imagine very similarly. Suppose that s and r are separated by a CSFR. This means that $s - r = C_f$ for some f. In other words, this means that if an

edge is present in s and incident to f, it is not in r, and if an edge is not present in s and incident to f, then it is present in r. Moreover, the status of every edge away from f is the same in s and r.

This means that $\Upsilon^{-1}s$ and $\Upsilon^{-1}r$ differ only in the edges which are adjacent to the vertex v in G, which corresponds to the face f in G^*. If an edge adjacent to v is present in the cut $\Upsilon^{-1}s$, it is not present in $\Upsilon^{-1}r$, and if an edge adjacent to v is not present in $\Upsilon^{-1}s$, then it is present in $\Upsilon^{-1}r$.

Taking it one step back through the diagram (fig. 3.5), we know now that $\Lambda^{-1} \circ \Upsilon^{-1}s$ and $\lambda^{-1} \circ \Upsilon^{-1}r$ differ by a single strategic change because, if the player v was using the same strategy as a neighbor in $\Lambda^{-1} \circ \Upsilon^{-1}s$, then it is not using the same strategy as that same neighbor in $\Lambda^{-1} \circ \Upsilon^{-1}r$. Likewise, if player v is using a different strategy as a neighbor in $\Lambda^{-1} \circ \Upsilon^{-1}s$, then it must use the same strategy as that same neighbor in $\Lambda^{-1} \circ \Upsilon^{-1}s$. This means that v has changes their strategy from $\Lambda^{-1} \circ \Upsilon^{-1}s$ to $\Lambda^{-1} \circ \Upsilon^{-1}r$ and these two strategy profiles are adjacent in $(\mathcal{B}_G, \tilde{D})$.

To finish the proof correctly, we need only note that by lemma 3.8, $\Lambda^{-1}\circ\Upsilon^{-1}s = \Phi^{-1}\circ\Psi^{-1}s$ for all $s \in C(G^*)$. This means that truly the spaces $(\mathcal{B}_G, \tilde{D})$ and $(C(G^*), D)$ are isometric and the isometry can be given as $\Psi \circ \Phi$. □

Notice that the definition of a CSFR does not always fit the definition of an SFR. This is because a CSFR can be defined without regard to the connectivity of the subgraph. Because there are only two strategies and so the cutset alone determines the strategy profile, we never encounter the situation wherein a CSFR results in the merging of two distinct strategic communities. This means that we can describe flows through the cycle space entirely locally.

Definition 3.4 (Synchronous Cycle Shortening Flow)**.** *A Synchronous Cycle Shortening Flow is a sequence $s_t \in C(G^*)$. For a particular s_t, if any face f of G^* has more edges than non edges in s_t, then add C_f to s_t.*

$$s_{t+1} = s_t + \sum_{f \in G^*} C_f H(f, s_t) \tag{3.5}$$

Where $H(F, s_t)$ is a Heavyside-like function which is 1 when the number of edges of f in s_t is strictly greater than the number of edges of f not in s_t and 0 otherwise.

Although it may be hard to picture, it is a rather simple concept. Each face of G^* is rewired to reduce the number of edges incident to it while still maintaining all of the departure vertices. To see an example of this, see appendix C.

The main result from 3.2.2 still holds in this setting, even with the mildly different metric on the cycle space, which is a subset of $\mathcal{SC}_{G^*}$. Indeed, the result can be stated more strongly because of the bijective correspondence between elements of the cyclespace and strategy profiles.

Theorem 3.4. *Consider a 3-edge connected and planar graph G and its simple dual G^* (which may depend on the planar embedding). $s \in C(G^*)$ satisfies*

$$size(s) \leq size(r) \, \forall r \in N(s)$$

Where $N(s) := \{r \in C(G^*); D(r, s) \leq 1\}$ if and only if $\Phi^{-1} \circ \Psi^{-1} s$ is a Nash Equilibrium

Proof. $\implies$ If s is a local size minimizer in $C(G^*)$ then there are no faces f for which $size(s + C_f) \leq size(f)$. By theorem 3.3, there are no single strategic changes that could decrease the size of the cut set of $\Psi^{-1} s$. By lemma 3.4, this means that there is no single strategic change that could increase the potential above $\mathcal{W}(\Phi^{-1} \circ \Psi^{-1} s)$ and thus, by the definition of potential game, $\Phi^{-1} \circ \Psi^{-1} s$ is a Nash equilibrium.

$\impliedby$ Lemma 3.4 and the definition of a potential game imply that, if u is a Nash equilibrium, there are no single strategic changes that can decrease the cutset of Φu, which by lemma 3.8 and by lemma 3.3 means that there are no CSFRs that could decrease the size of s. Therefore, s is a local size minimizer, meaning that

$$size(s) \leq size(r) \, \forall r \in N(s)$$

Where $N(s) := \{r \in C(G^*); D(r, s) \leq 1\}$. This completes the proof. □

Not only do the equilibrium results still hold, but the process of cycle shortening reflects the game dynamics directly. One critical thing to notice about the game with only two strategies is that there are never ties between two different new strategies. A player may be faced with the situation where their current strategy gives the same payoff as the opposite strategy, but in this case, by the ϵ-inertial condition, they do not change strategies. Therefore, the system with two strategies is entirely deterministic. In Chapter 1, we described the discrete time game as any flow such that

$$u_v(t+1) \in BR_v(u(t)) \; \forall v \in V. \tag{3.6}$$

with certain random tie breaking conditions.

Because now at each time step, one strategy profile is mapped to exactly one new strategy profile by the synchronous myopic best response, we can give it a name. For a strategy profile $u \in \mathcal{B}_G$, $f(u)$ is the unique strategy profile that satisfies $f(u)_v \in BR_v(u)$ for all $v \in V$ and where the player does not change strategy in the case of a tie. It is clear that every flow satisfying the more general myopic best response condition with only two strategies satisfies $u(t+1) = f(u(t))$.

Moreover, it will be convenient to give a name to a single step of the synchronous subgraph shortening flow. Let $g(s) = s_t + \sum_{f \in G^*} C_f H(f, s_t)$ as in equation (3.5) so that $s_{t+1} = g(s_t)$ in the synchronous cycle shortening flow.

Theorem 3.5. *The dynamics in $\mathcal{B}_G$ of the pure coordination game under synchronous Myopic best response are equivalent to the Synchronous Cycle Shortening Flow on $\mathcal{C}_{G^*}$. More specifically: Given a $u_0 \in \mathcal{B}_\mathcal{G}$ then the flows $u(t+1) = f(u(t)), u(0) = u_0$ and $s_{t+1} = g(s_t), g(0) = \Psi \circ \Phi u_0$ satisfy $\Psi \circ \Phi u(t) = s_t$ for all t.*

Proof. The only thing necessary to prove is that $f(u) = \Phi^{-1} \circ \Psi^{-1}(g(\Psi \circ \Phi u))$ Starting from the strategy profile u if $u' = f(u)$ that means that if v was playing a best response in u then it did not change strategies and so it is playing the same strategy in u'. If it was not playing a best response in u, then it is playing the opposite strategy in u'. Notice that if two players are playing the same strategy and they both change strategies, in the two strategy case,

they are still playing the same strategy. Likewise, if they are playing different strategies and both change strategies, then they are still playing different strategies. This is to say, if both players change strategies, then if the edge between those two players was in Λu then it is also in $\Lambda u'$. Moreover if it was not in Λu, it will not be in $\Lambda u'$. Likewise, if only one of two adjacent players changes its strategy, then if the edge was in Λu, it will not be in $\Lambda u'$, and if it was not in Λu, it will be in $\Lambda u'$.

This means we have captured the difference in the edges contained in $\Psi \circ \Phi u$ and $\Psi \circ \Phi f(u)$. Consider any edge in G^*. It separates two faces f_1 and f_2, which correspond to two players v_1 and v_2 in G. If exactly one of these vertices is not playing a best response, then the edge changes its stats (either it was included in $\Psi \circ \Phi u$ and is no longer included in $\Psi \circ \Phi f(u)$ or it was not included in $\Psi \circ \Phi u$ and is now included in $\Psi \circ \Phi f(u)$). If both or neither of the vertices are playing a best response, the edge does not change its status.

Observe that if a player, v, is not playing a best response in u, then, in the dual, the corresponding face f will have more edges than non-edges in $\Psi \circ \Phi u$. This is exactly the condition from the cycle shortening flow for when C_f is added to the subgraph. Using this logic, and the definition of the Synchronous Cycle Shortening Flow, we can say the following about $\Psi \circ \Phi u$ and $g(\Psi \circ \Phi u)$. Consider an edge in G^* which separates two faces f_1 and f_2. These faces correspond to two adjacent vertices in G, v_1 and v_2. If exactly one of these vertices is not playing a best response then exactly one of C_{f_1} or C_{f_2} is added to $\Psi \circ \Phi u$ and so (by addition in the field $\mathbb{Z}_2$ if the edge was in $\Psi \circ \Phi u$ it is not it $g(\Psi \circ \Phi u)$ and if it was not in $\Psi \circ \Phi u$ then it is in $g(\Psi \circ \Phi u)$. Likewise, if both or neither of v_1 and v_2 are playing a best response in u, then if the edge is in $\Psi \circ \Phi u$, it will remain in $g(\Psi \circ \Phi u)$ and if it was not in $\Psi \circ \Phi u$, then it will not be in $g(\Psi \circ \Phi u)$.

This is a long winded way of saying that, given any $u \in \mathcal{B}_G$, If an edge is in $\Psi \circ \Phi f(u)$, then it will also be in $g(\Psi \circ \Phi u)$, and if an edge is missing from $\Psi \circ \Phi f(u)$, then it will also be absent from $g(\Psi \circ \Phi u)$. This means that these subgraphs are identical and we can conclude, by lemma 3.8 that,

$$f(u) = \Phi^{-1} \circ \Psi^{-1} g(\Psi \circ \Phi u).$$

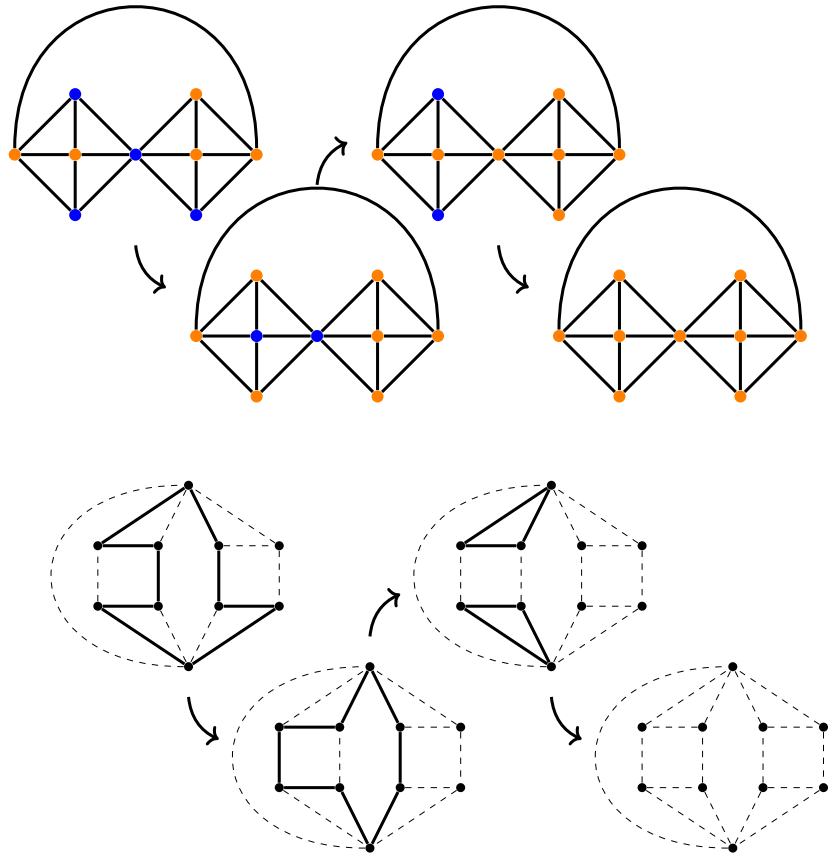

Figure 3.6: Top: A trajectory in the dynamic pure coordination game on the graph G with two strategies that leads to a consensus equilibrium. **Bottom** The corresponding synchronous cycle shortening flow in the dual G^*. The dotted edges are edges of G^* which are not included in the subgraph s_t, and the bold edges are included in s_t.

□

This equivalence is demonstrated in figures 3.6 and 3.7.

This method of understanding the coordination game on planar graphs with simple duals does not give us any improved computational techniques. Indeed, because of the non-uniqueness of the dual graph and issues with identifying faces in the dual, the algorithm for simulating these game dynamics is simpler using the strategic profile method than the subgraph method. However, the subgraph method gives us a much better idea, geometrically, of what equilibria look like and where we can search for them. The concept that Nash equilibria locally minimize the number of edges cut by the partition related to the strategy

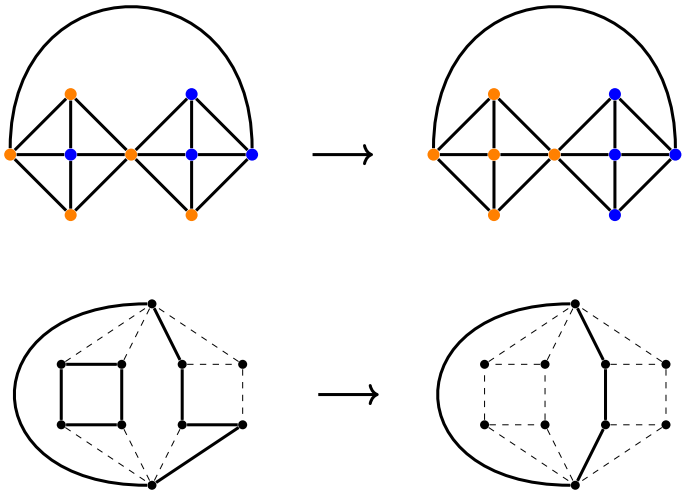

Figure 3.7: Top: A trajectory in the dynamic pure coordination game on the graph G with two strategies that leads to a non-consensus equilibrium. **Bottom** The corresponding synchronous cycle shortening flow in the dual G^*. The dotted edges are edges of G^* which are not included in the subgraph s_t and the bold edges are included in s_t. The Nash equilibrium corresponds to a local size minimizer in the cycle space.

profile by Φ is identical to the idea that the subgraph in the dual sense is locally minimal. The context of locality can be given by incremental rewiring, almost as if two subgraphs can be compared (at least locally) by their displacement across faces. This idea is quite natural to extend into the continuous player space where the player domain is continuous and the boundaries between strategic profiles form a manifold (or complex of manifolds) with codimension 1.

3.3 Continuous Player Spaces

3.3.1 Nonlocal Formulation

In the continuous player space, the game is much the same. The only real differences are to change the set of players to a domain $\Omega \subset \mathbb{R}^n$ and to change the adjacency matrix to an integrable kernel K. Consider the most general setting $K \in C_b^0(\Omega; L^1(\Omega))$, meaning that for every player $x \in \Omega$ there is an L^1 function $(K(x, \cdot) \in L^1(\Omega))$ where $K(x, y)$ describes how

frequently x interacts with y. We think of the strategy profile, $u : \Omega \to \mathbb{R}^m$ as a vector valued function so that $u(x) \in \Delta^{m-1}$ can describe a distribution over all m strategies available. This implies that $u \in L^\infty(\Omega)$. When we are talking about pure strategies, then $u(x) = \hat{e}_i$ for some i (these are the standard basis elements of $\mathbb{R}^m$).

All of this together makes the payoff function

$$w(x|u) = \int_\Omega K(x,y)\langle u(x), u(y)\rangle dy \tag{3.7}$$

and we have an equally sensible potential function

$$\mathcal{W}(u) = \frac{1}{2}\int_\Omega \int_\Omega K(x,y)\langle u(x), u(y)\rangle dxdy \tag{3.8}$$

It will also be helpful to put a name to the nonlocality itself

$$g[u](x) := \int_\Omega K(x,y)u(y)dy \tag{3.9}$$

so $w(x|u) = \langle u(x), g[u](x)\rangle$. Notice that, because of the assumption that K is continuous with respect to L^1 in the first argument, $g[u]$ is continuous whenever $u \in L^\infty(\Omega)$.

It is obvious that the image of a pure strategy profile will be discrete. We will now consider, as in the continuous setting, the strategic communities, which are the preimages $U^i = u^{-1}(\hat{e}^i)$ which partition Ω. It is equivalent to formulating problem by saying that $U_i \subset \Omega$ is the group of players playing strategy i in which case, if x plays strategy i

$$w(x|u) = \int_\Omega K(x,y)\chi_{U^i}(y)dy \tag{3.10}$$

and the potential function is written as

$$\mathcal{W}(u) = \frac{1}{2}\int_{\Omega\times\Omega} K(x,y)dxdy - \frac{1}{2}\sum_{i,j\in C}\int_{\Omega\times\Omega} K(x,y)\chi_{U^i}(x)\chi_{U^j}(y)dydx \tag{3.11}$$

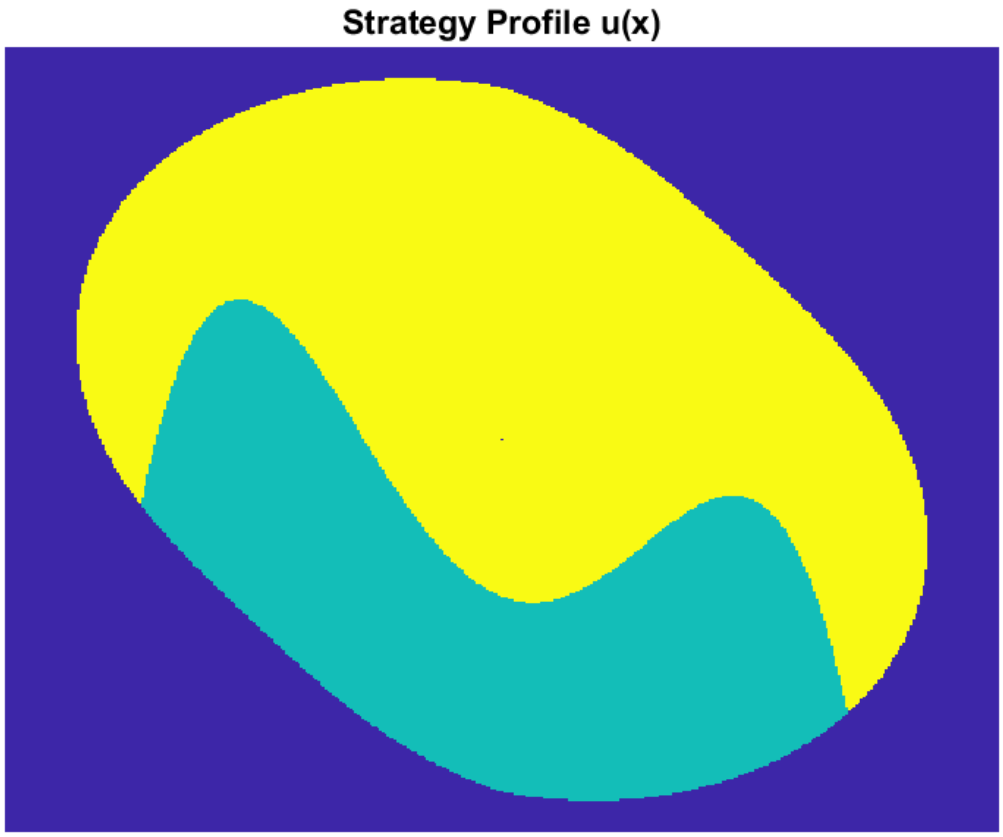

Figure 3.8: A strategy profile in a convex domain. The cyan region is playing strategy 1 and the yellow region is playing strategy 2. The dark blue is not in the player domain Ω.

As an example. Consider the strategy profile, u, described in figure 3.8. In this strategy profile the yellow region and the cyan region are strategic communities which share a strategic boundary. We can compute the payoff for each player if they played strategy 1 or 2 against the strategy profile u by taking the convolution $K * u^i(x) = K \star \chi_{U^i}(x)$ for $i = 1, 2$. These payoff functions are shown in figure 3.9

From the payoffs calculated here, we can compute easily the best response for each player. For the two strategy case, If $x \in \{z \in \Omega; g^1[u](z) - g^2[u](z) > 0\}$ then $BR_x(u) = \{1\}$. Likewise if $x \in \{z \in \Omega; g^1[u](z) - g^2[u](z) < 0\}$ then $BR_x(u) = \{2\}$. Wherever these two regions share a boundary point, the fitnesses are equal. Although the pairwise comparisons grow exponentially, the process for computing best responses is the same even in the case where there are more than 2 strategies. From this we have a way of determining what the strategy profile will look like if every player takes on a best response and we can identify the

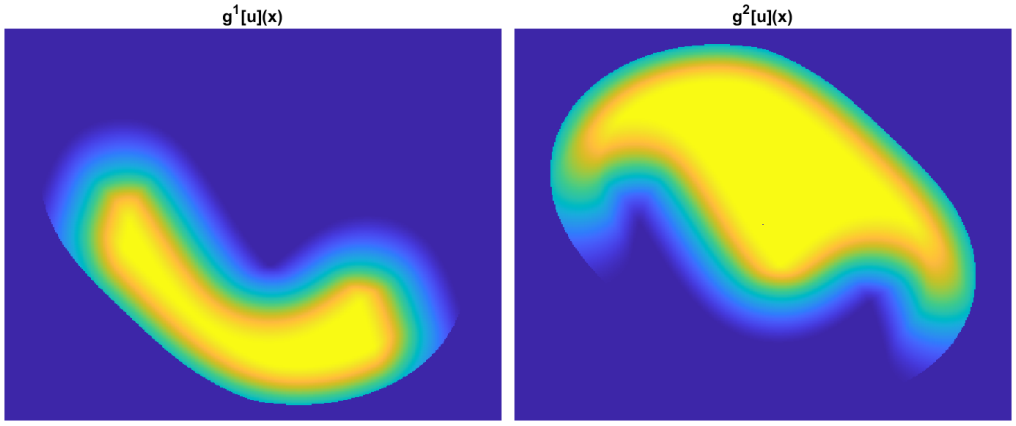

Figure 3.9: Left the payoff of each player in the domain from playing strategy 1 against the strategy profile u. **Right** the payoff of each player in the domain from playing strategy 2 against the strategy profile u. In both figures, the lighter color indicates the higher payoff.

boundaries of the updated strategic communities as the level set where $g^1[u](z) - g^2[u](z) = 0$ (Fig 3.10).

By doing this we can see that the boundary evolves in a familiar way under Myopic Best response. The boundary curve, at least from the example presented seems to move according to the free boundary curve shortening flow or mean curvature flow (which are equivalent in this setting. This is not surprising because the setup is identical to the nonlocal mean curvature formulation of Caffarelli et al. (2010).

Caffarelli, Roquejoffre, and Savin describe a non-local minimal surfaces in two ways. First the describe a time stepping non-local mean curvature flow which we will show to be equivalent to MBR in certain circumstances, then they show that non-local minimal surfaces minimize an energy which we will show is equivalent to maximizing game potential in certain settings. These similarities are remarkable because the dynamic process described here arise from game theoretic first principles alone. We will start by discussing the equilibrium (minimal surface) case.

3.3.2 Equilibrium Results

Caffarelli et al. (2010) examine nonlocal minimal surfaces with the kernel K being of the form $|y - x|^{-n-2\sigma}$ and show that these nonlocal minimal surfaces are the boundaries of sets

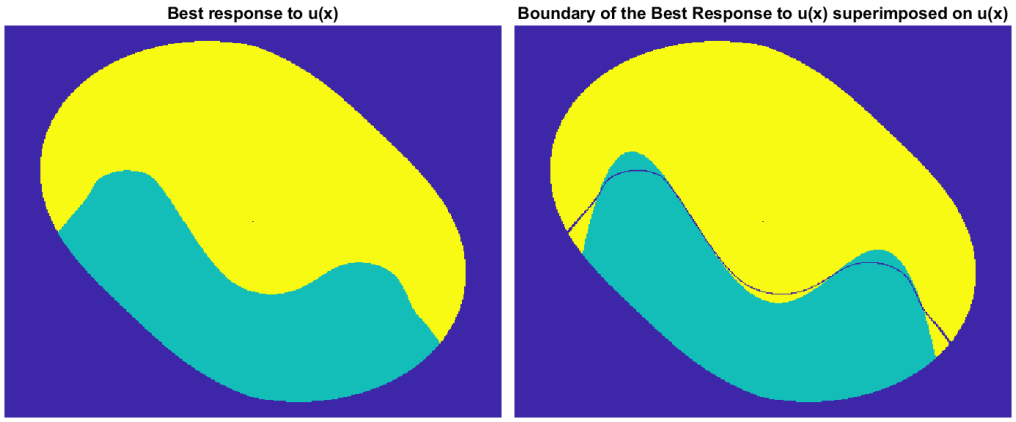

Figure 3.10: Left The strategy profile after every player changes strategy to take on their best response to the strategy profile u. **Right** the boundary of the updated strategy profile superimposed on the original strategy profile.

which minimize the energy

$$L(E, E^c) = \int_\Omega \int_\Omega K(x,y)\chi_E(x)\chi_{E^c}(y)dxdy$$

Although, their description of how such surfaces may interact with boundary data is more involved, in the "free boundary" case where there is no data outside of Ω it is easy to see that a minimizer of $L(U^1, (U^1)^c)$ would be a maximizer of (3.11) and thus (3.8). Thus we can take this result to mean that if there are only two strategies present and if the kernel is formed correctly, Nash equilibria are nonlocal minimal surfaces without boundary data. For a more detailed interpretation of what this results mean for the characteristics of nonlocal minimal surfaces from a differential geometric perspective, see Caffarelli and Souganidis (2008) or Savin (2025). Instead, I will present some results characterizing Nash equilibria in more generality from game theoretic first principles

Consider u a pure strategy profile that is a Nash equilibrium. Every player is playing a best response. If u is not constant on all of Ω, we must first characterize the behavior of the players on the boundary of a strategic community.

Lemma 3.9 (Players on the boundary of a strategic community)**.** *Let u be a Nash equilibrium strategy profile with multiple strategic communities. If there is an $x \in \partial C_i \cap \partial C_j$ then $g[u]^i(x) = g[u]^j(x)$.*

In words, this means that players on the boundary of multiple strategic communities get an equal payoff for playing each strategy of the communities to which they are associated. This means that players here can use any mixture of these strategies at Nash equilibrium.

Proof. Consider u with strategic communities C_1 and C_2 which share a boundary point x. Because u is assumed to be a Nash equilibrium, strategy 1 is a best response for every player in C_1 and strategy 2 is a best response for every player in C_2.

About the boundary point x any open ball $B_\eta(x)$ intersects with both C_1 and C_2. Suppose, by way of contradiction and without loss of generality $g^1[u](x) > g^2[u](x)$. $g[u]$ is continuous because of the continuity of $K(x, \cdot)$ in the L^1 sense. Thus $f(y) := g[u]^1(y) - g[u]^2(y)$ is also continuous. Because of the continuity, not only is $f(x) > 0$ but also there is an open ball around x such that $f(y) > 0$ for all $y \in B_\delta(x)$ for some $\delta > 0$. This open region must intersect C_2 which means that players in C_2 are playing strategy 2 even though strategy 1 would give a higher payoff. This means that u is not a Nash equilibrium.

Thus, for every boundary point of both C^1 and C^2, if u is a Nash equilibrium then $g^1[u](x) = g^2[u](x)$. □

Although $g[u]^i$ is always continuous regardless of the continuity of u, it can be difficult to imagine the strategic communities without some assumptions about the regularity of the strategic communities. As before, our discussion will be limited to domains of two dimensions. A strategy profile u partitions the domain Ω into strategic communities. For our purposes, we will assume that the strategic comminutes are uniformly weakly locally connected (uniformly connected im kleinen). This is sufficient to say that the boundary of each strategic community is a simple closed curve (Jordan curve) by a result from Moore (1918). This means, again, we will reduce our discussion to thinking of the boundaries of the strategic communities. This will be the union of simple closed curves. For a strategy profile u, we will call the complex of boundaries of strategy profiles s_u.

From this description, we can say that s_u is the union of finitely many continuous curves c^i and finitely many points p^i where at least two continuous curves meet. We will call these points junctions. For every curve one of the following is true: it is closed, both ends meet at a single junction, both ends hit the boundary of Ω, the ends meet two distinct junctions, or one end meets a junction and the other meets the boundary of Ω.

To get any results, we must assume that the support of the kernel K is very small. We will assume that $supp(K(x,\cdot)) \subset B_\epsilon(x)$ for all x for some $0 < \epsilon << 1$. We will also assume that for each curve in s_u, every point that is ϵ away from a junction is at least ϵ away from any other curve.

Lemma 3.10. *For a continuous domain with sufficiently smooth boundary and for players with a symmetric kernel and a sufficiently small detection radii, ϵ, if u is a Nash equilibrium, then, in s_u, any curve c^i with endpoints a and b lies is the strip centered on the line connecting a and b with width ϵ.*

Proof. Suppose that in s_u c^i connects two endpoint a and b. The two endpoints may be both junctions, both points on the boundary of Ω, or one of each. Let L be the line connecting a and b, and suppose c^i is not on L. Consider the point on c^i which has the furthest orthogonal distance from L, call that point p. If we imagine c^i on the x, y plane so that L is the x axis and, WLOG, a is the origin, c^i may not be a function, but the point p can be labeled as (x_p, y_p).

First, suppose that p is at least ϵ away from both a and b. Because p is on the boundary, that means the player p has equal payoff from playing either strategy separated by c^i. This means that c^i must bisect $B_\epsilon(p)$. Because p is assumed to have the greatest orthogonal distance from L, we know that c^i lies below or at the line $y = y_p$. Notice that the line $y = y_p$ bisects $B_\epsilon(p)$ and so if c^i lies below it at any point in $B_\epsilon(p)$ then c^i does not bisect $B_\epsilon(p)$. Therefore the curve c^i must be parallel to L on the interval $(x_p - \epsilon, x_p + \epsilon)$. We can repeat this argument at each endpoint of each interval until we reach a point that is within ϵ of a or b.

This means that c^i must reach its maximum orthogonal displacement away from L in the ϵ neighborhood of a or b. This implies that the curve c^i lies between the lines $y = \epsilon$ and $y = -\epsilon$. □

Corollary 3.3. *The curve c^i with endpoints a and b is in the rectangle formed by taking the strip from lemma 3.10 and keeping the connected interval between $x = a - \epsilon$ and $x = b + \epsilon$.*

Proof. Label every point of c^i with coordinates by the coordinate system described in the proof of lemma 3.10. If c_i has a point p which has $x_p < a - \epsilon$, then there must be a point q which has the smallest (most negative) x-coordinate. Because this point is on the boundary, the player q has an equal payoff from each of the strategies separated by c^i, so the line c^i must bisect $B_\epsilon(q)$. Because q has the minimum $x-$ coordinate the curve c_i cannot extend beyond the line $x = x_q$. By the same argument as before, the line c_i must be exactly the line $x = x_q$ while it intersects $B_\epsilon(q)$. This implies that either c^i escapes the strip from lemma 3.10 or that it reaches from the bottom of the strip to the top of the strip exactly, and so could repeat the same argument at $x_q, y_q + \frac{1}{2}\epsilon$ and get c^i to escape the strip. This contradiction shows that such a point is impossible. □

Corollary 3.4. *If u is a Nash equilibrium, and c^i is a curve in s_u, c^i cannot be a closed, isolated curve.*

Proof. By the same argument as in lemma 3.10, suppose there is a closed, isolated curve c^i in s_u and select any point $p \in c^i$. For any line Lthrough the point p, there is a point on the curve, q, which maximizes the orthogonal distance to the line L. Again, we can say that the diameter of $B_\epsilon(q)$, which is parallel to L, divides the sensing area of q in half and, because q is playing a best response, c^i must coincide with this diameter. Because the point on this diameter $\frac{\epsilon}{2}$ distance from q has the same property of maximizing the orthogonal distance for L, the process can be repeated in steps of $\frac{\epsilon}{2}$ indefinitely. Our assumptions provide us with the fact that these curves are rectifiable, and so we have reached a contradiction. □

From this result, we get the impression that as $\epsilon \to 0$ the curves in s_u approach straight lines between their endpoints, which gives us some heuristic connection between this game

and the curve shortening flow or the network flow. We cannot, at present, describe the relationship between minimal networks and these strategic boundary complexes rigorously, but we can provide a heuristic similar to that of the discrete case

Just as in the discrete game, any Nash equilibrium is a local maximizer of the potential function. We can rewrite the potential function here to be

$$\begin{aligned}\mathcal{W}(u) &= \int_\Omega \int_\Omega K(x,y)dxdy - \int_{N_\epsilon s_u} \int_{B_\epsilon(x)} K(x,y)(1-\langle u(x), u(y)\rangle)dydx \\ &= \int_\Omega \int_\Omega K(x,y)dxdy - \sum_{i,j\in C} \int_\Omega \int_\Omega K(x,y)\chi_{U^i}(x)\chi_{U^j}(y)dydx\end{aligned} \tag{3.12}$$

The minimization of the sum (and thus the maximization of the game potential) is not a straightforward extension of the minimization done by Caffarelli et al. (2010), but the form of this optimization problem point to a connection between the general many-strategy setting and a non-local minimal network analogous to the local minimal networks of Ilmanen et al. (2018).

This is far from rigorous but points to a connection between minimal surfaces with free boundaries in Ω and Nash equilibria of the pure coordination games in this setting. To strengthen this connection, we will examine numerical simulations of the game dynamics and show that these dynamics match the curve shortening flow or network flow very closely as $\epsilon \to 0$.

3.3.3 Dynamics in the Continuous Case

Just as in chapter 2, we will simulate a myopic best response dynamic coordination game where individuals are modeled as points in a mesh grid and their fitness is determined by (3.7) with $K(x,\cdot) = \chi_{B_\epsilon(x)}$. This simplistic model can demonstrate a rich set of dynamics. In the simulation (McAlister, 2026a), we model a continuous domain with a dense mesh grid and give every point in the grid a strategy. We then compute $g[u]^i(x)$ for each player x and strategy i and update each player's strategy so that they take on the best response. When there are only two strategies and u_s is a single curve, we see a striking resemblance to the

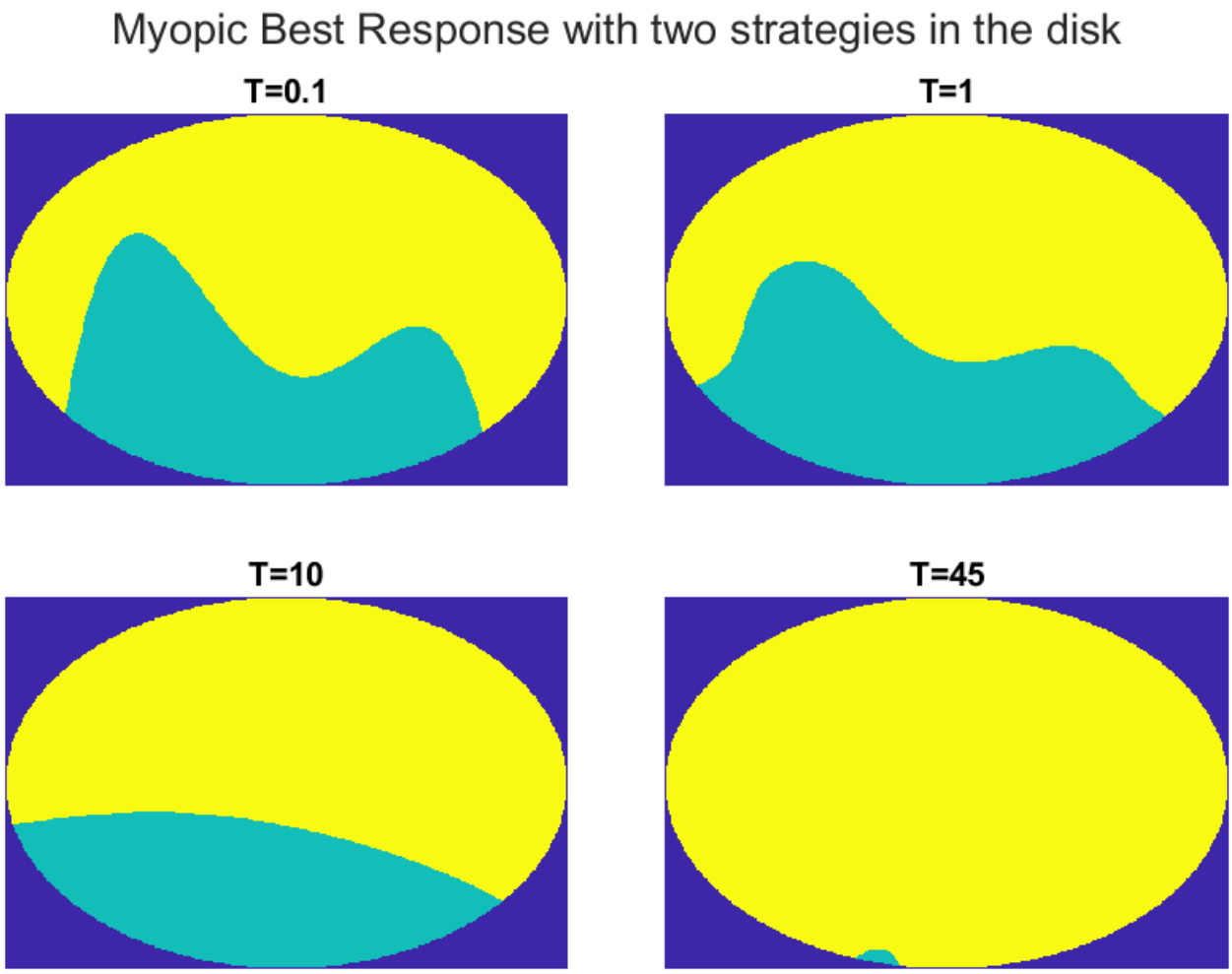

Figure 3.11: The myopic best response dynamics with two strategies in the disk. The boundary between the two strategic communities flows in a way that resembles the free boundary curve shortening flow.

free boundary curve shortening flow (Gage and Hamilton, 1986) (Fig. 3.11. The similarity between these two flows is not discussed rigorously here but the discussion of the conjecture in section 6.3 offers a game theoretic view of the a possible generalization of the results of Caffarelli and Souganidis (2008).

The myopic best response process in the setting with only two strategies can be described by a discrete evolution equation. For any strategy profile u which can be decomposed into

U^1 and U^2, let $g^1[u(t)] = K * \chi_{U^1}(x)$ and $[g^2(t)] = K * \chi_{U^2}(x)$. After a single update,

$$u(x, t + \Delta t) = \begin{cases} [1, 0] & g^1[u](x,t) > g^2[u](x,t) \\ [0, 1] & g^1[u](x,t) < g^2[u](x,t) \\ u(x,t) & g^1[u](x,t) = g^2[u](x,t) \end{cases}$$

It is easy to see that this is equivalent to the process described by Caffarelli and Souganidis (2008) for front propagation which they show recapitulates the mean curvature flow in certain settings. Before this nonlocal approach, Bence et al. (1992) had shown that, in a time stepping manner, if the characteristic functions for each set (strategic community) are allowed to diffuse for some time Δt then the maxima taken as in the computation for $BR_x(u)$, the motion of the boundaries can be described as mean curvature flow in the limit as $\Delta t \to 0$. According to Caffarelli and Souganidis (2008), it is a classical result that, if the kernel K is a rescaling of a Gaussian kernel $K(x - y) = (4\pi\epsilon)^{-n/2} e^{-|x-y|^2/-4\epsilon}$ (and thus the convolution with K is the semi-group operator for the heat equation) then if $\Delta t = \epsilon^2$, the time stepping process converges to the mean curvature flow in a variational sense.

Theorem 3.6 (Myopic Best Response Recapitulates the Mean Curvature Flow)**.** *Consider an initial strategy profile $u_0 : \mathbb{R}^n \to C$ is given as $U_0^2 = (U_0^1)^c$ so that $\partial U_0^1 = \partial U_0^2$. Let payoffs be given by equation (3.10) with the kernel $K_\epsilon(x, y) = (4\pi\epsilon)^{\frac{-n}{2}} e^{\frac{-|x-y|^2}{4\epsilon}}$. Under the myopic best response process with time step $\Delta t = \epsilon^2$, the strategic boundary ∂U^1 will move according to mean curvature flow in the limit as $\epsilon \to 0$*

Proof Sketch The MBR process is described first by convoluting $K * \chi_{U^1}(x)$ and $K * \chi_{U^2}(x)$. Because of the way K is defined, this convolution is the same as finding a solution $v_i(\cdot, \epsilon)$, where v_i solves $\frac{\partial}{\partial t} v_i - \Delta v_i = 0$ with $v_i(\cdot, 0) = \chi_{U^i}$. Having computed the payoffs in this way, which is equivalent to the semi-group approach of Bence et al. (1992), we compute the next strategy profile using the sub and super level sets of these convolutions. If we describe the new group of players playing strategy 1 after a single time step as $U^1_{\Delta t}$, we know that the

interior of this set is the super level set

$$U^1_{\Delta t} = \{x \in \mathbb{R}^n; K * \chi_{U^1}(x) - K * \chi_{U^1}(x) > 0\}$$

Likewise, the interior of $U^2_{\Delta t}$ is the corresponding sub level set. If there is a unique solution to the mean curvature flow for the initial surface ∂U^1_0 then the level set itself will have an empty interior by a result from Barles et al. (1993). It is very simple to use the linearity of the convolution to find that these sub and super level sets are

$$\begin{aligned} U^1_{(n+1)\Delta t} &= \{x \in \mathbb{R}^n; K * (\chi_{U^1_{n\Delta t}} - \chi_{U^2_{n\Delta t}})(x) > 0\} \\ U^2_{(n+1)\Delta t} &= \{x \in \mathbb{R}^n; K * (\chi_{U^1_{n\Delta t}} - \chi_{U^2_{n\Delta t}})(x) < 0\} = (U^1_{(n+1)\Delta t})^c \end{aligned}$$

This process is identical to the process described by Bence et al. (1992) and the convergence was proven rigorously in a series of papers by Evans and Spruck (1991, 1992a,b, 1995). This proof is similar to that of Caffarelli and Souganidis (2008) and thus we see that MBR recapitulates the mean curvature flow is this setting. □

This equivalence is exciting, not only because the MBR process recapitulates the curve shortening or mean curvature flow entirely from game theoretic first principles, it also means that studying the dynamics of the game in the continuous setting is made easier by the wealth of information available about the free boundary curve shortening flow. Moreover, our simulations show that the similarities between the mean curvature flow and MBR go beyond the narrow setting described in theorem 3.6. We do not dare to make a rigorous claim about the behavior of the strategic boundaries as they interact with domain boundaries, but we can observe through simulation that the MBR dynamics demonstrate a free boundary condition where strategic boundaries meet domain boundaries orthogonally for all positive time. Additionally, this method works for many strategies and can accommodate junctions of strategic boundaries which we do not describe rigorously here. The larger conjecture is that MBR recapitulates the free boundary network flow in the limit described above, and it can do so for any symmetric kernel, not only the gaussian of theorem 3.6.

In absence of a proof for this conjecture, I will give some general support by presenting several examples and numerical simulations which reproduce geometric analytical results about the free boundary curve shortening flow or network flow, entirely from a game theoretic perspective. More numerical support for the conjecture can be found in section 6.3.

Work of Bourni and Langford (2023) note that the stationary solutions of the free boundary curve shortening flow in a convex domain are diameters. For the circle, we can show analytically that for any ϵ, a strategy profile with s_u a diameter of the circle is a Nash equilibrium.

Example 3.2. *Consider a strategy profile u where s_u is a diameter of the circle Ω. Let $p \notin s_u$ and ϵ away from the boundary and observe that $d(p, s_u) > \delta$ for some positive δ. Without loss of generality, orient the diameter so that it is the x axis of the plane and assume p is above the x-axis. Consider the circle of radius ϵ around p. The top half of the circle does not intersect s_u or the boundary, so at least half of $B_\epsilon(p)$ is using the same strategy as p. This means, if the kernel is symmetric, that p is playing a best response.*

If $p \in s_u$, then the diameter must bisect $B_\epsilon(p)$, so it is playing a best response as well.

Lastly, we consider p close to the boundary. To see this, consider the circle $\partial B_\epsilon(p)$ which intersects $\partial\Omega$ and reorient Ω so that both the centers of both circles are on the x axis. The diameter meets the edge of Ω below the x axis and extends towards the center of Ω. With the assumption that the radius of the domain is much larger than the sensing radius ϵ, the diameter is below the x-axis in all of $B_\epsilon(p)$. This makes it clear that more of $B_\epsilon(p)$ is above the diameter than below the diameter, so p is playing a best response. From this, we have shown that every player is playing a best response (Fig. 3.12) and so certainly u is a Nash equilibrium.

For non-diameters, we can observe that, as long as they have not been designed to converge to a diameter under the myopic best response, the curve s_u will annihilate itself in finite time, as is expected in the curve shortening flow.

Although we cannot show the same thing for general convex domains analytically, we can observe through simulation that if s_u is a straight line that intersects the boundaries of

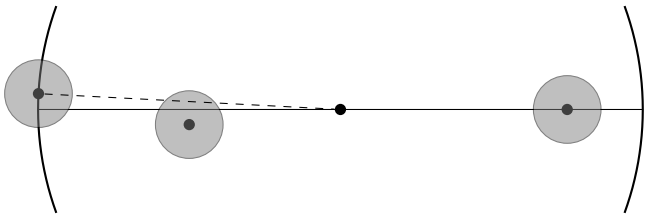

Figure 3.12: Three different players playing the continuous player space pure coordination game. The diameter is the boundary between two strategic communities. Any player on the boundary (left) is playing a best response. Any player on the diameter (right) is playing a best response because both strategies are best responses. Any player of the diameter (center) is playing a best response, and so the strategy profile is a Nash equilibrium.

the domain orthogonally, then it persists, otherwise the curve will annihilate itself as one strategy becomes semicircular against the boundary of the domain, shrinking in size until it is gone in finite time. This reflects the exact results of Bourni et al. (2025)

When there are many strategies, the dynamics are more complicated, just as they are with the varifold generalization of curve shortening or mean curvature flow (Brakke, 1978; Angenent, 1990, 1991) or the more restrictive network flow (Ilmanen et al., 2018). Nevertheless, through simulation we find striking results of strategy profiles evolving under myopic best response so that s_u evolves in accordance with the free boundary network flow (Figs. 3.14 and 3.15). Of course, in both of these figures, we see that there are differences in the flows. Namely, when two boundaries come within ϵ of one another, the two boundaries may meet and annihilate one another. This behavior is described by the MBR process, but it is not a feature of the Network flow. However, as $\epsilon \to 0$, this behavior does not occur.

In nonconvex domains, where non-consensus equilibria are more plentiful, we can even observe that stationary solutions have triple points where evenly rotationally spaced curves meet, as in Ilmanen et al. (2018). These simulation results lead us to the conjecture that as the sensing radius goes to zero, even when the kernel $\chi_{B_\epsilon(x)}(y)$, when the time step is scaled by ϵ^2 (the area being sensed), then the myopic best response process converges to the curve shortening or network flow. More detail about the conjecture and some numerical support for the idea can be found in chapter 6.3.

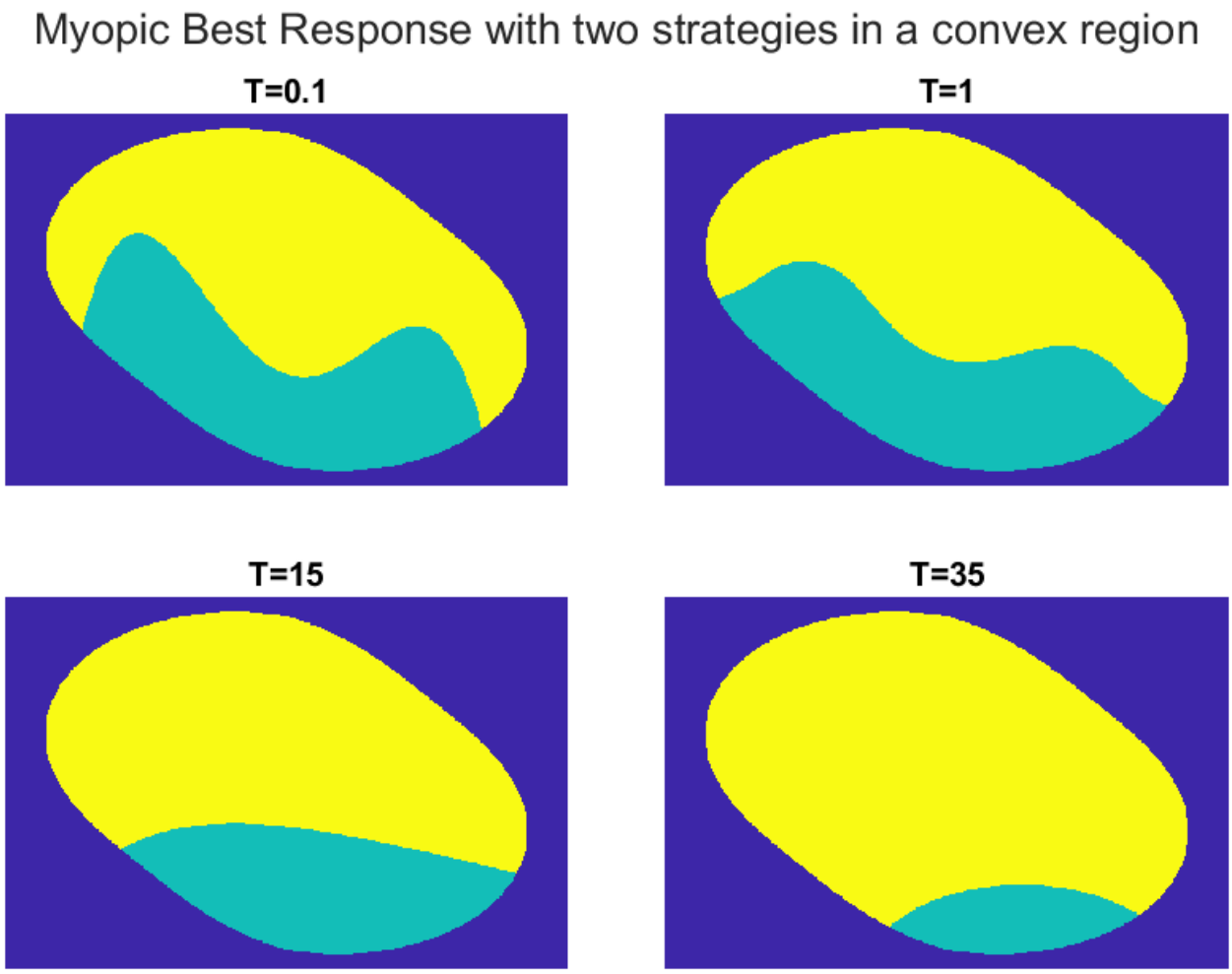

Figure 3.13: Myopic best response in a convex region with two strategies and a small sensing radius. With a sufficiently small sensing radius, the boundary curve between the strategic communities evolves in a way similar to the free boundary curve shortening flow.

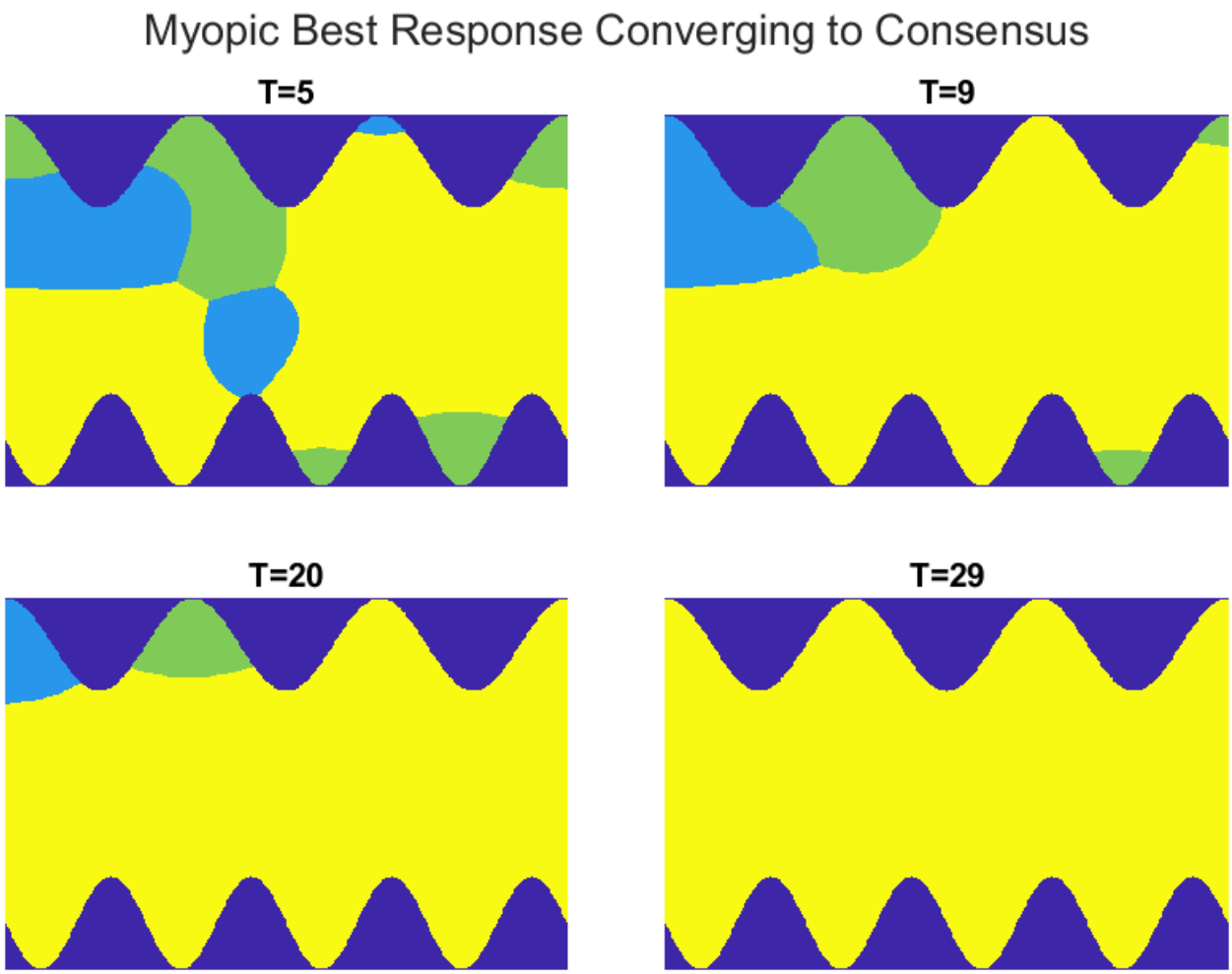

Figure 3.14: Under the myopic best response dynamics with a small sensing radius, the boundaries of the strategic communities flow in a manner similar to the free boundary network flow. Boundaries straighten, and sections of the boundary die at round points if the free boundary allows. Here, the boundaries find a path to the global minimal network (the empty network), and so the game reaches the consensus equilibrium.

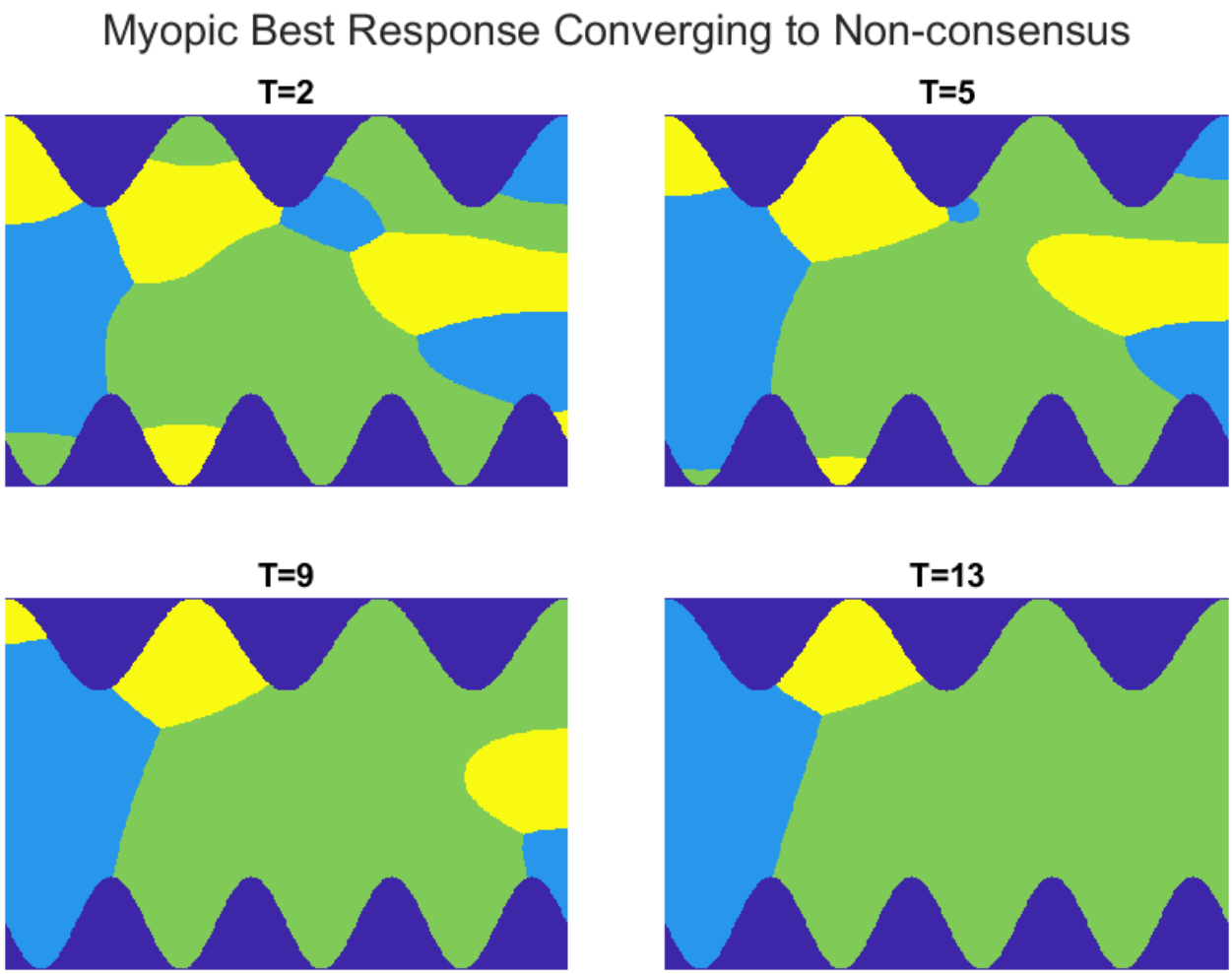

Figure 3.15: Under the myopic best response dynamics with a small sensing radius, the boundaries of the strategic communities flow in a manner similar to the free boundary network flow. Boundaries straighten, and sections of the boundary die at round points if the free boundary allows. Here, the boundaries find a locally minimal network which is not globally minimal, and so there is a non-consensus equilibrium.

The assumptions about the regularity of the boundary complex were necessary to describe the boundaries at equilibrium and observe how they move under MBR but they were not necessary to define the myopic best response. It is of note that the MBR process is smoothening. Because $g^i[u](x)$ is uniformly continuous even for pathological strategy profiles u, the level sets can be studied more easily. Although it is not the purpose of the present chapter, we propose that, even if a strategy profile u is too pathological to apply any of the corollaries presented here, it may be possible to apply the corollaries after a single step of MBR.

3.4 Discussion

Thinking of the pure coordination game on planar graphs through the dual does not give us any better computational power, but it does give us a much better geometric intuition for the structures that admit non-consensus equilibria. By proving that there is a quasiisometry between the strategy space $\mathcal{A}$ and the space of bridge-free subgraphs in the dual, $\mathcal{SC}_{G^*}$, we have demonstrated that a locally minimal subgraph always corresponds to a Nash equilibrium in the original graph.

This correspondence helps us understand several things about the pure coordination game. First, it makes the connection between the pure coordination game and the mincut partition quite obvious. Although this connection can be made without the use of the dual, the dual approach allows us to see that equilibrium partitions are to mincut partitions as local optima are to global optima. Excepting the degenerate case in which a part of a mincut partition has a single vertex, this makes the set containment immediate.

The correspondence also helps us imagine the kinds of planar graphs which admit non-consensus equilibria. If, in the dual, every cycle has at least one face, f, in which the majority of the edges of f are included in the cycle, then the graph G is not decomposable into two parts. This heuristic is easier for us to imagine than for computers to solve because it involves identifying minimal cycles with a locality which feels quite natural to us be is not clear algorithmically.

Although this method does not improve our ability to understand the discrete game algorithmically, it does make the connection to the continuous space game quite clear. When players are points in a continuum, and each player can sense some of the players around them, in the limit where the sensing radius goes to zero, we can observe a great many similarities to the curve shortening flow and to the network flow.

This correspondence is even more powerful than that of the discrete time system because the stationary solutions to these types of flows have been studied for years. In this setting, there is no continuous domain that is indecomposable. We can use stability results about the curve shortening flow as in Bourni and Franz (2026) to get a better picture of how resistant to perturbation certain Nash equilibria are. More clearly, we can say that non-convex domains have non-consensus equilibria, which we can construct by spanning the domain with a straight line from one part of the boundary to another.

Because the focus of this chapter is the dynamic game theory and not the network flow, I do not go into enough detail here to describe exactly the types of domains that are "stably" decomposable or even what it means to be a stable decomposition, but the intuition that the connection between these two seemingly unrelated flows provides is invaluable.

Being able to imagine the strategy space with a certain metric and being able to describe the dynamic game as flows through the strategy space makes it possible to draw equivalences between the game dynamics and other better understood flows, or at least other flows which are easier to define. These connections help us get a better intuitive understanding of the game dynamics and, in some cases, can show us where non-consensus equilibria can emerge.

Chapter 4

Structured Coordination through Replicator Dynamics

4.1 Introduction

When discussing coordination, or indeed any normal form game, in a dynamic sense, one of the challenges that we face is the issue with the best response function. For a player v and a strategy profile u, the best response function $BR_v(u)$ is set valued and highly discontinuous. For this reason, true best response dynamics can be difficult to describe using standard tools in dynamical systems without adding some constraints on available strategies or imposing a tie breaking rule. This is especially important when we consider pure coordination, in which all the strategies are equivalent because a tie breaking rule will corrupt the results. These challenges have been approached in different methods in recent years by Swenson et al. (2018a,b) with convergence results for best response flows in potential games and by So and Ma (2025), who used an incremental smoothing approach to achieve convergence results.

Because the best response dynamic, without modification, represents a difficult road block to overcome in the pursuit of understanding coordination behavior in structured settings and for more general applications, we take an approach that does not rely on the best response

dynamic but rather considers how replicator dynamics from evolutionary game theory may be of use.

$$\frac{d}{dt}p_i = p_i(f_i(p) - \varphi(p)) \tag{4.1}$$

The replicator equation (4.1), is a system of ODEs which describe a large well mixed population of individuals playing a game with normal form game with pure strategies Taylor and Jonker (1978). p_i is the proportion of the population playing strategy i and p is the strategy profile of the population. This model is built on the assumption of "pairwise proportional imitation," where the growth of p_i is proportional to p_i and to the fitness difference between playing strategy i among the current population ($f_i(p)$) and the average fitness of an individual in the population ($\varphi(p)$). This model has been used extensively to model well mixed populations (Bomze, 1983, 1995; Nowak, 2006). Here, I propose the use of this standard tool in a novel setting.

If we sought to use the replicator equation in a game with a structured player space, (i.e. players are vertices in a graph), we would violate the well mixed assumption and the large population assumption. This has been overcome in different ways in Ohtsuki and Nowak (2006); Lieberman et al. (2005), but these approaches still capture population averages rather than local information. Another approach by Coletti and de Lima (2025) uses competitive exclusion in geometric graphs to consider coexistence in a similar way, but is limited to only two strategies. However, by using mixed strategies and thinking of each player and mixed strategy as a patch of many players who are well mixed playing pure strategies, we can use this well established tool in a new setting. The result, for an n player game with m strategies, is an $n \times m$ system of ODEs, which allows us to use more powerful analytical tools to study dynamic games on networks.

The ultimate goal of this work is to take the tools that are available in the well behaved case of the replicator equation so that we can interrogate questions about structured normal form games in ways that may be impossible with best response dynamics alone. Because well understood notions of stability exist for simple ODE systems, whereas stability is harder

to describe in a best response system, we use the analytical tools from ODEs to partially classify Nash equilibria into stable and unstable. Moreover, because an ODE system has nice continuity with respect to parameters, this model gives us a continuous relationship between structure and behavior, at least for short times. The study of structured coordination aims to find a way to take the structure of a network and determine the types of Nash equilibria that network admits. Although this model does not provide a tool for that purpose, it does provide an easier way of conceptualizing the relationship between structure and game theoretic outcomes.

In section 4.2 we introduce the model formally for linear matrix form games. In section 4.3 we show that the model is mathematically well posed and that the results of the model stay meaningful for all time. In section 4.4, we show that the model satisfies the Folk Theorem of Evolutionary Game Theory and that, for coordination in particular, we can relate certain qualities of Nash equilibria to certain behaviors of the model. Although this model does little to directly address the question of how the relational structure determines game theoretic outcome on its own, in section 4.5 we show that it supports pervious conjectures about coordination in the continuous time setting, it can help identify critical structures in a graph that are stabilizing or destabilizing for particular games, and that it can be used for extensions into continuous player spaces. We do not accomplish it fully in this manuscript, but a robust theory of structured replicator dynamics brings us closer to understanding the relationship between relational structure and game theoretic outcomes.

4.2 Extensions of the Replicator Equation

Consider a linear multiplayer normal form game with payoff matrix A, and consider the players to be vertices on the graph $G(V, E)$ which has adjacency matrix W. Each player uses a mixture of m strategies, and so a strategy profile may look like $u : V \to \Delta^{m-1}$or we may also think of u as a collection of vectors $[u_1, u_2, ..., u_n]$. Later, to make computations more clear, we will use the convention that u_v is a column vector describing the strategy of player v and u is also a column vector as $u = [u_1^\intercal, u_2^\intercal, ..., u_n^\intercal]^\intercal$. In this case we will say

that $u \in (\Delta^{m-1})^V$ which is simply the cartesian product of $|V|$ simplices (importantly not a $|V| \cdot (m-1)$ dimensional simplex).

When two players v, w interact the fitness for player v is given as $\langle u_v, Au_w \rangle$, and so when we sum across all the vertices in the neighborhood of v, v's total fitness is given by $\langle u_v, \sum_{w \in V} W_{v,w} A u_w \rangle$ This linear combination of column vectors in the second argument of the inner product is used frequently, so we give it the shorthand

$$g_v = \sum_{w \in V} W_{v,w} A u_w. \tag{4.2}$$

Thus, the fitness of player v given the strategy profile u is

$$w_v(u_v|u) = \langle u_v, g_v \rangle. \tag{4.3}$$

In the strategy profile, u, the fitness benefit of changing to the pure strategy i is given as $w_v(\hat{e}^i|u) - w_v(u_v|u) = \langle \hat{e}^i - u_v, g_v \rangle$. From here, we can describe the full game dynamics by saying that a player v's use of the pure strategy i changes in proportion to their current familiarity with the strategy and in proportion to the fitness benefit of changing to take on that pure strategy. This is equivalent to the patch model conceptualization discussed in the introduction.

$$\frac{d}{dt} u_v^i = u_v^i \langle \hat{e}^i - u_v, g_v \rangle \tag{4.4}$$

Something crucial to mention is that in both the structured and unstructured cases, the system depends on *relative* payoffs and not absolute payoffs. For this reason, any payoff matrix A can be shifted so that all of the entries are non-negative without changing the dynamics of the game in any way.

Lemma 4.1. *The dynamics of a solution to equation (4.4) with payoff matrix A are identical to the dynamics of a solution to the same equation with payoff matrix $A + B$ where B is some constant matrix.*

Proof. The proof is a quick computation

$$\begin{aligned}\frac{d}{dt}u_v^i &= u_v^i\langle \hat{e}^i - u_v, (A+B)\sum_{w\in V} W_{v,w}u_w\rangle \\ &= u_v^i\langle \hat{e}^i - u_v, A\sum_{w\in V} W_{v,w}u_w\rangle + \langle \hat{e}^i - u_v, B\sum_{w\in V} W_{v,w}u_w\rangle\end{aligned} \tag{4.5}$$

If B is the constant matrix with entries b then $B\sum_{w\in V} W_{v,w}u_w$ is a constant vector with entries $b\sum_{i\in C}\sum_{w\in V} W_{v,w}u_w^i = b\sum_{w\in V} W_{v,w}$. Note that both $\hat{e}^i$ and u_v have entries that sum to 1 and so $\langle \hat{e}^i B\sum_{w\in V} W_{v,w}u_w\rangle = \langle u_v B\sum_{w\in V} W_{v,w}u_w\rangle = b\sum_{w\in V} W_{v,w}$. The result, therefore, is obvious. □

The model we have produced is a mild modification of the replicator equation for structured games without the assumptions of well mixed infinite populations, using a mixed strategy approach. The question that remains is whether this is meaningful and whether it is useful. In the following sections, I will address these questions in order. We will use lemma 4.1 and suppose that all payoff matrices are non-negative in the following sections.

4.3 Dynamic Results

To determine if the model is useful, we must first note that the model is well posed. It is clear from the Lipschitz continuity of the system of ODEs that solutions to an IVP (4.4) with initial conditions $u(0) = \underline{u}$ exist and are unique. Moreover, the following result shows that it will exist for all time.

Lemma 4.2. *If $u(t)$ solves the IVP (4.4) with $u_v(0) = \underline{u}_v \in \Delta^{m-1}$ then the solution exists for all positive time and $u_v(t) \in \Delta^{m-1}$ for all time $t \geq 0$.*

Proof. The proof is a simple computation

$$\begin{aligned}
\frac{d}{dt}\sum_{i\in C} u_v^i &= \sum_{i\in C} u_v^i \langle e_i - u_v, g_v\rangle \\
&= \sum_{i\in C} u_v^i \sum_{j\in C} (\delta_{i,j} - u_v^j) g_v^j \\
&= \sum_{i\in C}\sum_{j\in C} \delta_{i,j} u_v^i g_v^j - \sum_{i\in C}\sum_{j\in C} u_v^i u_v^j g_v^j \\
&= \sum_{i\in C} u_v^i g_v^i - \sum_{i\in C} u_v^i \sum_{j\in C} u_v^j g_v^j \\
&= \left(1 - \sum_{i\in C} u_v^i\right) \sum_{j\in C} u_v^j g_v^j
\end{aligned}$$

Therefore, by ODE uniqueness, if $\sum_{i\in C} u_v^i = 1$ at time t_0 then $\sum_{i\in C} u_v^i = 1$ for all $t > t_0$. This is equivalent to saying that a solution to the initial value problem with initial conditions $\underline{u}_v \in \Delta^{m-1}$ for all v is in $C^1([0,T], (\Delta^{m-1})^V)$. □

This result is proved in a similar way as the analogous result for the standard replicator equation. The meaning of this result is that the strategy profile u remains a meaningful strategy profile for all time. This result will also be useful as we have described an invariant manifold of the system. Indeed, you can observe by ODE uniqueness that if $u_v^i(t) = 0$ for any $t^\star$, then $u_v^i(t) = 0$ for all $t > t^\star$. Because of this, we can give the following corollary.

Corollary 4.1. *For the ODE system (4.4), Δ^{m-1} is an invariant manifold for any v. Moreover, any subsimplex of Δ^{m-1} is also an invariant manifold for any v.*

By ensuring that the state space is an invariant manifold, we have shown that the model is well posed, but we have also shown a shortcoming in the model, which is the fact that innovation is impossible regardless of the game. However, trajectories on the interior of $(\Delta^{m-1})^V$ are unaffected by this. For this reason, for a strategy profile u which is an equilibrium on the boundary of the domain, we cannot conclude that it is a Nash equilibrium of the game without considering the stability of that equilibrium.

Having shown that the model remains meaningful for all time, we must also show that the behavior is reasonable and consistent with the systems we are trying to model. In particular, we should expect that each individual is ascending the fitness gradient (as well as they can observe) at any time. A model which does this through direct gradient ascent encounters problems at the boundaries of Δ^{m-1}. Such a model would rewire the projection of the gradient onto the largest sub-simplex a player is a part of, and in doing this, we would lose the Lipschitz continuity of the ODE system, and the results we depend on for well posedness may no longer hold. That is to say that this model does not describe a best reply strategy revision protocol, but it does describe a *better reply*. That is to say, individuals are not changing their strategy to the strategy which maximizes their fitness relative to the present strategy profile, but they are changing their strategies so that their individual fitness increases relative to the present strategy profile. This result is proven through standard constrained optimization techniques on the interior, and on the boundary, we take advantage of the fact that the boundary of a simplex is a set of simplices.

Lemma 4.3. *If u solves the IVP (4.4) with $u_v(0) = \underline{u}_v \in \Delta^{m-1}$ for all $v \in V$ then*

$$\left.\frac{d}{d\zeta}\right|_{\zeta=0} w_v(u_v + \zeta \frac{d}{dt}u_v | u) \geq 0$$

with equality only when $\frac{d}{dt}u_v = \vec{0}$.

Proof. We will show that if $S_v(\zeta) = w_v(u_v + \zeta \frac{\partial}{\partial t}u_v|u)$, that $S_v'(0) \geq 0$ with equality only when $\frac{d}{dt}u_v = 0$. We compute $S_v'(0) = \left\langle \frac{\partial}{\partial t}u_v, \nabla_v w_v(u_v|u) \right\rangle$. Where $\nabla_v w_v(u_v|u) = \left(\frac{\partial}{\partial u_v^i} w_v(u_v^1, u_v^2, ...u_v^m|u) \right)_{i=1}^m$. When you carry out this computation, you see that $\nabla_v w_v(u_v|u) = g_v$. Thus, we need only show that $\left\langle \frac{d}{dt}u_v, g_v \right\rangle \geq 0$ with equality only in the case that $\frac{d}{dt}u_v = 0$. let $x := u_v$ and $y := g_v$. Now note that $\frac{d}{dt}u_v = x \circ y - \langle x, y \rangle x$ (where $\circ$ is the Hadamard product or element wise multiplication). Therefore, $\left\langle \frac{d}{dt}u_v, g_v \right\rangle = \langle x \circ y, y \rangle - \langle x, y \rangle^2$. Lemma A.1 in appendix A.1 tells us that this is non-negative, meaning that $\left\langle \frac{d}{dt}u_v, g_v \right\rangle \geq 0$ with equality only when $u_v^i = 0$ or $g_v^i = \langle u_v, g_v \rangle$ for all $i \in C$. This condition for equality is exactly the condition for $\frac{d}{dt}u_v = \mathbf{0}$. □

The fact that this system is a better reply revision protocol gives us some insight into the characteristics of equilibria. These characteristics are discussed more in section 4.4, but we present a simple corollary to theorem 4.3 here.

Corollary 4.2 (Nash equilibria are equilibria of the ODE system)**.** *A Nash Equilibrium to the game with payoff matrix A on graph G is an equilibrium point of the ODE system* (4.4)*.*

Proof. Suppose that $u^\star$ is a Nash equilibrium so for all v, $w_v(u_v^\star|u^\star) \geq w_v(s|u^\star)$ for all $s \in \Delta^{m-1}$ let $s \in \Delta^{m-1}$ and let $\nu_s = s - u_v^\star$. Because $u_v^\star$ is a Nash equilibrium and because $w_v(s|u^\star) \in C^\infty(\Delta^{m-1})$ we know that $\langle \nu_s, \nabla_v w_v(u_v^\star|u)\rangle \leq 0$ for all s.

By the proof of theorem 4.2 we know that $\frac{d}{dt}u_v$ cannot point outside of the simplex Δ^{m-1} so let ν be in the direction of $\frac{d}{dt}u_v$ and note that by 4.3, $\langle \nu, \nabla_v w_v(u_v^\star|u)\rangle \geq 0$. This means that this inequality is actually an equality and thus $\frac{d}{dt}u_v = \mathbf{0}$.

This is true for all $v \in V$, thus if $u^\star$ is a Nash equilibrium, it is a rest point of the system. This does not prove that it is a stable rest point. □

The dynamics of this system can be viewed as the coupled movement of n particles each in an $m-1$ dimensional simplex. As an example, the coordination game played on the graph P_4 can be seen in figure 4.1. Every Nash equilibrium is an equilibrium of the ODE system, and you can see that, in the coordination case, the consensus equilibrium is a locally asymptotically stable equilibrium for the ODE system. This is not always the case. For instance, if a Rock Paper Scissors (RPS) game is played on the same graph, although there is a mixed strategy Nash equilibrium where each player plays each strategy equally, this Nash equilibrium is not stable at all. In figure 4.2, solutions do not tend towards the Nash equilibrium but instead meander around the domain. The code for these visualizations and simulations can be found in the repository by McAlister (2026b).

The result of 4.3 is especially important for the case where the payoff matrix A is such that the game is an exact *potential game* (Monderer and Shapley, 1996; Lã et al., 2016). It is easy to construct such an A. For instance, if A is a symmetric matrix, then a potential function exists and it is simply half the sum of the fitnesses.

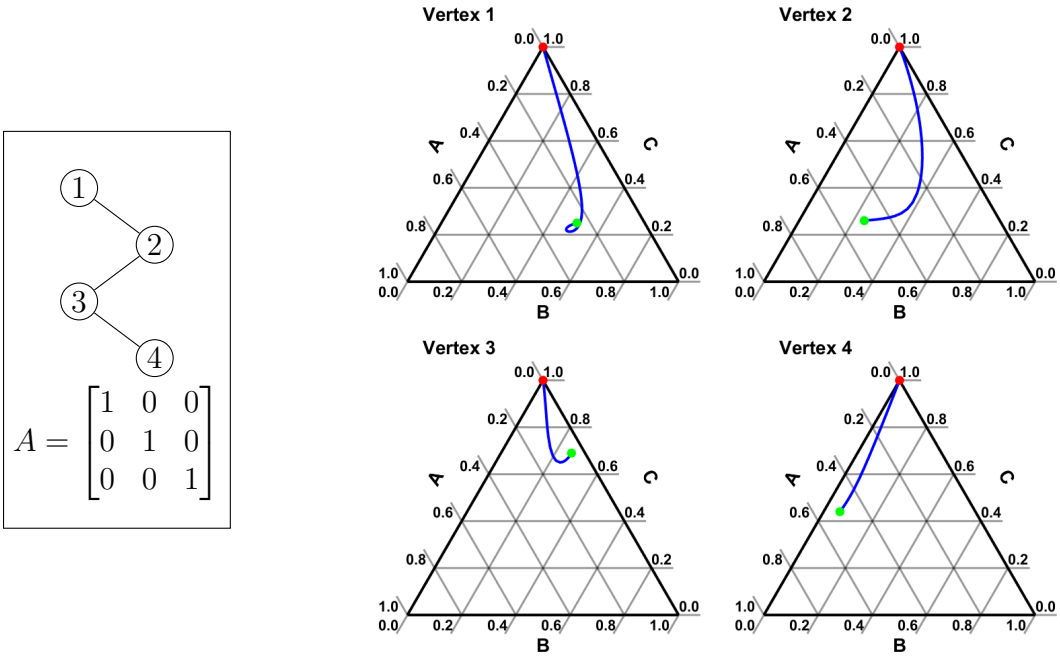

Figure 4.1: The pure coordination game played on P_4 with replicator dynamics converging to a consensus equilibrium. Solutions start at the green dot and proceed towards the red dot which is where the simulation terminates.

Proposition 4.1. *If the payoff matrix A is symmetric, then the structured linear game with fitnesses $w_v(u_v|u) = \langle u_v, g_v \rangle$, with g_v defined as in (4.2), is a potential game with the potential function*

$$\mathcal{W}(u) = \frac{1}{2} \sum_v w(u_v|u) = \frac{1}{2} \sum_{v \in V} \langle u_v, g_v \rangle \tag{4.6}$$

The proof of this proposition is included in the appendix A.1.

The fact that these games can be described as potential games is helpful in understanding them in the classical sense. It is well established that maxima of the potential functions are Nash equilibria of the game itself (Monderer and Shapley, 1996). In the dynamic sense, an exact potential function ensures the existence of Improvement paths in which each step involves a single player taking on their best response to the present strategy profile. The same concept of an improvement path can be translated into the continuous time evolutionary model by thinking about energy methods for ODEs. It is typical in ODEs to consider non-increasing energy in the system. It is typical in Game theory to think of the potential

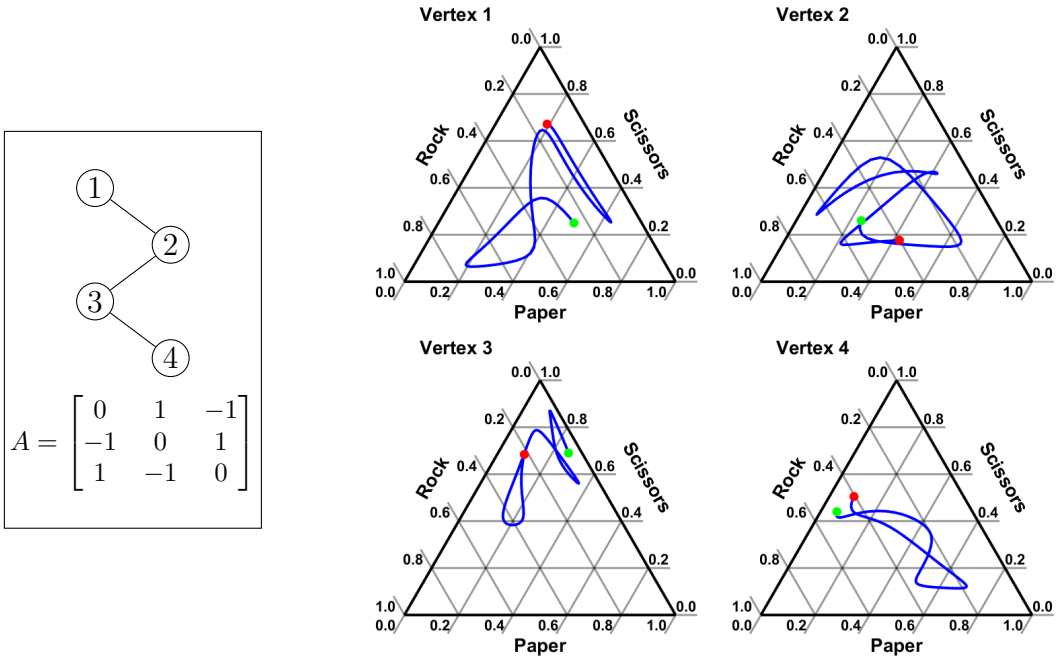

Figure 4.2: Rock Paper Scissors played on P_4 will not converge to an equilibrium. Solutions start at the green dot and proceed towards the red dot which is where the simulation terminates.

function in the opposite way. Here we continue with the convention of having non-decreasing potential in the game theoretic convention, although changing the sign of the function will not change the results meaningfully. This potential surface exists and can be used in this way for any potential game, not only those as in proposition 4.1.

Lemma 4.4. *If A describes a game on G which is an exact potential game with potential function $\mathcal{W}$ then, when a system acts according to the ODE system 4.4, $\mathcal{W}(u(t))$ is non-decreasing in time and is only constant when u is at an equilibrium.*

Proof. Consider the game with payoff matrix A on the graph G and assume it is an exact potential game with potential function $\mathcal{W}$. Recall from the definition of exact potential games that for all $v \in V$, for all $u_v, u'_v \in \Delta^{m-1}$ and for all $u \in (\Delta^{m-1})^V$ we know that

$$\mathcal{W}(u_v, u_{-v}) - \mathcal{W}(u'_v, u_{-v}) = w_v(u_v|u) - w_v(u'_v|u)$$

as in Monderer and Shapley (1996). We do a simple computation to see that

$$\begin{aligned}\frac{\partial}{\partial u_v^i}\mathcal{W}(u) &= \lim_{h\to 0}\frac{\mathcal{W}(u_v + h\hat{e}^i, u_{-v}) - \mathcal{W}(u_v, u_{-v})}{h} \\ &= \lim_{h\to 0}\frac{w_v(u_v + h\hat{e}^i|u) - w_v(u_v|u)}{h} \\ &= \frac{\partial}{\partial u_v^i}w(u_v|u)\end{aligned}$$

This nearly completes the proof because all that is left to do is write

$$\begin{aligned}\frac{d}{dt}\mathcal{W}(u(t)) &= \left\langle \nabla\mathcal{W}(u(t)), \frac{d}{dt}u(t)\right\rangle \\ &= \sum_{v\in V}\left\langle \nabla_v w_v(u_v|u), \frac{d}{dt}u_v\right\rangle \\ &= \sum_{v\in V}\langle g_v, \frac{d}{dt}u_v\rangle\end{aligned}$$

Finally, we notice that each of these components is nonnegative by lemma 4.3. Moreover, the observation that if each of these terms is 0, then $\frac{d}{dt}u = 0$ completes the proof. □

This result, like the existence of improvement paths in potential game theory, gives us a way to visualize the trajectory as populations moving up the fitness landscape (or a particle finding the plane of least potential if you prefer). The potential function is hard to imagine in general because the domain $(\Delta^{m-1})^V$ has dimension $(m-1)\cdot n$, but two trivial cases are shown in figure 4.3.

This result of theorem 4.4 helps us understand the game dynamics for games with symmetrical payoff matrices. In particular, we know that there are no limit cycles or homoclinic orbits because if $\frac{d}{dt}u \neq \mathbf{0}$ then total fitness is strictly increasing. Moreover, because $\mathcal{W}(u)$ is bounded above in $(\Delta^{m-1})^V$ it is certain that $\mathcal{W}(u(t))$ converges to a limit as $t \to \infty$. In the case of best response dynamics as in Swenson et al. (2018a), this is sufficient to show that solutions converge in finite time.

For the better response evolutionary case, finite time convergence is impossible. We do not, at this time, know that solutions necessarily converge, although we conjecture that they

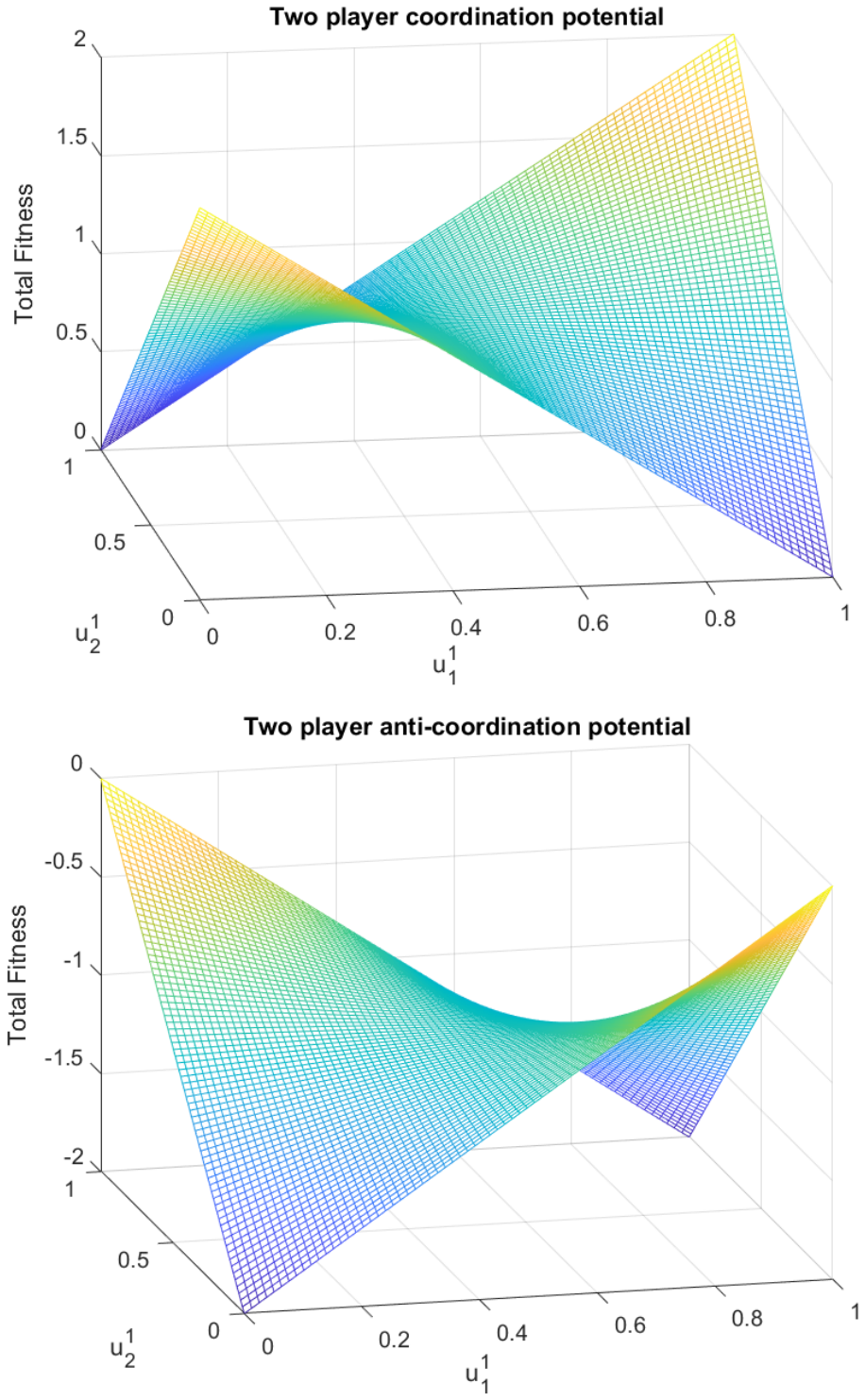

Figure 4.3: Top: The potential function for the two player coordination game with payoff matrix $A = I_2$. $\Delta^1 \times \Delta^1 = [0,1] \times [0,1]$ and the first component of each player's strategies is labeled along each axis. The potential reaches its maxima when $u_1^1 = u_2^1 = 1$ and $u_1^1 = u_2^1 = 0$. **Bottom:** The potential function for the two player anti-coordination game with payoff matrix $A = -I_2$. It is clearly the opposite of the potential function in the coordination case. It reaches its maxima whenever $|u_1^1 - u_1^2| = 1$.

do. However, if solutions do converge, we can characterize their limits. The final result of this section proves that if a trajectory is convergent, it must converge to a Nash equilibrium. The relevance of this result is discussed further in section 4.4.

Theorem 4.1 (Convergence to Nash equilibria)**.** *If $u(t)$ is a convergent trajectory in the interior of $(\Delta^{m-1})^V$, then $\lim_{t\to\infty} u(t)$ exists and is a Nash equilibrium.*

Proof. Suppose $u(t) \in (\Delta^{\mathring{m-1}})^V$ is a trajectory of (4.4). By ODE uniqueness $u_v^i(t) > 0$ for all $t \geq 0$. By way of contradiction, suppose that $\lim_{t\to\infty} u(t) = u^\star$ and $u^\star$ is *not* a Nash equilibrium. Because of this, we know that for some $v \in V$ and some $i \in C$, $g_v^i > \langle u_v, g_v\rangle$. This is equivalent to saying $\langle \hat{e}^i - u_v, g_v\rangle > 0$. Because the inequality is strict and the quantity is continuous in u, we know that there is a positive ϵ, δ pair so that for any $t \geq 0$,

$$|u(t) - u^\star| < \delta \implies \langle \hat{e}^i - u_v(t), g_v(t)\rangle > \epsilon$$

By assumption there is a T such that for $t > T$, $|u(t) - u^\star| < \delta$. This means that for all $t > T$, $\frac{d}{dt}u_v^i = u_v^i\langle \hat{e}^i - u_v, g_v\rangle \geq u_v^i\epsilon$. If $\frac{d}{dt}u_v^i \geq u_v^i\epsilon$ for all $t > T$ and $u_v^i(T) > 0$ then $u_v^i(t) \geq u_v^i(T)e^{\epsilon t}$ for all $t > T$ and thus we reach a contradiction. Therefore, if $u(t)$ is a convergent trajectory, then its limit is a Nash equilibrium. □

Not only do the results presented here help us make sense of the system. They demonstrate to us that the behavior of the system fits with our understanding of games of this type in other settings. Solutions flow up fitness landscapes in potential games just as best response improvement paths increase the potential at every step. The biologically reasonable domain is an invariant manifold for the system, so the system is well posed, and each player is acting in a way that is consistent with the "limited rationality" of evolutionary game theory. Now that we have shown that the model is reasonable, we turn our attention to the equilibria of the model to show that the model is useful.

4.4 Equilibrium Results

In Evolutionary Game Theory, a dynamic game theoretic model is considered against the Folk Theorem of Evolutionary Game Theory to determine if it is useful as a model (Cressman and Apaloo, 2018). The folk theorem of evolutionary game theory describes three benchmarks an evolutionary model must reach

a. A stable rest point is a Nash Equilibrium.

b. A convergent trajectory on the interior of $(\Delta^{m-1})^{|V|}$ evolves to a Nash Equilibrium.

c. A strict Nash equilibrium is locally asymptotically stable

By showing that each of these conditions is satisfied by the model, we can say that the model is useful as a way to understand game dynamics. Moreover, in showing these results, we will demonstrate the ways that this model can be used to evaluate the equilibria of games in classical game theory.

4.4.1 General Games

To start, observe that theorem 4.1 is exactly part (b) of the folk theorem. This is satisfied regardless of the payoff matrix A. Also observe that corollary 4.2 is a partial converse to (a) as it says that every Nash equilibrium is a stable rest point. The converse of this statement, which would be a generalization of (a), is not true. That is, not every rest point is a Nash equilibrium for any non-trivial game. Indeed, every pure strategy profile is an equilibrium of the model (as noted in corollary 4.1), but these are not always Nash equilibria for any nontrivial game. However, it is true, and proven later, that every *stable* rest point is a Nash equilibrium.

As a matter of notation, recall that $BR_v(u^\star)$ is the set of pure strategies $i \in C$ which maximize $w_v(\hat{e}^i|u^\star)$. To discuss the set of strategies that a player v is currently playing with non-zero probability (Called the support of player v's strategy), we write $C(u_v) \subset C$. Note that at equilibrium, because every player is playing a best response, we know that $C(u_v) \subseteq BR_v(u^\star)$ for all $v \in V$.

To interrogate this model against parts (a) and (c) of the folk theorem, we first compute the Jacobian matrix. In order to have a tractable Jacobian matrix, we consider u as a vector $u = [u_1^1, u_1^2, ..., u_1^m, u_2^1, ..., u_2^m, ..., u_n^m]^\intercal$. This will allow for the Jacobian matrix to be a tractable block matrix. If $f_v^i(u) := \frac{d}{dt}u_v^i = u_v^i\langle \hat{e}^i - u_v, g_v\rangle$, where $g_v = A\sum_{w\in V} u_w$ we note that

$$\frac{d}{du_w^j} g_v^i = A_{i,j}W_{v,w}.$$

and so we can compute all of the partial derivatives

$$\begin{aligned}
\frac{\partial}{\partial u_v^i} f_v^i(u) &= \langle \hat{e}^i - u_v, g_v\rangle - u_v^i g_v^i \\
\frac{\partial}{\partial u_v^j} f_v^i(u) &= -u_v^i g_v^j \\
\frac{\partial}{\partial u_w^i} f_v^i(u) &= u_v^i\langle \hat{e}^i, A(\hat{e}^i - u_v)\rangle W_{w,v} \\
\frac{\partial}{\partial u_w^j} f_v^i(u) &= u_v^i\langle \hat{e}^j, A(\hat{e}^i - u_v)\rangle W_{w,v}
\end{aligned} \tag{4.7}$$

With this, we can build up the Jacobian matrix as a block matrix.

$$J(u) = \begin{bmatrix} J_{1,1} & \cdots & J_{1,n} \\ \vdots & \ddots & \vdots \\ J_{n,1} & \cdots & J_{n,n} \end{bmatrix} \tag{4.8}$$

where the diagonal blocks are of the form $J_{v,v}(u) = diag(\langle \hat{e}^i - u_v, g_v\rangle) - u_v g_v^\intercal$ and the off diagonal blocks $J_{v,w}$ are given as $[J_{v,w}]_{i,j} = W_{v,w}u_v^i\langle \hat{e}^j, A(\hat{e}^i - u_v)\rangle$. Observe that if u is a pure strategy equilibria, meaning that for every v, $u_v = \hat{e}^i$ for some i, $J_{v,w} = 0$. This makes the pure strategy equilibria easy to investigate.

We will start by examining the eigenvalues of the Jacobian matrix only in the pure strategy case. This will not be sufficient to entirely determine the stability of the equilibria because of the possible existence of zero eigenvalues. However, it will provide important insights.

Lemma 4.5. *If $u^\star$ is a pure strategy equilibrium, then the spectrum of the Jacobian of the ODE system (4.4) evaluated at $u^\star$ is*

$$\sigma(J(u)) = \bigcup_{v \in V} (\{-g_v^{k_v}\} \cup \{(g_v^i - g_v^{k_v}) : i \neq k_v\})$$

where k_v is the unique strategy which player v is playing (i.e. $C(u_v) = \{k_v\}$).

Proof. The first thing to notice is that, if u is a pure strategy, then $J_{v,w}(u) = 0$ whenever $w \neq v$. This means that J is block diagonal and we need only determine the eigenvalues of $J_{v,v}(u)$ for each v. This too is an easy task because the outer product $u_v g_v^\intercal$ is very simple. Let k_v be the strategy that player v is playing, so $u_v = \hat{e}^{k_v}$. In this case

$$u_v g_v^\intercal = \begin{bmatrix} \mathbf{0}^\intercal \\ \vdots \\ -g_v^\intercal \\ \vdots \\ \mathbf{0}^\intercal \end{bmatrix}$$

In other words, the outer product is a matrix full of zeros except for the vector $g_v^\intercal$ in the k_vth row. Thus, if $P_{k_v,1}$ is the permutation matrix which switches the first and k_vth row when left multiplied, we can write that $P_{k_v,1} J_{v,v} P_{k_v,1}$ is upper triangular. The eigenvalues of this matrix (which are identical to the eigenvalues of $J_{v,v}$ are therefore immediate. We need only observe that $\langle \hat{e}^i - u_v, g \rangle = g^i - g^{k_v}$ to see that

$$P_{k_v,1} J_{v,v} P_{k_v,1} = \begin{bmatrix} -g_v^{k_v} & -g_v^2 & \cdots & -g_v^1 & \cdots & g_v^m \\ 0 & g_v^2 - g_v^{k_v} & \cdots & 0 & \cdots & 0 \\ \vdots & \vdots & & \vdots & & \vdots \\ 0 & 0 & \cdots & g_v^1 - g_v^{k_v} & \cdots & 0 \\ \vdots & \vdots & & \vdots & & \vdots \\ 0 & 0 & \cdots & 0 & \cdots & g_v^m - g_v^{k_v} \end{bmatrix}$$

The spectrum for each diagonal block is therefore immediate

$$\sigma(J_{v,v}(u)) = \{-g^{k_v}\} \cup \{(g^i - g^{k_v}) : i \neq k_v\}. \tag{4.9}$$

Thus, for the entire jacobian we get the eigenvalues

$$\sigma(J(u)) = \bigcup_{v \in V} (\{-g^{k_v}\} \cup \{(g^i - g^{k_v}) : i \neq k_v\}) \tag{4.10}$$

□

Lemma 4.6. *For a pure strategy profile, $u^\star$, there are no deficient eigenvalues and the invarient set $(\Delta^{m-1})^V$ is contained entirely by the span of $n(m-1)$ eigenvectors each corresponding to eigenvalues of the form $g_v^i - g_v^{k_v}$ where k_v is the strategy that v is playing in $u^\star$.*

Proof. Adopt the convention that in $u^\star$ player v plays the pure strategy k_v (thus $u_v = \hat{e}^{k_v}$). We can find the eigenvectors for each $J_{v,v}(u^\star)$ and build the corresponding eigenvectors for $J(u^\star)$ from there.

For a particular $v \in V$ $J_{v,v}(u^\star)$ has an eigenvector $\hat{e}_v^k$ corresponding to the eigenvalue $\lambda = -g_v^{k_v}$. This can be seen as $J_{v,v}(u^\star)e^{k_v}$ is the k_vth column of $J_{v,v}$. This column is clearly $-g_v^{k_v}\hat{e}^{k_v}$. Note that

$$\Delta^{m-1} \cap (u^\star + span(\hat{e}^{k_v})) = \{u^\star\}.$$

Partition all strategies $i \in C$ other than k_v into groups $S_v^{l_1}, ..., S_v^{l_L}$ so that, if $i, j \in S_v^{l_p}$, then $g_v^i = g_v^j = l_p$. For each $p \in 1, ..., L$, there is an $|S_v^{l_p}|$ dimensional eigenspace $E(S_v^{l_p})$, corresponding to the eigenvalue $\lambda = l_p - g_v^{k_v}$. The eigenspace is described in the following way: $x \in E(S_v^{l_p})$ if and only if $x_j = 0$ when $j \notin S_v^{l_p}$ and $x_{k_v} + \sum_{i \in S_v^{l_p}} x_i = 0$.

There are two possibilities. The first is that $l_p = g_v^{k_v}$ in which case the eigenvalue is zero. This means that $g_v^i = g_v^{k_v}$ for all $i \in S_v^{l_p}$. Consider the product $J_{v,v}(u^\star)x = diag(\langle \hat{e}^i - u_v, g_v \rangle)x - u_v g_v^\intercal x$ where $x \in E(S_v^{l_p})$.

Notice that for every j such that $x_v^j \neq 0$ we have that $\hat{e}^j g_v = g_v^j = g_v^{k_v}$ and that $\langle u_v, g_v \rangle = g_v^{k_v}$. Thus $[diag(\langle \hat{e}^i - u_v, g_v \rangle)x]_j = (g_v^j - g_v^{k_v})x_j = 0$

Moreover, notice that $u_v g_v^\intercal x = \hat{e}^{k_v} \langle g_v, x \rangle$. Of course $\langle g_v, x \rangle = x_{k_v} g_v^{k_v} + \sum_{i \in S_v^{l_p}} x_i g_v^i = g_v^{k_v} \left(x_{k_v} + \sum_{i \in S_v^{l_p}} x_i \right) = 0$, and so $u_v g_v^\intercal x = 0$. Thus, we have shown that, for $x \in E(S_v^{l_p})$, $J_{v,v}(u^\star)x = 0$, and therefore x is an eigenvector for the eigenvalue 0 when $l_p = g_v^{k_v}$.

Now consider the other case where $l_p \neq g_v^{k_v}$. In this case $g_v^j = l_p$ for all $j \in S_v^{l_p}$ and the corresponding eigenvalue we expect will be $\lambda = l_p - g_v^{k_v}$. We can do a similar computation to find that, if $x \in E(S_v^{l_p})$, then

$$diag(\langle \hat{e}^i - u_v, g_v \rangle)x_j = (g_v^j - g_v^{k_v})x_j = \begin{cases} \lambda x_j & j \neq k_v \\ 0 & j = k_v \end{cases}$$

In the same way, we can write

$$\begin{aligned} u_v g_v^\intercal x &= \hat{e}^{k_v} \left(g_v^{k_v} x_{k_v} + \sum_{S^{l_p}} g_v^j x_j \right) \\ &= \hat{e}^{k_v} \left(g_v^{k_v} (x_{k_v} + \sum_{S^{l_p}} x_j) + \sum_{S^{l_p}} (g_v^j - g_v^{k_v}) x_j \right) \\ &= \hat{e}^{k_v} \lambda \sum_{S^{l_p}} x_j \\ &= \hat{e}^{k_v} \lambda x_{k_v} \end{aligned}$$

Thus, when we sum these two terms together, we get that $J_{v,v}(u^\star)x = \lambda x$ whenever $\lambda = l_p - g_v^{k_v}$ and $x \in E(S^{l_p})$.

then again $[J_{v,v}(u^\star)x]_{k_v} = 0$ through an identical computation and $[J_{v,v}(u^\star)x]_i = (l_p - g_v^{k_v})x_i$. This completely characterizes the eigenspaces for every eigenvalue of the submatrix $J_{v,v}$. Let $E_v = E(S_v^1) + E(S_v^2) + ... + E(S_v^l)$ and note now that

$$\Delta^{m-1} \subset E_v.$$

This means for $J_{v,v}(u^\star) \in \mathbb{R}^{m\times m}$ we have m linearly independent eigenvectors in $\mathbb{R}^m$. This is true for each v. Thus to form the eigenvectors of $J(u^\star)$ we form block vectors so that if x is an eigenvector of $J_{v,v}(u^\star)$ then $y = [\mathbf{0}^\intercal, ..., \mathbf{0}^\intercal, x^\intercal, \mathbf{0}^\intercal, ..., \mathbf{0}^\intercal]^\intercal$ is an eigenvector for $J(u^\star)$ where x takes up the components of y corresponding to player v. This gives us nm linearly independent eigenvectors for $J(u^\star)$. for the n eigenvectors which correspond to eigenvalues of the form $-g_v^{k_v}$ we see the eigenspace intersects the invariant manifold only at $\{u^\star\}$. If $E = \sum_{v\in V} E_v$ is the span of all eigenvectors corresponding to an eigenvalue of the form $\lambda = g_v^i - g_v^{k_v}$, then $(\Delta^{m-1})^V \subset (u^\star + E)$.

Because of theorem 4.2, we know that u_v does not leave the invariant manifold of Δ^{m-1} for all time, we can describe the stability of the system using only the eigenvalues corresponding to the $n(m-1)$ eigenvectors in E_v for any v. □

It is of note that the signs of the eigenvalues $\lambda = -g_v^{k_v}$ do not impact the dynamics of the system qualitatively. This is consistent with the idea that the game does not depend on absolute payoff but rather relative payoff as in lemma 4.1. This means that the value of $g_v^{k_v}$ itself cannot impact the dynamics, and we can see that clearly here by characterizing this eigenspace.

Having characterized the eigensystem for the Jacobian in the pure strategy case, we can discuss the dynamics of the behavior near the equilibria. If there are no zero eigenvalues, the behavior of the system is described entirely by Hartman–Grobman theorem. For nonhyperbolic equilibria, we cannot use the linearization to characterize the equilibria in the same way. However, we fall under the assumptions of the center manifold theorem. That is to say, in a neighborhood around the equilibrium, there is a unique stable manifold, a unique unstable manifold, and a not necessarily unique center manifold which are tangent to the Eigenspaces of negative eigenvalues, positive eigenvalues, and zero eigenvalues, respectively. The nonlinearity makes it difficult to use this result in general, but we may find that it is possible to describe these manifolds with additional assumptions on the game in section 4.4.2.

Nevertheless, we can use the linearization to prove part (c) of the folk theorem of EGT for general games in the form of (4.4). First, we provide a proposition which is equivalent to the equal payoff principle for mixed strategies

Lemma 4.7. *For a structured coordination game, if $u^\star$ is a strict Nash equilibrium, then $u^\star$ is a pure strategy Nash equilibrium.*

Proof. Suppose that $u^\star$ is a mixed strategy Nash equilibrium, and without loss of generality, assume that $u_v^i > 0$ for $i = 1, 2$. By corollary 4.2, we know that at a Nash equilibrium $\frac{d}{dt}u_v^\star = 0$ and this can only be the case if $u_v^{\star i} = 0$ or $g_v^i = \langle u_v^\star, g\rangle$ for all $i = 1, ..., m$. By assumption $u_v^1 \neq 0$ and $u_v^2 \neq 0$ so it must be true that $g_v^1 = g_v^2 = \langle u_v^\star, g_v\rangle$. Now let $\vec{\varepsilon} = [\epsilon, -\epsilon, 0, ..., 0]^\intercal$ for some small $|\epsilon|$ so that $u_v + \vec{\varepsilon} \in \Delta^{m-1}$. Observe that

$$w(u_v^\star + \vec{\varepsilon}|u^\star) = \langle u_v^\star + \vec{\varepsilon}, g_v\rangle = \langle u_v^\star, g_v\rangle + \underbrace{\langle \vec{\varepsilon}, g_v\rangle}_{=0} = w_v(u_v^\star|u^\star)$$

Therefore, the Equilibrium is not strict. Thus, any mixed strategy Nash equilibrium cannot be strict, which is equivalent to saying any strict Nash equilibrium is a pure strategy Nash equilibrium. □

Having shown that any strict Nash equilibrium is a pure strategy Nash equilibrium, we can examine the Jacobian only for pure strategies in order to prove part (c) of the folk theorem for EGT.

Theorem 4.2 (Folk Theorem of EGT (c))**.** *If $u^\star$ is a strategy profile to the game, with payoff matrix A, played on the connected graph G, and $u^\star$ is a strict Nash equilibrium, then it is locally asymptotically stable.*

Proof. If $u^\star$ is a strict Nash equilibrium, then by lemma 4.7 it is a strict Nash equilibrium and, for all v, $w_v(u_v|u^\star) > w_v(s|u^\star)$ for all $s \in \Delta^{m-1}$. Let $s = \hat{e}^i$ for some $i \neq k_v$, where k_v is the strategy used by player v in $u^\star$ and get that $w_v(u_v|u^\star) > w_v(\hat{e}^i|u^\star)$ for all $ineqk_v$. This is equivalent to writing $g_v^i - g_v^{k_v} < 0$ for all $i \neq k_v$.

Lemma 4.5 tells us then that $(g_v^i - g_v^{k_v})$ are all eigenvalues of $J(u^\star)$ and thus we know that each of these eigenvalues are negative. By lemma 4.6, we know that the eigenspace associated to the negative eigenvalues contains the entire invariant manifold, and so this provides some assurance that, regardless of the value of $-g_v^{k_v}$, $u^\star$ is still stable to perturbations in the biologically reasonable domain. The easiest way to do this rigorously, however, is to cite lemma 4.1 and note that we can shift A so that it has only positive entries and thus at least one entry in g_v will be positive. Because $u^\star$ is a pure strategy Nash equilibrium, $\langle u_v, g_v \rangle = \max_i g_v^i > 0$ which is identical to saying $g_v^{k_v} > 0$ for every v,

Therefore, we have shown that $J(u^\star)$ has only negative eigenvalues and so Hartman-Grobman implies that $u^\star$ is locally asymptotically stable. In particular, it is stable against perturbations in Δ^{m-1}. □

The Jacobian method described here can also be used to show that part (a) is true for stable rest points that are strict pure strategies, but we have not computed the eigenvalues for mixed strategy equilibria. Moreover, we can see that if the Nash equilibrium is not strict, even in the pure strategy case, zero-eigenvalues will mean that our linearization approach is insufficient. Instead, we will use a less elegant approach to directly prove that if a rest point is not a Nash equilibrium, it cannot be stable, and thus any stable rest point must be a Nash equilibrium.

Theorem 4.3 (Folk Theorem of EGT (a))**.** *Stable rest points of the ODE system* (4.4) *are Nash equilibria of the game played on the graph G with adjacency matrix W and payoff matrix A.*

Proof. By way of contradiction, suppose that $u^\star$ is an equilibrium point and *not* a Nash equilibrium. Therefore, for some $v \in V$ and for some $s \in \Delta^{m-1}$, $w_v(s|u^\star) > w_v(u_v|u^\star)$. Thus, $\langle s, g_v^\star \rangle > \langle u_v, g_v^\star \rangle$. $u^\star$ is an equilibrium, so this means that whenever $u_v^i \neq 0$, $g_v^{\star i} = \langle u_v, g_v^\star \rangle$. Therefore, $\langle s, g_v^\star \rangle > \langle u_v, g_v^\star \rangle$ implies that there exists an $i \in C$ such that $g_v^{\star i} > \langle u_v, g_v^\star \rangle$. Crucially we will write this as $g_v^{\star i} - \langle u_v^\star - g_v^\star \rangle > \delta > 0$.

Having argued this point, consider the solution to the ODE system (4.4) $u(t) = u^\star(t) + x(t)$ where $u^\star(t) \equiv u^\star$. Clearly $\frac{d}{dt}u(t) = \frac{d}{dt}x(t)$. I will show that there exists a δ neighborhood of

$u^\star$ so that any $u(t)$ leaves the neighborhood in finite time if $u(0) \neq u^\star$. In the same way as before, let x_v be the portion of x with elements corresponding to the strategies of player v, so x_v^i describes the difference in the ith component of player $v's$ strategy between $u(t)$ and $u^\star$.

$$\frac{d}{dt}x_v^i = (u_v^{\star i} + x_v^i)\langle \hat{e}^i - u_v^\star - x_v, g_v^\star + \sum_{w\in V} W_{v,w}Ax_w\rangle$$

We first note that because $g_v^{\star i} > \langle u_v^\star, g_v^\star\rangle$, it must be the case that $u_v^{\star i} = 0$ because $u^\star$ is an equilibrium point of the ODE system. Thus, we can write out the ODE.

$$\frac{d}{dt}x_v^i = x_v^i(g_v^{\star i} - \langle u_v^\star, g_v^\star\rangle - \langle x_v, g_v^\star\rangle + \sum_{w\in V} W_{v,w}(\langle \hat{e}^i, Ax_w\rangle - \langle u_v, Ax_w\rangle - \langle x_v, Ax_w\rangle))$$

Now we write $x_v = |x_v|\eta_v$ so that $\eta_v \in S^{m-1}$ to show that

$$\frac{d}{dt}x_v^i = x_v^i(g_v^{\star i} - \langle u_v^\star, g_v^\star\rangle - |x_v|\langle \eta_v, g_v^\star\rangle + \sum_{w\in V} |x_w|W_{v,w}(\langle \hat{e}^i, A\eta_w\rangle - \langle u_v, A\eta_w\rangle - |x_v|\langle \eta_v, A\eta_w\rangle)).$$

Note that, because $\eta \in S^{m-1}$ and every term is continuous, we can write that $|\langle \eta_v, g_v^\star\rangle| \leq c_v$, $|\langle \hat{e}^i, A\eta_w\rangle| \leq c_w$, $|\langle u_v, A\eta_w\rangle| \leq c_{v,w}^{(1)}$ and $|\langle x_v, Ax_w\rangle| \leq c_{v,w}^{(2)}$. In all this means that

$$\begin{aligned} |B(x)| &:= \left| -|x_v|\langle \eta_v, g_v^\star\rangle + \sum_{w\in V} |x_w|W_{v,w}(\langle \hat{e}^i, A\eta_w\rangle - \langle u_v^\star, A\eta_w\rangle - |x_v|\langle \eta_v, A\eta_w\rangle)\right| \\ &\leq |x_v|c_v + \sum_{w\in V} |x_w|(c_w + c_{v,w}^{(1)} + |x_v|c_{v,w}^{(2)}) \\ &\leq |x|C \end{aligned} \tag{4.11}$$

where the relationship between $\sum |x_v|$ and $|x|$ is given simply by norm equivalence. Notice that C depends only on A and $u^\star$ not on x. The result of this computation is that, if $|x| < \frac{\delta}{2C}$,

then we have

$$\begin{aligned}\frac{d}{dt}x_v^i &= x_v^i(g_v^{\star i} - \langle u_v^\star, g_v^\star\rangle + B(x)) \\ &\geq x_v^i(g_v^{\star i} - \langle u_v^\star, g_v^\star\rangle - |x|C) \\ &\geq x_v^i(\delta - \frac{\delta}{2C}C) \\ &\geq \frac{\delta}{2}x_v^i\end{aligned} \tag{4.12}$$

Therefore, if $|x(t)| < \frac{\delta}{2C}$ for all time $t > 0$ then $x_v^i(t) \geq e^{\frac{\delta}{2}t}$ for all time $t > 0$ whenever $x_v^i(0) > 0$. This leads to an obvious contradiction so $|x(t)| > \frac{\delta}{2C}$ in finite time whenever $x_v^i(0) > 0$.

This means that if there is a neighborhood about $u^\star$ such that, for every $\epsilon > 0$ there is a perturbation $|u(0) - u^\star| < \epsilon$ which eventually escapes the δ neighborhood of $u^\star$. Therefore, $u^\star$ is unstable.

This shows that an equilibrium which is not a Nash equilibrium cannot be stable, and so a stable equilibrium must be a Nash equilibrium. □

Therefore, we have shown that indeed the structured replicator dynamics are well founded and pass the benchmark set by the folk theorem of evolutionary game theory. This type of system, however, is much different from other models in evolutionary game theory because we are limited in the ways we are able to discuss invasability. Just as Δ^{m-1} is an invariant manifold for every u_v, so is every subsimplex. This has the consequence that invasiability is impossible even in game settings where it should be selected for.

This main drawback does not prevent us, however, from examining games in which innovation is not selected for. In particular, coordination games, wherein the bandwagon principle of Kandori and Rob (1998) or, in a more general sense, the weak bandwagon principle of Cui and Shi (2022).

4.4.2 Coordination Games

The pure coordination game, ($A = I_n$) is an obvious example of a coordination game and will be the focus of the remainder of this chapter. The ODE system satisfies the folk theorem of EGT, but this theorem does not entirely classify the behavior of solutions around certain equilibria. Our goal in this section is to give a characterization of the behavior of solutions near equilibria, and in order to do this, we will first describe the Jacobian for the pure coordination game in particular. We would like to be able to use the ODE system, for which stability has a clear definition, to describe stability in the discrete-time system, in which the definition of stability is less clear. The goal of this section is to consider equilibrium strategy profiles and attempt to classify their stability through various ODE methods.

The spectrum of the Jacobian is unchanged in the pure strategy case from lemma 4.5. In general, the spectrum is still arduous to compute for mixed strategies, but for certain mixed strategies, the spectrum is as simple as before. In order to see this effectively, we will need to reorder the player strategy pairs in u. This reordering of the variables will be helpful for making the Jacobian tractable, but it is not straightforward, and so we will describe it here before we proceed to any results.

In the previous subsection, u has been in the shape $[u_1^\intercal, u_2^\intercal, ..., u_n^\intercal]^\intercal$ where every strategy of player 1 was listed, then every strategy of player 2, and so on until player n. We will now reorder these variables, and to do that, we must introduce notation for the "support" of a strategy player pair. We say that if a player v is playing a strategy i with some non-zero proportion, then i is in player v's support. The notation is that if i is in the support of v then $i \in C(u_v)$. Using this, we will split each strategy vector u_v into strategies in the support of v and those strategies not in the support of v. We will now give the order of the variables as

$$[[u_1^i]_{i\in C(u_1)}, [u_2^i]_{i\in C(u_2)}, ..., [u_n^i]_{i\in C(u_n)}, [u_1^i]_{i\notin C(u_1)}, [u_2^i]_{i\notin C(u_2)}, ..., [u_n^i]_{i\notin C(u_n)}]$$

as a column vector. This reordering of the variables makes the strategy profile itself easier because it will have the form

$$[[u_1^i]_{i\in C(u_1)}, [u_2^i]_{i\in C(u_2)}, ..., [u_n^i]_{i\in C(u_n)}, 0, 0, ..., 0]$$

More importantly, this reordering of the variables gives the Jacobian a helpful permutation. Having reordered the variables, we can separate the Jacobian into four blocks.

$$PJ(u^*)P = \begin{bmatrix} B & X \\ Y & D \end{bmatrix}$$

B is the submatrix of the Jacobian where we consider partial derivatives $\frac{\partial}{\partial u_w^j} f_v^i$ where $i \in C(u_v)$ and $j \in C(u_w)$. That is, this submatrix contains all of the partial derivatives in which both strategies in question are being used by their corresponding players. We can further break this matrix down into submatrices

$$B = \begin{bmatrix} B_{1,1} & \cdots & B_{1,n} \\ \vdots & & \vdots \\ B_{n,1} & \cdots & B_{n,n} \end{bmatrix} \text{ with } B_{v,w} = \begin{bmatrix} \frac{\partial}{\partial u_w^1} f_v^1 & \cdots & \frac{\partial}{\partial u_w^j} f_v^1 \\ \vdots & & \vdots \\ \frac{\partial}{\partial u_w^1} f_v^k & \cdots & \frac{\partial}{\partial u_v^j} f_v^k \end{bmatrix}$$

where $C(u_w) = \{1, ..., j\}$ and $C(u_v) = \{1, ..., k\}$.

X is the submatrix of the Jacobian where we consider partial derivatives $\frac{\partial}{\partial u_w^j} f_v^i$ where $j \notin C(u_w)$ but $i \in C(u_v)$. Thus, we are differentiating parts of f which correspond to strategy player pairs which are non-zero at u^*, but we are taking the derivative with respect to the variables which are 0 at u^*. Again, we can further break this matrix down into submatrices as before.

$$X = \begin{bmatrix} X_{1,1} & \cdots & X_{1,n} \\ \vdots & & \vdots \\ X_{n,1} & \cdots & X_{n,n} \end{bmatrix} \text{ with } X_{v,w} = \begin{bmatrix} \frac{\partial}{\partial u_w^{j+1}} f_v^1 & \cdots & \frac{\partial}{\partial u_w^m} f_v^1 \\ \vdots & & \vdots \\ \frac{\partial}{\partial u_w^{j+1}} f_v^k & \cdots & \frac{\partial}{\partial u_v^m} f_v^k \end{bmatrix}$$

where the compliment of the support of w is $C^c(u_w) = \{j+1, ..., m\}$ and the support of v is $C(u_v) = \{1, ..., k\}$.

Y is the submatrix of the Jacobian where we consider partial derivatives $\frac{\partial}{\partial u_w^j} f_v^i$ where $j \in C(u_w)$ but $i \notin C(u_v)$. This means we are differentiating parts of f which correspond to strategy player pairs which are zero in u^*, but we are taking the derivative with respect to the variables which are non-zero in u^*. The same submatrix decomposition can be done.

$$Y = \begin{bmatrix} Y_{1,1} & \cdots & Y_{1,n} \\ \vdots & & \vdots \\ Y_{n,1} & \cdots & Y_{n,n} \end{bmatrix} \text{ with } Y_{v,w} = \begin{bmatrix} \frac{\partial}{\partial u_w^1} f_v^{k+1} & \cdots & \frac{\partial}{\partial u_w^j} f_v^{k+1} \\ \vdots & & \vdots \\ \frac{\partial}{\partial u_w^1} f_v^m & \cdots & \frac{\partial}{\partial u_v^j} f_v^m \end{bmatrix}$$

where the support of w is $C(u_w) = \{1, ..., j\}$ and the compliment of the support of v is $C^c(u_v) = \{k+1, ..., m\}$.

Finally, D is the submatrix of the Jacobian where we are concerned with only those derivatives $\frac{\partial}{\partial u_w^j} f_v^i$ where $j \notin C(u_w)$ and $i \notin C(u_v)$. This means that we are differentiating parts of f which correspond to strategy player pairs which are zero in u^*, and we are taking the derivative with respect to the variables which are zero in u^*. The final submatrix decomposition is shown below.

$$D = \begin{bmatrix} D_{1,1} & \cdots & D_{1,n} \\ \vdots & & \vdots \\ D_{n,1} & \cdots & D_{n,n} \end{bmatrix} \text{ with } D_{v,w} = \begin{bmatrix} \frac{\partial}{\partial u_w^{j+1}} f_v^{k+1} & \cdots & \frac{\partial}{\partial u_w^m} f_v^{k+1} \\ \vdots & & \vdots \\ \frac{\partial}{\partial u_w^{j+1}} f_v^m & \cdots & \frac{\partial}{\partial u_v^m} f_v^m \end{bmatrix}$$

where the compliment of the support of w is $C^c(u_w) = \{j+1, ..., m\}$ and the compliment of the support of v is $C^c(u_v) = \{k+1, ..., m\}$.

This reordering of the variable will clearly not change the spectrum. $\sigma(J(u^*)) = \sigma(PJ(u^*)P)$. The reordering of the variables in a way that is particular to the strategy profile in question is clearly not helpful for the dynamic results, but we will see that this reorganization makes the Jacobian much easier to work with for equilibrium results.

Lemma 4.8. *If $u^\star$ is a mixed strategy profile in the pure coordination game on the graph G with adjacency matrix W, wherein, for every pair of players v and w, one of the following is true:*

a $|C(u_v)| = 1$ *or* $|C(u_w)| = 1$

b $W_{v,w} = 0$

c $C(u_v) \cap C(u_w) = \emptyset$

Then the spectrum of the Jacobian evaluated at $u^\star$ is given as

$$\sigma(J(u^\star)) = \bigcup_{v \in V} \left(\{-\langle u_v, g_v \rangle, 0\} \bigcup_{i \notin C(u_v)} \{g_v^i - \langle u_v, g_v \rangle\} \right)$$

where 0 has algebraic multiplicity $|BR_v(u^\star)| - 1$ for each v.

Proof. To prove this, I will claim that in the block matrix representation of the permuted Jacobian, B is block upper triangular, $Y = 0$, and D is diagonal. In addition to the permutation of the Jacobian matrix described above, we will assume that all of the players playing mixed strategies are listed first, then all of the players playing pure strategies. That is there is some r so that if $v \leq r$ then v is playing a mixed strategy ($|C(u)v)| > 1$) and if $v > r$ then v is playing a pure strategy ($|C(u_v)| = 1$).

$$PJ(u^*)P = \begin{bmatrix} B & X \\ Y & D \end{bmatrix}$$

If we show that (1) B is block upper triangular, (2) $Y = 0$, and (3) D is diagonal, we need not determine anything about X. Understanding the structure of X will not change the eigenvalues of PJP and thus will not change the eigenvalues of J.

(1) To show that B is block upper triangular consider $B_{v,w}$ for $v \neq w$. $\frac{\partial}{\partial u_w^j} f_v^i = W_{v,w} u_v^i (\delta_{i,j} - u_v^j)$ for $j \in C(u_w)$ and $i \in C(u_v)$. One of the assumptions (a), (b), or (c) must hold about v and w.

If $i = j$ then (c) cannot hold. If (b) holds then $\frac{\partial}{\partial u_w^j} f_v^i = 0$. If (b) does not hold, then (a) must hold, and so one player must have support of size 1. If player v has support of size one then $u_v^i = u_v^j = 1$ so $\frac{\partial}{\partial u_w^j} f_v^i = 0$. If player w has support of size 1, then $w > v$, so the block $B_{v,w}$ is above the diagonal, and so it may have non-zero elements in it.

If $i \neq j$ then we have $-W_{v,w} u_v^i u_v^j$. Again, if (b) holds, this is clearly 0, and if (a) holds, it is either 0 or above the diagonal. If (c) holds then $j \in C(u_w)$ implies that $u_v^j = 0$, Thus in every case $B_{v,w} = 0$.

(2) To show that $Y = 0$ consider first $Y_{v,v}$. $\frac{\partial}{\partial u_v^j} f_v^i = -u_v^i g_v^j$ for $j \in C(u_v)$ and $i \notin C(u_v)$. If $i \notin C(u_v)$ then $u_v^i = 0$ and thus all the elements of $Y_{v,v}$ are zero. For the off diagonal blocks, consider $Y_{v,w}$ for $w \neq v$. Here $\frac{\partial}{\partial u_w^j} f_v^i = W_{v,w} u_v^i (\delta_{i,j} - u_v^j)$ for $j \in C(u_w)$ and $i \notin C(u_v)$. Again, $u_v^i = 0$ and thus every element of the off diagonal blocks is also zero. Thus, we have shown that $Y_{v,v} = 0$ for all $w, v \in V$ and so $Y = 0$ regardless of what we assume about (a), (b), or (c).

(3) To show that D is a diagonal matrix itself, I will first demonstrate that all of the off diagonal blocks are zero. Consider $D_{v,w}$ for $w \neq v$. $\frac{\partial}{\partial u_w^j} f_v^i = W_{v,w} u_v^i (\delta_{i,j} - u_v^j)$ for $j \notin C(u_w)$ and $i \notin C(u_v)$. Again, clearly $u_v^i = 0$ so the off diagonal blocks are all zeros. For a diagonal block, we must show that the block itself is diagonal. Consider $D_{v,v}$. $\frac{\partial}{\partial u_v^j} f_v^i = -u_v^i g_v^j$ for $j \neq i$ and $j, i \notin C(u_v)$. For the final time, again $u_v^i = 0$, so all of the off diagonal elements must be zero. Lastly consider $\frac{\partial}{\partial u_v^i} f_v^i = g_v^i - \langle u_v, g_v \rangle - u_v^i g_v^i$ for $i \notin C(u_v)$. When $u_v^i = 0$, we are left with $g_v^i - \langle u_v, g_v \rangle$ on the diagonal.

Having shown this, we can say that the Jacobian is indeed block upper triangular and so the eigenvalues are easy observe. The eigenvalues of the block D are obviously

$$\sigma(D) = \bigcup_{v \in V} \bigcup_{i \notin C(u_v)} (g_v^i - \langle u_v, g_v \rangle)$$

The spectrum for B is provided by a calculation from lemma A.2 in appendix A.1

$$\sigma(B) = \bigcup_{v \in V} \sigma(B_{v,v}) = \bigcup_{v \in V} \{0, -\langle u_v, g_v \rangle\}$$

where 0 has multiplicity $|C(u_v)| - 1$.

Notice that this means that the spectrum is nearly unchanged from the pure strategy spectrum from theorem 4.2 (except for the inclusion of 0 with multiplicity $|C(u_v)| - 1$) because of the fact that $g_v^i = g_v^j$ whenever $i, j \in C(u_v)$ and u_v is at equilibrium. Thus, we can write the spectrum of the Jacobian for a mixed strategy $u^\star$ as

$$\sigma(J(u^\star)) = \bigcup_{v \in V} \left(\{0, -\langle u_v, g_v \rangle\} \cup \{g_v^i - \langle u_v, g_v \rangle; i \notin C(u_v)\} \right)$$

Importantly, we note that, with the inclusion of possible strategies $i \notin C(u_v)$ but $i \in BR(u_v)$, we get additional copies of 0 eigenvalues, bringing the total multiplicity of the zero eigenvalues to

$$\sum_{v \in V} (|BR_v(u^\star)| - 1)$$

□

Without the conditions (a), (b), and (c), we cannot easily compute the eigenvalues in general because B may not be block upper triangular. However, we can say that, when those conditions are not met, the equilibrium is unstable using a Chetaev instability argument.

Lemma 4.9 (Intersecting Best responses)**.** *For an Nash equilibrium of the ODE system 4.4, $u^\star$, in a pure coordination game game with payoff matrix $A = I_m$, If at least two adjacent players v and w satisfy the following*

h1) There exists an $i \in BR_v(u^\star) \cap BR_w(u^\star)$ such one of the following holds:

(a) $u_v^i > 0$ and $u_w^i > 0$

(b) $u_v^i = 0$ and $u_w^i < 1$

h2) $|BR_v(u^\star)| > 1$, and $|BR_w(u^\star)| > 1$

then $u^\star$ is unstable.

Proof. First, observe that the pure coordination game has a symmetric payoff matrix, so we can use the potential $\mathcal{W}(u) = \sum_v \langle u_v, g_v \rangle$. We will formulate a Chetaev instability theorem

argument, so we calculate first the conditions required for $\mathcal{W}(u^\star + x) - \mathcal{W}(u^\star) > 0$. This condition is exactly

$$\sum_{v\in V}\langle x_v, g_v\rangle + \frac{1}{2}\sum_{v\in V}\sum_{w\in V} W_{v,w}\langle x_v, x_w\rangle > 0 \tag{4.13}$$

Let $U_{u^\star} := \{x \in \mathbb{R}^{m\cdot n}; \mathcal{W}(u^\star + x) - \mathcal{W}(u^\star) > 0\}$ We will use the fact that (h1) and (h2) are true to tell us that certainly U is non-empty later.

Let $x \in U$ and observe that for some $v \in V$, $\langle x_v, g_v^\star\rangle + \frac{1}{2}\sum_{w\in W} W_{w,v}\langle x_v, x_w\rangle > \delta$ because the condition in (4.13) is satisfied. Because $u^\star$ is a Nash equilibrium, $\langle x_v, g_v\rangle = \langle u_v + x_v, g_v\rangle - \langle u_v, g_v\rangle \leq 0$, and so $\sum_{w\in V} W_{v,w}\langle x_v, x_w\rangle > 0$. Surely this means that $-\langle x_v, g_v\rangle - \sum_{w\in V} W_{v,w}\langle x_v, x_w\rangle < -\delta < -0$.

Consider now that player v and one of their strategies, $i \in C(u_v^\star)$. Let $|x|$ small enough so that $u_v^{\star i} + x_v^i \neq 0$. At $u^\star + x$, the time derivative of u_v^i is given as

$$\frac{d}{dt}u_v^i = (u_v^{\star i} + x_v^i)\left(\langle \hat{e}^i - u_v^\star - x_v, g_v^\star\rangle + \sum_{w\in V} W_{v,w}\langle \hat{e}^i - u_v^\star - x_v, x_w\rangle\right)$$

With the observation that $\langle \hat{e}^i - u_v^\star, g_v^\star\rangle = 0$, because $u^\star$ is an equilibrium, we get

$$\frac{d}{dt}u_v^i = (\underbrace{u_v^{\star i} + x_v^i}_{>0})\left(\underbrace{-\langle x_v, g_v^\star\rangle - \sum_{w\in V} W_{v,w}\langle x_v, x_w\rangle}_{<-\delta} + \sum_{w\in V} W_{v,w}\langle \hat{e}^i - u_v^\star, x_w\rangle\right)$$

Recall that $C(u_v)$ is the set of all strategies for which $u_v^{\star i} > 0$ and further let j be an index so that

$$j \in \operatorname*{argmin}_{i\in C(u_v)} \sum_{w\in V} W_{v,w}x_w^i.$$

Surely then $\sum_{w\in V} W_{v,w}x_w^j = \langle e^j, \sum_{w\in V} W_{v,w}x_v\rangle$ will be less than any weighted average over $C(u_v)$ of the components of $\sum_{w\in V} W_{v,w}x_w^i$. $\langle u_v^\star, \sum_{w\in V} W_{v,w}x_w^i\rangle$ is such a weighted average, so we can say that

$$\langle e^j, \sum_{w\in V} W_{v,w}x_v\rangle - \langle u_v^\star, \sum_{w\in V} W_{v,w}x_w\rangle \leq 0$$

This means, so long as $0 < \epsilon < \min_{v,i \in V, C(u_v^\star)} u_v^i$, then for any x such that $|x| < \epsilon$ and $\mathcal{W}(u^\star + x) - \mathcal{W}(u^\star) > 0$ it is true that $f_v^j < 0$ for some v and j. By lemma 4.4 We know that $\frac{d}{dt}\mathcal{W}(u(t)) > 0$ whenever $\frac{d}{dt} \neq 0$. Therefore if $x(t) = u(t) - u^\star$ (so $\frac{d}{dt}x(t) = \frac{d}{dt}u(t)$) and we let $\mathcal{V}(x) = \mathcal{W}(u^\star + x) - \mathcal{W}(u^\star)$ then we can say the following:

$$\mathcal{V}(x) > 0 \implies \mathcal{W}(u^\star + x) - \mathcal{W}(u^\star) > 0 \implies x \in U$$

and U is open.

$$x \in U \cap B_\epsilon(u^\star) \implies f_v^j(u^\star + x) \neq 0 \implies \frac{d}{dt}\mathcal{W}(u^\star + x(t)) > 0 \implies \frac{d}{dt}\mathcal{V}(x(t) > 0$$

This is sufficient for the Chetaev instability theorem to imply that $u^\star$ is unstable as long as we show that U is nonempty. More specifically, to show that it is unstable to perturbations in the invariant manifold, we want to show that $U \cap B_\epsilon(u^\star) \cap ((\Delta^{m-1})^V - u^\star) \neq \emptyset$. We can construct an element of this set using (h1) and (h2). Let v, w be a pair of adjacent players satisfying both hypotheses. Without loss of generality, let $v = 1$ and $w = 2$. Suppose $i, j \in BR_1(u^\star)$ and that $i, k \in BR_2(u^\star)$. So that (in case (a)) $i \in C(u_1) \cap C(u_2) \cap BR_1(u^\star) \cap BR_2(u^\star)$. Let $x_1 = \zeta(\hat{e}^i - \hat{e}^j)$, $x_2 = \zeta(\hat{e}^i - \hat{e}^k)$, and $x_v = \mathbf{0}$ for all other $v \in V$. Observe that $u^\star + x \in (\Delta^{m-1})^V$ and we can choose $\zeta < 0$ so that $x \in B_\epsilon(u^\star)$. If, instead, $i \in C^c(u_1) \cap BR_1(u^\star) \cap BR_2(u^\star)$, and $u_2^i < 1$, as in case (b), we can choose $\zeta > 0$ and, because $C(u_v) \subset BR_v(u^\star)$ is not empty we let $j \in C(u_1)$, still we can say that $u^\star + x \in (\Delta^{m-1})^V$ and still we can find a ζ so that $x \in B_\epsilon(u^\star)$. Finally, we do the computation to show that

$$\begin{aligned}\mathcal{W}(u^\star + x) =& \langle u_1^\star + x_1, g_1 + x_2\rangle + \langle u_2^\star + x_2, g_2 + x_1\rangle \\ &+ \sum_{v>3} \langle u_v, g_v + W_{v,1}x_1 + W_{v,2}x_2\rangle\end{aligned}$$

It is an easy next step to show that

$$\mathcal{W}(u^\star + x) - \mathcal{W}(u^\star) = \langle x_1 g_1^\star \rangle + \langle x_2, g_2^\star \rangle + \sum_{v \in V} W_{v,1} \langle u_v, x_1 \rangle + W_{v,2} \langle u_v, x_2 \rangle$$
$$+ 2\langle x_1, x_2 \rangle$$

From here, we note that because $i, j \in BR_1(u^\star)$, $g_1^i = g_1^j$. Likewise $g_2^i = g_2^k$ and so $\langle x_1, g_x \rangle = \langle x_2, g_2 \rangle = 0$. Moreover, we can move the sum into the inner products and see that $\sum_{v \in V} W_{v,1} \langle u_v, x_1 \rangle = \langle g_1, x_1 \rangle = 0$. The same can be done for player 2, and so we get

$$\mathcal{W}(u^\star + x) - \mathcal{W}(u^\star) = 2\langle x_1, x_2 \rangle = 2(1 + \delta_{j,k})\zeta^2 > 0$$

Therefore, we have shown that $x \in U$, and thus, the Chetaev instability theorem implies that $u^\star$ is unstable when it satisfies (h1) and (h2).

□

Not only does this lemma tell us something about when a mixed strategy equilibrium is unstable, but it also tells us something about the quality of stable mixed strategy equilibria.

Lemma 4.10 (Mixed strategies in manifolds of equilibria)**.** *For the pure coordination game, any stable mixed strategy equilibrium exists in a manifold of equilibria containing at least two pure strategy equilibria.*

Proof. Lemma 4.9 says that if (h1) and (h2) are both satisfied, then a mixed strategy equilibrium, u, cannot be stable. Therefore, if we suppose there is a stable mixed strategy equilibrium, it does not satisfy h1 and h2. Lemma 4.8 describes the eigenvalues in this case.

Suppose by way of contradiction that u is stable and that at v has $|C(u_v)| > 1$. In particular, u_v lies in some subsimplex of Δ^{m-1} which is the set of convex combinations of pure strategies in $C(u_v)$. Call this subsimplex Z. $\max\{\sigma(J(u))\} = 0$ because it can't be positive (lest it be unstable), and for a mixed strategy, 0 must always be an eigenvalue. Note that all the neighbors of v either are playing only 1 strategy or are not playing any strategy in $C(u_v)$.

For any neighbor, w whose support does not overlap, if v changes their strategy to any other strategy, $u' \in Z$,

$$\frac{d}{dt}u_w^i = u_w^i\langle \hat{e}^i - e_w, g_v + x\rangle$$

where $x = u' - u$. Clearly for strategies $i \in C(u_w)$ $\langle \hat{e}^i - u_w, x\rangle = 0$ because $i \neq C(u_v)$. Moreover, for $i \notin C(u_w)$ it is immediate that $\frac{d}{dt}u_w^i = 0$. Therefore, if v changes their strategy to any strategy in Z, all of the adjacent players with non-overlapping supports are still at equilibrium.

Any player that does have an overlapping support is also still at equilibrium because it must be playing a single strategy.

Finally, we show that the player v is still at equilibrium after changing their strategy to any strategy in Z

$$\frac{d}{dt}u_v^i = u_v^i(\langle \hat{e}^i - u_v, g_v\rangle - \langle x, g_v\rangle)$$

for any $i \notin C(u_v)$ this is obviously zero. For any $i \in C(u_v)$, $\langle \hat{e}^i - u_v, g_v\rangle = 0$ because u was assumed to be an equilibrium. Also $\langle x, g_v\rangle = 0$ because whenever $g_v^i = g_v^j$ for all $i, j \in C(u_v)$ and because of the construction of Z. Therefore $\frac{d}{dt}u_v = 0$.

We have shown that in this case the stable mixed strategy u exists in a manifold of equilibria, which connects the corners of the subsimplex Z in which the player v is playing a pure strategy.

If we start from the mixed strategy u which satisfies the hypotheses of lemma 4.8 and do this procedure to reach the (possible mixed) strategy u'. The number of players playing mixed strategies has decreased, and u' must still satisfy the hypotheses of the lemma 4.8, and so this procedure can be repeated until we reach a pure strategy.

Thus, every stable mixed strategy exists in a manifold of equilibria containing at least 2 pure strategies. The stability of every equilibrium in the manifold may change across the manifold. □

With these lemmas, we can partially characterize the behavior of solutions in the vicinity of a pure strategy equilibrium. If the pure strategy is a strict Nash equilibria it

is asymptotically stable. If the pure strategy is a non-strict Nash equilibrium satisfying the conditions of lemma 4.9 or if it is not a Nash equilibrium, it is unstable in the Lyapunov sense. However, we cannot, in general, give a description of the behavior in the vicinity of an equilibrium which does not satisfy the conditions of lemma 4.9 at present. We know that they are at best Lyapunov stable (not locally asymptotically stable) because of lemma 4.10. The stability of such an equilibrium is highly dependent on the payoff matrix A, and even the symmetry condition is not sufficient to complete the characterization of behaviors in the vicinity of equilibria. Our final approach in this manuscript is to use the center manifold theorem in a subcase of the case not yet characterized.

The reason that this is attainable for the pure coordination game, and not in general, is because of the form of the Jacobian matrix. For a coordination game, the diagonal blocks of the Jacobian remain unchanged, but the off diagonal blocks become rather simple. $J_{v,w}(u) = diag(u_v) - u_v u_v^\intercal$. With this simplified Jacobian, we can find the eigenvalues for some mixed strategies. First, notice that any mixed strategies wherein two adjacent players are both playing mixed strategies with intersecting support satisfy the hypotheses of lemma 4.9 and any such equilibrium is unstable. It is our next task to determine the stability of the Jacobian for a mixed strategy equilibrium which does not satisfy (h1) and (h2). We first introduce a lemma to characterize the 0-eigenspace in this case.

Lemma 4.11 (Eigenspaces for zero eigenvalues when (h1) or (h2) is not satisfied)**.** *If $u^\star$ is a Nash equilibrium and there are no two adjacent players for which (h1) and (h2) hold, then the eigenvalue $\lambda = 0$ is nondegenerate, and the eigenspace E_0 is described as $E_0 = \sum E_v^0$ where*

$$E_v^0 = \left\{ x \in \mathbb{R}^{m\cdot n}; x_w^i = 0 \text{ if } w \neq v, x_v^i = 0 \text{ if } i \notin BR_v(u^\star), \sum_i x_v^i = 0 \right\}$$

Proof. We begin by saying that if there are no adjacent players for which (h1) and (h2) hold, this means that for any pair of players v, w, one of the following must hold

a $|BR_v(u^\star)| = 1$ or $|BR_w(u^\star)| = 1$

b $W_{v,w} = 0$

c if $i \in BR_v(u^\star) \cap BR_w(u^\star)$ then $u_v^i = 1$ and $u_w^i = 0$ or $u_w^i = 1$ and $u_v^i = 0$

Negating the (h1) and (h2) is not immediate, but it is a simple exercise in Boolean algebra so it is presented here without proof. Point a here implies point a of lemma 4.8 that $|C(u_v)| = 1$ or $|C(u_w)| = 1$. Point b is equivalent to point b of lemma 4.8, and point c implies point c of lemma 4.8. Therefore, if there are no adjacent players for which (h1) and (h2) hold, then we are in the case discussed in lemma 4.8 and can therefore describe the eigenvalues directly. Importantly if 0 is an eigenvalue, it has multiplicity $\sum_{v \in V}(|BR_v(u^\star)| - 1)$.

Let $x \in E_v^0$ and without loss of generality let $v = 1$. Just as before, order the variable in x so that it may be expressed as $[x^1, x^2, ..., x^n, x_1, ...x_n]$ where the x^v corresponds to strategies played by player v and x_v corresponds to strategies not played by player v. This is now a vector which is indexed by a strategy player pair. For instance $[x]_{i,w} = [x_w]_i = x_w^i$. Likewise, when we apply the Jacobian, Jx is a vector which we index in the same way. $[Jx]_{i,w}$ is the the component of Jx corresponding to the player w and strategy i. With J organized as before we get that, for $i \in C(u_w)$

$$[Jx]_{i,w} = [B_{w,1}x^1 + B_{w,2}x^2 + ... + B_{w,n}x^n + X_{w,1}x_1 + ... + X_{w,n}x_n]_i$$

and for $i \in C^c(u_w)$

$$[Jx]_{i,w} = [Y_{w,1}x^1 + Y_{w,2}x^2 + ... + Y_{w,n}x^n + D_{w,1}x_1 + ... + D_{w,n}x_n]_i$$

Because $x^v = 0$ and $x_v = 0$ for all $v \neq 1$ we get can reduce this to write

$$[Jx]_{i,w} = B_{w,1}x^1 + X_{w,1}x_1 \text{ or } [Jx]_{i,w} = Y_{w,1}x^1 + D_{w,1}x_1$$

I will proceed to show that this is 0 for all i. First, if $i \in C^c(u_w)$ and $w \neq 1$, then $[Jx]_{i,w}$ is obviously 0 because $Y_{w,1} = 0$ and $D_{w,1} = 0$. Also, if $i \in C^c(u_1)$, but $w = 1$, then still $Y_{1,1} = 0$ and $[D_{1,1}x_1]_i = (g_1^i - \langle u_1, g_1 \rangle)[x_1]_i$. Whenever $[x_1]_i \neq 0$, it implies that $i \in BR_1(u^\star)$ and so

$g_1^i = \langle u_1, g_1 \rangle$. Thus $(g_1^i - \langle u_1, g_1 \rangle)[x_v]_i = 0$. Clearly, if $[x_1]_i = 0$, then it is also true that $(g_1^i - \langle u_1, g_1 \rangle)[x_1]_i = 0$. Therefore $[D_{1,1}x_1]_i = 0$, and thus, $[Jx]_{i,w} = 0$ for any $i \in C^c(u_w)$.

For $i \in C(u_1)$, we note that $[B_{1,1}x^1]_i = \sum_{j \in C(u_v)} u_1^i \langle u_v, g_v \rangle [x^1]_j$ by the computation from lemma A.2 from appendix A.1. Moreover $[X_{1,1}x_1]_i = \sum_{j \in C^c(u_v)} u_1^i g_1^j [x_1]_j$. Again, $[x_1]_j \neq 0$ only when $j \in BR_1(u^\star)$, and thus $g_1^j = \langle u_v, g_v \rangle$. Therefore,

$$[Jx]_{i,1} = \sum_j u_1^i \langle u_1, g_1 \rangle [x]_j = u_1^i \langle u_1, g_1 \rangle \sum_j [x]_j = 0$$

, and so $[Jx]_{i,1} = 0$ for any $i \in C^c(u_w)$ for any w.

Lastly, if we consider $i \in C(u_w)$ for $w \neq 1$, we must show that $B_{w,1}x^1 + X_{w,1}x_1 = 0$. This can be shown through an unfortunate number of steps. First we consider $B_{w,1}x^1$. We know that

$$[B_{w,1}x^1]_i = \sum_{j \in C(u_1)} W_{w,1} u_w^i (\delta_{i,j} - u_w^j) x_1^j.$$

Between vertices 1 and w, at least one of (a), (b), or (c) must be true. If (b) is true, then clearly this sum is 0. If (a) is true then either $|BR_1(u^\star)| = 1$ or $|BR_w(u^\star)| = 1$. If $|BR_1(u^\star)| = 1$ then $E_v^0 = \{0\}$ so again the sum is zero. If $|BR_w(u^\star)| = 1$ then $|C(u_w)| = 1$. Note that this means that $u_w^i(\delta_{i,j} - u_w^j) = 0$ for all j because if $i \neq j$ then at least one of u_w^i and u_w^j is zero and if $i = j$ then they are either both 0 or both 1. Therefore, again, the entire sum is 0.

If (c) is true, there are several cases. In the case where $BR_w(u^\star) \cap BR_1(u^\star) = \emptyset$ then if $x_1^j > 0 \implies u_w^j = 0$ because $C(u_w) \subset BR_w(u^\star)$. Examining each term, if $i \neq j$ then $(\delta_{i,j} - u_w^j) = 0$ so the entire term is 0. If $i = j$ then $u_w^i = 0$ so again the whole term is 0. Therefore, the entire sum is 0 in this case.

The next case is that there is a $k \in BR_w(u^\star) \cap BR_1(u^\star)$ and $u_w^k = 1$ and $u_1^k = 0$. If $u_w^k = 1$ then $|C(u_w)| = 1$ so, by the same argument as in the previous paragraph, $u_w^i(\delta_{i,j} - u_w^j) = 0$ for all j and so the sum is 0. In the last case $k \in BR_w(u^\star) \cap BR_1(u^\star)$ and $u_w^k = 0$ and $u_1^k = 1$. This means that if $x_1^j > 0$ then $j \in BR_1(u^\star)$ so either $j \notin BR_w(u^\star)$ which means that $j \notin C(u_w)$ so $u_w^j = 0$ or $j = k$ and $u_w^k = 0$. With this observation, if $i \neq j$ then

$\delta_{i,j} - u_w^j = 0$, and if $i = j$ then $u_w^i = 0$ so $u_w^i(\delta_{i,j} - u_w^j) = 0$. In either case, every term in the sum is 0, and so the entire sum is 0.

We have shown that if at least one of (a), (b), or (c) holds, then $B_{w,1}x^1 = 0$. Now we proceed to show that $X_{w,1}x_1 = 0$.

$$[X_{w,1}x_1]_i = \sum_{j \in C^c(u_1)} W_{1,w}u_w^i(\delta_{i,j} - u_w^j)[x_1]_j$$

Again, if (a) holds and $|BR_1(u^\star)| = 1$ then $x = 0$ so this sum is zero. If (a) holds and $|BR_w(u^\star)| = 1$ then $|C(u_w)| = 1$ and so $u_w^i(\delta_{i,j} - u_w^j) = 0$ for all j and so again the sum is 0. It is again obvious that if (b) holds, then this sum is 0. Thus, we have shown that if (c) holds, then the sum is equal to 0. Notice that because u_1 is not part of the sum, the same arguments that we used on $\sum_{j \in C(u_1)} W_{w,1}u_w^i(\delta_{i,j} - u_w^j)x_1^j$ hold for $\sum_{j \notin C(u_1)} W_{w,1}u_w^i(\delta_{i,j} - u_w^j)x_1^j$. This means the argument that $B_{w,1}x^1 = 0$ can be applied again to show that $X_{w,1}x_1 = 0$. Therefore we can say that $[Jx]_{i,w} = B_{w,1}x^1 + X_{w,1}x_1 = 0$ for $i \in C(u_w)$.

What we have shown is that for any strategy player pair (i, w), $[Jx]_{i,w} = 0$ and because our choice of $v = 1$ in E_v^0 was arbitrary, this proves the claim that $Jx = 0$ for $x \in E_v^0$ for any v whenever (h1) or (h2) is false. It is obvious that there are $|BR_v(u^\star)| - 1$ degrees of freedom for $x \in E_v^0$ and so the dimension of $E_v^0 = |BR_v(u^\star)| - 1$. Because $\langle x, y \rangle = 0$ for $x \in E_v^0, y \in E_w^0$ for $v \neq w$ we know that the sum of these eigenspaces has dimension $\sum_{v \in V}(BR_v(u^\star) - 1)$ which is exactly the multiplicity of the eigenvalue 0 by lemma 4.8. □

This characterization of the eigen-system coincides exactly with that of lemma 4.6 for pure strategies. This means that we are in the situation where, for an equilibrium of a coordination game, we can either characterize the kernel of the Jacobian evaluated at the equilibrium, or we can show that that equilibrium is unstable with the Chataev function. This is the last step we need to carry out the final method of this chapter involving the center manifold through equilibria, for which we can compute the kernel (also called the center space).

Lemma 4.12 (Stationary Solutions on the center manifold.)**.** *Suppose that $u^\star$ is a non-strict Nash equilibrium to the pure coordination game. If, for any pair of players v, w, one of the following holds:*

1. $W_{v,w} = 0$
2. $|BR_v(u^\star)| = 1$ *or* $|BR_w(u^\star)| = 1$
3. $BR_v(u^\star) \cap BR_w(u^\star) = \emptyset$

then solutions in the neighborhood of $u^\star$ converge to the center space E_0 on which solutions are stationary.

Proof. In the course of this proof, it will be convenient to describe all the strategy player pairs (i, v) so that $\hat{e}^i$ is contained in the 0 eigenspace corresponding to the player v. This condition is equivalent to saying that there is a vector $z \in E_0$ so that $z_v^i \neq 0$. For clarity, we will say that a strategy player pair is "in" E_0 if there is a $z \in E_0$ so that $E_v^i \neq 0$.

It is immediate, by the center manifold theorem, that, in a neighborhood of the equilibrium $u^\star$, because it is a Nash equilibrium and thus there is no unstable space, solutions converge to the center manifold.

In the case described in the hypotheses (which fall under the conditions of lemma 4.8 excluding the case wherein $W_{v,w} = 1$, $|BR_v(u^\star)| > 1, |BR_w(u^\star)| > 1$ and $i \in BR_v(u^\star) \cap BR_w(u^\star)$,$u_v^i = 1$ and $u_w^i = 0$) The center space solves the center manifold problem. In more detail, shift the ODE system so that the equilibrium $u^\star$ is at the origin. Call the new system $\tilde{f}$. Let $(x, y) = u$ where $x \in E_0$ and $y \in E_0^\perp$ and let our ODE system $\frac{d}{dt}u = \tilde{f}(u)$ be separated into

$$\frac{d}{dt}x = L_0 x + F(x, y)$$
$$\frac{d}{dt}y = L_1 y + G(x, y)$$

where L_0 and L_1 are the linearizations of $\tilde{f}$ about 0 and F, G are continuous functions with 0 gradient at $(0, 0)$.

Because, when the hypotheses are satisfied, all the eigenvalues are real by lemmas 4.5 and 4.8, it is certain that $L_0 = \mathbf{0}$. The center manifold can be described locally as $h : E_0 \to E_0^{\perp}$, so locally the dynamics are described as

$$\begin{aligned}\frac{d}{dt}x &= F(x, h(x)) \\ \frac{d}{dt}y &= L_1 h(x) + G(x, h(x))\end{aligned}$$

Because the center manifold is invariant under the dynamics of $\tilde{f}$, we get that $\frac{d}{dt}y = Dh(x)\frac{d}{dt}x$, which results in the following problem.

$$Dh(x)(F(x, h(x))) = L_1 h(x) + G(x, h(x)) \tag{4.14}$$

To show that the center manifold and the center space coincide, we need only show that $h(x) \equiv 0$ solves equation (4.14). That is equivalent to showing $G(x, 0) \equiv 0$.

Let $\tilde{f}(z) = f(u^\star + z)$ and subtract the linearization to get that

$$\begin{aligned}\tilde{f}_v^i(z) &= (u_v^{\star i} + z_v^i)\left(\langle \hat{e}^i - u_v^\star - z_v, g_v^\star\rangle + \sum_{w\in V} W_{v,w}\langle \hat{e}^i - u_v^\star - z_v, z_w\rangle\right) \\ &= \underbrace{u_v^{\star i}\langle \hat{e}^i - u_v^\star, g_v^\star\rangle}_{=0} + \\ &\quad \underbrace{z_v^i\langle \hat{e}^i - u_v^\star, g_v^\star\rangle + u_v^{i\star}\langle -z_v, g_v^\star\rangle + u_v^{i\star}\sum_{w\in V} W_{v,w}\langle \hat{e}^i - u_v^\star, z_w\rangle}_{[J(u^\star)z]_v^i} + \\ &\quad z_v^i\langle -z_v, g_v\rangle + z_v^i\sum_{w\in V} W_{v,w}\langle \hat{e}^i - u_v^\star, z_w\rangle + (u_v^i + z_v^i)\sum_{w\in V} W_{v,w}\langle -z_v, z_w\rangle\end{aligned} \tag{4.15}$$

Thus, $F(z)$ and $G(z)$ are the higher order terms of (4.15). In particular, $G_v^i(z)$ is the nonlinearity for player strategy pairs v, i not in the space E_0. $F_v^i(z)$ is the nonlinearity for the player strategy pairs v, i in the space E_0. The nonlinear terms are expressed as

$$G_v^i(z) = z_v^i\langle -z_v, g_v\rangle + z_v^i \sum_{w\in V} W_{v,w}\langle \hat{e}^i - u_v^\star, z_w\rangle + (u_v^{i\star} + z_v^i)\sum_{w\in V} W_{v,w}\langle -z_v, z_w\rangle. \tag{4.16}$$

For $z = (x, y)$, $y = 0$, we mean that the only nonzero components of z are in E_0. Thus if $z_v^i \neq 0$ then $i \in BR_v(u^\star)$ and $|BR_v(u^\star)| > 1$. From this, we can immediately conclude that $G_v^i \equiv 0$. If (i, v) is not a strategy player pair included in E_0, then $i \notin BR_v(u^\star)$. Therefore, for any strategy player pair not in E_0, $z_v^i = 0$. The first two terms are immediately evaluated to zero, and because $i \notin C(u_v)$, the third term is also evaluated to zero.

Moreover, we can show that $F_v^i(z) = 0$ for $z = (x, 0)$ as well. The first term in (4.16) is 0 because if $z_v^i \neq 0$ then $i \in BR_v(u^\star)$, Moreover, if $i, j \in BR_v(u^\star)$ then $g_v^i = g_v^j$. Thus $-\langle z_v, g_v\rangle = -g_v^i \sum_{i\in C} z_v^i = 0$.

We can prove that the second term is zero in the following way. If $z_v^i > 0$ then $i \in BR_v(u^\star)$ and $|BR_v(u^\star)| > 1$. If $W_{v,w} > 0$, then either $|BR_w(u^\star)| = 1$ or $BR_w(u^\star) \cap BR_v(u^\star) = \emptyset$. In the former case, $z_w = \mathbf{0}$ so $\langle \hat{e}^i - u_v^\star, z_w\rangle = 0$. In the latter case, this implies that $z_w^j = 0$ for any $j \in BR_v(u^\star)$. Because the only nonzero components of $(\hat{e}^i - u_v)$ are in $BR_v(u^\star)$, surely $\langle \hat{e}^i - u_v^\star, z_w\rangle = 0$. (recall that in F_v^i, (i, v) is a strategy player pair in E_0 so certainly $i \in BR_v(u^\star)$).

Finally, the last term is zero because if $(u_v^{i\star} - z_v^i) \neq 0$ then $i \in BR_v(u^\star)$ (because if not, both $u_v^i\star = 0$ and $z_v^i = 0$). Therefore if $W_{v,w} > 0$ then, again, either $|BR_w(u^\star)| = 1$ or $BR_w(u^\star) \cap BR_v(u^\star) = \emptyset$. In the former case, $z_w = \mathbf{0}$ so $\langle \hat{e}^i - u_v^\star, z_w\rangle = 0$. In the latter case, $z_w^i = 0$ if $i \in BR_v(u^\star)$, and $z_v^i = 0$ if $i \notin BR_v(u^\star)$, so $\langle z_v, z_w\rangle = 0$.

We have therefore shown that $G(x, 0) = 0$ and $F(x, 0) = 0$. This is equivalent to showing that $h \equiv 0$ is a center manifold and that solutions are stationary on this center manifold. Although the uniqueness of the center manifold is not guaranteed, we can be assured of the uniqueness of the dynamics on the center manifold.

Because $f \in C^\infty$, we know that any center manifold will also be C^∞ but not necessarily analytic. However, a result from Deng (2023) says that if two Center manifolds W_1^c and W_2^c exist and are both C^k then there is a $\kappa \in C^k$ where $\kappa : W_c^1 \to W_c^2$ so that $\kappa(f(x)) = f(\kappa(x))$

for all $x \in W_c^1 \cap B_\epsilon(u^\star)$. Because the dynamics on the center space are stationary, we know that the dynamics on any other center manifold (Which must also be C^k) are also stationary. Thus, locally, solutions near $u^\star$ converge to a center manifold, and the system is stationary on any center manifold.

Having shown this, it is an easy application of the reduction principle of Carr (1982) for the center manifold to say that, because on the center manifold $u^\star$ is Lyapunov stable, then $u^\star$ is Lyapunov stable for the entire system. □

This allows us to partially characterize the behavior of the system in the vicinity of different game states.

Theorem 4.4 (Partial characterization of pure strategy equilibria for pure coordination)**.** *Let $u^\star$ be a pure strategy equilibrium to a pure coordination game ($A = I_m$) played on the graph G for the ODE system (4.4). We can characterize the stability in the following way*

1. *If $u^\star$ is a strict Nash equilibrium, it is asymptotically stable*
2. *If it is a Nash equilibrium but it is not a strict Nash equilibrium and it satisfies the hypothesis of lemma 4.12, then it is Lyapunov stable*
3. *If it is a Nash equilibrium but not a strict Nash equilibrium and satisfies the hypothesis of lemma 4.9, then it is unstable in the Lyapunov sense*
4. *If it is not a Nash equilibrium, then it is unstable*

Proof. Conditions 1 and 4 are direct from theorem 4.2. Condition 2 is direct from lemma 4.12. Condition 3 is direct from lemma 4.9. □

This leaves a critical case missing. The case where (h1) and (h2) are not satisfied there are adjacent players who have overlapping, nontrivial best responses. This happens when two adjacent players, both with non unique best responses to $u^\star$ are playing distinct pure strategies, i and j, with $i, j \in BR_v(u^\star) \cap BR_w(u^\star)$. This case obscures the results because the center manifold is no longer trivial. It is certainly still true that solutions converge to a

solution on the center manifold, but the behavior of the center manifold is undetermined at present and so we cannot say that such an equilibrium is necessarily Lyapunov stable.

4.5 Discussion

The model presented here adapts the well known replicator equation and equips it to model local information in the space of mixed strategies on a static network. We have shown that it is a reasonable evolutionary model as it passes the benchmarks set out by the Folk theorem of evolutionary game theory. This set of results tells us that solutions of the ODE system can give us insight into the behavior of the game in the vicinity of Nash Equilibria. Moreover, when we consider a particular game like the coordination game, it is possible to gain insight in the other direction. This model poses a question that must be answered before we accept it as a reasonable evolutionary model: Does it make sense for an evolutionary model to keep track of local information?"

This question is crucial because evolution, acting on the population level, cannot be used to describe changes in individuals. The argument posed in section 4.1 describes the setting of social learning wherein an individual's use of a strategy changes in proportion to how familiar the individual is with the strategy already. Recently Chiba-Okabe and Plotkin (2024) showed that in the unstructured setting, a modification of the replicator equation was a reasonable model for social learning. However, while this setting may be of interest, it is not the only way in which this model can be helpful. In the present discussion, we will describe two ways that the model can be helpful. The first is proposed applications for its use in understanding elements of the discrete time game, which are difficult or time intensive to predict. The second is an extension of the model which we argue gives evolutionary meaning back to the model in the case where a population is distributed over space and the population is not well mixed (e.g. sessile plants).

4.5.1 Connection to the Discrete Time Game

Beyond being motivated by the same underlying payoff/fitness function. The continuous time game with replicator dynamics and the discrete time game under best response dynamics are closely related. Best response solutions to dynamic games have long been of interest to game theorists as well as those in the application areas. One of the issues is that the best response function is set valued, and even with a proper tie-breaking order it is highly discontinuous in general. There has been much work on the use of the best response dynamic with analytical tools from ODEs (Swenson et al., 2018a,b). In this same tradition, we can use the dynamics of this system to tell us about the best response dynamics of the discrete time game described in chapters 2 and 3

This can be seen rigorously by examining the Morse graph of the ODE system (4.4). The trajectory graph or the Morse graph is a graph of a dynamical system wherein each vertex is a distinct, disjoint, isolated invariant subset of the compact phase space with a directed edge from one vertex to another if the unstable manifold of the origin vertex intersects the stable manifold of the destination vertex. That is, if there is a heteroclinic orbit from one invariant set to another, then there is a directed edge between the associated vertices in the direction of the heteroclinic orbit (Adwani et al., 2025; Wiseman, 2020). The Morse graph is not unique because a heteroclinic orbit, together with its origin and destination, is itself invariant both forwards and backwards.

Recall from chapter 3 that the space of strategy profiles X can be given a discrete metric d where two strategy profiles u and u' are adjacent if one individual changing their strategy in u results in the strategy profile u'. When we used this space for pure coordination games in chapter 3, we modded out strategic permutations $((\mathcal{A}, \tilde{D}) = (X, d)/S_n)$. but this is not necessarily possible for games where strategies are not interchangeable.

Proposition 4.2. *For any Morse graph of the system (4.4) for a linear game with payoff matrix A on the graph G, and for $u, u' \in X$, with $d(u, u') = 1$, then if we represent $u, u' \in (\Delta^{m-1})^V$ and we say M is an invariant set containing u and M' is an invariant set containing u', one of the following is true*

- *There is an edge in the Morse graph from M to M'*
- *there is an edge from the Mores graph from M' to M*
- *M and M' are the same invariant set.*

Proof. If two strategy profiles u and u' are adjacent to one another, then the only difference is that a single player, v, changed their strategy. Let v be player 1 and we can say they changed from strategy 1 to strategy 2.

Translate these strategy profiles u and u' so that they can be described at vectors $u, u' \in (\Delta^{m-1})^V$. Certainly, u and u' are both in invariant sets because they are both equilibria. If they are in the same invariant set, then the proof is complete.

If they are not, we must prove there is a heteroclinic orbit from one to the other. Corollary 4.1 says that the line from u to u' in the domain is itself an invariant manifold. Call this line segment I. We need only show that the sign of f_1^1 does not change on I. By assumption $u' - u = [(\hat{e}^2 - \hat{e}^1)^\intercal, 0^\intercal, ..., 0^\intercal]^\intercal$.

$$f_1^1(u + t(u' - u)) = (g_1^1 - g_1^2)t(1 - t)$$

which does not change sign in t. (Note that g_1^1 and g_1^2 are not changed by player 1 changing their strategy.) This is the familiar logistic equation, and it is clear that trajectories in the 1-dimensional submanifold will move from u to u' if $g_1^1 - g_1^2 < 0$ and from u' to u if $g_1^1 - g_1^2 > 0$. This shows that there is a heteroclinic orbit. In the case where $g_1^1 = g_1^2$, $f_1^1(I) = 0$, and we can show that I is a manifold of equilibria. In this case, for every possible Morse graph of the system, u and u' are in the same invariant set.

This means that either u and u' are connected by a heteroclinic orbit or a manifold of equilibria. Therefore, the proof is complete. □

There are many corollaries to this result that allow us to use the Morse graph to describe trajectories through the strategy space, at least in the sequential update case. To discuss these corollaries, we must describe a particular Mores graph $\mathcal{M}_G$ and introduce an intermediate between X and $\mathcal{M}$.

Definition 4.1 (Morse Graph, $\mathcal{M}_G$)**.** *The Mores Graph M_G is the graph where vertices are isolated (forward and backward) invariant sets of the ODE system (4.4) so that two vertices M_1 and M_2 share an edge if, for any ϵ, there is a trajectory starting in $N_\epsilon(M_1) := \{x \in (\Delta^{m-1})^V; dist(x, M_1) < \epsilon\}$ has an ω-limit set contained in M_2.*

This is like saying the Mores graph with the smallest resolution (for the meaning of "resolution" see Wiseman (2020)).

Definition 4.2 (Contracted Strategy Space, B_G)**.** *Let B_G be the Contracted Strategy Space of (X, d), the directed graph constructed in the following way: Start with the graph (X, d). If two nodes u and u' share an edge in (X, d), they differ by a single player, v playing a different strategy.*

For any edge such that $w_v(u) = w_v(u')$ for that player v which is changing strategy, contract the edge into a single vertex (and if more than two nodes are connected by a sequence of such edges, contract all of the nodes into a single vertex).

The remaining edges represent single strategic changes where, for the player v changing strategy, $w_v(u) \neq w_v(u')$. The edges are directed so that point towards the strategy profiles where v has higher fitness.

With these definitions and the proposition 4.2, several results are immediately obvious.

Corollary 4.3. *Each of the following are true*

1. *B_G is weakly connected and, for potential games, acyclic*
2. *For potential games, $B_G \subset \mathcal{M}_G$*
3. *For a potential game, the partial order ($\prec$) on the isolated invariant sets induced by the Morse Graph satisfies the following $M_1 \prec M_2 \implies \mathcal{W}(u_1) < \mathcal{W}(u_2)$ where M_1, M_2 are isolated invariant sets in the dynamical system and $u_1 \in M_1$ and $u_2 \in M_2$.*
4. *For the pure coordination game, $B_G/S_m \subset \mathcal{M}_G/S_m$ where S_m is the group of permutations of m (the number strategies available). Moreover, B_G/S_m is constructed by doing the same contraction process on $(\mathcal{A}, \tilde{D}) = (X, d)/S_m$.*

5. *For the pure coordination game, if G is indecomposable then $\mathcal{M}_G/S_m$ has a single node with outdegree 0.*

6. *For the pure coordination game, if $\mathcal{M}_G/S_m$ has more than one node of outdegree 0, then there is a non-Consensus Nash Equilibrium.*

7. *For a potential game, if two equilibria u and u' are in the same isolated forward and backward invariant set, then they are connected by a manifold of equilibria which is contained in a connected component of $\mathcal{W}^{-1}(u)$*

8. *if G is indecomposable, a trajectory of the ODE system 4.4 with random initial data and with random noise will converge to a consensus equilibrium with probability 1.*

This demonstrates to us that the dynamics of the ODE system, which are characterized qualitatively by the Morse graph, give us information about how the discrete time system behaves on (X, d) at least in the sequential update case. Because, in the simultaneous update case, strategy profiles do not move around in (X, d), the connection is less obvious but still relevant. Several examples of the connection between these two objects are given in figure 4.4, 4.5. For non-potential games like Rock Paper Scissors, the Morse graph is less useful because of the existence of cycling behavior. The contracted strategy space may be strongly connected (fig. 4.6), and so clearly the subgraph relationship will not hold.

An additional challenge arises when considering a simultaneous update rule as in McAlister and Fefferman (2025); Ashkenazi-Golan et al. (2025) rather than an asynchronous best response update. Even when there are nice potential functions for games, the simultaneous updates may not obey the rule of increasing potential and thus there is no theory of finite improvement chains in this setting.

One of the open questions, in the simultaneous update case, considers the existence of $n-$cycles for $n > 2$. This was posed in detail for the coordination case based off of simulated data in McAlister and Fefferman (2025) (included in section 6) and posed as a more general question for potential games in Ashkenazi-Golan et al. (2025). Although the latter reference shows a proof that such cycles are impossible under simultaneous best response updates in

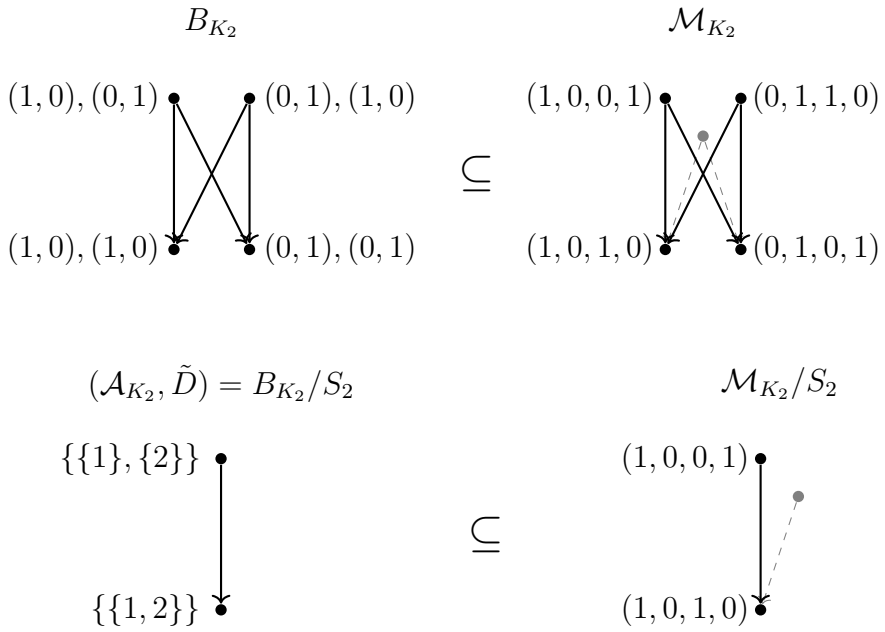

Figure 4.4: The Contracted Strategy Space the pure coordination game on K_2 in the top left, and the Morse graph for the the system on K_2 on the top right, the Contracted strategy space mod permutations in the bottom left, Morse graph with permutations of the equivalent strategies modded out in the bottom right. In the Morse graphs, the nodes which represent mixed strategies and the heteroclinic orbits which do not correspond to edges in $\mathcal{A}, \tilde{D}$ are dashed. Parts 1,2,4,5 of corollary 4.3 are demonstrated in this example. It is easy to see that this example also satisfies part 3 by computing the potentials for each pure strategy.

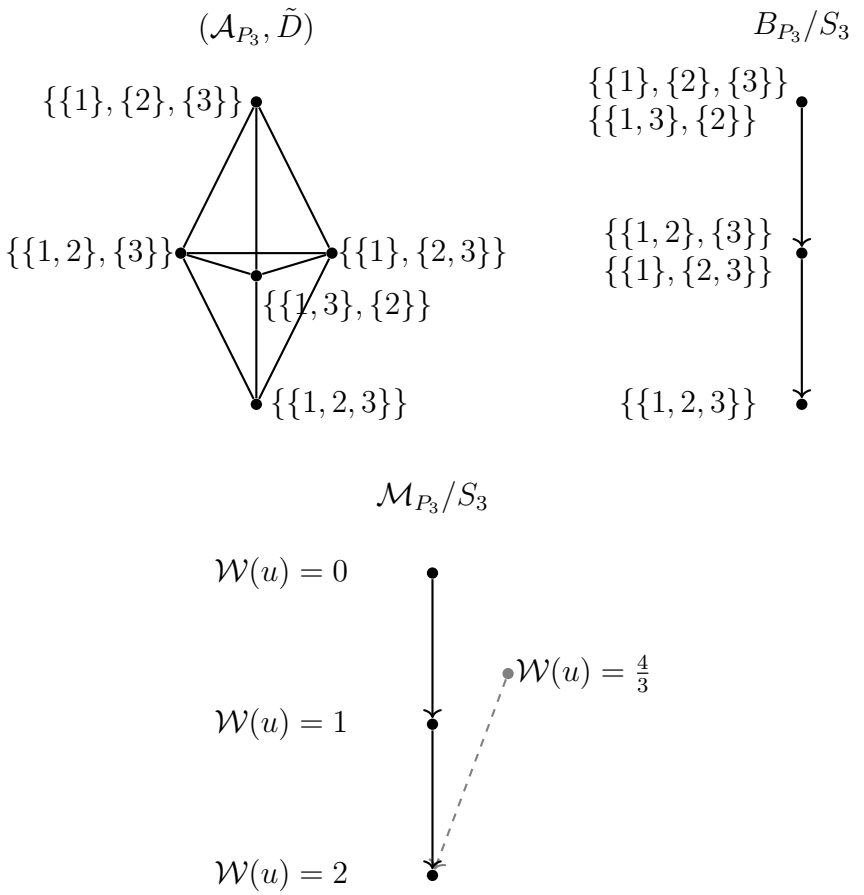

Figure 4.5: The state space $(\mathcal{A}_{P_3}, \tilde{D})$, the contracted strategy space B_{P_3}/S_3 and the Morse graph for the system $\mathcal{M}_{P_3}/S_n$. In the Morse graphs, the nodes which represent mixed strategies and the heteroclinic orbits which do not correspond to edges in $\mathcal{A}, \tilde{D}$ are dashed. Parts, 1-5 of corollary 4.3 are demonstrated here.

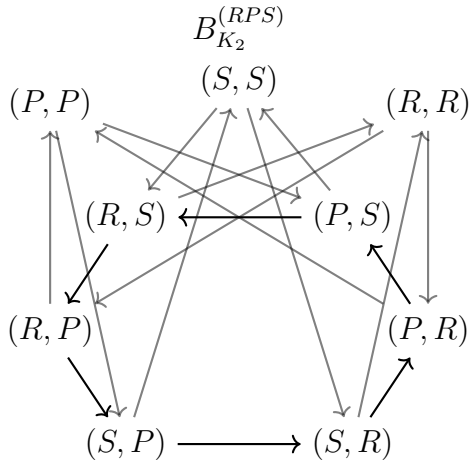

Figure 4.6: The contracted strategy space for Rock Paper Scissors on K_2. observe that it is strongly connected and for that reason, every pure strategy is included in the same isolated invariant manifold. For non-potential games, describing the Morse graph is exceedingly difficult, even for small systems like two player RPS.

two player games, the question is not resolved for larger games. In the continuous setting, however, the question is easily resolved. For exact potential games, cycling behavior is impossible simply by lemma 4.4. This does not present an obvious connection to the discrete time dynamic, but it does provide a new way to approach the question. A conjecture, which would resolve the $n-$cycle conjecture if proven, is that if the discrete time game with payoff matrix A has a deterministic n-cycle, $(u(1), u(2), ..., u(n))$ for $n > 3$ then there is a limit cycle in the simplicial set defined by this set of pure strategies $\{u(1), u(2), ..., u(n)\}$. If this conjecture were to be proven, then because there are no limit cycles in the ODE system for potential games, no potential game could admit an n-cycle for $n > 2$ under simultaneous best response dynamics.

A less speculative connection between this model and the discrete game is the way that this model can be used to evaluate the stability of equilibria. In particular, we can use the model to identify critical levels of connectedness which are required to stabilize or destabilize certain structures. In the most trivial way, for pure strategies and unweighted graphs, we can conduct the stability analysis with edge addition and removal to identify stabilizing or destabilizing edges and non edges. The stability of the continuous time game is given by

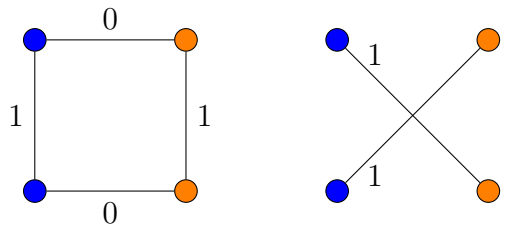

Figure 4.7: The graph C_4 with a non-trivial Nash equilibrium. Two adjacent players play the strategy "blue" while the other two play the strategy "orange". On the left, the edges of C_4 are labeled with their stabilizing weight. Every edge with a positive weight would be destabilizing if it was removed and every edge with a weight of zero can be removed and not change the stability of the equilibrium. Because we know that this graph is a non-strict Nash equilibrium (and so $\max(\sigma(J(u^\star)) = 0)$, any destabilization will result in a game state which is no longer a Nash equilibrium. On the right is the co-graph of C_4 with each edge weighted by its destabilizing effect. Both edges have an equivalent destabilizing effect.

$\lambda_0(u^\star, W) = \max \sigma(J(u^\star; W))$ and so it is an easy exercise to compute this for a modified adjacency matrix W'. If $W' = W - e$ then $\lambda_0(u^\star, W') - \lambda_0(u^\star, W)$ represents the change in stability from the removal of the edge e. If this quantity is positive, then the removal is destabilizing, and if it is negative, the removal is stabilizing.

We can examine to cograph in the same way to think about the effects of edge addition. If now $W' = W + e$, then $\lambda_0(u^\star, W') - \lambda_0(u^\star, W)$ represents the change in stability from the addition of the edge e. If this quantity is positive, then that edge is destabilizing, and if it is negative, the addition is stabilizing. An easy example of this is shown in figure 4.7.

To connect these results to the discrete time game observe that a corollary of lemma 4.5 is that, for pure strategies, when $\lambda_0(u^\star, W) < 0$ then $u^\star$ is a strict Nash equilibrium, if $\lambda_0(u^\star, W) > 0$ then $u^\star$ is not a Nash equilibrium, and if $\lambda_0(u^\star, W) = 0$ $u^\star$ is a Nash equilibrium but it is not strict. Using these facts, along with this method for describing the stabilizing effects of each edge, we can identify areas in graphs with nontrivial equilibria where structural changes to the graph may have large impacts on the game. This insight may be used to build networks with promote or suppress certain nontrivial equilibria even in settings more complicated than the pure coordination game, where the outcome is less obvious (Fig. 4.8)

$$A = \begin{bmatrix} 10 & 1 & -10 \\ 1 & 0 & 1 \\ -10 & 1 & 10 \end{bmatrix}$$

$$\lambda_0 = -6$$

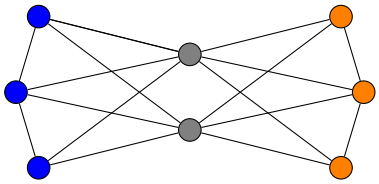

	graph (edge removal)	co-graph (edge addition)
critically destabilizing	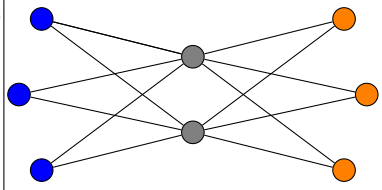	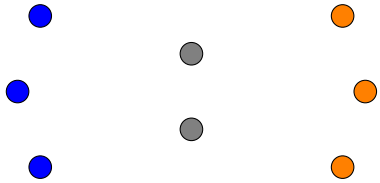
mildly destabilizing	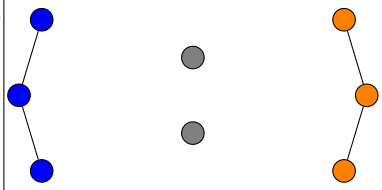	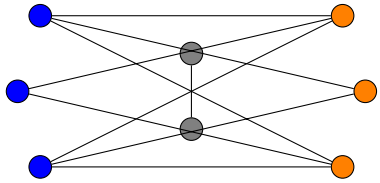
neutral or stabilizing	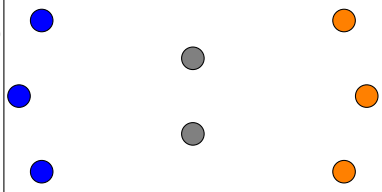	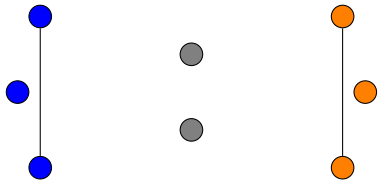

Figure 4.8: With the above adjacency matrix, A, the strategy profile on the graph shown (where strategy 1 is blue, strategy 2 is gray, and strategy 3 is orange) has a maximum eigenvalue of -6 and thus is locally asymptotically stable in the continuous time model (and therefore a strict Nash Equilibrium). In the table below, Edges of the graph are classified in the left column and edges of the co-graph are classified in the right column. An edge is critically destabilizing if its addition or removal would make the maximal eigenvalue positive (and thus make the strategy profile no longer a Nash Equilibrium). An edge is mildly destabilizing if its addition or removal would increase the maximal eigenvalue but not make it positive. An edge is neutral or stabilizing if its addition or removal would not change the maximal eigenvalue.

This means that, for any game described by a payoff matrix A over a set of players V with an undetermined relational structure, for a particular desired strategy profile, we can design a relational structure to maximize the stability of that strategy profile. In order to see this, we must permit $W \in [0,1]^{n\times n}$ to be a weighted adjacency matrix with bounded weights. We simply seek $W \in [0,1]^{n\times n}$ which minimizes $\lambda_0(u^\star; W)$. Although $\lambda_0(u^\star; W)$ does not have a derivative everywhere, we can argue, because of continuity with respect to parameters, and because of the finiteness of W, that this quantity is Lipschitz continuous and thus has a weak derivative. If we use a gradient descent method for weak derivatives, we can construct solutions to $\mathbf{0} = D_W\lambda_0(u^\star, W)$ where $\mathbf{0}$ is the zero matrix.

This method has the same drawbacks that all gradient descent methods have. Namely, finding the global minimum requires a good apriori estimate of the global minimizer. However, with more study for particular games about the size of the basins of stability for the weak gradient flow $\frac{d}{dt}W(t) = D_W\lambda_0(u^\star; W)$ could provide optimized methods for constructing maximally stable assemblages to achieve desired strategic outcomes. For the easy case of coordination, we know that this gradient flow will always result in different strategic communities being segregated into different connected components, each of which are themselves complete. Different games with complex structure may have more interesting results (Fig. 4.9).

We also note that the results of this optimization procedure for the linear game are not hard to predict through other methods. These networks are, in general, easy to construct by considering only the pairwise interactions. For the linear games, there are no critical points on the interior of the domain $[0,1]^{n\times n}$, any edge given a weight which is not 0 or 1 is due to the fact that changing that edge weight does not change λ_0 given the current adjacency matrix. Should this model and the associated optimization procedure be extended to work for nonlinear games, then this optimization procedure may be more useful. This method and related results are an area for future investigation.

A	$\begin{bmatrix} 1 & 0 & 0 \\ 0 & 1 & 0 \\ 0 & 0 & 1 \end{bmatrix}$	$\begin{bmatrix} -1 & 0 & 0 \\ 0 & -1 & 0 \\ 0 & 0 & -1 \end{bmatrix}$	$\begin{bmatrix} 10 & 1 & -10 \\ 1 & 0 & 1 \\ -10 & 1 & 10 \end{bmatrix}$
$W^\star$	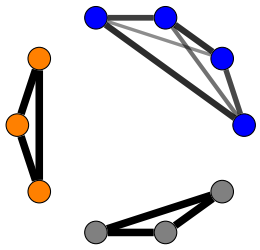	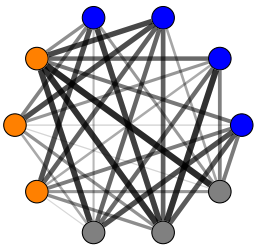	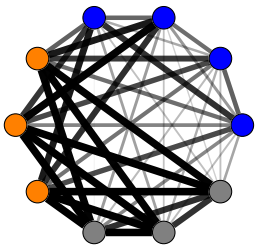
λ_0	-2	0	-5.46

Figure 4.9: For three different games, the same strategy profile can be made into a Nash equilibrium with a different community structure. In this figure, blue is strategy 1, orange is strategy 2, and gray is strategy three. On the left, when the game is a pure coordination game, the strategy profile can be made into a strict Nash equilibrium when the network is disconnected, and each connected component is a complete graph spanning the strategic communities. In the middle, the anti-coordination game can be made into a (non-strict) Nash equilibrium when the network is a complete multipartite network where each strategic community is a part. On the right, the strategy profile can be made into a Nash equilibrium with respect to the pairwise payoff A through the minimization of $\lambda_0(u^\star; W)$.

4.5.2 Further Extensions in Continuous Settings

Excitingly, the ability to use replication dynamics in structured player spaces opens the door for extensions into continuous player spaces. It is easy to extend when the player space is a subset of $\mathbb{R}^n$ by replacing the sum against the adjacency matrix with integration against an integrable kernel $K \in C_b^0(\Omega; L^1(\Omega))$ (meaning that for every value of $x \in \Omega$, $K(x, \cdot) \in L^1(\Omega)$ and $K(x, \cdot)$ is continuous and bounded in the L^1 sense in x. The result is the non-local equation

$$\frac{\partial}{\partial t} u^i = u^i \left\langle \hat{e}^i - u^i, A\left(\int_\Omega K(x, y) u(y) dy \right) \right\rangle.$$

Adopt the same notation as before and write the nonlocality as

$$g[u] = A(\int_\Omega K(x, y) u(y) dy)$$

and we get $\frac{\partial}{\partial t} u^i = u^i \langle \hat{e}^i - u^i, g[u] \rangle$. In settings where the population density in the player space is not uniform we can consider a population $P(x)$ and the nonlocality becomes $g[u] = \int_\Omega K(x, y) P(y) u(y) dy$ which will continue to satisfy the property that $\sum_i u^i(x) \equiv 1$. In this way, the evolution equation describes the evolution of a partition of unity across some population distribution. Through standard techniques like a Picard iteration approach, we can show that solutions to this equation exist and are unique for some time.

The main benefit of this extension is that the model can be used in an evolutionary biological context again. Consider a population occupying a continuous spatial domain Ω whose individuals are not well mixed. For each point in the domain $x \in \Omega$, $u(x)$ is a distribution of the strategies found in the subpopulation at x. Although the individuals are not well mixed, fitness is still determined by their ability to compete with the population in its vicinity (given by $K(x, \cdot)$), and so through time, the distribution of strategies changes in response to the distribution of strategies present around them.

Certainly, this is not the only way to describe the ways that a continuous strategic landscape changes in time. Other models where individuals move around in space up

strategic gradients also exist. Yao and Cooney (2025); Yao et al. (2025); Cheng et al. (2026) all examine such systems when limited to two strategies, which can be categorized as "cooperating" and "defecting." These PDE models capture movement within the domain from individuals and can exhibit highly oscillatory behavior and Turing instability. Our nonlocal approach can be adapted to any normal form game and can exhibit similar types of behavior.

Example 4.1 (Rock-Paper-Scissors Flowers)**.** *Consider a population of plants competing for the attention of pollinators. If a pollinator visits a plant at point x, the probability that it will also visit a plant at point y is given by $K(x, y)$. Suppose there are three flower variations this plant may have: the Rock variant, the Paper variant, or the Scissors variant. Given the choice between a Rock and a Paper flower, the pollinator will choose Paper. Given the choice between Paper and Scissors, the pollinator will choose Scissors, but (in order to make the example non-trivial), given the choice between Scissors and Rock, the pollinator will choose Rock. This gives us a Rock Paper Scissors type game with an adjacency matrix*

$$A = \begin{bmatrix} 0 & -1 & 1 \\ 1 & 0 & -1 \\ -1 & 1, & 0 \end{bmatrix}.$$

In this example, through forward Euler type numerical methods, simulated solutions to this model show propagating waves throughout the domain (Fig. 4.10). There is no motion of the population itself, but the behaviors that are selected for propagate through a static population.

Example 4.2 (Anti-coordination)**.** *Consider an infinite patch of flowers that covers $\mathbb{R}^2$. Suppose that a pollinator will visit two flowers on every trip and never visits the same color flower twice in a single trip. Because of this, any pair of flowers improves their chances of being visited by ensuring that they are a different color. If there are three colors present in the population, the pairwise payoff matrix becomes $A = -I_3$. Assume that the familiarity*

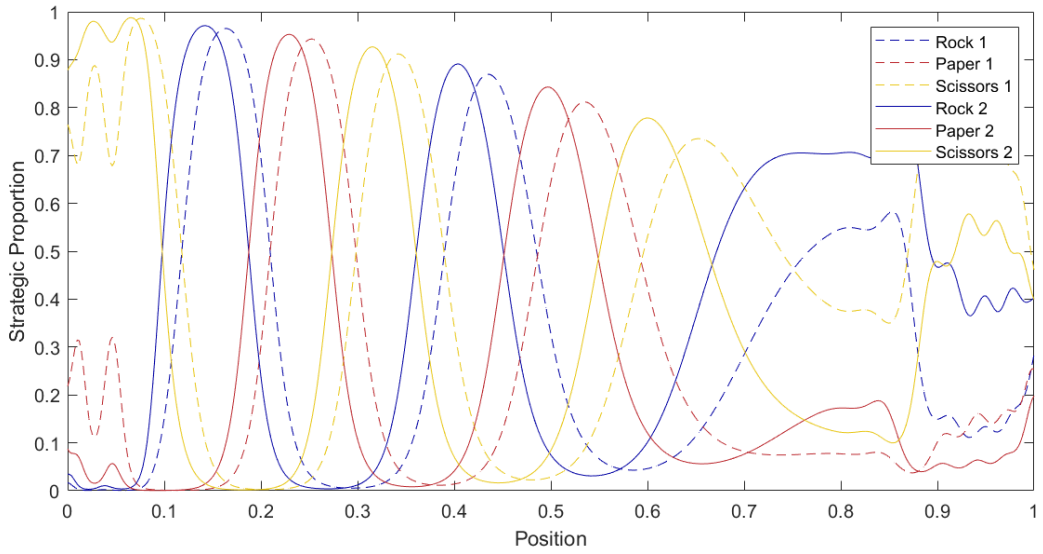

Figure 4.10: Two snapshots of the strategy profile of a Rock Paper Scissors type game played on the domain $[0, 1]$. The dotted line is the solution at $t = 5$, and the dotted line is the solution at $t = 5.2$. There are waves of rock propagating leftwards along the domain, each followed by waves of paper, which are followed by waves os scissors, which are themselves followed by waves of rock.

kernel is a Gaussian Kernel that depends only on the distance between two flowers $K(x, y) = Ce^{-\beta|x-y|^2}$*).*

In this example, our evolution equation is

$$\frac{\partial}{\partial t}u(x,t) = \underbrace{-u^i(x,t)\left\langle \hat{e}^i - u(x,t), \int_{\mathbb{R}^2} K(x-y)u(y)\right\rangle}_{F^i(x,t)}$$

It is obvious that $u(x, t) \equiv [1/3, 1/3, 1/3]$ is an equilibrium for the nonlocal equation. If we linearize about this equilibrium using the standard Gâteaux derivative, restricted only to the invariant manifold, we get that

$$DF\phi = -\frac{1}{3}\int_{\mathbb{R}^n} K(x-y)\phi(y)dy$$

Although we cannot solve for the eigenfunctions of the convolution, we do know that if ϕ is an eigen function then $DF\phi = \lambda\phi$

$$\mathcal{F}[DF\phi] = \mathcal{F}[-\frac{1}{3}K * \phi] = \frac{-1}{3}\hat{K} \cdot \hat{\phi} = \lambda\hat{\phi} = \lambda\mathcal{F}[\phi]$$

Thus to find eigenvalues we examine the spectrum of the multiplication operation which is contained in the range of $\hat{K(\xi)}$. Because K was a Gaussian Kernel so also is $\hat{K}$ and thus we know that the range of $-1/m\hat{K}$ is $(-\frac{C}{m}, 0)$ for some C. This means that the equilibrium is *spectrally* stable (Beck, 2020). This does not, however, imply stability in a stronger sense, but such stability is conjectured through numerical simulations.

Example 4.3 (Coordination)**.** *Consider a continuous patch of sessile individuals taking up* $\mathbb{R}^2$*, interacting at a distance with a Gaussian kernel and with a payoff matrix* $A = I$*. This is a pure structured coordination game. Consider a strategy profile where all players play every available strategy equally,* $u^i = \frac{1}{m}$

This example is exactly the opposite of the anti-coordination case, and thus the linearization is exactly the opposite of that of the anti-coordination case. From that, we know that this equilibrium is spectrally unstable, and thus we can say that it is unstable in L^∞. This mirrors the results of part 4 of theorem 4.4.

These examples are not meant to be illustrative for any model system in particular, but they are meant to demonstrate the usefulness of this model and the need for additional study into the dynamics in the continuous case.

4.5.3 Evolutionary Game Theoretic Discussion

Adding structure to the standard replicator equation makes it possible to describe new model systems in ways that were previously poorly described in an evolutionary sense. In the discrete space system at hand, one may still wish to understand how classical evolutionary game theoretic elements like invasibility and branching translate local information.

The concept of invasibility is difficult to translate because while a strategy profile may be invasible by a particular strategy at a particular position in the graph, it may resist invasion from that same strategy elsewhere. This means that invasibility is dependent not only on the relationship between a strategy profile and a strategy, but also on the structure on which the game is played. For a particular strategy profile, we can describe a certain location in the graph as vulnerable or invulnerable.

Typically, the notion of invasibility discusses the introduction of an entirely novel strategy into the population. This idea does not translate to the structured model exactly because of corollary 4.1, which says that once a strategy is expressed with probability 0 by a certain player, it cannot be expressed by that player again. To really talk about the invasibility of an entirely novel strategy, one must either consider whether a single player can come to play an entirely novel strategy after its introduction to that node, or if the entire graph (or subgraph) can come to learn a strategy after it is introduced in a small proportion over the entire population. Again, depending on the present strategy profile, a strategy being introduced at a small probability over the entire population may still invade in some parts of the population while being resisted in others.

Because there are so many different versions of invasibility for the structured game, the translation of these concepts is not obvious. In the table 4.1 we summarize four types but recognize that there may be other concepts which can equally be called "invasibility."

For coordination in particular, any strategy profile $u^\star$ is non-invasive in any sense to any strategy not already present. This is equivalent to the weak bandwagon property of Cui and Shi (2022). Anti-coordination games are, likewise, always invasible in every sense to any strategy not present in the current strategy profile. In general, these simple interactions are easy to predict for the simplest games. Because the work that we have done in this chapter is limited to linear games, we can argue that continuous invasibility implies shock invasibility in both the local and the global sense. This, however, would not be the case for games with nonlinear payoffs.

In addition to invasibility, branching is another concept that we might expect in an evolutionary model. Branching, in the classical sense, is the transition of a population

Table 4.1: A non-exhaustive list of invasibility types with descriptions and sufficient conditions for each. In all cases we consider a strategy i which is not present in the original strategy profile $u^\star$. When we only consider linear games we can say that global continuous invasibility implies global shock invasibility and local continuous invasibility implies local shock invasibility.

Invasibility Type	Description	Notes
local shock	A single player, v, changes their strategy to play i with probability 1, and all other players remain unchanged.	The strategy $u^\star$ is locally shock invasible to i at v if the new strategy profile is a stable fixed point of the ODE system
global shock	A single player, v, changes their strategy to play i with probability 1, and all other players change their strategy to play i with probability ϵ.	If strategy i becomes fixed in a subgraph $K \subset G$ (meaning the solution converges to an equilibrium with strategy i present with positive probability for all players in K) Then $u^\star$ is shock invasible to i on K.
local continuous	A single player, v, changes their strategy to play the strategy i with probability ϵ	If the solution converges to an equilibrium wherein player v plays strategy i with nonzero probability then $u^\star$ is locally continuously invasible to i at v.
global continuous	All players in the population change their strategy to play strategy i with probability ϵ.	If the solution converges to an equilibrium where every player in a subgraph K is playing i with non-zero probability, then $u^\star$ was continuously invasible to i on K

from a unimodal strategic distribution to a bimodal strategic distribution in time without a time dependent disruption (Dieckmann and Doebeli, 1999; Doebeli and Dieckmann, 2000; Wakano and Iwasa, 2013). These dynamics can occur, for instance, even in a coordination game, if the initial population has strategies centered around the center of the simplex, but the graph is such that a non-consensus equilibrium has a large basin of stability, then the system may converge to a bimodal distribution. Of course, this "branching" is not entirely in the spirit of how branching processes are discussed because the initial unimodal distribution was transient and unstable.

It is difficult to use a structured model to discuss evolutionary dynamics, and for good reason. Evolution, being a population level process, makes the individual level information difficult to use or even incorrect in some settings. However, in the correct settings, such as social learning or even through continuous extensions in the player space, the structured replicator equation becomes meaningful as a well founded and well posed evolutionary model. Insight can be drawn from the ODE model to make game theoretic determinations, and in certain settings, game theoretic information can be used to predict the dynamics of the ODE system. The way that these two domains are connected makes the model potent to help us understand questions even outside of the area of evolutionary game theory, like those questions posed in the classical game theoretic paradigm. Understanding these kinds of structured games through any modeling techniques gives us more insight into the way that relational or spatial structure determines outcomes in complex systems.

Chapter 5

Structured Coordination through Nonlocal Diffusion

5.1 Introduction

Having considered continuous extensions with continuous time and space, we consider one more extension with a slightly modified formulation to examine the case when strategies are directly comparable. In this chapter, we will discuss a broad class of games, which we call Toeplitz games, where payoffs for each pairwise interaction depend only on the "distance" between the strategies of each player. Neutral Coordination games (games wherein players receive a payoff which is maximized when they play the same strategy as their co-player but is independent of the strategy itself) fall under this category, as well as neutral anti-coordination and dis-coordination games. We call this the comparable strategy concept (c.f. the mixed strategy concept from chapter 4). This chapter is taken directly from the *preprint* McAlister et al. (2025), which is under review at the Journal of Mathematical Biology. Again, the introduction has been moved to chapter 1. The brief discussion of the mixed strategy concept has been moved to chapter 4, and the supplementary results have been moved to the appendix A.

All of the early studies about coordination mentioned in 1 have considered discrete strategies with discrete player spaces. These models are helpful for thinking of particular examples (e.g., the selection of a coordinated computer operating system among coworkers in an office) but are unable to be translated to conditions where strategy may vary continuously (e.g., language conventions). Further, using a continuous player space to represent general behaviors of replaceable individuals organized in space, rather than discrete player spaces with explicit interaction behavior unique to each player, changes the required analysis for the system. The purpose of the present study is to introduce a rigorous continuous extension of Toeplitz-type games so that the questions in the application areas may be investigated with a new set of tools.

When other games have previously been considered with continuous strategies, integral equations have been of use. Indeed, many of these authors have extended beyond the present study to consider mixed continuous strategies in the space of distributions (i.e., Stackelberg equilibrium, nonlocal replicator dynamics (Kavallaris and Suzuki, 2018)), but these often rely on a finite number of players. In the same way, studies of a continuum of players often require a discrete strategy. In the present study, we seek to understand a system with continuous players and strategies that cannot be considered as a potential game (Sandholm, 2001; Lã et al., 2016). Moreover, the non-monotonicity and nonlinearity of the nonlocal equation in our problem are of interest beyond its applications here.

In particular, we propose a way to translate the Toeplitz-type games into continuous strategic and player domains through the use of a nonlinear, nonlocal diffusion equation. We start in the present section with some game theoretic background, then we present a rigorously supported extension into the continuous setting resulting in a nonlocal equation model. In section 5.3 we prove classical existence and uniqueness of solutions. We strengthen these results for true coordination games in subsection 5.3.2 by way of a weak maximum principle. In addition to this, in subsection 5.3.3, we consider the problem in the Cauchy setting to show strengthened results. In particular, we get regularity estimates so that, after showing several analytical examples in section 5.4, we can approximate them through simple numerical methods in section 5.5 and consider other properties of the nonlocal equations.

In section 5.6, we consider what the theory tells us about coordination in continuous space by examining stationary solutions and conducting several numerical examples. Finally, in section 5.7 we note that this model is compatible with an inhomogeneity which provides a way for us to extend the model to an even larger class of games.

5.2 Continuous Extension through Comparable Strategies

5.2.1 Toeplitz Games

We are interested in a class of games which we call Toeplitz games. These are the discrete two player games which have Toeplitz payoff matrices. Equivalently each player has a set of pure strategies which can be ordered as $S_1 = S_2 = \{s^{(1)}, s^{(2)}, ..., s^{(m)}\}$ so that if the payoff matrix A is given where $a_{i,j}$ describes the payoff $w(s^{(i)}, s^{(j)})$ against strategy j, A is diagonal-constant (AKA Toeplitz). Three examples below, from left to right, are the pure coordination game, an anti-coordination game, and a game which is neither coordination nor anti-coordination.

$$\begin{bmatrix} 1 & 0 & 0 & 0 \\ 0 & 1 & 0 & 0 \\ 0 & 0 & 1 & 0 \\ 0 & 0 & 0 & 1 \end{bmatrix} \qquad \begin{bmatrix} 0 & 1 & 2 & 4 \\ 1 & 0 & 1 & 2 \\ 2 & 1 & 0 & 1 \\ 4 & 2 & 1 & 0 \end{bmatrix} \qquad \begin{bmatrix} 0 & 1 & 2 & 3 \\ -1 & 0 & 1 & 2 \\ -2 & -1 & 0 & 1 \\ -3 & -2 & -1 & 0 \end{bmatrix}$$

The ordering required to write the payoff matrix as a Toeplitz matrix, $(s^{(1)}, s^{(2)}, ..., s^{(m)})$, induces a metric on the strategy space $d(s^{(i)}, s^{(j)}) = |i - j|$. With a metric and a complete ordering, this kind of game can be reduced to a two player game in which each player v selects a number $n_v \in \{1, ..., m\}$ and their payoff is determined by $w_v(n_v, n_u) = \rho(n_v - n_u)$. This ordering is not unique. For instance, in the pure coordination game, any ordering of the strategies will satisfy this condition.

Those Toeplitz games that are also coordination games are of particular interest to us. A two-player coordination game is a type of strategic form game that satisfies the Bandwagon Property described in chapter 1. These coordination and anti-coordination games, which can be expressed as a Toeplitz game, are of particular interest because they model the homogeneous impact of cooperative or uncooperative behavior. In a Toeplitz game, a particular strategy does not give any fitness benefit independent of its proximity to a co-player's strategy. That is to say that any fitness benefit is only the result of the interaction between players (whether the interactions are sympathetic or antagonistic). If the strategies were reorganized by some permutation p so that all the players playing $s^{(l)}$ take on the strategy $s^{(p(l))}$, the payoff for every player will have remained the same. If several methods of communication are equally efficient but the benefit of communication is only achieved when two players are using the same method, this can be described as a Toeplitz coordination game. Building a foundational theory of this homogeneous problem will then allow for better treatment of inhomogeneous coordination and anti-coordination processes.

Recall from chapter 1 that the dyadic interactions of this type are easy to understand. Therefore, when we seek to understand multiplayer Toeplitz games, we easily generalize the two-player interactions and say that a player's payoff is the sum (or equivalently the arithmetic mean) of the payoffs from each dyadic interaction. As is typical, we will start by considering the players as vertices in a graph where (possibly weighted) edges describe the strength of interaction between individuals. Suppose the game is played on the graph $G(V, E)$ with weighted adjacency matrix W and that each player has pure strategies $B = \{\hat{e}_1, \hat{e}_2, ..., \hat{e}_m\}$, which is the standard basis for $\mathbb{R}^m$. Then, if we consider a strategy profile as a function $u : V \to B$ rather than an element of the Cartesian product $B^{|v|}$ (although the two spaces are clearly identical), we can write our payoff function as

$$w(v|u) = \sum_{i \in V} W_{i,v} u(v)^T A u(i) \tag{5.1}$$

where A is the payoff matrix as described in 1. This formulation holds true for any symmetric game with a payoff matrix A, it need not be Toeplitz.

If instead of a collection of discrete players we considered an uncountable continuum of players, we might think of our player domain as a subset of $\mathbb{R}^n$, and instead of summing, we could integrate over the entire domain. The weighted adjacency matrix is replaced by a nonnegative integrable kernel $K \in C_b^0(\Omega; L^1(\mathbb{R}^n))$ (That is a kernel $K(x,y)$ which is continuous x, in the L^1 sense, and integrable in y where $\sup_{x\in\Omega} \|K(x,\cdot)\|_{L^1(\mathbb{R}^n)} < \infty$). Replacing the sum in (5.1) with the integral, we get that a strategy profile $u : \Omega \to B$ gives the payoff

$$w(x|u) = \int_\Omega K(x,y)u(x)^T Au(y)dy. \tag{5.2}$$

Again, this extension does not require the game to be a Toeplitz game.

5.2.2 Continuous Strategic Extensions

To truly study cooperative and non-cooperative behavior, we may also consider extending the existing model to include continuous strategies. There are two ways to do this. The first is the mixed strategy case, which is discussed in a different light in chapters 3 and 4. The other is the comparable strategy case, described here, which is exceptionally helpful when we have a Teoplitz type game.

If our payoff matrix is a Toeplitz matrix, we can express the pairwise payoff simply as some function $\rho(dd(u(x), u(y))$ where dd is the directed metric which is natural from the ordering induced by the Toeplitz matrix. The continuous extension from this point is clear. The ordering of the strategies means that they can be considered as elements of $\mathbb{R}$ and we can allow $\rho : \mathbb{R} \to \mathbb{R}$ so that our payoff can be expressed as $\rho(u(x) - u(y))$. Therefore we can write our payoff function as

$$w(x|u) = \int_\Omega K(x,y)\rho(u(x) - u(y))dy. \tag{5.3}$$

To make this extension, all we have done is replace the bilinear form in (5.2) with our payoff function induced by the Teoplitz matrix. We are especially interested in this type of game, both because of its implications in the application areas but also because, in the continuous

form, we will see that it has great similarities to a class of important nonlocal equations called nonlocal diffusive equations. Indeed, the time dependent model will be a nonlinear, nonlocal diffusion equation, and understanding this model will contribute to the understanding of nonlocal diffusion problems in general.

With this fitness function, we have now described a strategic form game completely as we have a set of players Ω, a set of strategies $\mathbb{R}$, and a payoff function (5.3). However, the search for Nash equilibria to this game is exceedingly difficult, and the primary difficulty is the size of the function space in which we must work. Notice that if $\rho(z) = \chi_{\{0\}}(z)$ then any constant function is a Nash equilibrium to this game. This is clear because if $u \equiv c$ then

$$\begin{aligned} BR_x(u) &= \underset{z\in\mathbb{R}}{\operatorname{argmax}}\{\int_\Omega K(x,y)\chi_{\{0\}}(z-c)dy\} \\ &= \underset{z\in\mathbb{R}}{\operatorname{argmax}}\{\chi_{\{0\}}(z-c)\|K(x,\cdot)\|_{L^1(\Omega)}\} \\ &= c \end{aligned}$$

so $BR_x(u) = u(x)$ in Ω. However, if $\tilde{u}$ differs from u as a non-empty set of measure 0, then it will certainly not be a Nash equilibrium. This causes a problem because it means that we cannot search for equilibria in any L^p space (as elements of these spaces are equivalence classes of functions that differ at sets of measure 0).

Because of this issue, in order to understand the game in this setting, we will follow in the example of those who have studied the game in the discrete setting and consider it as a dynamic game through myopic best response (e.g Ellison (1993); Raducha and San Miguel (2022)). Myopic best response is a replication dynamic for an evolutionary game in which a set of players, who chosen to update their strategies, take on their best response (often pure strategy best response) to the current strategy profile. By repeating this process, we can study a sequence of strategy profiles which, if it terminates, will result in a strategy profile in which every player is playing a best response. Under myopic best response, we can see that the evolution of strategy profiles for the game with payoff function (5.3) will evolve according to a particular nonlocal equation.

Proposition 5.1. *Under myopic best response, bounded strategy profiles of the game with players $\Omega \subseteq \mathbb{R}^n$ choosing strategies in $\mathbb{R}$, with fitness as in (5.3), will evolve as*

$$\frac{\partial}{\partial t}u(x,t) = \int_\Omega K(x,y)\rho'(u(x,t)-u(y,t))dy$$

so long as the following three hypotheses are met

(H1) Players change their strategies in arbitrarily small time steps Δt

(H2) Players incur a quadratic cost $\frac{h^2}{\Delta t}$ for changing their strategy

(H3) $\rho \in C^{1,1}(\mathbb{R})$ and $\rho(z) \leq Cz^2 + A$ for some nonnegative C, A

Proof. Consider a bounded strategy profile $u(\cdot,t) : \Omega \to \mathbb{R}$. Every player will seek to update their strategy by some amount h in order to take on their best response to $u(\cdot,t)$ after a time step of Δt and in doing so they will incur a cost of $\frac{h^2}{2}$. Let

$$S_x(h) := \int_\Omega K(x,y)\rho(u(x,t)+h-u(y,t))dy$$

be the payoff that player x will receive after updating their strategy by h. Because ρ is subquadratic (H3), we can see that

$$\begin{aligned} S_x(h) &\leq C\int_\Omega K(x,y)(h+(u(x,t)-u(y,t))^2dy + \underbrace{A\sup_{x\in\Omega}\|K(x,\cdot)\|_{L^1(\Omega)}}_{A_1} \\ &\leq \underbrace{C\int_\Omega K(x,y)dy}_{C_1}h^2 + 2hC\int_\Omega K(x,y)(u(x,t)-u(y,t))dy \\ &\quad + C\int_\Omega K(x,y)(u(x,t)-u(y,t))^2dy + A_1 \end{aligned}$$

Since $K \in C_b^0(\Omega; L^1(\mathbb{R}^n))$, C_1 and A_1 can be bounded by constant independent of x. Now because u is bounded we know that $|u(x,t)-u(y,t)|$ is bounded by some M and thus we

can write

$$S_x(h) \leq C_1 h^2 + \underbrace{2CM \sup_{x\in\Omega} \|K(x,\cdot)\|_{L^1(\Omega)}}_{B_1} h + \underbrace{CM^2 \sup_{x\in\Omega} \|K(x,\cdot)\|_{L^1(\Omega)} + A_1}_{A_2}$$
$$\leq C_1 h^2 + B_1 h + A_2$$

Having shown that $S_x(h)$ is uniformly subquadratic in h, we also note that when $\rho \in C^{1,1}$ (H3), $S_x(h)$ is also in $C^{1,1}$. Observe that

$$\frac{d}{dh} S_x(h) = \int_\Omega K(x,y)\rho'(u(x,t) + h - u(y,t))dy$$

And so clearly for any compact subdomain $I \subset \mathbb{R}$ we can write

$$\begin{aligned}
&\left| \frac{d}{dh} S_x(h_1) - \frac{d}{dh} S_x(h_2) \right| \\
&\leq \int_\Omega |K(x,y)||\rho'(u(x,t) + h_1 - u(y,t)) - \rho'(u(x,t) + h_2 - u(y,t))|dy \\
&\leq \int_\Omega K(x,y) L_\rho |h_1 - h_2| dy \\
&\leq \sup_{x\in\Omega} \|K(x,\cdot)\|_{L^1(\Omega)} L_\rho |h_1 - h_2|
\end{aligned} \tag{5.4}$$

Because u is bounded, the choice of a compact subdomain I gives us a Lipschitz constant for ρ' on the subdomain $[-2\sup|u| - \sup I, 2\sup|u| + \sup I]$ which is called L_ρ in (5.4). Therefore $\frac{d}{dh} S_x(h)$ is locally Lipschitz.

This is important because it means that, for any x, when Δt is small enough, $S_x(h) - \frac{h^2}{\Delta t} \leq C_2 h^2 + A_3$ for some negative C_2 and some A_3. Thus $S_x(h) - \frac{h^2}{\Delta t}$ must have a global maximizer, h^* and that global maximizer will satisfy

$$\frac{d}{dh} S_x(h^*) = 2\frac{h^*}{\Delta t}$$

because everything is continuously differentiable.

Having observed this, we note also that there must be a negative h^- so that when $h < h^-$ then $S_x(h) - \frac{(h)^2}{\Delta t} < S_x(0)$. Likewise there must be an h^+ so that $h > h^+ \implies S_x(h) - \frac{(h)^2}{\Delta t} < S_x(0)$. These h^- and h^+ will form a compact interval which will surely contain h^*. Moreover, from the chosen interval, we have a Lipschitz constant for $\frac{d}{dh}S_x$ which we call L_S. The next step is to put bounds on h^*. In order to do this, we will consider different cases: when $h^* > 0, h^* < 0$, and $h^* = 0$.

If $h^* > 0$ we write that

$$-h^* L_S \leq \frac{d}{dh}S_x(h^*) - \frac{d}{dh}S_x(0) \leq h^* L_S$$
$$-h^* L_S \leq \frac{h^*}{2} - \frac{d}{dh}S_x(0) \leq h^* L_S$$

Reorganization on each side of the inequality, with the knowledge that Δt can be made small enough so that $2 - L_S \Delta t > 0$, will yield

$$\frac{d}{dh}S_x(0)\frac{\Delta t}{2 + L_S \Delta t} \leq h^* \leq \frac{d}{dh}S_x(0)\frac{\Delta t}{2 - L_S \Delta t}$$

Likewise we can show that if $h^* < 0$ we will get the inequality

$$\frac{d}{dh}S_x(0)\frac{\Delta t}{2 - L_S \Delta t} \leq h^* \leq \frac{d}{dh}S_x(0)\frac{\Delta t}{2 + L_S \Delta t}$$

We also note here that if $h^* = 0$ this requires that $\frac{d}{dh}S_x(0) = 0$.

Now that we have bounds on h^*, recall that h^* is the change in strategy in one time step. That it $h^* = u(x, t + \Delta t) - u(x, t)$. If we make this substitution and divide our inequalities by Δt we see that

$$\frac{d}{dh}S_x(0)\frac{1}{2 + L_S \Delta t} \leq \frac{u(x, t + \Delta t) - u(x, t)}{\Delta t} \leq \frac{d}{dh}S_x(0)\frac{1}{2 - L_S \Delta t} \qquad h^* > 0$$
$$\frac{d}{dh}S_x(0)\frac{1}{2 - L_S \Delta t} \leq \frac{u(x, t + \Delta t) - u(x, t)}{\Delta t} \leq \frac{d}{dh}S_x(0)\frac{1}{2 + L_S \Delta t} \qquad h^* < 0$$

Both inequalities trivially hold in the case that $h^* = 0$. In any case, when we take $\Delta t \to 0$, we see that by the squeeze theorem

$$\frac{\partial}{\partial t}u(x,t) = \frac{1}{2}\frac{d}{dh}S_x(0)$$

To complete the proof, we need only note that

$$\frac{d}{dh}S_x(0) = \int_\Omega K(x,y)\rho'(u(x,t) - u(y,t))dy$$

and do a trivial rescaling of space-time to arrive at the desired nonlocal equation. □

Thus, we have shown that, for any Toeplitz type game, we can make a continuous extension and describe how bounded strategy profiles will evolve in time with a nonlocal equation. We will call the nonlocality

$$g[u](x,t) := \int_\Omega K(x,y)\rho'(u(x,t) - u(y,t))dy \tag{5.5}$$

and express the nonlocal equation as $u_t = g[u]$. Notice that if K and ρ are selected appropriately, a certain Toeplitz coordination game extends directly to the nonlocal heat equation (Andreu-Vaillo et al., 2010; Gomez and Rossi, 2020) and a certain Toeplitz anti-coordination game extends directly to the nonlocal backward heat equation. Being able to study these games with a new suite of tools from PDEs and nonlocal equations will allow us to understand coordination and anti-coordination in space more fully. Moreover, the present investigation into this game will also extend our understanding of nonlinear nonlocal diffusion equations.

5.3 Existence, Uniqueness, and Regularity for Toeplitz Type Games

5.3.1 General Toeplitz Games

Now that we have a nonlocal equation which captures the behavior we are interested in, we will proceed with some classical existence and uniqueness results for the initial value problem (IVP) wherein an initial strategy profile u_0 is given in Ω, and there are no boundary data prescribed. The assumption is that no information is entering the system from outside the domain, and so it is argued by Chasseigne et al. (2006) that this is the analogue to the Neumann boundary condition for nonlocal diffusion type problems. It is important to note that these results for the nonlocal equation do not depend on the assumptions that make the model appropriate for the application area ($H1-3$ from proposition 5.1). Namely, ρ need not be subquadratic. However, we will require that $\rho \in C^{1,1}$.

The main result of this section is a Picard iteration type proof relying on the contraction mapping principle. In order to achieve this, we will first state and prove two important lemmas. The first will show that the nonlocality, g, maps continuous and bounded functions to continuous and bounded functions. The second will show that g is locally Lipschitz with respect to the sup norm in C_b^0. For the following, let $\Omega \subset \mathbb{R}^n$ be an open domain and let $\Omega_T := \Omega \times [0,T]$.

Lemma 5.1 (g is well defined)**.** *The non local operator* $g[u](x,t) = \int_\Omega K(x,y)\rho'(u(x) - u(y))dy$ *is well defined from* $C_b^0(\Omega_T, \mathbb{R})$ *into* $C_b^0(\Omega_T, \mathbb{R})$.

Proof. To show that g is well defined in this space, let $u \in C_b^0(\Omega_T)$, and we will show that $g[u]$ is continuous on Ω_T and bounded. To show that $g[u]$ is bounded, first note that, when u is bounded, because $\rho \in C^{1,1}$, surely there is a W such that $|\rho'(u(x,t_1) - u(y,t_2))| < W$ for all $x, y \in \Omega$ and $t_1, t_2 \in [0,T]$ by a continuous on compact argument. This means that $|g[u](x,t)| \leq \int_\Omega |K(x,y)|W dy \leq W\|K(x,\cdot)\|_{L^1(\Omega)}$. By assumption $\|K(x,\cdot)\|_{L^1(\Omega)}$ is uniformly bounded so $\sup_{x\in\Omega} \|K(x,\cdot)\|_{L^1(\Omega)} \leq D$ for some $D < \infty$. Thus, we have shown that $\|g[u]\|_\infty < WD$, so $g[u]$ is bounded whenever u is continuous and bounded.

Consider the sequence $(x_n, t_n)_{n=1}^{\infty} \subset \Omega_T$ with $(x_n, t_n) \to (x, t) \in \Omega$. Furthermore, consider the difference

$$\begin{aligned}
&|g[u](x_n, t_n) - g[u](x, t)| \\
&\qquad = \left| \int_\Omega K(x_n, y)\rho'(u(x_n, t_n) - u(y, t_n)) - K(x, y)\rho'(u(x, t) - u(y, t))dy \right| \\
&\qquad \leq \int_\Omega |(K(x_n, y) - K(x, y))\rho'(u(x_n, t_n) - u(y, t_n))|dy \\
&\qquad\quad + \int_\Omega |K(x, y)(\rho'(u(x_n, t_n) - u(y, t_n)) - \rho'(u(x, t) - u(y, t)))|dy \\
&\qquad \leq I_1 + I_2
\end{aligned}$$

We will consider each integral separately. Let $\epsilon > 0$. Note that there is an R such that $\int_{\Omega \setminus B_R(0)} K(x, y)dy < \frac{\epsilon}{8W}$. Now consider x_n and y inside $\overline{B_R(0)}$. $\rho \in C^{1,1}$ so $\exists \delta$ such that $|x - y| < \delta \Rightarrow |\rho'(x) - \rho'(y)| < \frac{\epsilon}{4D}$. Because u is continuous, $\exists M_1$ such that $|u(x_n, t_n) - u(x, t)| < \delta/2$ whenever $n > M_1$. Furthermore, In $\Omega \cap \overline{B_R(0)}$ there is surely a M_2 such that $n > M_2 \implies |u(y, t_n) - u(y, t)| < \delta/2$ for any $y \in \Omega \cap \overline{B_R(0)}$. It is an easy application of the triangle inequality to see that this implies $|(u(x_n, t_n) - u(y, t_n)) - (u(x, t) - u(y, t))| < \delta$ when $n > \max\{M_1, M_2\}$ and thus, when n is sufficiently large

$$|\rho'(u(x_n, t_n) - u(y, t_n)) - \rho'(u(x, t) - u(y, t))| \leq \frac{\epsilon}{4D} \quad \forall y \in \Omega \cap \overline{B_R(0)}.$$

Therefore, we can see that

$$\begin{aligned}
I_2 &\leq 2W \int_{\Omega \setminus B_R(0)} K(x, y)dy + \int_{\Omega \cap B_R(0)} K(x, y)\frac{\epsilon}{4D}dy \\
&\leq 2W\frac{\epsilon}{8W} + D\frac{\epsilon}{4D} = \frac{\epsilon}{2}
\end{aligned}$$

Now we consider I_1. It is clear that

$$I_1 \leq W \int_\Omega |K(x_n, y) - K(x, y)|dy.$$

From the assumed continuity of $\|K(x,\cdot)\|_{L^1(\Omega)}$ we get immediately that $\exists M_3$ such that for $n > M_3$, $\|K(x_n,\cdot) - K(x,\cdot)\|_{L^1(\Omega)} \leq \frac{\epsilon}{2W}$.

Thus, if $M = \max\{M_1, M_2, M_3\}$, then $n > M \implies$

$$|g[u](x_n,t_n) - g[u](x,t)| \leq I_1 + I_2 \leq \frac{\epsilon}{2} + W\frac{\epsilon}{2W} = \epsilon$$

This clearly works for any $\epsilon > 0$ so we have shown that $g[u]$ is continuous at (x,t) for any $(x,t) \in \Omega_T$. Therefore we have proved that $g : C_b^0(\Omega_T,\mathbb{R}) \to C_b^0(\Omega_T,\mathbb{R})$ is well defined. □

Lemma 5.2 (Lipschitz Continuity of g)**.** *For any bounded (in the sup norm sense) subset $X_R := \{u \in C_b^0(\Omega_T); \|u\|_\infty \leq R\} \subset C_b^0(\Omega_T)$, there exists a $C^g \geq 0$ such that for every $u, v \in X_R$*

$$\|g[u](\cdot,t) - g[v](\cdot,t)\|_\infty \leq C^g \|u(\cdot,t) - v(\cdot,t)\|_\infty$$

Proof. Let $u, v \in X_R$. Then we observe that for each $0 < t < T$,

$$\begin{aligned}
\|g[u](\cdot,t) - g[v](\cdot,t)\|_\infty &= \left\| \int_\Omega K(x,y)(\rho'(u(x,t) - u(y,t)) - \rho'(v(x,t) - v(y,t))dy \right\|_\infty \\
&\leq \sup_{x\in\Omega} \int_\Omega |K(x,y)||\rho'(u(x,t) - u(y,t)) - \rho'(v(x,t) - v(y,t))|dy \\
&\leq \sup_{x\in\Omega} \|\rho'(u(x,t) - u(\cdot,t)) - \rho'(v(x,t) - v(\cdot,t))\|_\infty \int_\Omega K(x,y)dy.
\end{aligned}$$

Recall that $\rho \in C^{1,1}(\mathbb{R})$ and ρ' has Lipschitz constant L_ρ for the compact interval $[-2R, 2R]$. Now note that for any $(x,t) \in \Omega_T$

$$\begin{aligned}
&\sup_{y\in\Omega} |\rho'(u(x,t) - u(y,t)) - \rho'(v(x,t) - v(y,t))| \\
&\qquad \leq \sup_{y\in\Omega} L_\rho |u(x,t) - u(y,t) - v(x,t) + v(y,t)| \\
&\qquad \leq \sup_{y\in\Omega} L_\rho (|u(x,t) - v(x,t)| + |u(y,t) - v(y,t)|) \\
&\qquad \leq L_\rho (|u(x,t) - v(x,t)| + \|u(\cdot,t) - v(\cdot,t)\|_\infty)
\end{aligned}$$

so naturally

$$\sup_{x\in\Omega} \|\rho'(u(x,t)-u(\cdot,t)) - \rho'(v(x,t)-v(\cdot,t))\|_\infty \leq 2L_\rho \|u(\cdot,t)-v(\cdot,t)\|_\infty$$

This, and the fact that $\|K(x,\cdot)\|_{L^1(\Omega)} \leq D$ uniformly for some finite D, gives us the result that for any $t \in [0,T]$

$$\|g[u](\cdot,t) - g[v](\cdot,t)\|_\infty \leq 2L_\rho D \|u(\cdot,t)-v(\cdot,t)\|_\infty$$

Clearly, then we have $C^g = 2L_\rho D$ and

$$\sup_{t\in[0,T]} \|g[u](\cdot,t) - g[v](\cdot,t)\|_\infty \leq C^g \sup_{t\in[0,T]} \|u(\cdot,t)-v(\cdot,t)\|_\infty.$$

It is important to notice that L_ρ may depend on the choice of R so C^g depends on R. □

Having shown that g is well defined and Lipschitz continuous, we can now prove short time existence and uniqueness of the solution to the initial value problem $u_t = g[u]$ in Ω_T with $u(0,t) = u_0 \in C_b^0(\Omega)$ through a contraction mapping principle.

Theorem 5.1 (Short Time Existence and Uniqueness)**.** *The initial value problem $u_t = g[u]$ in Ω_τ has a unique continuous and bounded solution in Ω_τ for some τ, when $u(x,0) = u_0 \in C_b^0(\Omega)$, $\rho \in C^{1,1}(\mathbb{R})$, and $K \in C_b^0(\Omega; L^1(\Omega))$.*

Proof. Let $\Omega_T = \Omega \times [0,T]$ with T to be chosen later. Equip the function space $C_b^0(\Omega_T)$ with the standard sup norm $\|u\| = \sup_{t\in[0,T]} \|u(\cdot,t)\|_\infty$. Now, for some $R > \|u_0\|_\infty$, let $E_{R,T} := \{u \in C_b^0(\Omega_T, \mathbb{R}); u(x,0) = u_0, \|u\| \leq R\}$. Observe that $E_{R,T}$ is nonempty as the map $(x,t) \mapsto u_0(x)$ belongs in $E_{R,T}$. Moreover, observe that $E_{R,T}$ is complete with respect to the sup norm, so we will be able to proceed with a Banach Fixed Point Theorem (BFPT) argument. It is clear that a solution to the IVP will also satisfy

$$u(x,t) = u_0(x) + \int_0^t g[u](x,s)ds.$$

Let $\Theta : C_b^0(\Omega_T, \mathbb{R}) \to C_b^0(\Omega_T, \mathbb{R})$, where $\Theta u = u_0 + \int_0^t g[u]ds$, and notice that if this operator has a unique fixed point in $E_{R,T}$ then we have a unique solution to the IVP.

First, we show that $\Theta : E_{R,T} \to E_{R,T}$ for some T. It is easy to say that $\Theta u \in C_b^0(\Omega_T, \mathbb{R})$ and that $\Theta u(x,0) = u_0(x)$. Because of lemma 5.1, we know that $g[u] \in C_b^0(\Omega_T)$ so its time antiderivative is obviously continuous in space and time.

In order to show that $\|\Theta u\| \leq R$, we note that $g[u]$ is bounded whenever u is bounded. In particular, $g[u] \leq WD$ where W is the bound for ρ' on $[-2R, 2R]$ which, of course, depends on R, and D is the uniform bound on $\|K(x,\cdot)\|_{L^1(\Omega)}$. Therefore we can always find a T_R such that $\|\Theta u(\cdot,t)\|_\infty \leq \|u_0\|_\infty + \int_0^t WD \leq R$ for all $t \in [0, T_R]$. Let $T < T_R$ and we have that $\Theta : E_{R,T} \to E_{R,T}$.

Now that we have shown that Θ indeed maps from $E_{R,T}$ to $E_{R,T}$ for some T, we need only show that Θ is a contraction in $E_{R,T}$ for some, possibly smaller, value of T. Let $u, v \in E_{R,T}$ and note that

$$\begin{aligned}\|\Theta u - \Theta v\| &= \sup_{t\in[0,T]} \left\| \int_0^t g[u](\cdot,s) - g[v](\cdot,s) ds \right\|_\infty \\ &\leq \sup_{t\in[0,T]} \int_0^t \|g[u] - g[v]\| ds\end{aligned}$$

By lemma 5.2 we get immediately that

$$\|\Theta u - \Theta v\| \leq C^g T \|u - v\|.$$

Notice here that C^g depends on R because the Lipschitz constant for g is defined for a particular compact subset. With this Lipschitz constant for Θ, when $T \leq \frac{1}{2C^g}$ we know that Θ is a contraction. Thus, by the BFPT, there is a unique $u \in E_{R,T}$ such that $\Theta u = u$. Thus, there is a continuous and bounded u so that $u_t = g[u]$ on Ω_T and $u(0,t) = u_0 \in C_b^0(\Omega)$ so long as $T < \min\{T_R, \frac{1}{2C^g}\}$. This completes the proof of short time existence and uniqueness by way of the Banach Fixed Point Theorem. We can use an extension principle to get a longer existence time. Note that for a given u_0, we can choose an R_1 and find a resulting T_1 so that there is a unique solution on $[0, T_1]$. Take $u(\cdot, T_1 - \epsilon)$ for some $\epsilon > 0$ as our initial condition, take a new R_2 and resulting T_2 to find a new solution on $[T_1 - \epsilon, T_2]$. Wherever these solutions overlap, they must be identical because of the uniqueness proved here. We

cannot use this extension to say that the solution is global in time because we have no lower bound on the minimal existence time. As R grows, the resulting T may shrink quickly enough so that we cannot extend the solution beyond some finite time τ. □

We have shown that for any continuously extended Teoplitz game with certain hypotheses on K and ρ, and with a bounded and continuous initial strategy profile, there is exactly one way the strategy profile will evolve for some time. Next, we will show that if there is a finite maximal existence time, T, (i.e., $u(x,t)$ cannot be extended beyond time T as a solution of the IVP) then there is necessarily a finite time blowup.

Lemma 5.3 (Finite Time Blow up)**.** *If $T < \infty$ is the maximal time of existence for a solution u to the IVP $u_t = g[u]$ with $u(\cdot,0) = u_0 \in C_b^0(\Omega)$ then $\|u(\cdot,t)\|_\infty \to \infty$ as $t \to T$.*

Proof. Suppose that u is a solution to the IVP $u_t = g[u]$ with $u(\cdot,0) = u_0 \in C_b^0(\Omega)$ that has a maximal time of existence $T < \infty$. Moreover, by way of contradiction, suppose there is a bounded subset $E_R := \{v \in C_b^0(\Omega); \|v\|_\infty \leq R\}$ such that for all $t \in [0,T)$ $u(\cdot,t) \in E_R$. Note that E_R is a closed subset of $C_b^0(\Omega)$.

Consider now a sequence of times t_n which have $t_n \to T$ as $n \to \infty$. This is necessarily a Cauchy sequence in the reals. We will show that $u(\cdot,t_n)$ is a Cauchy sequence in E_R with respect to the sup norm. Note that for any $\delta > 0$ there is an N so that $n,m > N \implies |t_n - t_m| < \delta$.

$$\begin{aligned}
\|u(\cdot,t_n) - u(\cdot,t_m)\|_\infty &= \left\| \int_0^{t_n} g[u](\cdot,s)ds - \int_0^{t_m} g[u](\cdot,s)ds \right\|_\infty \\
&= \left\| \int_{t_n}^{t_m} g[u](\cdot,s)ds \right\|_\infty \\
&\leq \delta \sup_{s\in[t_n,t_m]} \|g[u](\cdot,s)\|_\infty
\end{aligned}$$

By assumption, $\|u\|_\infty$ is bounded for all time $t \in [t_n,t_m] \subset [0,T)$ uniformly in time by R. By lemma 5.1 we know that if u is bounded by R then there is an R_g so that $\|g[u]\|_\infty \leq R_g$ and, crucially, this upper bound only depends on the choice of R (see proof of lemma 5.1). Thus we can say that $\sup_{s\in[t_n,t_m]} \|g[u](\cdot,s)\|_\infty \leq R_g$. Thus, we have that

$$\|u(\cdot,t_n)-u(\cdot,t_m)\|_\infty \le \delta R_g$$

Therefore, for any $\epsilon>0$, we let $\delta=\frac{\epsilon}{2R_g}$ and from this we get an appropriate N so that $|t_n-t_m|<\delta$ and thus $\|u(\cdot,t_n)-u(\cdot,t_m)\|\le\epsilon$. Thus $u(\cdot,t_n)$ is a Cauchy sequence from the closed subset of a Banach space, E_R, and so it has a limit $\tilde{u}_0\in E_R$. (Note carefully that $\tilde{u}_0$ is continuous because the convergence is uniform). Now consider another arbitrary sequence of times τ_k with $\lim\tau_k\to T$ and we will show that $u(\cdot,\tau_k)\to\tilde{u}_0$. Of course, $u(\cdot,t)$ is differentiable in time on $[0,T)$ and that derivative is uniformly bounded by R_g as above, so $|u(x,t)-u(x,\tau)|\le R_g|t-\tau|$. Thus, we can write

$$\begin{aligned}\|u(\cdot,\tau_k)-\tilde{u}_0\| &\le \|u(\cdot,\tau_k)-u(\cdot,t_n)\|_\infty+\|u(\cdot,t_n)-\tilde{u}_0\|_\infty\\ &\le R_g|\tau_k-t_n|+\|u(\cdot,t_n)-\tilde{u}_0\|_\infty\end{aligned}$$

Both τ_k and t_n approach T from the left and so if $\epsilon>0$ there is an n_1 such that $k,n>n_1 \implies |t_k-t_n|<\frac{\epsilon}{2R_g}$. Furthermore, we already showed that $\|u(\cdot,t_n)-\tilde{u}_0\|\to 0$ so there is an n_2 such that $n>n_2 \implies \|u(\cdot,t_n)-\tilde{u}_0\|_\infty\le\frac{\epsilon}{2}$. Therefore we get that when $k>\max\{n_1,n_2\}$ then surely

$$\|u(\cdot,\tau_k)-\tilde{u}_0\|\le\epsilon.$$

This is true for any sequence of $\tau\to T$ from the left thus we write that $\lim_{t\to T^-}u(\cdot,t)=\tilde{u}_0\in C_b^0(\Omega)$.

Because we have a $\tilde{u}_0\in C_b^0(\Omega)$, by theorem 5.1 we can find a solution $\tilde{u}$ to the IVP $\tilde{u}=g[\tilde{u}]$ with $\tilde{u}(\cdot,T)=\tilde{u}_0$ on some interval $[T,T+\eta)$. Now let $\hat{u}(\cdot,t)=u(\cdot,t)$ when $t\in[0,T)$ and $\hat{u}(\cdot,t)=\tilde{u}(\cdot,t)$ when $t\in[T,T+\eta)$. We will show now that $\hat{u}\in C_b^0(\Omega_{T+\eta})$. The boundedness is immediate from the hypothesis and from the details of the proof of theorem 5.1. Also, we know that $\hat{u}$ is continuous on $[0,T)$ and on $(T,T+\eta)$. To see that is also continuous at T observe that $\lim_{t\to T^-}\hat{u}(\cdot,t)=\hat{u}(\cdot,T)$ by the previous result and that

$\lim_{t\to T^+} \hat{u}(\cdot,t) = \hat{u}(\cdot,T)$ by the details in the proof of 5.1. This convergence is uniform and so we can say that $\hat{u} \in C_b^0(\Omega_{T+\eta})$.

Lastly, we show that $\hat{u}$ is a solution to the IVP, that is, in the integral form,

$$\hat{u}(x,t) = u_0(x) + \int_0^t g[\hat{u}](x,s)ds. \tag{5.6}$$

This is obviously true when $t < T$. Moreover, we can see that when $t = T$, we can write

$$\begin{aligned} u_0(x) + \int_0^T g[\hat{u}](x,s)ds &= u_0(x) + \int_0^{T-\epsilon} g[u](x,s)ds + \int_{T-\epsilon}^T g[u](x,s)ds \\ &= u(x,T-\epsilon) + \int_{T-\epsilon}^T g[u](x,s)ds \end{aligned} \tag{5.7}$$

Recall that, because $\|\hat{u}\|_\infty = \|u\|_\infty \leq R$ when $t < T$, $\|g[\hat{u}]\|_\infty = \|g[u]\|_\infty \leq R_g$ when $t < T$. Therefore if we take the limit as $\epsilon \to 0$ in equation (5.7) we get $u_0(x) + \int_0^T g[u](x,s)ds = \lim_{t\to T^-}(x,t) = \tilde{u}_0(x) = \hat{u}(T)$.

Finally, when $t > T$ we observe that

$$\begin{aligned} u_0(x) + \int_0^t g[\hat{u}](x,s)ds &= u_0(x) + \int_0^T g[\hat{u}](x,s)ds + \int_T^t g[\hat{u}](x,s)ds \\ &= \tilde{u}_0 + \int_T^t g[\tilde{u}](x,s)ds \\ &= \tilde{u}(x,t) = \hat{u}(x,t) \end{aligned}$$

Therefore $\hat{u} \in C_b^0(\Omega_{T+\eta})$ and $\hat{u}$ satisfies that integral equation (5.6). Thus $\hat{u}$ extends the solution to the IVP $u_t = g[u]$ with $u(\cdot,0) = u_0$ beyond the assumed maximal time of existence. This contradicts the assumption that T was the maximal time of existence. Thus, if there is a finite maximal time of existence, the solution must leave every compact subset of $C_b^0(\Omega_T)$. Because the limit $u(\cdot,t_n)$ is continuous for $t_n \leq T < \infty$ we know that $\|u(\cdot,t)\|_\infty \to \infty$ as $t \to T$. □

Note that this result only discusses the consequences of having a finite time of existence. It is made less interesting by the fact that we have no example of a solution which exhibits

finite time blowup. These results are for general continuous extensions of Toeplitz games with appropriate ρ. These general games are interesting, but we can achieve more specific results when we constrain our study to Toeplitz coordination games.

5.3.2 Coordination Toeplitz Games

In the discrete case, if a Toeplitz game has a positive Strictly Diagonally Dominant (SDD) payoff matrix, then it is necessarily a coordination game. We can see this because, for any mixed strategy $t \in \Delta^{m-1}$, the payoff of playing a pure strategy $k \in \{1, ..., m\}$ is $w(e_k, t) = e_k^T A t$. It is immediate to see that if k is such that $t_k = 0$ then $e_k^T A t = \sum_{j=1}^m a_{kj} t_j < a_{kk} \|t\|_{\ell^\infty}$ and if l is such that $t_l = \|t\|_{\ell^\infty}$ then $e_l^T A t = \sum_{j=1}^m a_{lj} t_j \geq a_{ll} t_l = a_{kk} \|t\|_{\ell^\infty}$. Therefore, if k is not in the support of a strategy t, it cannot be a pure strategy best response to t and so $BR(t) \subset C(t)$.

Although the translation between an SDD matrix and the function ρ used to describe pairwise payoff is not clear, we consider the continuous coordination Toeplitz game as games where

$$\rho'(z) \begin{cases} \leq 0 & z > 0 \\ = 0 & z = 0 \\ \geq 0 & z < 0 \end{cases} \tag{5.8}$$

This implies that ρ achieves its global maximum at $z = 0$ and so the pairwise interaction with pure strategies governed by such a ρ will satisfy the bandwagon property (and thus, this is indeed a coordination game). This restriction on ρ allows us to think more specifically about how coordination behavior evolves in time.

It is appropriate to make the comparison between the continuous Toeplitz coordination games and nonlocal diffusion equations, which are well covered in Andreu-Vaillo et al. (2010). Indeed, if we choose $\rho(z) = \frac{-1}{2} z^2$ our coordination equation becomes exactly the linear nonlocal diffusion equation $u_t = \int_\Omega K(x, y)(u(y) - u(x))dy$. Moreover, regardless of our choice of ρ, if we assume it is even and $C^{1,1}$, near zero $\rho'(z) \approx -z$. Because of this similarity, we will expect some of the same behavior as the nonlocal diffusion equation. In particular,

we will see that there is a weak maximum principle, and thus solutions to the IVP will exist globally in forward time. In the same way, it is appropriate to compare a continuous Toeplitz anti-coordination game to the backward nonlocal diffusion equation.

Lemma 5.4 (Weak Maximum Principle)**.** *If u solves $u_t = g[u]$ in Ω_T with $u(\cdot, 0) = u_0 \in C_b^0(\Omega)$ and if ρ satisfies (5.8), then*

$$\|u(\cdot, t_2)\|_\infty \leq \|u(\cdot, t_1)\|_\infty$$

whenever $t_1 \leq t_2$.

Proof. Notice that it is no loss of generality to assume $t_1 = 0$, so we will prove that $\|u(\cdot, t)\|_\infty \leq \|u_0\|_\infty$ for all $t \in [0, T)$ where T is the maximal existence time which may be infinite. Let $\epsilon > 0$ and let $v = \|u_0\|_\infty + \epsilon$. Now observe that if u solves $u_t = g[u]$ and $\tilde{u} := u - \epsilon t$, then $\tilde{u}_t = g[\tilde{u}] - \epsilon$. This is because $g[u - \epsilon t] = g[u]$ (More generally, g is invariant under vertical shifts, even if they are time-dependent). Suppose that $\tilde{u}(x^\star, t^\star) = v$ for the first time at some $x^\star \in \Omega$ and some $t^\star > 0$. That means that when $t < t^\star$, $\tilde{u}(y, t) < v$ for all $y \in \Omega$ and by continuity of u, $\tilde{u}(y, t^\star) \leq v$ for all $y \in \Omega$. Using the fact that $\rho'(z) \leq 0$ when $z \geq 0$, we obtain that

$$g[\tilde{u}](x^\star, t^\star) = \int_\Omega K(x, y)\rho'(\tilde{u}(x^\star, t^\star) - \tilde{u}(y, t^\star))dy \leq 0,$$

and therefore, $\partial_t \tilde{u}(x^\star, t^\star) \leq 0 - \epsilon < 0$. However, because $\tilde{u}$ is continuously differentiable in time (see proof of theorem 5.1), and because $\tilde{u} = v$ for the first time at $t = t^\star$, we can say $\partial_t \tilde{u}(x^\star, t^\star) \geq 0$. This is a contradiction, so we can say that $\tilde{u} < v$, which means $u < \|u_0\|_\infty + \epsilon + \epsilon t$. This is true for any ϵ so let $\epsilon \to 0$ and we see that $\|u(\cdot, t)\|_\infty < \|u_0\|_\infty$ for all finite time. This proves the result. □

This is tremendously helpful because it will allow us to give a uniform lower bound on existence time if we seek to extend solutions forward in time. Because we know that, if we select an $R \in \mathbb{R}$, a solution to the initial value problem with ρ satisfying (5.8) will exist on a

time interval $[0, T)$ and surely have $\|u(\cdot, T-\epsilon)\|_\infty < R$ and so it will be in the same closed subset of $C_b^0(\Omega_T)$, $E_{R,T} = \{u \in C_b^0(\Omega_T); u(\cdot, t) = u_0, \|u\|_\infty \leq R\}$. Because the provable existence time depended only on the forms of K, ρ, and the bound R, when we consider a coordination game, we can extend it by the same amount of time in each iteration. We can repeat the process indefinitely to get global existence. Global existence can be proven this way, but we may also prove the same result just by considering the previous two lemmas.

Theorem 5.2 (Global existence and uniqueness with particular $\rho \in C^{1,1}$)**.** *Let $\rho \in C^{1,1}(\mathbb{R})$ satisfy (5.8). Under this strengthened hypothesis, the Initial Value Problem $u_t = g[u]$ with $u(x, 0) = u_0 \in C_b^0(\Omega)$ has a unique continuous and bounded solution for all finite time.*

Proof. Observe that for any time t, the solution $u(\cdot t)$ must be in the compact subset

$$E_0 := \{u \in C_b^0(\Omega); \|u\|_\infty \leq \|u_0\|_\infty\} \subset C_b^0(\Omega)$$

because of lemma 5.4. If the maximal time of existence is $T < \infty$ then it must leave this compact subset before time T by lemma 5.3. This is a contradiction, so u cannot have a finite maximal time of existence. □

Lemma 5.4 and Theorem 5.2 are consistent with our understanding of the coordination game in the discrete case. For multiplayer coordination, it is an easy extension of the bandwagon property to say that innovation outside of the support of the current strategy profile is never a best response. Indeed, lemma 5.4 is the continuous version of the Weak Bandwagon Property of Cui and Shi (2022), which says that it is never optimal for an individual to take on a strategy not used by any opponent in a multiplayer coordination game.

The boundedness of solutions for the coordination game enables us to give a weak regularity result. This result will be especially important when we attempt to approximate solutions through numerical methods.

Theorem 5.3 (Regularity for the coordination game without boundary conditions)**.** *Let $\Omega \subseteq \mathbb{R}^n$. Suppose u solves the Initial Value Problem $u_t = g[u]$ with the coordination assumption*

(5.8) *and with* $u_0 \in C_b^{0,1}(\Omega)$ *with a uniform Lipschitz constant* L_0*, If* K *is uniformly Lipschitz in the first variable with respect to the* L^1 *norm, then for any finite time* t*,* $u(\cdot,t) \in C^{0,1}(\Omega)$*. Moreover, if* Ω *is open and bounded with a* C^1 *boundary,* $u \in W^{1,\infty}(\Omega)$*. Furthermore, for some positive* c *and* C*,*

$$\|D_x u(\cdot,t)\|_{L^\infty(\Omega)} \leq (L_0 + Ct)e^{ct}$$

Where C *depends only on* K *and* u_0 *and* c *depends only on* K *and* ρ*.*

Proof. Let $\phi(h,x,t) = u(x+h,t) - u(x,t)$ for some $h \in \mathbb{R}^n$ so that both x and $x+h$ are in Ω and observe that by simply subtracting the two solutions from one another

$$\phi(h,x,t) = \phi(h,x,0) + \int_0^t (g[u](x+h,s) - g[u](x,s))\,ds. \tag{5.9}$$

Let L_ρ be the Lipschitz constant for ρ' on the interval $[-2\|u_0\|_\infty, 2\|u_0\|_\infty]$. Recall by lemma 5.4 that $u \in [-\|u_0\|_\infty, \|u_0\|_\infty]$ for all $x,t \in \Omega_T$ so surely $u(x,t)-u(y,t) \in [-2\|u_0\|_\infty, 2\|u_0\|_\infty]$ regardless of x and y. Also note that ρ' is bounded by some W on the same interval. Now observe that this integrand is

$$\begin{aligned}
&|g[u](x+h,s) - g[u](x,s)| \\
&\quad = \left| \int_\Omega K(x+h,y)\rho'(u(x+h,s)-u(y,s)) - K(x,y)\rho'(u(x,s)-u(y,s))dy \right| \\
&\quad \leq \int_\Omega K(x+h,y)|\rho'(u(x+h,s)-u(y,s)) - \rho'(u(x,s)-u(y,s))|dy \\
&\qquad + \int_\Omega [K(x+h,y)-K(x,y)]|\rho'(u(x,s)-u(y,s))|ds \\
&\quad \leq \int_\Omega K(x+h,y)L_\rho|u(x+h,s)-u(x,s)|dy \\
&\qquad + W\|K(x+h,\cdot)-K(x,\cdot)\|_{L^1(\Omega)} \\
&\quad \leq L_\rho \int_\Omega K(x+h,y)|\phi(x,h,s)|dy + WL_K h \\
&\quad \leq L_\rho \sup_{z\in\Omega} \|K(z,\cdot)\|_{L^1(\Omega)} \|\phi(h,\cdot,s)\|_\infty + WL_k h
\end{aligned}$$

Let $c = L_\rho \sup_{z\in\Omega} \|K(z,\cdot)\|_{L^1(\Omega)}$ and $C = WL_k$ and make this replacement into equation (5.9) and take the sup norm over Ω to see that

$$\|\phi(h,\cdot,t)\|_\infty \leq \|\phi(h,\cdot,0)\|_\infty + \int_0^t [c\|\phi(h,\cdot,s)\|_\infty + Ch]ds$$

It is an easy application of Grönwall's inequality to see that

$$\|\phi(h,\cdot,t)\|_\infty \leq (\|\phi(h,\cdot,0)\|_\infty + Cht)e^{ct}$$

Note also that $\|\phi(h,\cdot,0)\|_\infty \leq |h|L_0$, so the difference from any $x \in \Omega$ on any finite time interval $[0,T]$ is controlled by

$$|u(x,t) - u(x+h,t)| \leq |h|(L_0 + Ct)e^{cT}$$

Notice that we have shown that for each t, $u(\cdot,t)$ is globally Lipschitz continuous in Ω with Lipschitz constant $L_T = (L_0 + CT)e^{cT}$. Note that this constant is uniform in t. This means, when Ω is open and bounded, we can use the characterization of $W^{1,\infty}(\Omega)$ Evans (1998) to conclude that u is weakly differentiable and the weak derivative is bounded by the Lipschitz constant.

$$\|D_x u(\cdot,t)\|_{L^\infty(\Omega)} \leq L_T = (L_0 + Ct)e^{cT}$$

□

Note that, in the above proof, the Lipschitz continuity of u holds without restrictions on the domain. Indeed, if Ω is not bounded, we have a global Lipschitz constant. Also note that in any open domain Ω and for each t, $u(\cdot,t) \in W^{1,\infty}_{loc}(\Omega)$.

Corollary 5.1. *For $\Omega \subseteq \mathbb{R}^n$, suppose that u solves the IVP $u_t = g[u]$ under the assumptions in theorem 5.3 on a finite time domain $[0,T]$. In this case, u is globally Lipschitz in $\Omega \times [0,T]$*

Proof. By theorem 5.3, u is Lipschitz continuous in space and the Lipschitz constant is uniform on a bounded time interval. Moreover, we know that $u(x,\cdot)$ is continuously

differentiable because $u_t(x,t) = g[u](x,t)$, which is continuous in space and time by 5.1. $g[u]$ is bounded above by a constant related to the form of K, ρ, and the bounds on u. Under the hypothesis of theorem 5.3, $\|u(\cdot,t)\|_\infty \leq \|u_0\|_\infty$ so we obtain

$$\begin{aligned}|u(x,t) - u(y,s)| &\leq |u(x,t) - u(y,t)| + |u(y,t) - u(y,s)| \\ &\leq C_T|x-y| + C_0|t-s| \\ &\leq L(|x-y| + |t-s|)\end{aligned}$$

Where L is a constant which depends only on T, K, ρ and u_0. Of course, we can adjust this norm to say that

$$|u(x,t) - u(y,s)| \leq C\sqrt{|x-y|^2 + |t-s|^2}$$

so that we can express it using the Euclidean norm in $\Omega_T \subset \mathbb{R}^{n+1}$ □

5.3.3 The Cauchy Problem with a Translation Invariant Kernel

The results presented in the previous subsections are rather general and do not rely on heavy assumptions about the domain or the form of K or ρ beyond what is strictly necessary for the model to be well posed. The analysis of this model is made exceedingly difficult, however, by the nonlinear nature of the nonlocality. Because the nonlocality is both nonlinear and non-monotonic, we currently have no comparison principle as in dos Santos et al. (2022), nor can we use Fourier analysis or semigroup theory, as is the standard for linear nonlocal diffusion problems Bucur and Valdinoci (2016); Andreu-Vaillo et al. (2010); Kavallaris and Suzuki (2018) to directly analyze the model. To take our analysis further, we present a strengthening of the regularity in the Cauchy setting with a different assumption on K.

Much of the existing literature on nonlocal problems focuses on the use of translation invariant or even radial kernels. In that tradition, we will examine the improved result we can obtain through using a kernel of the form $K(z) \in L^1(\Omega)$. This assumption means that every player has the same pattern of interaction distributed spatially. In the case that

$\Omega = \mathbb{R}^n$ we can mildly strengthen the regularity result from theorem 5.3. The purpose of this strengthening is to remove the dependence on the shape of K from the Lipschitz constant. In future work, we will seek to investigate the "zero-horizon limit" or the "local limit" of this nonlinear nonlocal diffusion problem (i.e., the limit as the support of K goes to $\{0\}$). In the case that ρ' is linear, we see that the results on non-local limits from Du et al. (2015, 2022); Mengesha and Du (2015); Andreu-Vaillo et al. (2010); Tao et al. (2017, 2019) will hold. For the nonlinear case, the scaling of the kernel to achieve the non-local limit poses a problem for the provable regularity of solutions, which has, at present, prevented us from characterizing the local limit of this diffusion equation. However, this strengthened regularity result will be crucial in this pursuit.

Theorem 5.4 (Regularity for the coordination game with a Translation Invariant Kernel)**.** *Consider the domain $\mathbb{R}^n$. Suppose that u solves the Initial Value Problem $u_t = g[u]$ with the coordination assumption (5.8) and with $u_0 = C_b^{0,1}(\mathbb{R}^n)$ with the uniform Lipschitz constant L_0. If K is a translation invariant Kernel (i.e. $K(x,y) = J(x-y)$) then $u(\cdot,t) \in C^{0,1}(\mathbb{R}^n)$ for any finite time. Moreover the global Lipschitz constant for $u(\cdot,t)$ on $\mathbb{R}^n$ is given as $L_0 e^{cT}$ where c depends only on the Lipschitz constant for ρ' and on $\|u_0\|_\infty$.*

Proof. Without loss of generality, we normalize the kernel $J(z)$ so that $\|J\|_{L^1(\mathbb{R}^n)} = 1$. We will proceed with this proof in much the same way as theorem 5.3. As before we let $\phi(h,x,t) = u(x+h,t) - u(x,t)$ for some $h \in \mathbb{R}^n$ with some magnitude r and a bearing $\theta \in S^{n-1}$ and again observe the equation (5.9) holds.

Let L_ρ be the Lipschitz constant for ρ' on the interval $[-2\|u_0\|_\infty, 2\|u_0\|_\infty]$ and by lemma 5.4 we know that $u \in [\|u_0\|_\infty, \|u_0\|_\infty]$ for all $x,t \in \Omega_T$. We take the same computation as

before to find that the quantity

$$\begin{aligned}
&|g[u](x+h,s) - g[u](x,s)| \\
&\leq \underbrace{\int_{\mathbb{R}^n} J(x+h-y)|\rho'(u(x+h,s)-u(y,s)) - \rho'(u(x,s)-u(y,s))|dy}_{I_1} \\
&\quad + \underbrace{\int_{\mathbb{R}^n} |(J(x+h-y)-J(x-y))\rho'(u(x,s)-u(y,s))|dy}_{I_2}
\end{aligned}$$

As before, $I_1 \leq L_\rho \|J(x-\cdot)\|_{L^1(\mathbb{R}^n)} \|\phi(h,\cdot,s)\|_\infty = L_\rho \|\phi(h,\cdot,s)\|_\infty$. For I_2 we can see that

$$\begin{aligned}
I_2 &= \left| \int_{\mathbb{R}^n} [J(x+h-y) - J(x-y)]\rho'(u(x,s)-u(y,s))dy \right| \\
&= \left| \int_{\mathbb{R}^n} J(x+h-y)\rho'(u(x,s)-u(y,s))dy - \int_{\mathbb{R}^n} J(x-y)\rho'(u(x,s)-u(y,s))dy \right| \\
&= \left| \int_{\mathbb{R}^n + h} J(x-y)\rho'(u(x,s)-u(y-h,s))dy - \int_{\mathbb{R}^n} J(x-y)\rho'(u(x,s)-u(y,s))dy \right| \\
&= \left| \int_{\mathbb{R}^n} J(x-y)[\rho'(u(x,s)-u(y-h,s)) - \rho'(u(x,s)-u(y,s))]dy \right| \\
&\leq \int_{\mathbb{R}^n} J(x-y)L_\rho \big|u(x,s)-u(y-h,s)-u(x,s)+u(y,s)|dy \\
&\leq L_\rho \|J\|_{L^1(\mathbb{R}^n)} \|u(\cdot-h,s)-u(\cdot,s)\|_{L^\infty(\mathbb{R}^n)} \\
&\leq L_\rho \|\phi(-h,\cdot,s)\|_{L^\infty(\mathbb{R}^n)}
\end{aligned}$$

Now instead of considering only the supremum of $\phi(-h,x,s)$ for $x \in \mathbb{R}^n$, we will decompose h into r and θ and consider

$$\psi(r,s) := \sup_{x,\theta \in \mathbb{R}^n \times S^{n-1}} \phi(r,\theta,x,s).$$

From our inequalities on I_1 and I_2 We can see that

$$\phi(h,\cdot,t) \leq \phi(h,\cdot,0) + \int_0^t L_\rho \|\phi(h,\cdot,s)\|_{L^\infty(\Omega)} ds + \int_0^t L \|\phi(-h,\cdot,s)\|_{L^\infty(\Omega)} ds$$

So we can make the replacement that

$$\psi(r,t) \leq \psi(r,0) + 2L_\rho \int_0^t \psi(r,s)ds$$

From here, we can use our standard Grönwall's inequality to see that

$$\psi(r,t) \leq \psi(r,0)e^{2L_\rho t}$$

Recall that $\psi(r,0) \leq rL_0$ and so

$$|u(x,t) - u(x+h,t)| \leq |h|L_0 e^{2L_\rho t}.$$

Therefore, for each t, $u(\cdot,t)$ is Lipschitz continuous for any finite time and the global Lipschitz constant is $L_0 e^{2L_\rho T}$. □

In this section, we have shown that this model has unique solutions and, for particular ρ, those solutions exist globally and are as regular as we can expect. Unlike local diffusion models, nonlocal diffusion problems do not exhibit a smoothening of initial data, so we suspect that to gain higher regularity, the regularity of the initial data would have to be increased.

5.4 Analytical Examples

Having shown that solutions to the IVP without boundary conditions exist and are unique, we now turn our attention to the behavior and properties of solutions. We begin by showing several examples wherein we can write down solutions easily.

Example 5.1 (Unstructured Coordination)**.** *Consider a bounded domain Ω. If $\rho = -\frac{z^2}{2}$ and $K(x,y) = \frac{1}{Vol(\Omega)}$, we call this the continuous version of the unstructured coordination game (because every player interacts with every other player equally). In this case, the solution can be written down for any $u_0 \in C_b^0(\Omega)$.*

$$u(x,t) = e^{-t}\left(u_0(x) - \fint_\Omega u_0(y)dy\right) + \fint_\Omega u_0(y)dy$$

Proof. Observe that our nonlocality g reduces to

$$g[u] = \frac{1}{Vol(\Omega)} \int_\Omega u(y,t) - u(x,t) dy = \fint_\Omega u(y,t) dy - u(x,t)$$

Once we show that $\fint_\Omega u(y,t)dy$ is constant in time, we can solve point-wise as an ODE. Observe that

$$\begin{aligned}
u(x,t) &= u_0(x) + \int_0^t \left[\fint_\Omega u(y,s)dy - u(x,s) \right] ds \\
\fint_\Omega u(x,t)dx &= \fint_\Omega u_0(x)dx + \fint_\Omega \int_0^t \left[\fint_\Omega u(y,s)dy - u(x,s) \right] dsdx \\
\fint_\Omega u(x,t)dx &= \fint_\Omega u_0(x)dx + \int_0^t \left[\fint_\Omega \fint_\Omega u(y,s)dydx - \fint_\Omega u(x,s)dx \right] ds
\end{aligned}$$

Note that $\fint_\Omega \fint_\Omega u(y,s)dydx = \fint_\Omega u(y,s)dy \fint_\Omega dx = \fint_\Omega u(y,s)dy$ and observe that this implies $\fint_\Omega u(x,t)dx = \fint_\Omega u_0(x)dx$ for all t. Therefore, we can write our nonlocal equation as

$$u_t(x,t) + u(x,t) = \fint_\Omega u_0(y)dy$$

Now it is a simple exercise in ODEs to see that the solution to this is

$$u(x,t) = e^{-t} \left(u_0(x) - \fint_\Omega u_0(y)dy \right) + \fint_\Omega u_0(y)dy$$

In particular, if we adjust the initial strategy profile so that it has $\fint_\Omega u_0(y)dy = 0$, then $u(x,t) = e^{-t}u_0(t)$. □

The example is illustrative because it validates our model with the expected result in the discrete case. It is easy to see that in the unstructured case here, the only equilibrium is a consensus equilibrium. Later in section 5.6, we will be able to extend result in the unstructured case and say that the only stationary solution (and thus the only equilibrium strategy profile) is the consensus solution whenever ρ' is nonzero away from zero. This is consistent with the result of Kandori et al. (1993), which found that in the case where all individuals interact, the consensus equilibrium is the only stable equilibrium. The

consistency breaks down in the case that ρ' is compactly supported, but in the discrete case, all strategies are comparable, and so the compact support of ρ' does not have a discrete analog.

Example 5.2 (Unstructured Anti-coordination)**.** *Consider a bounded domain Ω with $\rho(x) = \frac{z^2}{2}$ and $K(x,y) = \frac{1}{Vol(\Omega)}$. The initial value problem with initial date $u_0 \in C_b^0$ will have the solution*

$$u(x,t) = e^t \left(u_0(x) - \fint_\Omega u_0(y)dy \right) + \fint_\Omega u_0(y)dy$$

Example 5.2 is an anticoordination game in the sense that it is the opposite of the coordination game in example 5.1. It is equivalent to considering the solutions to the coordination game in backward time, and for this reason, the solution is immediate. Observe that in this example, the coordination condition (5.8) is not met, and thus the solution does not abide by a maximum principle. However, the solution does exist globally in time.

Example 5.3 (Structured asymmetric-Toeplitz game)**.** *Consider a domain Ω with a Kernel $K \in C_b^0(\Omega; L^1(\Omega))$. If $\rho(z) = cz$ (and thus the game is a dis-coordination game), then the solution is*

$$u(x,t) = u_0(x) + tc\|K(x,\cdot)\|_{L^1(\Omega)}.,$$

Proof. It is easy to see that the nonlocality in this case becomes

$$g[u] = \int_\Omega cK(x,y)dy$$

so finding the solution to the IVP is trivial. □

In example 5.3, we see a glimpse of different behaviors present in Toeplitz games. In example 5.1, solutions remain bounded and always converge to the consensus equilibrium. Example 5.2 is simply the backward time solution of the coordination game, and so any constant solution represents an unstable equilibrium, but starting from any non-constant

initial data will result in a solution growing without bound. In example 5.3, we have a game wherein every player wants to be as far above (or below) the population average as possible, so the strategy profile will increase (or decrease) monotonically depending on the kernel K. If we combine these elements, we can get a situation wherein players are acting under coordination but also seeking to be above-average.

Example 5.4 (unstructured coordination and advection)**.** *Let Ω be a compact domain. If $K(x,y) = \frac{1}{Vol\Omega}$ and $\rho = \frac{-z^2}{2} + cz$ then the solution will be*

$$u(x,t) = e^{-t}(u_0(x) - \bar{u_0}) + \bar{u_0} + ct$$

where $\bar{u_0} = \fint_\Omega u_0(y)dy$

Proof. Again the nonlocality will be

$$g[u] = \frac{1}{Vol\Omega}\int_\Omega u(y,t) - u(x,t) + cdy$$

Let w be a general from example 5.1 with K as described, and let $v = ct$. v is only a vertical translation so $w(x) - w(y) = (w(x) + v(x)) - (w(y) + v(y))$. Let $u = w + v$ and note that $w(x,t) - w(y,t) = u(x,t) - u(y,t)$. Thus

$$\begin{aligned} u_t &= w_t + v_t \\ &= \frac{1}{Vol\Omega}\int_\Omega w(y,t) - w(x,t)dy + \frac{1}{Vol\Omega}\int_\Omega cdy \\ &= \frac{1}{Vol\Omega}\int_\Omega u(y,t) - u(x,t) + cdy \\ &= g[u] \end{aligned}$$

Therefore, we can easily see that the solution to the IVP is

$$u(x,t) = e^{-t}\left(u_0(x) - \bar{u_0}\right) + \bar{u_0} + ct.$$

□

It appears as though we have combined solutions from examples 5.1 and 5.3. However, this linear combination of solutions only works because solutions are still solutions under vertical translation. This is the same thing as saying if $u_t = g[u]$ and $w = u + ct$ then $w_t = g[u] + c$. In general, linear combinations of solutions do not solve linear combinations of IVPs.

5.5 Numerical Results

The examples in the previous subsections help us to understand the kinds of behavior we may expect from these kinds of games, but we cannot, in general, solve the IVP analytically. However, because of theorem 5.3, we can use numerical methods to find solutions, at least in the coordination case.

Let us begin on the unit square $\Omega = \prod_{i=1}^{n}[0,1]$ in $\mathbb{R}^n$ and let $\Omega_T = \Omega \times (0,T)$. If $u_t = g[u]$ on Ω_T and $u(x,0) = u_0 \in C^{0,1}(\Omega)$ then we will try to approximate u with the grid function $w \in \mathcal{V}(\Omega_T^{(h,\tau)})$. Here $\mathcal{V}$ is the set of grid functions which are defined on a discretization of $\overline{\Omega_T}$,

$$\Omega_T^{(h,\tau)} = \Omega^h \times \{\tau l\}_{l=0}^{\frac{T}{\tau}} = \prod_{i=1}^{n} \left(\{hk\}_{k=0}^{\frac{1}{h}} \right)_i \times \{\tau l\}_{l=0}^{T/\tau}. \tag{5.10}$$

In particular the set of grid functions we are interested in are $\mathcal{V}(\Omega_T^{(h,t)}) = \{v; v : \Omega_T^{(h,t)} \to \mathbb{R}\}$ and $\mathcal{V}(\Omega^h) = \{v; v : \Omega^h \to \mathbb{R}\}$ These grid function spaces are different ways of imagining $\mathbb{R}^{\frac{1}{h}^n \cdot \frac{T}{\tau}}$ and $\mathbb{R}^{\frac{1}{h}^n}$ respectively. We use this reimagining so that the comparisons between $v \in \mathcal{V}(\Omega_T^{(h,\tau)})$ and $u \in C^{0,1}(\Omega_T)$ are more natural.

Let $\pi^h : C^0(\Omega) \to \mathcal{V}(\Omega^h)$ be the operator which takes a function on Ω and returns the grid function which is equal to the input function at every point of the grid Ω^h. In the present study, we will deal only with the case that $K \in C_b^0(\Omega; C_0^{0,1})$ so $\pi^h K(x,\cdot) \in \mathcal{V}(\Omega^h)$ for every $x \in \Omega^h$. A generalization is possible, but is not immediately necessary for the main results of the paper. There are some cases of $K \in C_b^0(\Omega; L^1(\Omega))$ for which this method is not appropriate. (For example $K(x,y) = d(x,\partial\Omega)^{-n} J(\frac{x-y}{d(x,\partial\Omega)})$ where $J \in L^1(B(0,1))$).

Let $w(\cdot,0) = \pi^h u_0$ on Ω^h, and compute for an $\mathbf{x} \in \Omega^h$,

$$w(\mathbf{x}, t_{i+1}) = w(\mathbf{x}, t_i) + \tau \sum_{\mathbf{y} \in {}^-\Omega^h} K(\mathbf{x}, \mathbf{y}) \rho'(w(\mathbf{x}, t_i) - w(\mathbf{y}, t_i)) h^n \tag{5.11}$$

where ${}^-\Omega^h = \prod_{i=1}^n (\{hk\}_{k=0}^{\frac{1}{h}-1})_i$. We will show for this particular domain that the method (5.11) is consistent and convergent.

Lemma 5.5 (Consistency of Forward Euler Method)**.** *The numerical scheme* (5.11) *is consistent to order* $\tau + h$ *for the nonlocality* (5.5) *with a bounded* $w \in C^{1,1}$ *with no boundary data when* $K \in C_b^0(\Omega; C_0^{0,1})$ *with a uniform bounds on* $\|K(x,\cdot)\|_\infty$ *and on the Lipschitz constant for* $K(x,\cdot)$*.*

Proof. First, we compute the error of the right-hand numerical quadrature

$$\mathcal{G}^h[w](\mathbf{x}, t_i) := \sum_{\mathbf{y} \in {}^-\Omega^h} K(\mathbf{x}, \mathbf{y}) \rho'(w(\mathbf{x}, t_i) - w(\mathbf{y}, t_i)) h^n \tag{5.12}$$

for a bounded $w \in C^{0,1}$. Let $\mathbf{y} \in {}^-\Omega^h$ and observe that in the hyperrectangle $\omega_{\mathbf{y}} := \prod_{k=1}^n [\mathbf{y}_k, \mathbf{y}_k + h]$, $|w(y, t_i) - w(\mathbf{y}, t_i)| \le L c_n h$ for all $y \in \omega_{\mathbf{y}}$, where L is the Lipschitz constant for w and c_n is a constant depending on the dimension of Ω.

As such, for any $y \in \omega_{\mathbf{y}}$, $\mathbf{x} \in \Omega^h$, and $\mathbf{y} \in {}^-\Omega^h$, we have $|\rho'(w(\mathbf{x}, t_i) - w(y, t_i)) - \rho'(w(\mathbf{x}, t_i) - w(\mathbf{y}, t_i))| \le L_\rho L c_n h$ where L_ρ is the Lipschitz constant for ρ' on the interval containing the compact range of w, $[-2\|w\|_\infty, 2\|w\|_\infty]$. By assumption, $\|K(\mathbf{x},\cdot)\|_\infty \le B < \infty$ uniformly over Ω^h and has a Lipschitz constant, $L_K < \infty$ which is an appropriate Lipschitz constant for $K(x,\cdot)\, \forall x \in \Omega$. This, along with the fact that ρ' attains its maximum on $[-2\|u\|_\infty, 2\|u\|_\infty]$, which we call W, allows us to do the following computation. First note

that $K(\mathbf{x},\mathbf{y})\rho'(u(\mathbf{x},t_i)-u(\mathbf{y},t_i))h^n = \int_{\omega_y} K(\mathbf{x},\mathbf{y})\rho'(u(\mathbf{x},t_i)-u(\mathbf{y},t_i))dy$. Thus we write,

$$\begin{aligned}
&\left| \int_{\omega_{\mathbf{y}}} K(\mathbf{x},y)\rho'(u(\mathbf{x},t_i)-u(y,t_i))dy - K(\mathbf{x},\mathbf{y})\rho'(u(\mathbf{x},t_i)-u(\mathbf{y},t_i))h^n \right| \\
&\quad \leq \int_{\omega_{\mathbf{y}}} \left| K(\mathbf{x},y)\rho'(u(\mathbf{x},t_i)-u(y,t_i))dy - K(\mathbf{x},\mathbf{y})\rho'(u(\mathbf{x},t_i)-u(\mathbf{y},t_i) \right| dy \\
&\quad \leq \int_{\omega_{\mathbf{y}}} |K(\mathbf{x},y)-K(\mathbf{x},\mathbf{y})||\rho'(u(\mathbf{x},t_i)-u(y,t_i))|dy \\
&\qquad + \int_{\omega_{\mathbf{y}}} |K(\mathbf{x},\mathbf{y})||\rho'(u(\mathbf{x},t_i)-u(y,t_i)) - \rho'(u(\mathbf{x},t_i)-u(\mathbf{y},t_i))|dy \\
&\quad =: I_1 + I_2
\end{aligned}$$

As we have before, we will deal with each integral separately. The second integral is controlled by $I_2 \leq L_\rho L c_n h \int_{\omega_{\mathbf{y}}} |K(\mathbf{x},\mathbf{y})|dy \leq B L_\rho L c_n h^{n+1}$. Now notice that for I_1

$$\begin{aligned}
I_1 &\leq W \int_{\omega_{\mathbf{y}}} |K(\mathbf{x},y)-K(\mathbf{x},\mathbf{y})|dy \\
&\leq W \int_{\omega_{\mathbf{y}}} L_K h dy \\
&\leq W L_K h^{n+1}
\end{aligned}$$

Thus, the original difference is controlled by

$$C_1 h^{n+1} := (W L_K + B L_\rho L c_n) h^{n+1}$$

Now when we sum across every $\mathbf{y} \in^- \Omega_T^h$ we see that

$$|g[w](\mathbf{x},t_i) - \mathcal{G}^h[w](\mathbf{x},t_i)| \leq C_1 h^{n+1} \frac{1}{h^n}$$

Therefore, we have shown that

$$g[w] = \mathcal{G}^h[w](\mathbf{x},t_i) + \mathcal{O}(h)$$

Now, suppose w is continuously differentiable in time. It is easy to see that the forward difference

$$\frac{\partial}{\partial t} w(\mathbf{x}, t_i) = \frac{w(\mathbf{x}, t_i) - w(\mathbf{x}, t_{i+1})}{\tau} + \mathcal{O}(\tau).$$

Thus we can say that the numerical scheme (5.11) is consistent to order $\tau + h$ for functions w which are bounded, C^1 in time, and $C^{0,1}$ in space. □

For a linear problem, the consistency from lemma 5.5 and stability from a discrete maximum principle would complete the proof of convergence. The discrete maximum principle holds for this method and is proved in the appendix A.2, however, it only provides a sanity check that this method makes sense when τ and h are sufficiently small. Because the equation is nonlinear, we cannot use the Lax principle and lemma A.3 to prove convergence. Instead, we will recapitulate in the discrete case the argument about the Lipschitz continuity of $\mathcal{G}^h$ in $\Omega_T^{(h,\tau)}$.

Lemma 5.6 (Lipschitz continuity of $\mathcal{G}^h$)**.** *For any bounded (in the sup norm sense) subset of* $X_R := \{w \in \mathcal{V}(\Omega_T^{(h,\tau)}); \|w\|_{\ell^\infty} \leq R\}$*, there is a* $C^{\mathcal{G}} \geq 0$ *such that for every* $w_1, w_2 \in X_R$

$$\|\mathcal{G}[w_1](\cdot, t_i) - \mathcal{G}[w_2](\cdot, t_i)\|_{\ell^\infty(\Omega^h)} \leq C^{\mathcal{G}} \|w_1(\cdot, t_i) - w_2(\cdot, t_i)\|_{\ell^\infty(\Omega^h,)}$$

so long as $K \in C_b^0(\Omega; C_0^{0,1})$ *with a uniformly bounded* $\|K(x, \cdot)\|_\infty$ *and* $\mathcal{G}$ *is defined as in* (5.12)*.*

Proof. Consider $w_1, w_2 \in X_R$ and observe that $\|\mathcal{G}[w_1] - \mathcal{G}[w_2]\|_{\ell^\infty}$

$$\leq \max_{\mathbf{x} \in \Omega^h} \left\{ \sum_{\mathbf{y} \in {}^-\Omega^h} |K(\mathbf{x}, \mathbf{y})| |\rho'(w_1(\mathbf{x}, t_i) - w_1(\mathbf{y}, t_i)) - \rho'(w_2(\mathbf{x}, t_i) - w_2(\mathbf{y}, t_i))| h^n \right\}$$

$$\leq \max_{\mathbf{x} \in \Omega^h} \left\{ \|\rho'(w_1(\mathbf{x}, t_i) - w_1(\cdot, t_i)) - \rho'(w_2(\mathbf{x}, t_i) - w_2(\cdot, t_i))\|_{\ell^\infty(\Omega^h)} \sum_{y \in {}^-\Omega^h} |K(\mathbf{x} - \mathbf{y})| h^n \right\}$$

Notice that, because the domain in question has volume $vol(\Omega) = 1$, we have

$$\begin{aligned}\sum_{\mathbf{y}\in^{-}\Omega^h} |K(\mathbf{x},\mathbf{y})|h^n &\leq \sum_{\mathbf{y}\in\Omega^h} \|\pi^h K(\mathbf{x},\mathbf{y})\|_{\ell^\infty(\Omega^h)} h^n \\ &\leq \|\pi^h K(\mathbf{x},\cdot)\|_{\ell^\infty(\Omega^h)} \sum_{\mathbf{y}\in^{-}\Omega^h} h^n \\ &\leq \|K(\mathbf{x},\cdot)\|_{\ell^\infty(\Omega^h)} vol(\Omega) \\ &\leq B := \sup_{\mathbf{x}\in\Omega^h} \|K(\mathbf{x},\cdot)\|_{\ell^\infty(\Omega^h)}\end{aligned}$$

for all $\mathbf{x} \in \Omega^h$ and so we proceed with a very similar argument about ρ' as in lemma 5.2.

$$\begin{aligned}&\|\rho'(w_1(\mathbf{x},t_i) - w_1(\cdot,t_i)) - \rho'(w_2(\mathbf{x},t_i) - w_2(\cdot,t_i))\|_{\ell^\infty(\Omega^h)} \\ &\qquad \leq L_\rho \|w_1(\mathbf{x},t_i) - w_1(\cdot,t_i) - w_2(\mathbf{x},t_i) + w_2(\cdot,t_i)\|_{\ell^\infty(\Omega^h)} \\ &\qquad \leq L_\rho \left(|w_1(\mathbf{x},t_i) - w_2(\mathbf{x},t_i)| + \|w_1(\cdot,t_i) - w_2(\cdot,t_i)\|_{\ell^\infty(\Omega^h)}\right)\end{aligned}$$

So naturally we see, as before, that

$$\begin{aligned}&\max_{\mathbf{x}\in\Omega^h} \|\rho'(w_1(\mathbf{x},t_i) - w_1(\cdot,t_i)) - \rho'(w_2(\mathbf{x},t_i) - w_2(\cdot,t_i))\|_{\ell^\infty(\Omega^h)} \\ &\qquad \leq 2L_\rho \|w_1(\cdot,t_i) - w_2(\cdot,t_i)\|_{\ell^\infty(\Omega^h)}\end{aligned}$$

Therefore, we get the result that

$$\|\mathcal{G}[w_1](\cdot,t_i) - \mathcal{G}[w_2](\cdot,t_i)\|_{\ell^\infty(\Omega^h)} \leq 2L_\rho M \|w_1(\cdot,t_i) - w_2(\cdot,t_i)\|_{\ell^\infty(\Omega^h)}$$

Let $C^{\mathcal{G}} = 2L_\rho M$ to complete the proof. Again L_ρ may depend on R so $C^{\mathcal{G}}$ will depend on R. □

With these two results, we can show that the numerical scheme (5.11) is convergent in the case that $K \in C_b^0(\Omega; C_0^{0,1})$ with uniformly bounded $\|K(x,\cdot)\|_\infty$ and with a global Lipschitz constant. The general case wherein $K \in C_b^0(\Omega; L^1(\Omega))$ requires a choice of approximate K which are bounded and defined everywhere to manage the case in which $K(x,\cdot)$ has a

singularity for some $x \in \Omega$, which makes this method inappropriate in some cases. There are more sophisticated numerical methods for non-local equations, which are equipped to handle the more general case D'Elia et al. (2020), but we do not use them in the analysis in section 5.6. For this reason, we only consider the finite difference method in this nonlinear setting, which mildly extends the results from Du et al. (2019) for the linear setting.

Theorem 5.5 (Convergence of the Forward Euler Scheme)**.** *In a domain with discretization* (5.10)*, the IVP* $u_t = g[u]$ *on* Ω*, with* $u(x,0) = u_0 \in C_b^{0,1}(\Omega)$*, and with* ρ *satisfying* (5.8)*, the numerical scheme* (5.11) *is convergent in the case where* $K \in C_b^0(\Omega; C_0^{0,1})$ *with uniformly bounded* $\|K(x,\cdot)\|_\infty$ *and a uniform global Lipschitz constant.*

Proof. Let $\pi_{h,\tau} : C^0(\Omega_T) \to \mathcal{V}(\Omega_T^{(h,\tau)})$ discretize u, a solution of the IVP $u_t = g[u]$ with $u(x,0) = u_0 \in C_b^{0,1}(\Omega)$. Let w be a grid function which solves the numerical scheme (5.11) with $w(\mathbf{x},0) = \pi_h u_0$. Further let $e = \pi_{h,\tau} u - w$. Now notice that

$$\begin{aligned}
\frac{e(\mathbf{x},t_{i+1}) - e(\mathbf{x},t_i)}{\tau} &= \frac{u(\mathbf{x},t_{i+1}) - u(\mathbf{x},t_i)}{\tau} - \mathcal{G}^h[w](\mathbf{x},t_i) \\
&= u_t(\mathbf{x},t_i) - \mathcal{G}^h[w](\mathbf{x},t_i) + \mathcal{O}(\tau) \\
&= g[u](\mathbf{x},t_i) - \mathcal{G}^h[w](\mathbf{x},t_i) + \mathcal{O}(\tau) \\
&= \mathcal{G}^h[u](\mathbf{x},t_i) - \mathcal{G}^h[w](\mathbf{x},t_i) + \mathcal{O}(\tau + h)
\end{aligned} \tag{5.13}$$

by lemma 5.5. $\mathcal{G}^h$ is not linear, so the stability of the method does not complete the proof. Instead, we use lemma 5.6 to show that

$$\begin{aligned}
e(\mathbf{x},t_{i+1}) &= e(\mathbf{x},t_i) + \tau\left(\mathcal{G}^h[u](\mathbf{x},t_i) - \mathcal{G}^h[w](x,t_i) + \mathcal{O}(\tau+h)\right) \\
\|e(\cdot,t_{i+1})\|_{\ell^\infty(\Omega^h)} &\le \|e(\cdot,t_i)\|_{\ell^\infty(\Omega^h)} + \tau\|\mathcal{G}^h[u](\mathbf{x},t_i) - \mathcal{G}^h[w](x,t_i)\|_{\ell^\infty(\Omega^h)} + \tau|\mathcal{O}(\tau+h)| \\
&\le \|e(\cdot,t_i)\|_{\ell^\infty(\Omega^h)} + \tau C^{\mathcal{G}}\|\pi^h u(\mathbf{x},t_i) - w(x,t_i)\|_{\ell^\infty(\Omega^h)} + \tau|\mathcal{O}(\tau+h)| \\
&\le (1+\tau C^{\mathcal{G}})\|e(\cdot,t_i)\|_{\ell^\infty(\Omega^h)} + \tau|\mathcal{O}(\tau+h)|
\end{aligned}$$

We now employ Grönwall's lemma in the discrete forward difference case to say that

$$\|e(\cdot,t_{i+1})\|_{\ell^\infty(\Omega^h)} \le (1+\tau C^{\mathcal{G}})^i\|e(\cdot,0)\|_{\ell^\infty(\Omega^h)} + \frac{1}{C^{\mathcal{G}}}((1+\tau C^{\mathcal{G}})^i - 1)C(\tau+h)$$

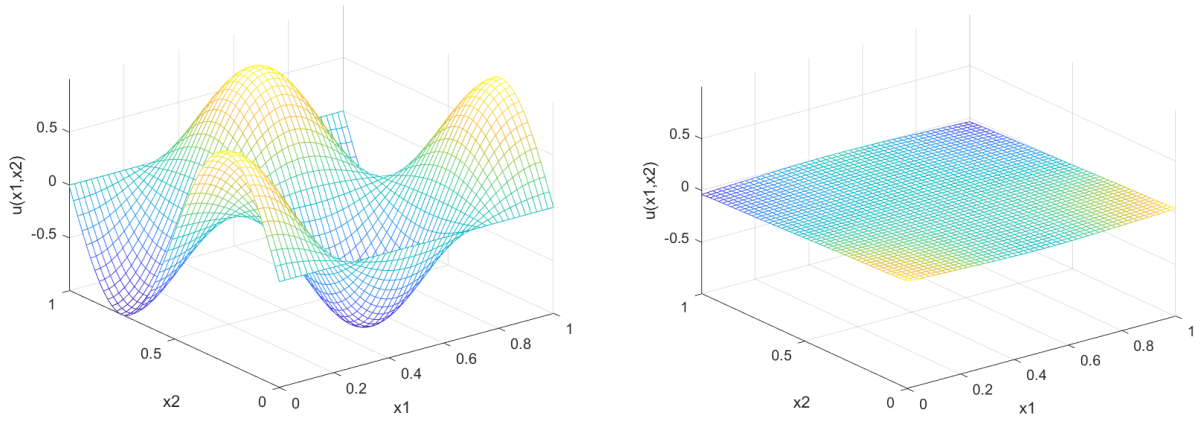

Figure 5.1: The Initial condition (**left**) and solution after $T = 10$ (**right**) to the IVP $u_t = g[u]$ approximated by the numerical scheme (5.11). Here the recognition function has non-zero derivative on all of $\mathbb{R} \setminus \{0\}$

Naturally, $e(\cdot, 0) \equiv 0$ and for finite time T we have a maximum $i \leq T/\tau$ so we can say that

$$\|e\|_{\ell^\infty(\Omega_T^{(\tau,h)})} \leq \tilde{C}((1 + \tau C^{\mathcal{G}})^{\frac{T}{\tau}} - 1)(\tau + h)$$

Observe that $C^{\mathcal{G}}$ does not depend on h or τ. It only depends on R, but because of lemma 5.4 and its discrete analogue (lemma A.3), R is the same at each time step; therefore, so is $C^{\mathcal{G}}$. Also observe that $\lim_{\tau \to 0}(1 + \tau C^{\mathcal{G}})^{\frac{T}{\tau}}$ exists and so this quantity is bounded for any sufficiently small τ and indeed as $(\tau, h) \to \mathbf{0}$, $\|e\|_{\ell^\infty} \to 0$. □

This proof was done for the unit cube, but each part is easily generalizable to any bounded domain with constants which may depend on the volume of the domain itself. Now that we are certain that this numerical scheme appropriately approximates solutions to the IVP, we can show several examples.

Interrogating the system with numerical methods allows us to observe some curious properties of solutions to the coordination equation. One such interesting observation is the qualitatively different behavior seen for solutions which depends on the support of ρ as in figures 5.1 and 5.2. This will be discussed further in the modeling results.

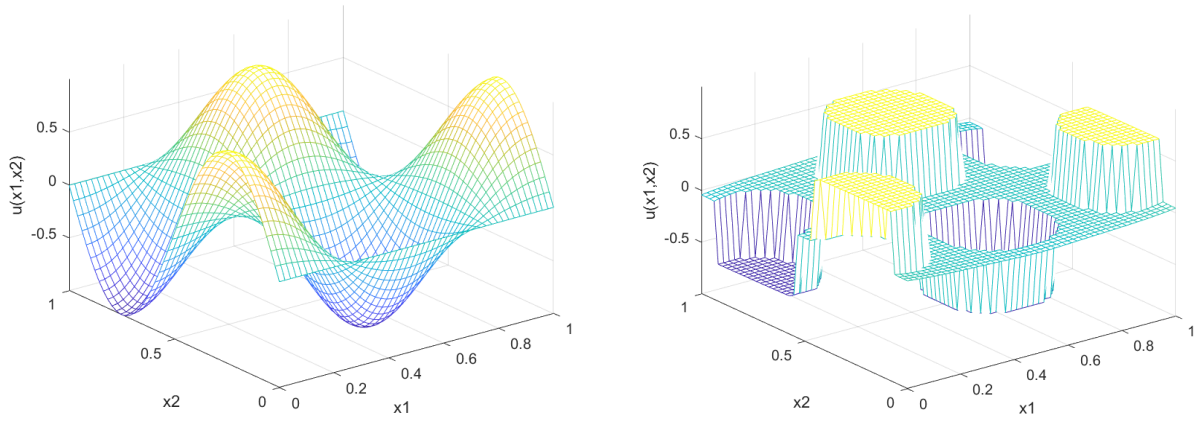

Figure 5.2: The Initial condition (**left**) and solution after $T = 10$ (**right**) to the IVP $u_t = g[u]$ approximated by the numerical scheme (5.11). Here the recognition functions is identically 0 outside $B_{1/4}(0)$.

5.6 Modeling Results

Having shown that the model is well posed, solutions exist, and that solutions can be approximated through simple numerical methods, we turn our attention now to what this model may reveal about coordination in continuous settings. The first, and most striking observation is the apparent discontinuities which emerge in the limit at $t \to \infty$ when ρ' has compact support (Fig. 5.2). It has not been proven that solutions to the IVP will converge, even pointwise to a limit, but we do know that, if they do converge, they will clearly converge to a solution to the problem $g[u] = 0$ in Ω. Without imposing boundary data, solutions to this problem obviously exist (e.g. $u \equiv 0$). The existence of non-trivial solutions and solutions with boundary data are not discussed in the present study. We will, however, discuss several results about stationary solutions and present some results from numerical experiments.

5.6.1 Stationary Solutions

Recall that, as the game was introduced in section 5.2, we are not only interested in the dynamic results but in fact may wish to consider the classical game with no time component. Results about stationary solutions in the dynamic game can, unsurprisingly, reveal more

effective ways of searching for Nash equilibria in the classical game. If u is a Nash equilibrium in the classical game, by definition, it will have the property that

$$J[u] := \inf_{(x,s)\in\Omega\times\mathbb{R}} \{w(x|u) - w(x|u + t\chi_{\{x\}})\} = 0. \tag{5.14}$$

This is exactly the condition that each player is playing their best response.

Proposition 5.2. *If u is a Nash Equilibrium to the game with players in $\Omega \subset \mathbb{R}^n$, strategies in $\mathbb{R}$ and payoffs as in (5.3), then u is necessarily a stationary solution in the system $u_t = g[u]$.*

Proof. In the same way as in the proof of proposition 5.1 let $S_x(h) := \int_\Omega K(x,y)\rho(u(x) + h - u(y))dy$ and note that, so long as $\rho \in C^{1,1}(\mathbb{R})$ then $S_x(h) \in C^{1,1}(\mathbb{R})$ and $\frac{d}{dh}S_x(0) = \int_\Omega K(x,y)\rho'(u(x,t) - u(y,t))$. Because $u(x)$ is a best response to u, it is certain that $S_x(h)$ attains a global maximum at $h = 0$ and because the strategic domain is unbounded, we know that $\frac{d}{dh}S_x(0) = \int_\Omega K(x,y)\rho'(u(x) - u(y))dy = 0$. This is true for every x and thus $g[u] = 0$ in Ω. □

It should be noted that the opposite direction does not hold. It is easy to construct a stationary solution which is not a Nash equilibrium.

Example 5.5. *Consider a coordination game where $\rho \in C^{1,1}(\mathbb{R})$ satisfies $\rho(0) > 0, \rho'(0) = 0$, and $supp(\rho') \subset [-a, a]$.*

$$u = \begin{cases} 0 & x \neq 0 \\ 2a & x = 0 \end{cases}$$

is a stationary solution because $g[u] \equiv 0$. However, u is not a Nash equilibrium because $w(0|u) = 0$ but when $\tilde{u} = 0$ on all of Ω, (so $\tilde{u} = u - 2a\chi_{\{0\}}$) then $w(0|\tilde{u}) = \rho(0)\|K(0,\cdot)\|_{L^1(\Omega)}$. Thus we have that $J[u] \leq w(x|u) - w(x|\tilde{u}) = -\rho(0)\|K(0,\cdot)\|_{L^1(\Omega)} < 0$ where J is defined as in (5.14).

This means that understanding stationary solutions will inform our understanding of the classical game, even if we cannot connect, rigorously, our understanding of the stationary

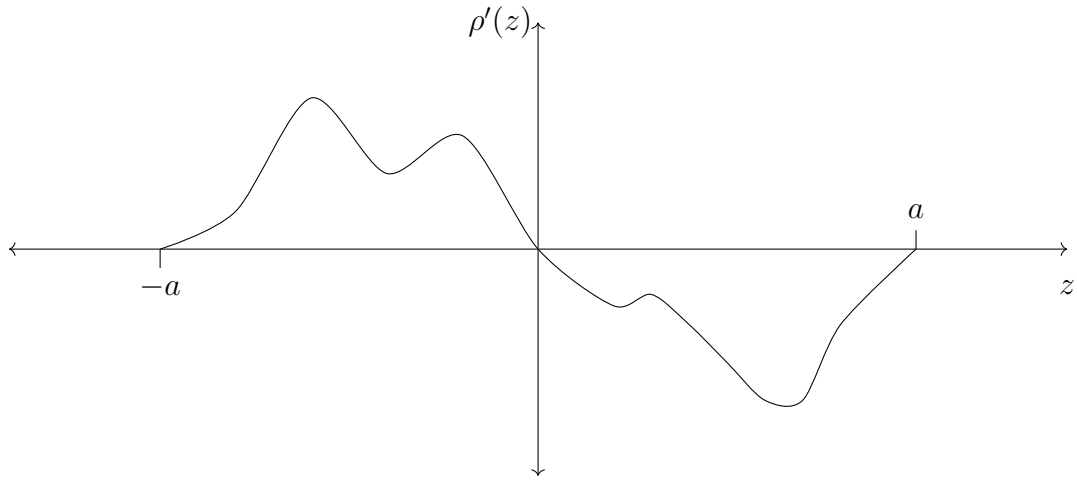

Figure 5.3: A diagram showing an appropriate ρ' for theorem 5.6. ρ' must be non-zero on $(-a, a) \setminus \{0\}$ and satisfy (5.8) so that on $(-a, 0)$ ρ' is positive and on $(0, a)$, ρ' is negative. ρ' is Lipschitz continuous, but no more regularity is required for this argument.

solutions to the dynamics of the IVP we have been studying. In the following theorem, we characterize stationary solutions in the case that Ω is bounded and there is no boundary data whenever K is supported on all of Ω.

Theorem 5.6 (Stationary Solutions when $supp(\rho')$ is compact)**.** *Let Ω be a bounded domain in $\mathbb{R}^n$. Let $K(x, y) \in C_b^0(\Omega; L^1(\Omega))$ so that for any x, $\Omega \subseteq supp(K(x, \cdot))$ and $\lambda \leq K(x, y)$. Finally, let ρ' satisfy (5.8) and have support $(-a, a) \subset \mathbb{R}$, with the assumption that ρ' has only one zero in this interval at $z = 0$ (Fig. 5.3). If u is a solution to $g[u] = 0$ in Ω and u is bounded, then the image, $u(\Omega)$, is a finite set of points separated by at least $|a|$ except possibly at a set of measure 0.*

Proof. First note that by the assumption on K, $C^K \geq \|K(x, \cdot)\|_{L^1(\Omega)} > \lambda Vol(\Omega) =: C_K$ for all x. Let $M_0 = \sup_\Omega u(x)$. Whether or not it is attained, there is a sequence of x_k so that $u(x_k) \to M_0$ and $k \to \infty$. For each k, we partition the domain into three parts

$$\Omega_k^+ := \{x \in \Omega, u(x) > u(x_k)\}$$
$$\Omega_k^o := \{x \in \Omega; u(x) = u(x_k)\}$$
$$\Omega_k^- := \{x \in \Omega; u(x) < u(x_k)\}$$

and so $g[u]$ is partitioned into three parts

$$g[u](x_k) = \underbrace{\int_{\Omega_k^+} K(x_k,y)\rho'(u(x_k)-u(y))dy}_{:=I_k^+\geq 0} + \underbrace{\int_{\Omega_k^o} K(x_k,y)\rho'(u(x_k)-u(y))dy}_{:=I_k^o=0}$$
$$+ \underbrace{\int_{\Omega_k^-} K(x_k,y)\rho'(u(x_k)-u(y))dy}_{:=I_k^-\leq 0}$$

Note that for every k, $I_k^+ = -I_k^-$ because $g[u] = 0$.

Let $\beta > 0$ and note that we can find a K_β so that $u(x_k) > M_0 - \frac{\beta}{C^K L_\rho}$ for all $k > K_\beta$ where L_ρ is the Lipschitz constant for ρ'. Because ρ' is Lipschitz continuous and $\rho'(0) = 0$, if $-\frac{\beta}{C^K L_\rho} < u(x_k) - u(y) < 0$ for all $y \in \Omega_k^+$, then $\rho'(u(x_k)-u(y)) \leq \frac{L\beta}{C^K L} = \frac{\beta}{C^K}$ for all $y \in \Omega_k^+$. This means that for any β we can find a K_β so that when $k > K_\beta$,

$$I_k^+ < \|K(x_k,\cdot)\|_{L^1(\Omega)} \frac{L\beta}{C^K L} \leq \frac{C^K L\beta}{C^K L} = \beta.$$

This means that for every β sufficiently small, we must see that there exists a K (indeed, the same K_β should do) such that $|I_k^-| \leq \beta$ for all $k > K_\beta$.

Now, consider $\epsilon > 0$ sufficiently small and suppose there is an $S \subset \Omega$ with positive measure $\mu(S) > 0$ and satisfying the inequality $M_0 - a + \epsilon < u(s) < M_0 - \epsilon$. Let K_ϵ be the index so that $k > K_\epsilon \implies M_0 - u(x_k) < \frac{\epsilon}{2}$. Note that when $k > K_\epsilon$, $S \subset \Omega_k^-$. Moreover, because $\frac{\epsilon}{2} \leq u(x_k) - u(s) \leq a - \epsilon$, and ρ' has no zeros in this compact interval, there is a C_ϵ such that $\rho'(u(x) - u(s)) \leq C_\epsilon < 0$. This means that when $k > K_\epsilon$ we can bound I_k^- away from 0

$$-I_k^- \geq -\int_S K(x,y)\rho'(u(x_k)-u(y))dy \geq -\lambda C_\epsilon \mu(S) > 0.$$

This contradicts the fact that $I_k^- \to 0$ as $k \to \infty$ so we conclude that for any subset $S \subset \Omega$ with $M_0 - a + \epsilon_0 \leq u(S) \leq M_0 - \epsilon_0$, we know that $\mu(S) = 0$. Restated, we have

shown that in the bounded domain Ω,

$$u(s) \geq M_0 - \epsilon \quad \text{or} \quad u(s) \leq M_0 - a + \epsilon \quad \text{almost everywhere.} \tag{5.15}$$

Importantly, every step taken to arrive at (5.15) can still be done when ϵ is made smaller, and so in the limit as $\epsilon \to 0$ we can conclude that

$$u(s) = M_0 \quad \text{or} \quad u(s) \leq M_0 - a \quad \text{almost everywhere.} \tag{5.16}$$

To see the convergence argument, observe that if (5.16) was not true we would surely have that $|\{s \in \Omega; M_0 - a < u(s) < M_0\}| > 0$ and we can write this as the countable union

$$|\{s \in \Omega; M_0 - a < u(s) < M_0\}| = \left| \bigcup_{\epsilon = \frac{1}{n}} \{s \in \Omega; \epsilon - a < u(s) < M_0 < \epsilon\} \right| > 0.$$

In order for this to be positive, it must be positive for at least one ϵ, and this could contradict (5.15).

Now, consider $\{u(x); x \in \Omega, u(x) \neq M_0\}$. If this set has measure 0, then we have completed the proof. If it has positive measure, let $M_1 := \operatorname{ess\,sup}\{u(x); x \in \Omega, u(x) \neq M_0\}$ and note that $M_1 \leq M_0 - a$. Let $x_k \in \Omega$ so that $u(x_k) \leq M_1$ and $u(x_k) \to M_1$. Now partition the domain into

$$\begin{aligned}
\Omega_k^{++} &:= \{x \in \Omega; u(x) \geq u(x_k) + a\} \\
\Omega_k^{+} &:= \{x \in \Omega, u(x_k) < u(x) < u(x_k) + a\} \\
\Omega_k^{o} &:= \{x \in \Omega; u(x) = u(x_k)\} \\
\Omega_k^{-} &:= \{x \in \Omega; u(x) < u(x_k)\}
\end{aligned}$$

and again, we can split the integral into

$$g[u](x_k) = \underbrace{\int_{\Omega_k^{++}} K(x_k,y)\rho'(u(x_k)-u(y))dy}_{:=I_k^{++}=0} + \underbrace{\int_{\Omega_k^{+}} K(x_k,y)\rho'(u(x_k)-u(y))dy}_{:=I_k^{+}\geq 0}$$
$$+ \underbrace{\int_{\Omega_k^{o}} K(x_k,y)\rho'(u(x_k)-u(y))dy}_{:=I_k^{o}=0} + \underbrace{\int_{\Omega_k^{-}} K(x_k,y)\rho'(u(x_k)-u(y))dy}_{:=I_k^{-}\leq 0}$$

In this way, we are left with the same situation as before. $I_k^{++} = 0$ because when $u(y) \geq u(x_k) + a$ then $u(x_k) - u(y) \leq -a$ and so $\rho'(u(x_k) - u(y)) = 0$ for all $y \in \Omega_k^{++}$. Thus, we note that $I_k^+ = -I_k^-$ for all k. Again, for any β we can find a K_β so that $I_k^+ < \beta$ for all $k > K_\beta$. This is because we proved in the first part of the proof that $u(x) \notin (M_0 - a, M_0)$ except for possibly at a set of measure 0. Thus, the entire contribution to I_k^+ comes from $x \in \Omega_k^+$ with $u(x_k) < u(x) \leq M_1$ and we can repeat our previous argument exactly. Thus $u(x) \notin (M_1, M_1 + a)$ except possibly at a set of measure 0. Because the nonlocality will not see a set of measure 0, it is an identical argument to extend the result in (5.16) to say that in Ω,

$$u(s) = M_0 \quad \text{or} \quad u(s) = M_1 \quad \text{or} \quad u(s) \leq M_1 - a \quad \text{almost everywhere}$$

This argument can be repeated indefinitely, but notice that between each of the resulting bands in $u(\Omega)$ there is a gap of at least a. This means that, after a finite number of repetitions, we will cover the entire range of the bounded solution, u. This means that, except for a possible set Q which has measure 0, the image of $u(\Omega \setminus Q)$ is a finite set of points. Further, we can partition Ω into $A_0, ..., A_m$ where $A_k := \{x \in \Omega; u(x) = M_k\}$ (by the process described above each of these A_i will have positive measure) and represent the solution u as a simple function

$$u(x) = \sum_{k=0}^{m} M_k \chi_{A_i = k}(x) \in L^\infty(\Omega)$$

□

This result is remarkable and gives us some insight into coordination dynamics at equilibrium. Although we cannot rule out the existence of a set of players with measure zero that do not adhere to one of a finite set of strategies, we can say that, in a weak sense, at equilibrium, when no outside influences are acting on the system (i.e., no boundary data or inhomogeneity), the solution will be piecewise constant. If we know apriori that the solution is continuous, then we can go even further.

Corollary 5.2. *If u is a continuous, bounded, stationary solution on a bounded domain with ρ having only 1 zero in the interior of its support at $z = 0$ and K supported on the entire domain, then u is constant*

In order to see continuous and non-constant solutions, at least one of these assumptions must be broken. An easy example is when the boundedness of the solution and of the domain is violated. There are clear examples of solutions to $g[u] = 0$ which are unbounded and not piecewise constant.

Example 5.6. *Let $k(x, y) = J(|x - y|)$ be a radial, translation invariant kernel. Let ρ be even, so ρ' is odd. For the domain $\mathbb{R}$, the solution $u(x) = x$ satisfies $g[u] = 0$.*

Proof. ρ' is odd so for any x, $\rho'(u(x)-u(y)) = \rho'(x-y)$ is odd in y. J is even and translation invariant so again for any x it is even in y. Thus $g[u](x) = \int_{\mathbb{R}^n} J(x - y)\rho'(x - y)dy = 0$ for all $x \in \Omega$. □

Another example may be if ρ' is not supported in an interval around $z = 0$. In this case, regardless of K, we can construct a continuous non-constant stationary solution

Example 5.7. *K is translation invariant and has support in $B_\delta(0)$, and ρ satisfies*

$$\rho(z) = \begin{cases} 1 & |z| < r_0 \\ 0 & |z| \geq r_1 \end{cases}$$

where $r_0 < r_1$ and $0 \leq \rho(z) \leq 1$ when $r_0 \leq |z| \leq r_1$. than any u which is globally Lipschitz with Lipschitz constant $\frac{r_1}{\delta}$ or which satisfies $\sup(u) - \inf(u) < r_0$ is a stationary solution.

These results about stationary solutions are helpful because they give us a way of narrowing down the search for Nash equilibria in the classical game. By proposition 5.2 and by Theorem 5.6, we know that any bounded Nash equilibrium of the game with appropriate K and ρ' on a bounded domain will have a finite image when at most a set of measure 0 is excluded from the domain. We do not expect this result to hold in the case that there are boundary data, nor do we expect this to hold if we consider the inhomogeneous problem discussed in section 5.7.

From the proof of Theorem 5.6, we can see that there is an upper bound on the number of points present in the image of a stationary solution. Namely, if b is the number of points in the image (which will appear as bands on a bifurcation diagram in the next subsection), $R := \sup_{x\in\Omega} u(x) - \inf_{x\in\Omega} u(x)$ and r is the radius of $supp(\rho')$, then $b \leq \lfloor \frac{R}{r} \rfloor + 1$. Notably, this means that if ρ' is supported on all of $\mathbb{R}$ and has only one zero at $z = 0$, then a stationary solution will be constant except possibly at a set of measure zero. This upper bound is sharp, as we can construct stationary solutions which satisfy $b = \lfloor \frac{R}{r} \rfloor + 1$ easily.

$$u(x) = \sum_{k=1}^{b} rk\chi_{S_k} = \begin{cases} r & x \in S_1 \\ 2r & x \in S_2 \\ \vdots & \\ br & x \in S_b \end{cases}$$

Where $\{S_i\}_{i=1}^{b}$ partitions Ω. This result characterizes the stationary solutions, but because of the lack of a time convergence result, we cannot yet unite the dynamics described in the diffusion problem $u_t = g[u]$ with their apparent limits rigorously. In order to get some idea of how the time dependent coordination process proceeds towards equilibrium, we use several numerical experiments.

5.6.2 Numerical Experiments

From the above results about stationary solutions, we seek to investigate the behavior of solutions as time tends towards infinity. We conducted several numerical experiments employing the numerical methods described in section 5.5. The code used to run the experiments can be found at McAlister (2025). The first experiment considered the interval $I = [-1/2, 1/2]$ and the initial data $u_0(x) = lx$ where l was varied from 0 to 4. With a Gaussian kernel $K(x, y) = \frac{1}{s\sqrt{2\pi}} e^{\frac{(x-y)^2}{-2s^2}}$ (where the kernel concentrates around x as s increases) and a compactly supported recognition function $\rho(z) = e^{\frac{-1}{1-(z/r)^2}}$ when $|z| < r$ and 0 otherwise, the experiment examines the profile of the solution after the IVP has been solved until $t = 20$. The system parameters were chosen as $s = 0.5$ and $r = 0.2$. The results are shown in figure 5.4

An interesting observation about the number of bands present at time $t = 20$ is the approximate equal spacing between the non-central bands. All of the non-central bands are separated by 0.4, which is the diameter of the support of ρ'. This is unlike the example from subsection 5.6.1 where the minimum distance between bands could be only the radius of the support. When there are two central bands, they can achieve this minimum separation but will grow apart as l increases. It is exactly when the distance between the bands exceed 0.4 when the appearance of a single central band between them emerges. Following this pattern, we can predict, for a linear initial condition, how many bands there will be. No two bands can be closer than 0.2 (half the support ρ'), and no two bands can be further than 0.4. For this setting in particular, at most 2 spaces between bands will be less than 0.4. Therefore, we can arrive at the bound that the number of bands b is limited by

$$b \leq \frac{R}{2r} + 1$$

where again R is the length of the range of u_0 and r is the radius of the support of ρ'. This bound is smaller than the upper bound from subsection 5.6.1, which may be related to the stability of these stationary solutions.

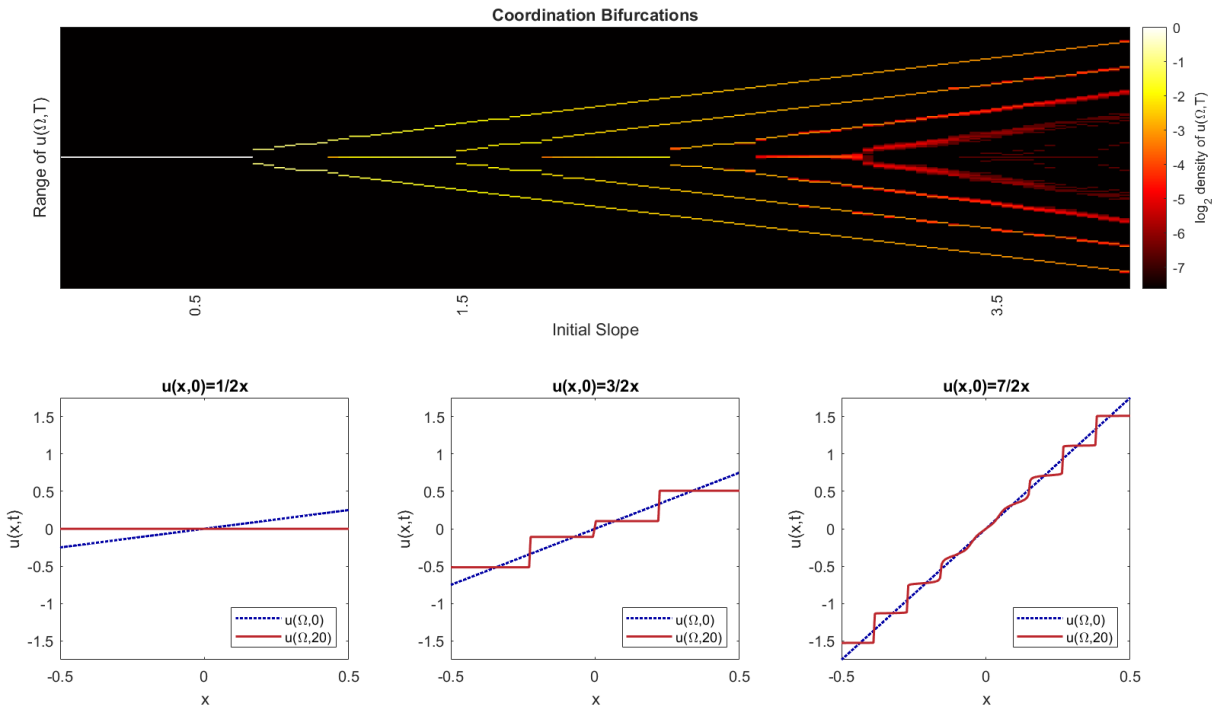

Figure 5.4: Top A bifurcation-type diagram showing that as the slope of the initial data increases, the distribution of the solution $u(x, 20)$ changes. On the far left, when the slope is low, the image is entirely distributed at $u(x) - = 0$. As the initial slope increases, there are more bands. The colors on the heat map represent the log_2 of the density of $u(x, 20)$. **Bottom** Three examples of initial conditions (dotted in blue) and solutions at time $t = 20$ (solid in red). The corresponding slices in the bifurcation diagram are labeled in order on the x axis of the heatmap above.

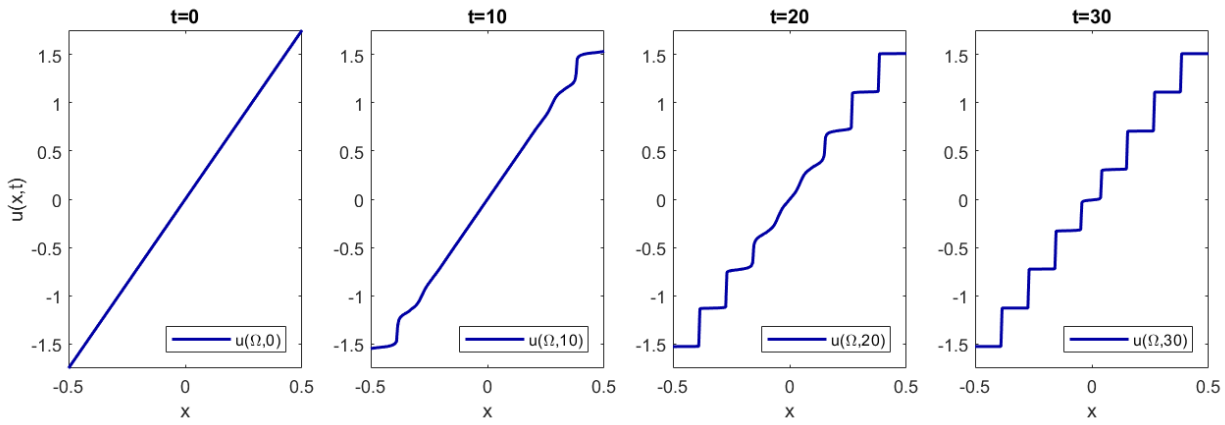

Figure 5.5: Four time slices of the solution to $u_t = g[u]$ when $u_0 = 7/2x$ on the domain $\Omega = [-2, 2]$. The collapse into discrete strategies starts at the edge of the domain and propagates towards the center.

Another interesting observation, which is not explored further in the present study, is the fact that the bands seem to start to form from the outside and then proceed in. In the case where $l = 3.5$ in figure 5.4, we can see that the most central bands have not formed by the time $t = 20$. This points to a possible finite propagation speed. As in example 5.6, when the solution $u(x, t)$ is odd about a point x_0 and the kernel is even, then $u_t(x_0, t) = 0$. In the exact center, the solution is odd for all time in each of these experiments. Close to the center, the solution "almost" has odd symmetry, and near the edge of the range, the solution has no odd symmetry. For points near the center, the lack of odd symmetry far away is hidden by the fact that the kernel K is small at that distance. For points close to the edge of the range, the immediate lack of odd symmetry results in an immediate collapse into discrete strategies. This collapse ruins the odd symmetry closer to the center, and so the collapse propagates to the center (Fig. 5.5).

We use the next two numerical experiments to test the hypothesis about the minimum band separation. Using a sigmoid function instead of a linear function for the initial data, we can investigate the number of bands that emerge while the range of the initial data is constrained. For the same kernel and recognition function as before, we run the same experiment with $u_0 = (1 + \exp(-lx))$ for $l \in [0, 15]$. The results are shown in figure 5.6

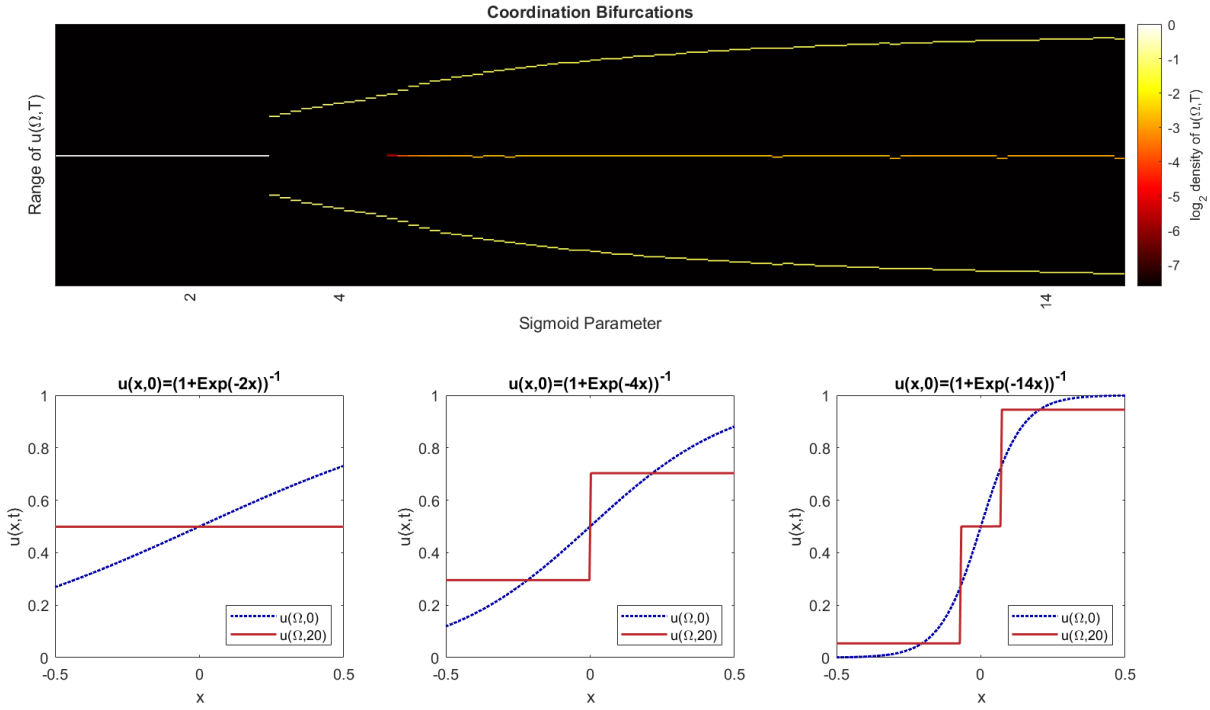

Figure 5.6: **Top** A bifurcation-type diagram showing that as the sigmoid parameter of the initial data increases, the distribution of the solution $u(x, 20)$ changes. On the far left, when the sigmoid parameter is low, the image is entirely distributed at $u(x) = 0$. As the sigmoid parameter for the initial data increases, there are two, then later three bands, but as the sigmoid parameter tends towards its maximum, the bands level out. The colors on the heat map represent the log_2 of the density of $u(x, 20)$. **Bottom** Three examples of initial conditions (dotted in blue) and solutions at time $t = 20$ (solid in red). The corresponding slices in the bifurcation diagram are labeled in order on the x axis of the heatmap above.

Again, we notice that the number of bands increases with the range of the initial data. It is straightforward to observe that the relationship from the first numerical experiment holds in this case too. Because the range of the initial data is constrained to $(0, 1)$ we never see more than three bands emerge. This is precisely what is predicted from the hypothesis previously stated.

The sigmoid example also shows us that it is not a critical gradient threshold that results in discontinuities in the limit. The derivative is greatest at $x = 0$ initially in every example. However, the discontinuities do not always emerge at the center. When the sigmoid parameter is greater than 5, and there are three bands present, the central band is centered around $x = 0$, and the discontinuities are present on either side of this band. Therefore, when trying to predict the location of bands present at equilibrium (assuming a solution converges to an equilibrium) is not as simple as finding where the gradient might surpass a certain threshold.

To further test this hypothesis, we vary the support of the recognition function rather than the initial data. In the third numerical experiment, the parameter r in the recognition function

$$\rho(z) = \begin{cases} e^{\frac{-1}{1-(z/r)^2}} & |z| < r \\ 0 & |z| \geq r \end{cases}$$

is varied from 0 (the limit in which $\rho(z) = \chi_{\{0\}}(z)$) to 0.8. The results are shown in figure 5.7

The results of the experiment are predicted exactly by our hypothesis. Again, in every case, the number of bands is bounded above by $(R/2r) + 1$.

These numerical experiments obviously fall far short of a real proof, and without a time-convergence result, such a proof is likely impossible. However, they do force us to consider which stationary solutions are discoverable (i.e., they have a non-trivial basin of stability) and which are not.

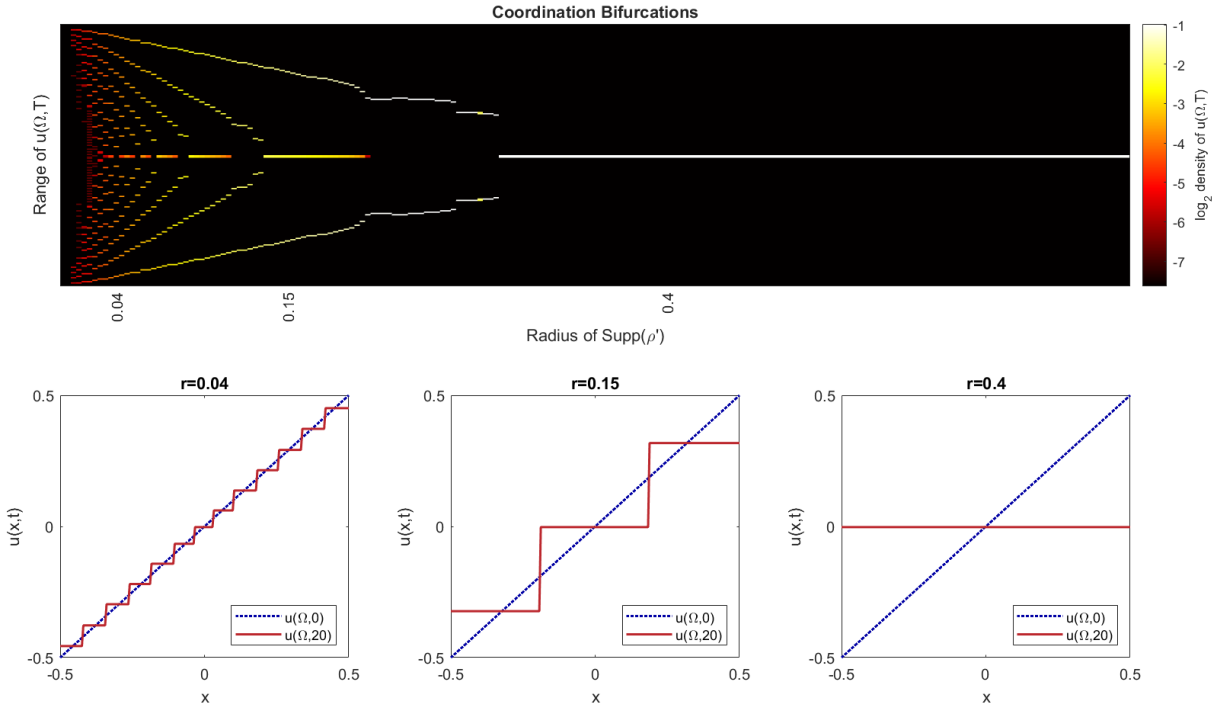

Figure 5.7: Top A bifurcation-type diagram showing that as the support of the recognition function changes, the distribution of the solution $u(x, 20)$ changes. On the far left, when the support of ρ is near 0, there are many bands. As the support of the recognition function increases, there are fewer and fewer bands until the solution collapses to $u(x) = 0$. The colors on the heat map represent the log_2 of the density of $u(x, 20)$. **Bottom** Three examples of initial conditions (dotted in blue) and solutions at time $t = 20$ (solid in red). The corresponding slices in the bifurcation diagram are labeled in order on the x axis of the heatmap above.

5.7 Towards an Inhomogeneous Problem

Recall that this model is inspired by a game theoretic situation in which two players are interacting and the payoff of their interaction depends only on the "distance" between their strategies. We can extend this idea to consider payoff separated into two parts: the extrinsic payoff, which will still only depend on the distance between the strategies, and the intrinsic payoff, which will depend only on the position of the player and, perhaps, the time. Consider, as in section 5.2, a game with a discrete number of strategies where every pairwise interaction is subject to the same extrinsic payoff, given by the payoff matrix A but there is an additional intrinsic payoff which is dependent on the player x, their strategy $u(x)$ and the time t. The payoff matrix, therefore, can be decomposed as

$$A = B + C(x,t)$$

where B is Toeplitz as before and $C(x,t)$ has constant rows for every $(x,t) \in \Omega_T$ (i.e. $C(x,t) = [c(x,t)\ c(x,t)\ \dots\ c(x,t)]$ where $c(x,t)$ is a column vector). We can rewrite our equation (5.2) as

$$w(x|u) = \int_\Omega K(x,y)u(x)^T Bu(y)dy + \int_\Omega K(x,y)u(x)^T C(x,t)u(y)dy.$$

However, because of the form of $C(x,t)$, $C(x,t)u(y) = c(x,t)\sum u(y)_i$. In both the pure strategy and mixed strategy cases, $\sum u(y)_i = 1$ so this is independent of y, and we can write

$$w(x|u) = \int_\Omega K(x,y)u(x)^T Bu(y)dy + \langle u(x), c(x,t)\rangle \|K(x,\cdot)\|_{L^1(\Omega)}$$

In the same way as before, the extension into continuous strategy space is easy. the matrix B and vector c become infinite dimensional and we replace them with the functions ρ and F respectively. Thus, we get our continuous strategy space functions

$$w(x|u) = \underbrace{\int_\Omega K(x,y)\rho(u(x)-u(y))dy}_{extrinsic} + \underbrace{F(u(x,t),x,t)}_{intrinsic} \tag{5.17}$$

We will now consider the requirements on F that ensure that the model is still well founded.

Proposition 5.3. *Bounded strategy profiles of the game with players in $\Omega \subset \mathbb{R}^n$ choosing strategies in $\mathbb{R}$ by myopic best response with fitness as in (5.17) will evolve as*

$$\frac{\partial}{\partial t}u(x,t) = g[u](x,t) + \partial_1 F(u(x,t),x,t)$$

Under the hypotheses of proposition 5.1 with the additional hypothesis that

(H4) F has a Lipschitz derivative with respect to its first argument and $F(z,x,t) \leq C_2 z^2 + A_3$ for some non-negative C_2 and A_3 uniformly in Ω_T

Proof. As in proposition 5.1, we will consider a bounded strategy profile $u(\cdot,t) : \Omega \to \mathbb{R}$. Every player will seek to update their strategy by some amount h in order to take on their best response to $u(\cdot,t)$ after a time step of Δt and in doing so they incur a cost of $\frac{h^2}{\Delta t}$. Let

$$S_x(h) := \int_\Omega K(x,y)\rho(u(x,t) + h - u(y,t))dy + F(u(x,t)+h,x,t)$$

be the payoff player x receives after changing their strategy by h. From the computations in the proof of proposition 5.1, we know that

$$\int_\Omega k(x,y)\rho(u(x,t) + h - u(y,t))dy \leq C_1 h^2 + B_1 h + A_2$$

Additionally from $(H4)$ $F(u(x,t)+h,x,t) \leq C_2 h^2 + A_3$ for some C_2 and A_3. Therefore we have immediately that

$$S_x(h) \leq C_3 h^2 + A_4$$

We also need to show that $S_x(h)$ has a Lipschitz derivative. As in proposition 5.1, the first term of $S_x(h)$ has a locally Lipschitz derivative. Moreover, by $(H4)$ the second term also has a locally Lipschitz derivative with respect to h.

Having argued that $S_x(h)$ is uniformly subquadratic in h and has a locally Lipschitz derivative in h, we note that the quantity $S_x(h) - \frac{h^2}{\Delta t} \leq C_4 h^2 + A_5$ for some negative C_4 when Δt is sufficiently small. Therefore, there is certainly a global maximizer h^*, and that maximizer satisfies

$$\frac{d}{dh} S_x(h^*) = 2\frac{h^*}{\Delta t}.$$

It is the same process as in proposition 5.1 that allows us to find that in the limit as $\Delta t \to 0$

$$\frac{\partial}{\partial t} u(x,t) = \frac{1}{2}\frac{d}{dh} S_x(0)$$

We note that

$$\frac{\partial}{\partial h} S_x(0) = \int_\Omega K(x,y)\rho'(u(x,t) - u(y,t))dy + \partial_1 F(u(x,t),x,t)$$

and do a trivial rescaling of space time to complete the proof. □

For the proceeding, let $f(u,x,t) := \partial_1 F(u(x,t),x,t)$, and we are left with the simple inhomogeneous version of the nonlinear nonlocal diffusion problem we have been discussing

$$u_t - g[u](x,t) = f(u,x,t) \tag{5.18}$$

where ρ and f are both subquadratic for the game theoretic application to be sensible. It is not a difficult task to prove short-time existence and uniqueness for solutions in this case. The theorem is written here and the proof is included in appendix A.2 because of its similarity to the proof of theorem 5.1

Theorem 5.7 (Short time existence and Uniqueness for the inhomogeneous case)**.** *The initial value problem $u_t - g[u] = f(u,x,t)$ has a unique continuous and bounded solution in Ω_T for some T when $u(x,0) = u_0 \in C_b^0(\Omega), \rho \in C^{1,1}(\mathbb{R})$, $K \in C_b^0(\Omega; L^1(\Omega))$ and f is*

Lipschitz continuous with respect the the first variable with a Lipschitz constant which does not depend on time, is continuous with respect to space and time, and is bounded

The proof proceeds practically identically to that of existence and uniqueness in the homogeneous case, as it uses a BFPT argument. Finding global existence or even a finite time blow up result in the inhomogeneous case is certainly much harder. The Main issue is the nonlinearity of the nonlocality, and so the standard Duhamel's property does not apply in this case.

5.8 Discussion

In this study, we have extended the game theoretic treatment of structured coordination to allow for continuous pure strategies and provide novel critical insights, extending the application areas beyond those for which only the traditional, discrete pure strategies of discrete player spaces are appropriate. With certain reasonable hypotheses on the components of the fitness function, we were able to show rigorously that through a myopic best response like update rule the situation can be modeled in continuous time by way of a nonlinear nonlocal equation, similar to existing nonlocal diffusion problems.

The nonlinearity in this model prevents the use of Fourier analysis, semi-group theory, or comparison principles in proving our results, but through elementary analysis and PDE techniques, we were able to determine short time existence and uniqueness for the general setting. With some additional requirements on ρ, we can strengthen this to find global existence and uniqueness. In addition to these results, we found that solutions with Lipschitz initial data remain Lipschitz continuous, although the modulus of continuity may increase exponentially. In the special case of the Cauchy problem, the Lipschitz constant does not depend on the shape of the kernel, K, as long as it is translation invariant.

After giving several trivial analytical examples, we showed that simple numerical methods are stable and convergent, which allows us to visually examine solutions to the initial value problem without boundary data prescribed. Using these results, we were able to carry out several numerical examples which supported the analytical results about stationary solutions.

Finally, we considered the inhomogeneous problem and again showed short time existence and uniqueness of solutions to the IVP with no boundary data.

Not only do these results help us understand the model as a way of discussing coordination in space, but they also represent advances in our understanding of nonlinear, nonlocal diffusion problems. On the modeling side, we see examples of solutions seeming to converge towards non-constant equilibria, the continuous analog of the non-trivial equilibria in the discrete case. Moreover, when discontinuities in strategy emerge, we can determine how quickly and how severely they can appear. By characterizing stationary solutions, we can significantly advance our understanding of both the classical game and nonlinear nonlocal diffusion problems. The concentration of strategies appears as a smoothening in some parts of the domain and tends to create discontinuities in other parts of the domain. Further study into nonlinear nonlocal diffusion problems is required to describe the asymptotic behavior of solutions and the stability of stationary solutions. From this study, it is clear that understanding coordination as a nonlinear nonlocal diffusion problem allows us to examine the system in exciting and novel ways, making accessible insights that were previously impossible.

Chapter 6

Conclusion

Coordination is an exceedingly simple game theoretic interaction and yet, in attempting to model it dynamically, we see a rich variety of model behavior across several types of domains. After a numerical treatment in chapter 2, in chapter 3, we examined the ways that considering only the boundaries of strategic communities can give us a better intuition for the game. In chapter 4 we used ODE methods inspired by evolutionary game theory to describe the dynamics of coordination, among other games, in continuous time. We also showed in that same chapter that a nonlocal model can be used to describe the same type of dynamics in continuous player spaces. Finally, in chapter 5 we showed that a different concept of strategic continuity results in a different nonlocal model which has a rich diversity of behaviors. Each of these models addresses a different modeling challenge, but none of them, of course, provide us with a perfect understanding of the system. Taken together, however, we can gain a better understanding of coordinating systems as a whole.

6.1 Comparison of Modeling Techniques

When modeling coordinating systems, the perfect model would be numerically fast to simulate, analytically understandable, and should bear a close similarity to the game at hand. In trying to describe dynamic coordinating systems through myopic best response, we can get very close but we cannot achieve all three of these goals simultaneously.

When we model this system through simulation, we can take steps to make the numerical methods fast and, because of the simplicity of the system, we can recreate it perfectly. However, we cannot draw any analytical understanding of the system from the simulation. In chapter 2, the best that we can do is provide a catalogue for very small graphs and make some observations about the large graphs. These observations are helpful. For instance, we know that non-consensus equilibria appear near the "boundary of connectedness" in random graphs, but we cannot make that claim rigorous through simulation alone. The simulation certainly gives us a better understanding of the system through observation and was crucial in making conjectures about the behavior of the system in other settings, but it cannot be used to achieve any analytical results.

We get closer to analytical results through the dual approach. With the dual approach in chapter 3, although we must restrict the types of graphs on which the game is played, we maintain a perfect representation of the best response dynamic perfectly. This means that we can use this model, which is more analytically tractable than the simulation, to gain a more general understanding of coordination dynamics, so long as the graph is restricted in a certain way. Moreover, if we restrict the strategy space even further, we can improve our ability to study the system analytically because, with only two strategies, the system can be modeled by simple operations in a vector space. The analytical power of this model is exciting, but it still does not achieve all three goals we are interested in because it is numerically very slow. Indeed, the fastest way to simulate the system in this way is to revert from the dual setting and simulate the game as it was done in chapter 2. This makes it harder for us to use the model and make observations about the system. Nevertheless, the main achievement of this model is in providing intuition for the system. The "minimal subgraph" concept is an intuitive concept which not only allows us to understand how equilibrium partitions relate to similar partitions but also gives us a way to think about which graphs may admit non-consensus equilibria. Furthermore, the intuition from this model allows us to think of interesting extensions into different domains. The similarities we can observe between the dual system and continuous systems, like curve shortening and network flows,

help us to solidify our intuition for the system and connect seemingly unrelated evolution equations.

With the observations we can make through simulation and with the intuition we built through the dual approach, the ODE model can give us an even better understanding of coordinating systems. ODE systems are numerically very fast to solve and analytically rather easy to understand. In chapter 4, we can analytically show that equilibria of the model system are semi-stable equilibria of the ODE system, and we can further characterize the behavior of solutions to the ODE system in the vicinity of equilibria, depending on their characteristics in the model system. The tools available to us to analyze ODE systems make this model very helpful to use, but we must recognize that it does not exactly capture the myopic best response dynamic that we are interested in studying. Although the replicator equation still can be described as a "better response" strategic revision protocol, the difference between the best response dynamics and the better response dynamics changes the shape of basins of stability and the behavior of trajectories themselves. The equilibria of the model system and of the ODE system can be almost perfectly united rigorously through the use of Morse graphs, but the transient dynamics of the systems may not necessarily reflect one another. For this reason, the main achievement of this model is that it provides an analytical way to discuss stability. The stability criteria of the ODE system and the way that they are connected to the model system give us a way of comparing the stability of solutions and a way of maximizing stability through adjustments to the relational structure. This model adds to our understanding of coordinating systems because the stability results give us a rigorous way to say that strategic gradients (in the mathematical sense but also in sense of gradual change along a discrete sequence) are unstable.

In order to achieve analytical tractability, fast numerical methods, and the ability to use Myopic Best Response, we consider the non-local, non-linear diffusion model of chapter 5. Indeed, this model has fast numerical methods and is analytically tractable. Through both numerical experiments and analytical tools, we can describe the equilibria of this model depending on the way that the continuous player space is connected. However, the game that we are studying in chapter 5 is considerably different from the original game. Although

Table 6.1: A table describing the pros and cons of each of the models presented in chapters 2-5.

	Simulation	Dual Model	ODE Model	Non-local Model
Numerically Fast	✓	X	✓	✓
Analytically Tractable	X	✓	✓	✓
Representation of the game	✓	✓	X	X
Main achievement	Observation	Intuition	Stability	Extensions

the myopic best response dynamic is maintained, the idea that strategies are differentially comparable, and that strategic change has a quadratic cost, are not elements of the original game. This game, being studied with the non-local model, is so different that, although it still used myopic best response, we cannot say it is a very close representation of the dynamic game in question. Despite this, we learn a great deal about coordination from this modified game. For instance, we can analytically understand how discontinuities form even when coordination itself is a centralizing process. This insight, and others described in chapter 5, mean that the main achievement of the non-local model is to provide insights about coordination that extend beyond the strict setting in which the question was originally described.

Although no model can tell us everything about the system, each of these models can tell us something new about the system, and by considering them together, we get a better understanding of coordination as a whole. A summary of the pros and cons of each model can be found in table 6.1.

6.2 Uniting the Domains

The main reason for using a diversity of models is to examine their similarities so that we may understand certain inherent properties of coordination. It is easy to observe that higher connectivity, in general, means that non-consensus equilibria are less likely. This is a

main result of the simulation model, but can also be seen by considering how, in the dual, more edges in the graph means a more connected cutspace, and a more connected cutspace results in fewer local minima. Likewise, with the ODE model, we can see that with more edges, the for players on the boundary of strategic communities decreases. Even though the non-local model models the game in a different way, still we can see that when every player is connected to every other player, the required distance between strategies must exceed the players' comparison distance in order to achieve non-consensus equilibria. If all strategies are comparable, then the only equilibrium is the consensus equilibrium.

In addition to this similarity, which is easy to see, there are two other similarities, which are admittedly more speculative. The first is the discretizing effect of coordination. When strategies are not mixed, then clearly the end point of dynamic coordination games must be discrete, but even when we allow for mixed strategies or comparable strategies, the equilibria that we observe only have a discrete set of strategies present when the familiarity Kernel covers the entire domain. This is proved for the nonlocal diffusion model and only conjectured for the nonlocal replicator model (see conjecture 6.6, however, on a fundamental level, this makes sense. Coordination is a centralizing process in evolutionary terms; those individuals away from the mean are selected against. In the classical setting, we say that individuals using uncommon strategies have a lower payoff. In this light, it is clear to see that, by pure coordination alone, distributions should localize around their "averages." The fact that there may be multiple such "averages" relates to the fact that the meaning of "average" for a particular player depends on the neighborhood around that player.

More surprising than the discretizing nature of coordination, we also observe the diffusive nature of coordination across many domains. The numerical simulations do not treat this point well, but we do see this commonality across chapters 3, 4, and 5. Regarding minimal subgraphs, and in particular the continuous player space extensions, we see that the stationary solutions have boundaries which are "almost" minimizers of arclength. In simulations, we have observed a close connection between the movements of these boundaries and the curve shortening flow. More information about how these are related is described in section 6.3. Of course, the curve shortening flow or the network flow is closely related to

the heat equation, and thus to diffusion. Although the entire connection is not made formal here, we show that the myopic best response dynamics of the pure coordination game have a diffusive effect on the boundary of strategic communities.

The diffusive behavior of the replicator equation model is not as directly related to the diffusion equation, but it can be seen especially in the continuous case. It is not difficult to rearrange the nonlocal version of the replicator model in section 4 so that it looks like

$$\frac{\partial}{\partial t}u^i(x,t) = u^i\mathcal{L}_K u^i + (u^i)^2 - \langle u, (K * u)\rangle$$

where $\mathcal{L}_K u$ is the nonlocal Laplacian $K * u(x) - u(x)$. The connection is not as exact as in the previous example, but it would be correct to classify this as a non-linear nonlocal parabolic equation. Whether the behavior can be described as "diffusive" does not have a clear answer, and so the diffusive connection in this setting is less clear. However, in the other continuous time model, the connection is very apparent.

Of course, in the non-local model, the similarities to diffusion are obvious. If the recognition function is chosen correctly, the model becomes exactly the non-local diffusion model. The non-linearities, which make it possible to get non-consensus equilibria, mean that the model is not, in general, diffusive on the entire domain, but certainly near consensus equilibria the dynamics of the non-local model are practically identical to the non-local diffusion equation.

From this comparison, we understand that the non-consensus dynamics of pure coordination happen in the case where the domain is only just connected. Moreover, we can see, at least thematically, that coordination is both discretizing and diffusive. These two forces compete whenever there are strategic gradients and the force that wins out is determined, not by qualities of the strategy profile alone, but by qualities of the payoffs (Fig 6.1).

These connections are only heuristics for how we can understand coordination, but key to our understanding is comparing the competing effects of discretization and diffusion. Near consensus, diffusion will win. Far from consensus, discretization will win, and diffusion may

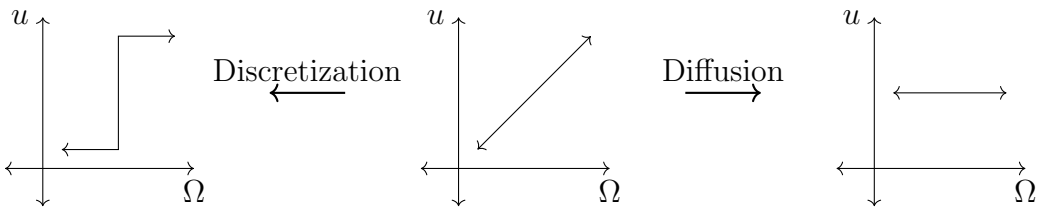

Figure 6.1: A strategic gradient is, in general, unstable. It can collapse in two mutually exclusive ways. Either it collapses in the strategy space to consensus in a diffusive manner or is collapses in the player space in a discretizing manner. The direction of collapse is not determined by the gradient of the strategy profile but the gradient of the payoffs.

take place along the boundary. In either case, we have shown that coordination, at least heuristically, can be thought of as a combination of these two effects.

6.3 Future Work

There are still many questions to be asked about this system in every domain that we have explored in this dissertation. Here, I describe some of the conjectures that we are left with after studying this model system and some support which has been provided by each of the models.

6.3.1 Conjectures Regarding the Simulation Study

The ultimate goal of the numerical investigation in chapter 2 was not to have a statistical understanding of this system, but rather an analytical understanding. The numerical understanding provided the basis for the later chapters, but there are still questions which were not addressed. With the help of the numerical results, we propose and discuss three conjectures here. The first is that when graphs grow infinitely large, the probability of an ER graph being indecomposable approaches zero so long as the number of edges is below some threshold function. The second is that as graphs grow infinitely large, $\phi(Q_0)$ converges to 1 so long as the number of edges is above some threshold function. These two conjectures together would imply the existence of a region wherein infinitely large graphs are almost

surely decomposable, but the non-trivial equilibria are almost never discoverable. The last is that n-cycles are impossible for $n > 2$.

These conjectures will help shape the way we understand this critical case of the coordination game and will, along with the results of the present numerical treatment, inform our understanding of the application areas of this system. For instance, if conjecture 2 is shown to be true, it would imply that, for the canonical example of a growing company selecting between operating systems, there is a critical amount of interconnectedness, above which the company will eventually converge to a consensus, almost surely, without intervention. If conjecture 3 is proven, it may give us further theoretical support for the idea that cyclical trends in fashion cannot be described only by individuals choosing to mimic one another (Acerbi et al., 2012).

Conjecture 6.1. *There is a function $A(n)$ which is monotonic increasing with $\lim_{n\to\infty} A(n) = \infty$ so that, if $P_{id}(n, N(n))$ is the probability that $\Gamma_{n,N(n)}$ is indecomposable,*

$$\lim_{n\to\infty} P_{id}(n, N(n)) = \begin{cases} 0 & \lim_{n\to\infty} \frac{N(n)}{A(n)} = 0 \\ 1 & \lim_{n\to\infty} \frac{N(n)}{A(n)} = \infty \end{cases} \tag{6.1}$$

From the catalogue, we start to see that as n grows, a smaller proportion of graphs of order n are indecomposable. Clearly, we cannot draw meaningful asymptotic results from observations of $n \in \{1, 2, ..., 7\}$, but we can support this conjecture with some facts about the system. First, it is clear that any disconnected graph is decomposable. This means immediately that any lower threshold function (a la (Erdős and Rényi, 1960)) for connectedness, like $A(n) = \frac{1}{2} n \log n$, is also obviously a lower threshold function for indecomposability. That is, if we consider random graphs $\Gamma_{n,N(n)}$ and let $n \to \infty$, the probability that $\Gamma_{n,N(n)}$ is indecomposable goes to zero when $\lim \frac{N(n)}{A(n)} = 0$.

We propose that a threshold function exists and is much stronger than the obvious lower threshold function already mentioned. It is not true that every graph of size n is indecomposable when $n \to \infty$. For instance, K_n and $K_n - e$ (for $n > 3$) are always indecomposable, as is $K_{n,m}$ when n and m are coprime (recall theorems 1.1 and 1.2).

Obviously then, if $N(n) \geq \binom{n}{2} - 1$, then $\Gamma_{n,N(n)}$ is indecomposable. Certainly, we know that if a threshold function exists, it will satisfy $\lim \frac{\binom{n}{2}-1}{A(n)} = \infty$ and $\lim \frac{(\frac{1}{2})n \log n}{A(n)} = 0$. The path toward finding such a threshold function, we believe, will involve the study of the separating sets of critically large subgraphs.

A proof of this conjecture would provide some idea about the behavior of very large networks and community formation. In the same way that McDiarmid and Skerman (2020) discusses the modularity of ER networks towards understanding the community properties of large graphs, we may be able to discuss the properties of community formation in very large graphs, as this system provides a similar, but more local, conception of the community structure in a network. A separate goal of this work is to be able to algorithmically find equilibrium partitions of finite graphs to describe community formation, just as Newman (2006) and Clauset et al. (2004) do with modularity, but this conjecture would inform our understanding of the system in a way that algorithms cannot.

For the next conjecture, recall that the consensus strategy profiles make up the equivalence class associated with the trivial partition Q^0.

Conjecture 6.2. *There exists a function $B(n)$ which is monotonic with $\lim_{n\to\infty} B(n) = \infty$ so that, if $\phi(Q^0_{\Gamma_{n,N(n)}})$ is the probability of a random initial strategy profile evolving into a consensus strategy profile, under the dynamics in (1.4) in the random graph $\Gamma_{n,N(n)}$, then*

$$\lim_{n\to\infty} \phi(Q^0_{\Gamma_{n,N(n)}}) = \begin{cases} 0 & \lim_{n\to\infty} \frac{N(n)}{B(n)} = 0 \\ 1 & \lim_{n\to\infty} \frac{N(n)}{B(n)} = \infty \end{cases} \tag{6.2}$$

The results of the second simulation suggest that $B(n) = \frac{1}{2}n\log(n)$ (which, again, is a threshold function for connectedness Erdős and Rényi (1960)) could be such a threshold function. The results shown in figures 2.11 and 2.12 show that as graph order increases, once edge density passes a threshold close to the threshold for connectedness, the probability of reaching the consensus equilibrium (or equivalently having a cluster number of 1) approaches 1. These results are the basis for the conjecture.

Again, as discussed in section 2.3, when the graph is disconnected, the relative size of the consensus basin of stability grows as $\frac{1}{r^{c-1}}$, where r is the number of components and $c \geq 2$. By theorem 6 of Erdős and Rényi (1960), we see that if $N(n) \sim cn$ for any $c < 1$, the expected number of components will tend to infinity as $n \to \infty$, and so the relative size of the consensus basin of stability will go to zero. This implies that $B(n) \sim cn$ is certainly a lower threshold function for this property. We conjecture the existence of a threshold function which is a stronger lower threshold function than cn. Progress on this question will include examining the stability of equilibria.

It is clear that, should a threshold function exist for both indecomposability ($A(n)$) and for the basin of stability for the consensus equilibrium being 1 ($B(n)$), then $A(n) \geq B(n)$. Moreover, we conjecture that, should these two exist, this inequality will be strict. That is, there will be a region wherein, asymptotically, almost every $\Gamma_{n,N(n)}$ has non-trivial equilibria, but they are discoverable with probability 0. This conjecture further gives insight into the nature of community formation in large networks. Specifically, it shows that through these dynamics of community formation, the non-trivial equilibria are only finite-size effects that do not appear in the infinite system.

Conjecture 6.3. *There is no graph G such that there exists $n > 2$ strategy profiles $\{u(1), u(2), ..., u(n)\}$ such that $|\, argmax_{c \in C}\{w_v(c|u(t))\}| = 1$ for all $t = 1, 2, ..., n$ and*

$$\begin{aligned} u_v(2) &= \underset{c \in C}{argmax}\{w_v(c|u(1))\} \\ u_v(3) &= \underset{c \in C}{argmax}\{w_v(c|u(2))\} \\ &\vdots \\ u_v(1) &= \underset{c \in C}{argmax}\{w_v(c|u(n))\} \end{aligned} \tag{6.3}$$

Throughout this entire project, throughout every attempt to run each simulation, neither a true 3-cycle nor a true 4-cycle was ever discovered. This suggests that, at least, these kinds of limits are exceedingly unstable, but we further conjecture that n-cycles with $n > 2$ exist with probability 0.

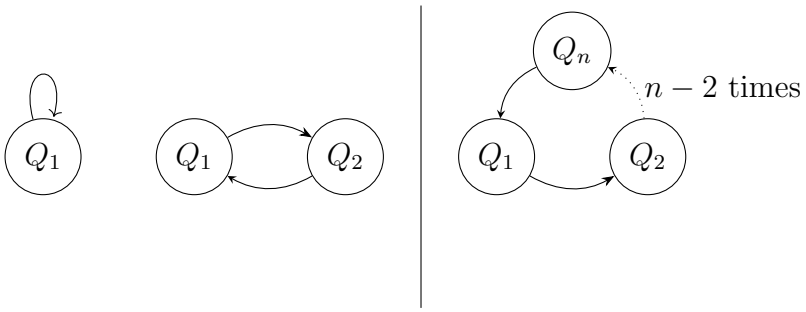

Figure 6.2: Q_i are elements of the state space. On the left, 1-cycles (which are equilibria) and 2-cycles are frequently observed and behave deterministically. On the right an n-cycle with $n > 2$ is never observed deterministically and stochastically will exist with probability 0.

Frequently, we observe fixed points and 2-cycles which, in the state space, behave as in figure 6.2. These exist deterministically and are uncomplicated to understand. Indeed, K_2 will exhibit a 2-cycle whenever the initial condition is non-trivial. It is not yet clear why $n > 2$-cycles do not appear as readily. If such a cycle exists stochastically, it will continue to cycle for all time with probability zero, so to prove our conjecture, we will need to show that deterministic $n > 2$ cycles are impossible.

This conjecture is strongly supported by the simulation results, as none of the 6×10^6 attempted IVPs resulted in a cycle of size greater than 2. In the simulations, the conditional statements which check for an n-cycle have a false positive rate of $\leq 2^{n-T}$, where T is the tolerance (which was set to 34 so that the false positive rate, even for $4-$ cycles, is $< 10^{-9}$), but during early iterations of the simulation (when the filter had a false positive rate of only $\leq 2^{-\lfloor \frac{T-n}{n} \rfloor}$) we would see rare false positive 4-cycle which could pass through the filter with probability 2^{-7} with the behavior demonstrated in figure 6.3

These pseudo 4 cycles give some suggestions as to why true deterministic n cycles with $n > 2$ do not appear in our observation. In order for a state to be reached deterministically, every best response set must be of size 1. The resulting strict inequalities present the main limitation. Aside from being a remarkable feature of this dynamical system, the impossibility of large cycles, again, would offer new insights into the process of community formation when is driven by local interactions alone.

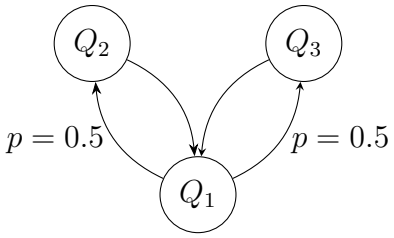

Figure 6.3: A pseudo 4-cycle which "starts" at Q_1 then with probability 0.5 proceeds to either Q_2 or Q_3. At either of these states, it certainly returns to Q_1. This behavior can appear like a 4-cycle with non-zero probability but will continue to behave as a 4-cycle with probability zero as time extends to infinity.

6.3.2 Conjectures Regarding Minimal Subgraphs and Surfaces

The first conjecture arising from the exploration of equilibrium partitions in the dual sense considers the relationship between an equilibrium partition and the maximum modularity partition.

Conjecture 6.4. *If the graph G is amodular and decomposable, then any non-consensus equilibria are not-strict.*

The basis for this conjecture is the similarity between the maximum modularity partition and the equilibrium partition as described in the introduction of chapter 3. Unfortunately the relationship between the two is difficult to tease apart because the modularity partition is defined globally and the equilibrium partition is defined locally. For this reason, the only real support for this conjecture is the lack of counterexamples.

Heuristically, a strict Nash equilibrium means that putting any vertex into a different strategic community will result in a strict decrease in game potential (and thus a strict increase in cut edges). In some way, modularity can be seen as a measure of the difference between the likelihood of selecting a non-cut edge at random in the graph G and selecting such an edge in a graph where edges are placed randomly. If the number of cut edges can be strictly increased by changing the strategy of a single vertex, then our intuition leads us to believe that the modularity of the original partition was not maximized. Unfortunately, this intuition is all the progress we have on this conjecture.

The next conjecture shows a great deal of promise and has a great deal of numerical support. However, because of the magnitude of the conjecture it remains an area of future work.

Conjecture 6.5. *Let $u_\epsilon(t)$ be a sequence of strategy profiles evolving under myopic best response with $K(x,y) = \chi_{B_\epsilon(x)}(y)$ and with time step Δt. Let $s_u^\epsilon(t)$ be the sequence of associated strategic boundary complexes. If $\Delta t = \epsilon^2 \to 0$ then $s_u^\epsilon(t) \to S(t)$, a smooth continuous one parameter family of curves (networks) which satisfy the free boundary curve shortening (network) flow.*

The support for the conjecture goes beyond the simulations presented in 3.3. During a single step of myopic best response the comparison between the the payoffs along a boundary match exactly with the threshold dynamics described by Caffarelli and Souganidis (2008) in their work on nonlocal threshold dynamics and wave prorogation only using a different kernel. The similarities between the two systems supports the conjecture that in the game theoretically informed model, the propagation of the "fronts" or strategic boundaries should conform to a mean curvature type flow. The conjecture presented here proposes a generalization of the results of Caffarelli et al. (2010) informed not by mechanics but rather by game theory.

If a point p on $s_u(t)$ has a positive curvature, then it is easy to see that $s_u(t+\Delta t)$ will intersect the ray from p in the direction of the curvature. If we describe this as motion in the normal direction, we can say

$$s_u(t+\Delta t) - s_u(t) = d(s_u, x)\vec{n}$$

where $d(s_u, x)$ is a function that describes how far in the direction of $\vec{n}$ does a player needs to travel before they would have an equal payoff between the two strategies separated by the curve. This is difficult to compute in general, but the ultimate goal is to take the limit

$$\lim_{\Delta t \to 0} \frac{s_u(t+\Delta t) - s_u(t)}{\Delta t} = \lim_{\epsilon \to 0} \frac{d(s_u, x)}{\epsilon^2}\vec{n}$$

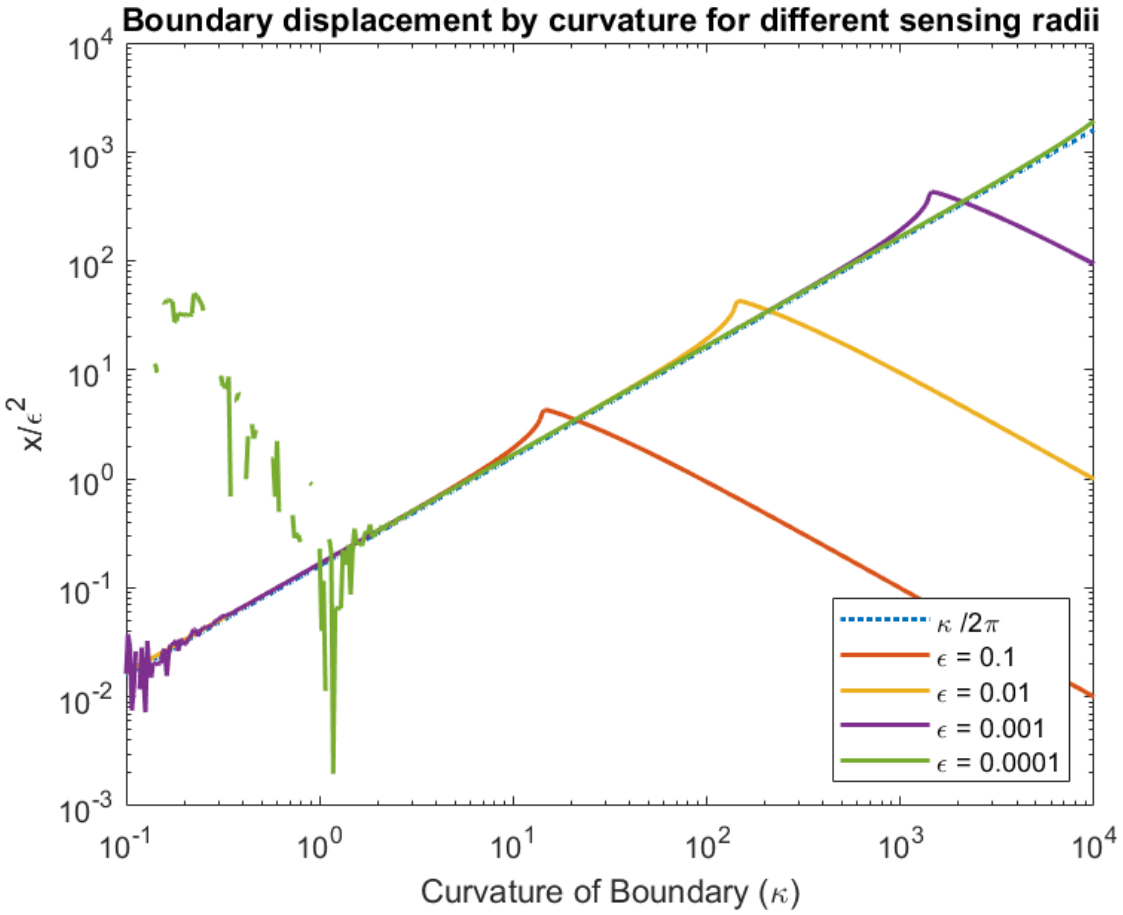

Figure 6.4: For several different choices of ϵ, x describes how far the circle of radius ϵ must be from the circle of radius R (with curvature $1/R$) so that the larger circle bisects the smaller one. We see that x/ϵ^2 converges to the curve representing the curvature of the large circle divided by 2π. This convergence gives support to the conjecture that the myopic best response flow converges to the curve shortening flow in the limit as $\epsilon \to 0$.

In the limit, we can approximate the curve as a circle because the curvature changes continuously and is bounded away from $\frac{1}{\epsilon}$. Even still, getting an analytical expression for how far from the curve the center of a circle of radius ϵ must be from a circle of radius $R >> \epsilon$ in order for the larger circle to bisect the smaller circle is not easily computed. We can, however, investigate numerically to find as $\epsilon \to 0$ it seems that $\frac{d(S_u,x)}{\epsilon^2} \to \frac{\kappa}{2\pi}$ where κ is the curvature of the boundary which is represented as $1/R$.

The result is the heuristic that in the limit as the sensing radius goes to zero,

$$\frac{ds}{dt} = \frac{\kappa}{2\pi}\vec{n}$$

almost everywhere. The meaning of almost everywhere is not yet rigorous, so this does not complete the conjecture. This is an exciting area continue future work.

6.3.3 Conjectures Regarding Structured Replicator Dynamics

The final conjecture relates to the replicator dynamics in the continuous player setting. It is again supported by numerical observation but was beyond the scope of chapter 4 at the time that it was written, and so it remains only a conjecture.

Conjecture 6.6. *For the pure coordination game in continuous player space, if u is a stationary solution satisfying the structured replicator equation*

$$0 = u^i(x)\langle \hat{e}^i - u^i(x), g[u](x)\rangle$$

for all i and for all $x \in \Omega$ then the image of u has measure 0 and u is piecewise constant.

Much like the result from 5.6 in the non-local non-linear diffusion case. Numerical experiments show that time dependent solutions converge to piecewise constant functions. However, these piecewise constant functions cannot be treated like those of chapter 5 exactly because there is no compact recognition range. Every strategy is comparable to every other strategy. Instead, we must examine the solutions which maximize the potential

$$\mathcal{W}[u] = \int_\Omega \int_\Omega K(x,y)\langle u(x), u(y)\rangle dxdy$$

Subject to the constraints that $u(x) \in \Delta^{m-1}$. We suspect that progress on this conjecture can be made by examining the regularized version of the problem where, instead of the domain being represented by a characteristic function in $\mathbb{R}^n$, we use a smooth population

function $P(x)$ with compact support. The reason this may be helpful is because it allows the use of the Fourier transform, which makes it easier to deal with the convolution.

The observed discretizations would be consistent with the findings of the other chapters, namely that continuous and non-constant Nash equilibria do not exist for pure coordination games in non-degenerate circumstances.

6.4 Concluding Remarks

When Caesar noted the differences in the people groups in first century Gaul, he did not describe this as the necessary emergent outcome of coordinating processes with spatial and relational structure. Nevertheless, the payoff from speaking the same language and using the same customs as one's close associates made it so that there were three distinct yet adjacent groups in the region. Mathematicians and scientists in network science, political science, game theory, and other fields have thought about situations like these for the past century to try to make sense of them. Even before the mathematicians, the philosophers and theologians, from Cicero saying that "no man lives for himself alone" to John Donne claiming that "no man is a Island" considered this type of emergence in their own way.

Since the question was posed, none of these mathematicians or philosophers have been able to give an answer: Given some relational structure, what non-consensus equilibria can emerge? I do not claim to have answered this question here, but I hope to have made a solution more attainable through a variety of models, each of which provides a different insight into coordinating systems. Each model described here gives a new insight into coordination as a whole, and the comparison of these models helps paint the picture of coordinating systems trying to balance the trade off between discretization and diffusion.

Bibliography

Acerbi, A., Ghirlanda, S., and Enquist, M. (2012). The logic of fashion cycles. *PLOS ONE*, 7(3):1–9. doi:10.1371/journal.pone.0032541. 205

Adwani, C., de Leo, R., and Yorke, J. (2025). What is the graph of a dynamical system. doi:10.48550/arXiv.2410.05520. Preprint. 124

Andreu-Vaillo, F., Mazón, J. M., Rossi, J. D., and Toledo-Melero, J. (2010). *Nonlocal Diffusion Problems*. American Mathematical Society. 151, 160, 165, 166

Angenent, S. (1990). Parabolic equations for curves on surfaces part i. curves with p-integrable curvature. *Annals of Mathematics*, 132(3):451–483. doi:10.2307/1971426. 76

Angenent, S. (1991). Parabolic equations for curves on surfaces: part ii. intersections, blow-up and generalized solutions. *Annals of Mathematics*, 133(1):171–215. doi:10.2307/2944327. 76

Apt, K. R., de Keijzer, D., Rahn, M., Schäfer, G., and Simon, S. (2017). Coordination games on graphs. *International Journal of Game Theory*, 46:851–877. doi:10.1007/s00182-016-0560-8. 7

Arditti, L., Como, G., Fagnani, F., and Vanelli, M. (2024). Robust coordination of linear threshold dynamics on directed weighted networks. *IEEE Transactions on Automatic Control*, pages 1–15. doi:10.1109/TAC.2024.3371882. 7

Ashkenazi-Golan, G., Mergoni Cecchelli, D., and Plumb, E. (2025). Simultaneous best-response dynamics in random potential games. doi:10.48550/arXiv.2505.10378. 127

Barles, G., Soner, H. M., and Souganidis, P. E. (1993). Front propagation and phase field theory. *SIAM Journal on Control and Optimization*, 31(2):439–469. doi:10.1137/0331021. 74

Beck, M. (2020). Spectral stability and spatial dynamics is partial differential equations. *Notices of the American Mathematical Society*, 67(4). doi:10.1090/noti2070. 138

Bence, J., Merriman, B., and Osher, S. (1992). Diffusion generated motion by mean curvature. Technical report, University of California Los Angeles. 73, 74

Bierwirth, M. and Lenger, J. (2025). Stable boundaries of opinion dynamics in heterogeneious spatial complex networks. In *Complex Networks & Their Applications XIV*. 6

Blondel, V. D., Guillaume, J.-L., Lambiotte, R., and Lefebvre, E. (2008). Fast unfolding of communities in large networks. *Journal of Statistical Mechanics: Theory and Experiment*, 2008(10):P10008. doi:10.1088/1742-5468/2008/10/P10008. 6

Bomze, I. M. (1983). Lotka-volterra equation and replicator dynamics:a two dimensional classification. *Biological Cybernetics*, 48:201–211. doi:10.1007/BF00318088. 83

Bomze, I. M. (1995). Lotka-volterra equation and replicator dynamics: new issues in classification. *Biological Cybernetics*, 72:447–453. doi:10.1007/BF00201420. 83

Bóna, M. (2017). *A Walk Through Combinatorics*. World Scientific. 19, 43

Bourni, T., Burns, N., and Catron, S. (2025). Classification of convex ancient solutions to free boundary curve shortening flow in convex domains. *Journal of Geometric Analysis*, 35:210. doi:10.1007/s12220-025-02036-x. 76

Bourni, T. and Franz, G. (2026). Ancient solutions to free boundary mean curvature flow. doi:10.48550/arXiv.2602.08850. 81

Bourni, T. and Langford, M. (2023). Classification of convex ancient free-boundary curve-shortening flows in the disc. *Analysis and PDEs*, 16(9):2225–2240. doi:10.2140/apde.2023.16.2225. 75

Brakke, K. A. (1978). *The motion of a surface by its mean curvature*. Princeton University Press. 76

Brandes, U., Delling, D., Gaerlet, M., Görke, R., Hoefer, M., Nikoloski, Z., and Wagner, D. (2006). On modularity - np-completeness and beyond. Technical report, Univeristy of Konstanz. 8, 37

Bucur, C. and Valdinoci, E. (2016). *Nonlocal Diffusion and Applications*. Springer. 165

Buskens, V. and Snijders, C. (2016). Effects of network characteristics on reaching the payoff-dominant equilibrium in coordination games: A simulation study. *Dynamic Games and Applications*, 6(4):477 – 494. doi:10.1007/s13235-015-0144-4. 7, 34

Caffarelli, L., Roquejoffre, J.-M., and Savin, O. (2010). Nonlocal minimal surfaces. *Communications on Pure and Applied Mathematics*, 63(9):1111–1144. doi:10.1002/cpa.20331. 66, 71, 210

Caffarelli, L. A. and Souganidis, P. E. (2008). Convergence of nonlocal threshold dynamics approximations to front propagation. *Archive for Tational Mechanics and Analysis*, 195:1–23. doi:10.1007/s00205-008-0181-x. 67, 72, 73, 74, 210

Cai, Y. and Daskalakis, C. (2011). On minmax theorems for multiplayer games. In *Proceedings of the 2011 Annual ACM-SIAM Symposium on Discrete Algorithms (SODA)*, pages 217–234. doi:10.1137/1.9781611973082.20. 7

Campigotto, R., Guillaume, J.-L., and Seifi, M. (2013). The power of consensus: random graphs have no communities. In *Proceedings of the 2013 IEEE/ACM International Conference on Advances in Social Networks Analysis and Mining*, page 272–276, New York, NY, USA. Association for Computing Machinery. 34

Carr, J. (1982). *Applications of Centre Manifold Theory*. Springer. 122

Chasseigne, E., Chaves, M., and Rossi, J. D. (2006). Asymptotic behavior for nonlocal diffusion equations. *Journal de Mathématiques Pures et Appliquées*, 86(3):271–291. doi:https://doi.org/10.1016/j.matpur.2006.04.005. 152

Cheng, H., Wang, H., and Meng, X. (2026). Spatio-temporal evolution of cooperation: multistability, pattern formation, and chaos in resource-driven eco-evolutionary games. *Journal of Mathematical Biology*, 92(12). doi:10.1007/s00285-025-02326-6. 136

Chiba-Okabe, H. and Plotkin, J. B. (2024). Social learning with complex contagion. *Proceedings of the National Academy of Sciences*, 121(49):e2414291121. doi:10.1073/pnas.2414291121. 123

Clauset, A., Newman, M. E. J., and Moore, C. (2004). Finding community structure in very large networks. *Physical Review E*, 70:066111. doi:10.1103/PhysRevE.70.066111. 6, 8, 36, 206

Coletti, C. F. and de Lima, L. R. (2025). Coexistence of species in a competition model on random geometric graphs. doi:10.48550/arXiv.2501.10611. Preprint. 6, 83

Cressman, R. and Apaloo, J. (2018). *Handbook of Dynamic Game Theory*, chapter Evolutionary Game Theory. Springer. 95

Cui, Z. and Shi, F. (2022). Bandwagon effects and constrained network formation. *Games and Economic Behavior*, 134:37–51. doi:https://doi.org/10.1016/j.geb.2022.03.014. 5, 104, 139, 162

Cvetković, D. and Petrić, M. (1984). A table of connected graphs on six vertices. *Discrete Math*, 50:37–49. doi:10.1016/0012-365X(84)90033-5. 23

Degroot, M. H. (1974). Reaching a consensus. *Journal of the American Statistical Association*, 69(345):118–121. doi:10.1080/01621459.1974.10480137. 6

Deng, B. (2023). Theory of invariant manifold and foliation and uniquenss of center manifold dynamics. *Journal of Dynmamics of Dynamics and Differential Equations*, 35:3075–3111. doi:10.1007/s10884-023-10265-3. 121

Dieckmann, U. and Doebeli, M. (1999). On the origin of species by sympatric speciation. *Nature*, 400(6742):354–357. 141

Doebeli, M. and Dieckmann, U. (2000). Evolutionary branching and sympatric speciation caused by different types of ecological interactions. *The american naturalist*, 156(S4):S77–S101. 141

dos Santos, B. C., Oliva, S. M., and and, J. D. R. (2022). A local/nonlocal diffusion model. *Applicable Analysis*, 101(15):5213–5246. doi:10.1080/00036811.2021.1884227. 165

Du, Q., Lehoucq, R., and Tartakovsky, A. (2015). Integral approximations to classical diffusion and smoothed particle hydrodynamics. *Computer Methods in Applied Mechanics and Engineering*, 286:216–229. doi:https://doi.org/10.1016/j.cma.2014.12.019. 166

Du, Q., Tao, Y., Tian, X., and Yang, J. (2019). Asymptotically compatible discretization of multidimensional nonlocal diffusion models and approximation of nonlocal green's functions. *IMA Journal of Numerical Analysis*, 39(2):607–625. doi:10.1093/imanum/dry011. 177

Du, Q., Tian, X., and Zhou, Z. (2022). Nonlocal diffusion models with consistent local and fractional limits. doi:10.48550/arXiv.2203.00167. Preprint. 166

D'Elia, M., Du, Q., Glusa, C., Gunzburger, M., Tian, X., and Zhou, Z. (2020). Numerical methods for nonlocal and fractional models. *Acta Numerica*, 29:1–124. doi:10.1017/S096249292000001X. 177

Ellison, G. (1993). Learning, local interaction, and coordination. *Econometrica*, 61(5):1047–1071. doi:10.2307/2951493. 4, 8, 32, 147

Ellison, G. (2000). Basins of attraction, long-run stochastic stability, and the speed of step-by-step evolution. *The Review of Economic Studies*, 67(1):17–45. doi:10.1111/1467-937X.00119. 5

Ely, J. C. (2002). Local conventions. *Advances in Theoretical Economics*, 2:1–29. doi:10.2202/1534-5963.1044. 5

Erdős, P. and Rényi, A. (1959). On random graphs i. *Publicationes Mathematicae Debrecen*, 6:290–297. 19, 32

Erdős, P. and Rényi, A. (1960). On the evolution of random graphs. *Publications of the mathematical institute of the Hungarian acadamy of science*, 5(1):17–60. 32, 205, 206, 207

Evans, L. C. (1998). *Partial Differential Equations*. American Mathematical Society. 164

Evans, L. C. and Spruck, J. (1991). Motion of level sets by mean curvature i. *Journal of DIfferential Geometry*, 33(3):635–681. doi:10.4310/jdg/1214446559. 74

Evans, L. C. and Spruck, J. (1992a). Motion of level sets by mean curvature ii. *Transactions of the American Mathematical Society*, 330(1):321–332. doi:10.2307/2154167. 74

Evans, L. C. and Spruck, J. (1992b). Motion of level sets by mean curvature iii. *Journal of Geometric Analysis*, 2(2):121–150. doi:10.1007/BF02921385. 74

Evans, L. C. and Spruck, J. (1995). Motion of level sets by mean curvature iv. *Journal of Geometric Analysis*, 5(1):77–114. doi:10.1007/BF02926443. 74

Foster, D. and Young, P. (1990). Stochastic evolutionary game dynamics. *Theoretical Population Biology*, 38:219–232. 4

Foulds, L. (1992). *Graph Theory Applications*. Springer. 11, 43, 55

Friedkin, N. E. and Johnsen, E. C. (1990). Social influence and opinions. *Journal of mathematical sociology*, 15(3-4):193–206. 6

Gage, M. and Hamilton, R. S. (1986). The heat equation shrinking convex plane curves. *ournal of Differential Geometry*, 23:69–96. 72

Gilboa, I. and Matsui, A. (1991). Social stability and equilibrium. *Econometrica*, 59(3):859–867. 4

Godsil, C. and Royle, G. (2001). *Algebraic Graph Theory*. Springer. 44

Gomez, C. and Rossi, J. D. (2020). A nonlocal diffusion problem that approximates the heat equation with neumann boundary conditions. *Journal of King Saud University - Science*, 32(1):17–20. doi:10.1016/j.jksus.2017.08.008. 151

Gross, J. L. and Jay, Y. (2005). *Graph theory and its applications*. CRCPress. 55

Hartvigsen, D. and Mardon, R. (1994). The all-pairs min cut problem and the minimum cycle basis problem on planar graphs. *SIAM Journal on Discrete Mathematics*, 7(3):403–418. doi:10.1137/S0895480190177042. 56

Helfgott, H. A., Bajpai, J., and Dona, D. (2017). Graph isomorphisms in quasi-polynomial time. doi:10.48550/arXiv.1710.04574. 20

Ilmanen, T., Nevis, A., and Schulz, F. (2018). On short time existence for the planar network flow. doi:10.48550/arXiv.1407.4756. Preprint. 71, 76

Jackson, M. O. and Storms, E. (2025). Behavioral communities and the atomic structure of networks. doi:10.2139/ssrn.3049748. Available at SSRN. 8

Kandori, M., Mailath, G. J., and Rob, R. (1993). Learning mutation and long run equilibria in games. *Econometrica*, 61:29–56. doi:10.2307/2951777. 3, 32, 169

Kandori, M. and Rob, R. (1995). Evolution of equilibria in the long run: A general theory and applications. *Journal of Economic Theory*, 65:383–414. doi:10.1006/jeth.1995.1014. 4

Kandori, M. and Rob, R. (1998). Bandwagon effects and long run technology choice. *Games and Economic Behavior*, 22(1):30–60. doi:10.1006/game.1997.0563. 5, 104

Karoński, M. (1982). A review of random graphs. *Journal of Graph Theory*, 6(4):349–389. doi:10.1002/jgt.3190060402. 32

Kavallaris, N. I. and Suzuki, T. (2018). *Non-Local Partial Differential Equations for Engineering and Biology*. Springer International. 143, 165

Lã, Q. D., Chew, Y.-H., and Soong, B.-H. (2016). *Potential Game Theory*. Springer. 40, 89, 143

Levin, S. A., Milner, H. V., and Perrings, C. (2021). The dynamics of political polarization. *Proceedings of the National Academy of Sciences*, 118(50):e2116950118. doi:10.1073/pnas.2116950118. 6

Li, J., Lai, S., Shuai, Z., Tan, Y., Jia, Y., Yu, M., Song, Z., Peng, X., Xu, Z., Ni, Y., Qiu, H., Yang, J., Liu, Y., and Lu, Y. (2024). A comprehensive review of community detection in graphs. *Neurocomputing*, 600:128169. doi:https://doi.org/10.1016/j.neucom.2024.128169. 6

Lieberman, E., Hauert, C., and Nowak, M. A. (2005). Evolutionary dynamics on graphs. *Nature*, 433:312–316. doi:10.1038/nature03204. 83

Maschler, M., Solan, E., and Zamir, S. (2013). *Game Theory*. Cambridge University Press. doi:10.1017/CBO9780511794216. 3

McAlister, J. S. (2024). Structured coordination with neutral options. doi:10.5281/zenodo.11237078. 25

McAlister, J. S. (2025). Nonlinear nonlocal diffusion model for continuous coordination. doi:10.5281/zenodo.15287893. 187

McAlister, J. S. (2026a). Continuous coordination in the plane. doi:10.5281/zenodo.18488638. 71

McAlister, J. S. (2026b). Structured replicator dynamics. doi:10.5281/zenodo.18436284. 89

McAlister, J. S. and Fefferman, N. H. (2025). Insights into the structured coordination game with neutral options through simulation. *Dynamic Games and Applications*. doi:10.1007/s13235-024-00612-4. 2, 11, 13, 16, 127

McAlister, J. S., Fefferman, N. H., and Mengesha, T. A. (2025). Nonlinear nonlocal diffusion equations for the analysis of continuous coordination and anti-coordination type games. doi:10.48550/arXiv.2506.13929. Under Review at Physical Reviews E. 2, 142

McDiarmid, C. and Skerman, F. (2020). Modularity of erdős-rényi random graphs. *Random Structures & Algorithms*, 57(1):211–243. doi:10.1002/rsa.20910. 8, 34, 206

Mengesha, T. and Du, Q. (2015). On the variational limit of a class of nonlocal functionals related to peridynamics. *Nonlinearity*, 28(11):3999. doi:10.1088/0951-7715/28/11/3999. 166

Monderer, D. and Shapley, L. S. (1996). Potential games. *Games and Economic Behavior*, 14(1):124–143. doi:10.1006/game.1996.0044. 40, 89, 90, 92, 229

Moore, R. L. (1918). A characterization of jordan regions by properties having no reference to their boundaries. *Proceedings of the National Academy of Sciences of the United States of America*, 4(12):364–370. 68

Morris, S. (2000). Contagion. *Review of EAconomic Studies*, 67:57–78. 7

Nash, J. (1950). Equilibrium points in n-person games. *Proceedings of the National Acadamy of Sciences*, 36:48–49. doi:10.1073/pnas.36.1.48. 3

Nash, J. (1951). Non-cooperative games. *The Annals of Mathematics*, 54:286–295. 2

Newman, M. E. (2003). *Handbook of Graphs and Networks: From the Genome to the Internet*. Wiley - VCH. 34

Newman, M. E. J. (2006). Modularity and community structure in networks. *Proceedings of the Nathonal Acadamy of Science*, 103(23):8577–8582. doi:10.1073/pnas.0601602103. 8, 206

Nisan, N., Schapira, M., Valiant, G., and Zohar, A. (2011). Best-response mechanisms. In *Innovations in Computer Science*, pages 155–165. 11

Nishizeki, T. and Chiba, N. (1988). *Planar Graphs, theory and algorithms*. Dover. 43, 55

Nowak, M. A. (2006). *Evolutionary Dynamics*. Harvard University Press. 6, 83

Nowak, M. A., Tarninta, C. E., and antal, T. (2010). Evolutionary dynamics in structured populations. *Philosophical Transactions of The Royal Society B*, 365:19–30. doi:10.1098/rstb.20090215. 6

Oechssler, J. (1997). Decentralization and the coordination problem. *Journal of Economic Behavior and Organization*, 32:119–135. doi:10.1016/S0167-2681(96)00022-4. 4

Oechssler, J. (1999). Competition among conventions. *Computational and Mathematical Organization Theory*, 5:31–44. doi:10.1023/A:1009646410168. 5

Ohtsuki, H. and Nowak, M. A. (2006). The replicator equation on graphs. *Journal of Theoretical Biology*, 243:86–97. doi:10.1016/j.jtbi.2006.06.004. 83

Paarporn, K., Alizadeh, M., and Marden, J. R. (2021). A risk-security tradeoff in graphical coordination games. *IEEE Transactions on Automatic Control*, 66(5):1973–1985. doi:10.1109/TAC.2020.3002499. 7

Raducha, T. and San Miguel, S. (2022). Coordination and equilibrium selection in games: the role of local effects. *Scientific Reports*, 12:3373. doi:10.1038/s41598-022-07195-3. 147

Robson, A. J. and Vega-Redando, F. (1995). Efficient equilibrium selection in evolutionary games with random matching. *Journal of Economic Theory*, 70:65–92. doi:10.1006/jeth.1996.0076. 4

Sandholm, W. H. (2001). Potential games with continuous player sets. *Journal of Economic Theory*, 97(1):81–108. doi:https://doi.org/10.1006/jeth.2000.2696. 143

Savin, O. (2025). The work of luis caffarelli on fully nonlinear elliptic pdes. *Bulletin of the Americal Mathematical Society*, 62(2):327–357. doi:10.1090/bull/1862. 67

Smith, J. M. (1982). *Evolution and the Theory of Games*. Cambridge University Press. 4

So, G. and Ma, Y.-A. (2025). Learnable mixed nash equilibria are collectively rational. doi:10.48550/arXiv.2510.14907. Preprint. 82

Swenson, B., Murray, R., and Kar, S. (2018a). On best-response dynamics in potential games. *SIAM Journal on Control and Optimization*, 56(4):2734–2767. doi:10.1137/17M1139461. 82, 92, 124

Swenson, B., Murray, R., Kar, S., and Poor, H. V. (2018b). Best-response dynamics in continuous potential games: Non-convergence to saddle points. In *2018 52nd Asilomar Conference on Signals, Systems, and Computers*, pages 310–315. doi:10.1109/ACSSC.2018.8645541. 82, 124

Tao, Y., Tian, X., and Du, Q. (2017). Nonlocal diffusion and peridynamic models with neumann type contraints and their numerical approximations. *Applid Mathematics and Computation*, 305:282–298. doi:10.1016/j.amc.2017.01.061. 166

Tao, Y., Tian, X., and Du, Q. (2019). Nonlocal models with heterogeneous localization and their application to seamless local-nonlocal coupling. *Multiscale Modeling & Simulation*, 17(3):1052–1075. doi:10.1137/18M1184576. 166

Taylor, P. D. and Jonker, L. B. (1978). Evolutionary stable strategies and game dynamics. *Mathematical Biosciences*, 40(1):145–156. doi:10.1016/0025-5564(78)90077-9. 83

Tomassini, M. and Pestelacci, E. (2010). Evolution of coordination in social networks: A numerical study. *Internation Journal of Modern Physics C*, 21(40):1277–1296. doi:10.1142/S012918311001583X. 7

von Neumann, J. (1928). Zur theorie der gesellschaftsspiele. *Mathematische Annalen*, 100:295–320. doi:10.1007/BF01448847. 1

von Neumann, J. and Morgenstern, O. (1944). *THeory of Games and Economic Behavior*. Princeton University Press. 1

Wakano, J. Y. and Iwasa, Y. (2013). Evolutionary branching in a finite population: Deterministic branching vs. stochastic branching. *Genetics*, 193(1):229–241. doi:10.1534/genetics.112.144980. 141

Waugh, A. S., Pei, L., Fowler, J. H., Mucha, P. J., and Porter, M. A. (2009). Party polarization in congress: A network science approach. doi:10.48550/arXiv.0907.3509. preprint. 6

Weidenholzer, S. (2010). Coordination games and local interactions: A survey of the game theoretic literature. *Games*, 1(4):551–585. doi:10.3390/g1040551. 6, 32

Wiseman, J. (2020). Persistence of morse decompositions over grid resolution for maps and time series. doi:10.48550/arXiv.2012.05297. Preprint. 124, 126

Yao, T. and Cooney, D. B. (2025). Spatial pattern formation in eco-evolutionary games with einvironment-driven motion. doi:10.48550/arXiv.2502.06723. Preprint. 136

Yao, T., Xu, C., and Cooney, D. B. (2025). Pattern formation in agent-based and pde models for evolutionary games with payoff-driven motion. doi:10.48550/arXiv.2509.20538. Preprint. 136

Zha, Q., Kou, G., Hengjie, Z., Liang, H., Chen, X., Li, C.-C., and DOng, Y. (2020). Opinion dynamics in finance and buisness: a literature review and research opportunites. *Financial Innovation*, 6. doi:10.1186/s40854-020-00211-3. 6

Appendices

A Supplementary Results

A.1 Results Regarding Replicator Dynamics

Proofs Regarding System Dynamics

Lemma A.1. *$f(x,y) = \langle x \circ y, y\rangle - (\langle x, y\rangle)^2 \geq 0$ for $x \in \Delta^{m-1}$, and equality is attained only when $x_i = 0$ or $y_i = \langle x, y\rangle$ for all i.*

Proof. The proof of this important point is surprisingly difficult. We must induct on the dimension. Before we get there we must make a point to use a Langrange multiplier argument to characterize local extrema of f given the constraint $g(x,y) = \sum x_i = 1$.

Let $\mathcal{L}(x,y,\lambda) = f(x,y) + \lambda g(x,y)$. Clearly we can write

$$\begin{aligned}
\frac{\partial}{\partial x_i}\mathcal{L}(x,y,\lambda) &= y_i(y_i - 2\langle x, y\rangle) + \lambda \\
\frac{\partial}{\partial y_i}\mathcal{L}(x,y,\lambda) &= 2x_i(y_i - \langle x, y\rangle) \\
\frac{\partial}{\partial \lambda}\mathcal{L}(x,y,\lambda) &= \sum_{i\in C} x_i
\end{aligned} \tag{4}$$

And so we see that for (x,y) to be a local extremum of f subject to the constraint, it must be true that $x_i = 0$ or $y_i = \langle x, y\rangle$ for all $i \in C$. When this condition is satisfied it is easy to compute that $f(x,y) = 0$. So we can conclude that at all the local extrema, subject to the constraint, $f(x,y) = 0$. To show that local extremum is a minimum and it is a global minimum we must consider the boundaries.

To do this, we begin the issue of induction. In the base case consider $m = 2$. We have already shown that at any local extrema of $f : \Delta^1 \times \mathbb{R}^2 \to \mathbb{R}$, $f(x,y) = 0$. Notice that we can use the fact that $f(x,ay) = a^2 f(x,y)$ to rewrite f as $f(\Delta^1, S^1, \mathbb{R}_+) \to \mathbb{R}$ where $f(x,y,a) \mapsto f(x,ay)$. We also notice that changing a (the magnitude of y) does not change the sign of $f(x,y,a)$. This rewriting has not changed the fact that at local extrema, $f(x,y,a) = 0$

Select any a_0 and let $f_{a_0} : \Delta^1 \times S^1 \to \mathbb{R}$ so that $f_{a_0}(x, y) = a_0^2 f(x, y)$ and consider its global extrema (which must be attained because the domain is compact and f is continuous). A global extrema must occur at the boundary or at a local extremum. Notice that $\partial(\Delta^{m-1} \times S^{m-1}) = \partial\Delta^{m-1} \times cl(S^{m-1}) \cup \partial(S^{m-1}) \times cl(\Delta^{m-1}) = \partial\Delta^{m-1} \times S^{m-1}$ and when $m = 2$, $\partial\Delta^1 \times S^1 = \{\hat{e}^1, \hat{e}^2\} \times S^1$. Now we can easily compute that $f(e_1, y) = 2y_1^2$ and $f(e_2, y) = 2y_2^2$. In either case it is positive unless is coincides with a local extremum.

The global minimum of $f(x, y, a)$ must be the global minimum of $f_{a_0}(x, y) = a_0^2 f(x, y)$ among all a_0. In the case $m = 2$ we have just shown that $\min f_{a_0} = \min\{2a_0^2 y_2^2, 2a_0^2 y_1^2, 0\} = 0$ and therefore, any a_0, $\min f_{a_0}(x, y) = 0$. Thus $f : \Delta^1 \times \mathbb{R}^1 \to \mathbb{R}$ has a global minimum $f(x, y) = 0$ which is attained only when $x_i = 0$ or $y_i = \langle x, y\rangle$ for all i. (If that is not true then it cannot be a local minimum and it cannot satisfy $f(x, y) = 0$ on the boundary so it cannot be global minimum). Restated $f(x, y) \geq 0$ with equality when $x_i = 0$ or $y_i = \langle x, y\rangle$ for all i when $m = 2$.

Now for the inductive step we must notice that the characterization of local extrema was independent of the dimension. Suppose that the statement is true for $m = 2, ..., M$ and consider the statement when $m = M + 1$. By the same argument, $f : \Delta^M \times \mathbb{R}^{M+1} \to \mathbb{R}$ can be rewritten as $f : \Delta^M \times S^M \times \mathbb{R} \to \mathbb{R}$ and again we will pick any a_0. Still it is true that the local minima are achieved when $x_i = 0$ or $y_i = \langle x, y\rangle$ for all i in which case $f(x, y, a_0) = 0$. Now consider $(x, y) \in \partial(\Delta^M \times S^M) = \partial\Delta^M \times S^M$. There is at least one $i \in C$ so that $x_i = 0$ let $(\tilde{x}, \tilde{y}) = ([x_j]_{j\neq i}, [y_j]_{j\neq i})$ and do an easy computation to see that $f(x, y) = \tilde{f}(\tilde{x}, \tilde{y})$ and $f(x, y, a_0) = \tilde{f}(\tilde{x}, \tilde{y}, a_0)$, where $\tilde{f} : \Delta^{M-1} \times \mathbb{R}^M \to \mathbb{R}$ and $\tilde{f} : \Delta^{M-1} \times S^{M-1} \times \mathbb{R} \to \mathbb{R}$. By the inductive hypothesis $a_0^2 f(\tilde{x}, \tilde{y}) \geq 0$ with equality only when $\tilde{x}_j = 0$ or $\tilde{y}_j = \langle \tilde{x}, \tilde{y}\rangle$ for all i. Therefore $a^2 f(x, y) \geq 0$ and because this was in the case where $x_i = 0$ for some i, the conditions for equality are equivalent.

Thus in any finite dimension, for $f : \Delta^{m-1} \times \mathbb{R}^m \to \mathbb{R}$ where $f(x, y) = \langle x \circ y, y\rangle - \langle x, y\rangle^2$, we have shown that $f(x, y) \geq 0$ with equality only when $x_i = 0$ or $y_i = \langle x, y\rangle$ for all i. □

The proof of proposition 4.1:

Proposition. *If the payoff matrix A is a symmetric matrix then the structured linear game with fitnesses $w_v(u_v|u) = \langle u_v, g_v \rangle$ with g_v defined as in (4.2), then the game is a potential game with the potential function*

$$\mathcal{W}(u) = \frac{1}{2}\sum_v w(u_v|u) = \frac{1}{2}\sum_{v\in V}\langle u_v, g_v\rangle \tag{5}$$

Proof. As in Monderer and Shapley (1996) we will show that $w_v(u_v|u) - w_v(x|u) = \mathcal{W}(u_v, u_{-v}) - \mathcal{W}(x, u_{-v})$. where u_{-v} is the strategy profile u without the strategy of v. without loss of generality we call $v = 1$ and write the new strategy x as $u_1 + \eta$ for some η

$$\begin{aligned} w_1(u_1|u) - w_1(u_1+\eta, u) &= \langle u_1, g_v\rangle - \langle u_1+\eta, g_1\rangle \\ &= -\langle \eta, g_1\rangle \end{aligned} \tag{6}$$

Now consider the differences in total fitness

$$\begin{aligned} \mathcal{W}(u_1, u_{-1}) - \mathcal{W}(u_1+\eta, u_{-1}) = \frac{1}{2}&\left(\langle u_1, g_1\rangle + \sum_{v>1}\langle u_v, g_v\rangle\right) - \\ &\frac{1}{2}\left(\langle u_1+\eta, g_1\rangle + \sum_{v>1}\langle u_v, g_v + AW_{v,1}\eta\rangle\right) \\ = \frac{1}{2}&\left(-\langle \eta, g_v\rangle - \sum_{v>1} W_{v,1}\langle u_v, A\eta\rangle\right) \end{aligned} \tag{7}$$

Use the fact that A is symmetric and real to say $\langle u_v, A\eta\rangle = \langle \eta, Au_v\rangle$, then observe that

$$\sum_{v>1} W_{v,1}\langle \eta, Au_v\rangle = \left\langle \eta, A\sum_{v\in V} W_{1,v}u_v\right\rangle = \langle \eta, g_1\rangle$$

so long as the adjacency matrix is undirected and there are no loops. Therefore we get the result

$$\mathcal{W}(u_1, u_{-1}) - \mathcal{W}(u_1+\eta, u_{-1}) = -\langle \eta, g_1\rangle$$

This completes the proof that the game is a potential game and $\mathcal{W}$ is a potential function. □

Jacobian Computations

Call the vector with all zeros except for a 1 in the position corresponding to player v and strategy k "$\hat{e}(v,k)$." In this way, for each player $v \in V$ there is an eigenvector, $e(v,k_v)$, associated to the eigenvalue $-g_v^{k_v}$ where k_v is the strategy used by player v. Note that there are clearly n linearly independent such eigenvectors. Moreover, notice that

$$\Delta^{m-1} \cap u^\star + span(\{\hat{e}(v,k_v); \forall v \in V\}) = \{u^\star\}$$

Now consider the eigenspaces associated to the eigenvalues $g_v^i - g_v^{k_v}$ for each v. Let $S(v,i) = \{j \in 1,...,m; g_v^i = g_v^j, j \neq k_v\}$. For a particular block $J_{v,v}$ it is easy to see that the eigenspace associated to $g_v^i - g_v^{k_v}$ contains the space of vectors where $x_j = 0$ if $j \notin S(v,i)$ and $x_{k_v} + \sum_{j \in S(v,i)} x_j = 0$. Call this subspace of $\mathbb{R}^m$, $E(v,i)$, and note that this space has dimension the same size as $|S(v,i)|$. Also note that

$$u^\star + E(v,i) \cap \Delta^{m-1} = \Delta^{|S(v,i)|}$$

(that is, the intersection of the $m-1$ simplex with the eigenspace $E(v,i)$ is a subsimplex of dimension $|S(v,i)|$ and it contains $\hat{e}^{k_v}$ and $\hat{e}^j$ for each $j \in S(v,i)$.) Let x be a block vector with all zeros except in the spots corresponding to player v where we include any vector from $E(v,i)$. x is an eigenvector of $J(u^\star)$. This means for each vertex v we can partition the strategies other than k_v and get eigenspaces whose geometric multiplicity is equal to their algebraic multiplicity. Thus we get $n(m-1)$ linearly independent eigenvectors. Combine these eigenvectors with the original n eigenvectors to get mn linearly independent eigenvectors.

To summarize so far we have found all mn eigenvectors, we can name them each x_v^i because the correspond to a single player and strategy. They are all linearly independent. There are exactly n eigenvectors, $x_v^{k_v}$, each one corresponding to $-g_v^{k_v}$ for some $v \in V$ for which $\Delta^{m-1} \cap u^\star + span(x_v^{k_v}) = \{u^\star\}$. This is not true for any of the remaining eigenvectors. For each vertex v and each value of g_v^i taken on by some $i \neq k_v$,

Lemma A.2. *Let $u^\star$ be an equilibrium to the ODE system (4.4) in which player v plays a mixture of strategies in $I \subset \{1, 2, ..., m\}$. Let $u_v^I = [u_v^i]_{i \in I}$. The submatrix of a jacobian matrix evaluated at an equilibrium $u^\star$ corresponding to the rows and columns of player v and the strategies in I has the form*

$$\langle u_v, g_v \rangle \begin{bmatrix} -u_v^1 & -u_v^2 & \dots & -u_v^r \\ -u_v^1 & -u_v^2 & \dots & -u_v^r \\ \vdots & \vdots & \ddots & \vdots \\ -u_v^1 & -u_v^2 & \dots & u_v^r \end{bmatrix}$$

With a spectrum $\{0, -\langle u_v, g_v \rangle\}$. The eigenspace corresponding to 0, E_0, satisfies

$$\Delta^{|I|-1} \subset u^\star + E_0$$

Proof. Consider $u_v^\star$ with $I = C(u_v)$. Without loss of generality suppose that $I = \{1, 2, ..., r\}$ and recall that if u is an equilibrium then $u_v^i \neq 0 \implies g_v^i = \langle u_v, g_v \rangle$.

Thus we can examine $J_{v,v}(u^\star) = diag(g_v^i - \langle u_v, g_v \rangle) - u_v g^\intercal$. Because of the assumption that $u_v^i = 0$ for $i > r$ and because $g_v^i = \langle u_v, g_v \rangle$ for $i \leq r$. It is clear that $J_{v,v}$ is the block matrix

$$J_{v,v}(u^\star) = \begin{bmatrix} -\langle u_v, g_v \rangle (u_v^I \mathbf{1}^\intercal) & A \\ 0 & diag(g_v^i - \langle u_v, g_v \rangle \end{bmatrix}.$$

where A is some real matrix. The submatrix corresponding only to the strategies in I, is $-\langle u_v, g_v \rangle (u_v^I \mathbf{1}^\intercal)$ and the eigenpairs are easy to compute.

Any vector x which satisfies $\sum_{i \in I} x_1 = 0$ will satisfy $-\langle u_v, g_v \rangle (u_v^I \mathbf{1}^\intercal) x = \mathbf{0}$ so 0 is an eigenvalue with eigenspace E_0 and certainly for any $x \in (u_v^I + E_0)$, $\sum_i x_i = 1$. That is if $x \in \Delta^{|I|-1}$ then $x \in (u_v^I + E_0)$.

0 has geometric multiplicity, and thus algebraic multiplicity, of $|I| - 1$. Note also that $-\langle u_v, g_v \rangle$ is an eigenvalue with eigenvector u_v^I. $-\langle u_v, g_v \rangle (u_v^I \mathbf{1}^\intercal) u_v^I = -\langle u_v, g_v \rangle u_v^I$. We note that the eigenspace of $-\langle u_v, g_v \rangle$, $E_{-g} = span(\{u_v^I\})$, because it can have dimension at most 1. Moreover, $\Delta^{|I|-1} \cap (u_v^I + E_{-\langle u_v, g_v \rangle}) = \{u_v^I\}$.

Thus for the submatrix corresponding to the block in the upper left of $J_{v,v}(u^\star)$ is nondeficient and the spectrum is $\{0, -\langle u_v, g_v\rangle\}$. Moreover, 0 has multiplicity equal to $|I|-1$, where $I = C(u_v)$.

□

Proofs Connecting the Continuous and Discrete Time Models

Corollary A.1. *B_G is weakly connected and, for a potential game, acyclic*

Proof. Because X is connected and B_G is a contraction of X, B_G must also be connected. Because the direction of edges always go in the direction of increasing potential, $\mathcal{W}$, there can be no cycles □

Corollary A.2. *For a potential game, $B_G \subseteq \mathcal{M}_G$*

Proof. Let P be the subset of $V(\mathcal{M}_G)$ so that every invariant set in P contains a pure strategy profile. Construct the mapping $\gamma : P \to V(B_G)$ so that $\gamma(M) = v$ if $\exists u \in M$ so that, if it is expressed as a strategy profile, $u \in v$.

It is clear that every $M \in P$ is mapped to at least one vertex in $V(B_G)$. Moreover, for a potential game, γ is well posed because if an invariant set in $\mathcal{M}$ contains two pure strategies, then those two pure strategies must be connected by a path made up of manifolds of equilibria. (For the pure coordination game this is achieved by 4.10. For other potential games, this is because the potential function from lemma 4.4 rules out the possibility of cycling. Therefore these two pure strategies will correspond to partitions which are contained in the same vertex of B_G. This means that Every vertex in $\mathcal{M}_G$, containing a pure strategy profile, is mapped to exactly 1 vertex in B_G and Γ is a surjection. Additionally if $\gamma(M_1) = \gamma(M_2) = v$ then there is a strategy profile $u_1 \in M_1$ and a strategy profile $u_2 \in M_2$ so that $u_1, u_2 \in v$. If two strategy profiles are in the same element of $v \in V(B_G)$. Then they are connected by a sequence of single strategic changes that do not change potential. Again this means that they are contained in a single isolated invariant set. Therefore M_1 and M_2 are the same. Thus γ is a bijection.

Moreover, any forward path in B_G also must exist in $\mathcal{M}_G$. Consider a forward path in B_G from v to w. This forward path corresponds to at least one path in (X, d) because each forward step represents a single strategic change of increasing potential and any two vertices in (X, d) which are contracted into a single vertex in B_G are connected by a path of single strategic changes that leave potential unchanged. Therefore Every forward path in B_G represents a path in (X, d) with (not necessarily strict) increasing potential. Moreover, by the proof of proposition 4.2 we know that between any two adjacent strategy profiles, there is either a heteroclinic orbit from one to the other increasing in potential or there is a manifold of equilibria connecting the two if they are of equal potential. Therefore any such path can be described as a path of heteroclinic orbits connecting isolated invariant sets increasing in potential.

Therefore, for any path in B_G from v to w there must be a path in $\mathcal{M}$ from $\gamma^{-1}(v)$ to $\gamma^{-1}(w)$. This complete the proof that $B_G \subseteq \mathcal{M}_G$. □

Corollary A.3. *The partial order $(\prec)$ on the isolated invariant sets induced by the Morse Graph satisfies the following:*

$$M_1 \prec M_2 \implies \mathcal{W}(u_1) < \mathcal{W}(u_2)$$

where M_1, M_2 are isolated invariant sets in the dynamical system and $u_1 \in M_1$ and $u_2 \in M_2$.

Proof. This is direct from corollary A.2 because if $M_1 \prec M_2$ then there is a forward path from $\gamma(M_1)$ to $\gamma(M_2)$ in B_G. By construction forward paths in B_G are increasing in potential. □

Corollary A.4. *For the pure coordination game $B_G/S_m \subset \mathcal{M}_G/S_m$ where S_m is the group of permutations of m (the number of available strategies). Moreover B_G/S_m is constructed by doing the same construction process as in the definition of B_G on $(\mathcal{A}, \tilde{D}) = (X, d)/S_m$*

Proof. Two vertices in B_G are joined into a single vertex in B_G/S_m if there two strategy profiles in the two vertices are equivalent under some permutation of strategies. In the same way, two vertices in $\mathcal{M}_G$ are joined into a single vertex in $\mathcal{M}_G/S_m$ if there are two strategy profiles in the two vertices which are equivalent under some strategic permutation.

Let p be some strategic permutation so if u is a strategy profile then pu is that strategy profile where the strategies have been relabeled according to p. $\gamma(pu) = p\gamma(u)$ so the reductions on both B_G and $\mathcal{M}_G$ are equivalent. □

Corollary A.5. *For the pure coordination game, if G is indecomposable then $\mathcal{M}_G/S_m$ has a single node with outdegree 0*

Proof. Lemma 4.10 shows that any mixed strategy equilibrium is either unstable or in a manifold of equilibria that contains at least two other pure strategy profiles. In an indecdomposable graph, every non-consensus strategy profile is unstable because it is not a Nash equilibrium. This means that the only isolated invariant sets for the system that have no heteroclinic orbits leaving them are the consensus equilibria. When permutations are modded out, all of the consensus equilibria are joined in a single vertex and that single vertex is the only vertex with outdegree 0. □

Corollary A.6. *For the pure coordination game, if $\mathcal{M}_G/S_m$ has more than one node of outdegree 0 then there is a non-consensus Nash equilibrium*

Proof. This is the contrapositive of A.5 □

Corollary A.7. *If two equilibria u and u' are in the same isolated forward and backward invariant set, then they are both contained in a component of a level set of $\mathcal{W}$.*

Proof. If two equilibria are both contained in a single vertex $M \in V(\mathcal{M}_G)$, from corollaryA.1, we know that the corresponding strategy profiles are contained in the same vertex $v \in V(B_G)$. By the construction of B_G every vertex strategy profile contained in a single vertex must have the same potential.

If the two equilibria are in the same forward and backward invariant set then, for any ϵ we can create a chain $u(i)$ so that $u(i) \in B_\epsilon(\omega(u(i-1)))$ with $u(0) = u$ that reaches u' in a finite number of steps (because the invariant set is isolated).

The two equilibria are in the same level set of $\mathcal{W}$ meaning they must both satisfy $\mathcal{W}(u) = \mathcal{W}(u') = c$ for some c. Moreover they must be in a connected component of this level set

because if they are not path connected in the levels set, any path between the two in $(\Delta^{m-1})^V$ must leave the level set and intersect some point x with $\mathcal{W}(x) \neq \mathcal{W}(u)$. Because there is a strict difference, and trajectories can only increase in potential, there exists a $\square$

Corollary A.8. *If G is indecomposable, a trajectory of the ODE system (4.4) for a pure coordination game with random initial data and any amount of random noise will converge to a consensus equilibrium with probability 1*

Proof. The fact that the the potential function $\mathcal{W}$ is a polynomial implies that any level set of $\mathcal{W}$ has measure 0 in $(\Delta^{m-1})^V$.

Thus corollary A.7 implies that, with random noise, every trajectory will eventually leave every invariant set and thus, if a unstable manifold exists, every trajectory with random noise will eventually leave every invariant set and not return with the exception of the consensus equilibrium $\square$

A.2 Results Regarding Nonlocal Diffusion

Alternative Proof for Global Existence

Recall theorem 5.2 when $\rho \in C^{1,1}$ satisfies the coordination property (5.8). Under these conditions the a solution to the the initial value problem $u_t = g[u]$ exists and is unique for all finite time. The short proof is included in the main text, but there is also an alternative proof which reveals the repeatability of the extension principle as described in the proof of theorem 5.1

Theorem (Global existence and uniqueness with particular $\rho \in C^{1,1}$)**.** *Let $\rho \in C^{1,1}(\mathbb{R})$ satisfy (5.8). Under this strengthened hypothesis, the Initial Value Problem $u_t = g[u]$ with $u(x,0) = u_0 \in C_b^0(\Omega)$ has a unique continuous and bounded solution for all finite time.*

Proof. We modify our proof from Theorem 5.1. Equip the function space $C_b^0(\overline{\Omega}_T)$ with the standard sup norm $\|u\| = \sup_{t\in[0,T]} \|u(\cdot,t)\|_\infty$. Now let

$$E_T := \{u \in C_b^0(\overline{\Omega}_T; \mathbb{R}); u(x,0) = u_0, \|u\| \leq \|u_0\|\}$$

for some T to be determined later. Observe again that $u(x,t) \equiv u_0(x)$ is in E_T so it is non-empty. Also, observe that E_T is complete. Consider the same operator $\Theta : C_b^0(\overline{\Omega}_T, \mathbb{R}) \to C_b^0(\overline{\Omega}_T, \mathbb{R})$ as in theorem 5.1. We will show again that $\Theta : E_T \to E_T$.

We again use lemma 5.1 to say that Θu is clearly continuous and indeed continuously differentiable in time. To say that $\|\Theta u\| \leq \|u_0\|_\infty$ we need only repeat our argument from lemma 5.4.

Suppose there is a time t_0 and position x_0 where $\Theta u(x_0,t_0) - \epsilon t_0 \geq v := \|u_0\| + \epsilon$. Θu is differentiable in time so, supposing that t_0 is the first time this inequality is satisfied we can say that $\frac{\partial}{\partial t}\Theta u(x_0,t_0)) - \epsilon \geq 0$. We also have that $\frac{\partial}{\partial t}(\Theta u(x_0,t_0)) = g[u](x_0,t_0)$. We already know that u and Θu are continuous so $u(x,t_0) \leq v$ for all $x \in \mathbb{R}^n$. Because $\rho'(z) \leq 0$ whenever $z \geq 0$ we know that $\rho'(u(x_0,t_0) - u(y,t_0)) \leq 0$ for all y and thus $g[u](x_0,t_0) \leq 0$. Therefore we get a contradiction

$$0 \geq g[u](x_0,t_0) = \frac{\partial}{\partial t}(\Theta u(x_0,t_0)) \geq \epsilon > 0$$

Thus we conclude that $\|\Theta u(\cdot,t) - \epsilon t\|_\infty \leq \|u_0\| + \epsilon$ for all $t \in [0,T)$. This inequality holds for any epsilon so we have shown that regardless of the choice of T, $\|\Theta u\| \leq \|u_0\|_\infty$. Therefore we have that $\Theta : E_T \to E_T$

Next we must show that Θ is a contraction on E_T. The argument here is exactly the same as the argument in theorem 5.1. We will have the Lipschitz constant for g, $2L_{\|u_0\|}$ by lemma 5.2 so we get that

$$\|\Theta u - \Theta v\| \leq C^g T \|u - v\|.$$

We are assured that such a C^g exists because we are working in a compact subset of $C_b^0(\Omega_T)$, namely E_T. As before we now know that if $T \leq \frac{1}{2C^g}$ then Θ is a contraction from E_T to E_T and therefore there is a unique solution to the IVP.

Now we want to show that we can extend this solution to any finite time. consider any $u_0 \in C_b^0(\Omega)$ and note that we know that a solution exists and is unique on $[0,T)$. Take $u(\cdot, T-\eta)$ for some $\eta > 0$ to be our new initial condition and note again that because

$\|u(\cdot, T-\eta)\| \leq \|u_0\|$ the original Lipschitz constant for g given the bound from u_0, is still an appropriate Lipschitz constant for g given the bound on the new initial data $\|u(\cdot, T-\eta)\|$. Therefore we can prove existence for the same length of time, $T = \frac{1}{2C^g}$, and we have a solution on $[T-\eta, 2T-\eta)$. Moreover, when the solutions overlap they are identical so the solution on $[0, T)$, overlaps perfectly with the solution on $[T-\eta, 2T-\eta)$ and is continuous and differentiable in time, therefore, it is a solution on $[0, 2T-\eta)$. We can repeat this process any number of times to show that our solution exists for all finite times. This completes the proof of global existence and uniqueness. □

Additional Numerical Result

Lemma A.3 (discrete maximum principle (Forward Euler))**.** *If Ω_T is a bounded time cylinder with discretization $\Omega_T^{(h,\tau)}$, and $w \in \mathcal{V}(\Omega_T^{(h,\tau)})$ which satisfies (5.11) with $K(x,y) \in C_b^0(\Omega; C_b^0)$ with $w(\mathbf{x}, 0) = \pi^h u_0(\mathbf{x})$, then, when $\tau \leq L_\rho \sup_{\mathbf{x}\in\Omega^h} \|\pi^h K(\mathbf{x}, \cdot)\|_{\ell^\infty(\Omega)}$*

$$\|w\|_{\ell^\infty\left(\Omega_T^{(h,\tau)}\right)} \leq \|u_0\|_{L^\infty(\Omega)}$$

where L_ρ is the Lipshitz constant for ρ' on $[-2\|u_0\|_{L^\infty(\Omega)}, 2\|u_0\|_{L^\infty(\Omega)}]$.

Proof. Suppose that $\|w(\cdot, t_i)\|_{\ell^\infty} = M$. We seek to show that $w(\mathbf{x}, t_{i+1}) \leq M$ for all $\mathbf{x} \in \Omega^h$. Consider $\mathbf{x} \in \Omega^h$, we will break the proof of this claim into two cases, the first if $w(\mathbf{x}, t_i) = M$ and the second, $w(\mathbf{x}, t_i) < M$.

In the first case, observe that, because $w(\mathbf{x}, t_i) - w(\mathbf{y}, t_i) \geq 0$ for all $\mathbf{y} \in^- \Omega^h$, we have that $\rho'(w(\mathbf{x}, t_i) - w(\mathbf{y}, t_i)) \leq 0$ for all $\mathbf{y} \in^- \Omega^h$. It is clear then that

$$w(\mathbf{x}, t_{i+1}) = M + \tau h^n \sum_{\mathbf{y}\in^-\Omega^h} K(\mathbf{x}, \mathbf{y})\rho'(u(\mathbf{x}, t_i) - u(\mathbf{y}, t_i)) \leq M$$

Now we consider the case that $w(\mathbf{x}, t_i) < M$. If we show that

$$\tau h^n \sum_{\mathbf{y}\in^-\Omega^h} K_\epsilon(\mathbf{x} - \mathbf{y})\rho'(u(\mathbf{x}, t_i) - u(\mathbf{y}, t_i)) \leq M - w(\mathbf{x}, t_i) \tag{8}$$

then surely $w(\mathbf{x}, t_{i+1}) \leq M$. We can show this by observing that ρ' is Lipschitz with Lipschitz constant L_ρ on the range of w and that, $w(\mathbf{x}, t_i) - w(\mathbf{y}, t_i) \geq w(\mathbf{x}, t_i) - M$. Because of the assumption that $\rho'(z) \geq 0$ when $z < 0$ and $\rho'(z) \leq 0$ when $z > 0$, in order to show the upper bound of the sum in (8) we assume the worst case which is that $w(\mathbf{x}, t_i) - w(\mathbf{y}, t_i)) \leq 0$ for all $\mathbf{y} \in^- \Omega^h$. In this worst case we know that

$$0 \leq \rho'(w(\mathbf{x}, t_i) - w(\mathbf{y}, t_i)) \leq L_\rho(M - w(\mathbf{x}, t_i))$$

for each $\mathbf{y} \in^- \Omega^h$. Thus we have that

$$\begin{aligned}
&\tau h^n \sum_{\mathbf{y} \in^- \Omega^h} K(\mathbf{x}, \mathbf{y}) \rho'(u(\mathbf{x}, t_i) - u(\mathbf{y}, t_i)) \\
&\qquad \leq \tau h^n L_\rho (M - w(\mathbf{x}, t_i)) \sum_{\mathbf{y} \in^- \Omega^h} K(\mathbf{x}, \mathbf{y}) \\
&\qquad \leq \tau L_\rho D (M - w(\mathbf{x}, t_i))
\end{aligned}$$

Where $D = \sup_{\mathbf{x} \in \Omega^h} \|\pi^h K(\mathbf{x}, \cdot)\|_{\ell^\infty(\Omega)}$. Therefore, when $\tau < \frac{1}{L_\rho D}$, inequality (8) is satisfied, so we have proved that, whenever $\tau < \frac{1}{L\rho D}$, $\|w(\cdot, t_{i+1})\|_{\ell^\infty(\Omega^h)} \leq \|w(\cdot, t_i)\|_{\ell^\infty(\Omega^h)}$. The desired result is an obvious consequence.

□

Additional Inhomogeneous Result

Theorem A.1 (Short time existence and uniqueness for the inhomogeneous problem)**.** *The initial value problem $u_t - g[u] = f(u, x, t)$ has a unique continuous and bounded solution in Ω_T for some T when $u(x, 0) = u_0 \in C_b^0(\Omega), \rho \in C^{1,1}(\mathbb{R})$, $K \in C_b^0(\Omega; L^1(\Omega))$ and $f : \mathbb{R} \times \Omega \times \mathbb{R} \to \mathbb{R}$ is Lipschitz continuous with respect the the first variable with a Lipschitz constant, L_f, which does not depend on time, is merely continuous in space and time, and is bounded.*

Proof. Let $\Omega_T = \Omega \times [0, T]$ with T to be chosen later. Equip the function space $C_b^0(\Omega_T)$ with the standard sup norm $\|u\| = \sup_{t \in [0,t]} \|u(\cdot, t)\|_\infty$. Now for some $R > \|u_0\|_\infty$ let $E_{R,T} := \{u \in$

$C_b^0(\Omega_T, \mathbb{R}); u(x,0) = u_0, \|u\| \leq R\}$ and observe that $u(x,t) = u_0(x)$ for all t is in this closed subset of the Banach space. As before we will use the BFPT. Clearly a solution to the IVP will satisfy

$$u(x,t) = u_0(x) + \int_0^t g[u](x,s) + f(u(s),x,s)ds \tag{9}$$

Let $\Psi : C_b^0(\Omega_T, \mathbb{R}) \to C_b^0(\Omega_T, \mathbb{R})$ where $\Psi u = u_0 + \int_0^t g[u](x,s) + f(u(s),x,s)ds$. Clearly if there is a solution to $\Psi u = u$ then we have a solution to (9) and thus the IVP.

We start by showing that $\Psi : E_{R,T} \to E_{R,T}$. By lemma 5.1 we know that $g[u]$ is continuous so its time antiderivative is clearly continuous. Moreover, by assumption f is continuous so its time antiderivative will also be continuous.

To show that $\|\Psi u\| \leq R$ we note that both $g[u]$ and f are bounded. g is bounded exactly as described in theorem 5.1 so there is a T_R before which

$$\sup_{t\in[0,T)} \| \int_0^t g[u](\cdot,s)ds\|_\infty \leq \frac{R - \|u_0\|_\infty}{2}.$$

$f(u(x,s),x,s)$ is bounded, by assumption, so likewise there is a T_{Rf} so that

$$\int_0^t f(u(x,s),x,s)ds < \frac{R - \|u_0\|_\infty}{2}$$

when $t < T_{Rf}$. Thus there is a T_1 so that when $T < T_1$, $\Psi : E_{R,T} \to E_{R,T}$.

To show that this is a contraction consider

$$\begin{aligned}
\|\Psi u - \Psi v\| &= \sup_{t\in[0,T)} \left\| \int_0^t g[u](\cdot,s) - g[v](\cdot,s)ds + \int_0^t f(u(\cdot,s),\cdot,s) - f(v(\cdot,s),\cdot,s)ds \right\|_\infty \\
&\leq \int_0^T \|g[u](\cdot,s) - g[v](\cdot,s)\|_\infty ds + \int_0^T |f(u(\cdot,s),\cdot,s) - f(v(\cdot,s),\cdot,s)|ds \\
&\leq TC^g\|u - v\| + L_f T\|u - v\|
\end{aligned}$$

Thus if $T < \frac{1}{2(c^g + L_f)}$ then $\|\Psi u - \Psi v\| \leq \frac{1}{2}\|u - v\|$.

Therefore when $T < \min\{T_1, \frac{1}{2(c^g+L_f)}\}$ then $\Psi : E_{R,T} \to E_{R,T}$ is a contraction and thus it has a unique fixed point. Thus we have shown that there is a unique solution to the integral

equation (9) and thus the IVP for some short time. We can extend this in the same way as in 5.1 but can not extend this to global existence without a maximum principle. □

B Visual Catalogue of Equilibria

All of the distinct equilibrium partitions of connected graphs of order 6 are pictured in this appendix. In figure B.1 are all the graphs which are indecomposable and thus admit only the equilibrium partition. In figure B.2 are all the graphs with a unique non-trivial partition. These graphs, therefore, admit two equilibrium partitions, one trivial and one non-trivial. The trivial partition is not pictured. In figure B.3 are all the graphs with two distinct non-trivial equilibrium partitions. Again, this means these graphs have three total distinct equilibrium partitions, the trivial partitions are not pictured. Likewise, in figures B.4 and B.5 are pictured the graphs with exactly 3 and exactly 4 non-trivial equilibrium partitions respectively. They all obviously admit the trivial partitions although it is not pictured in this catalogue.

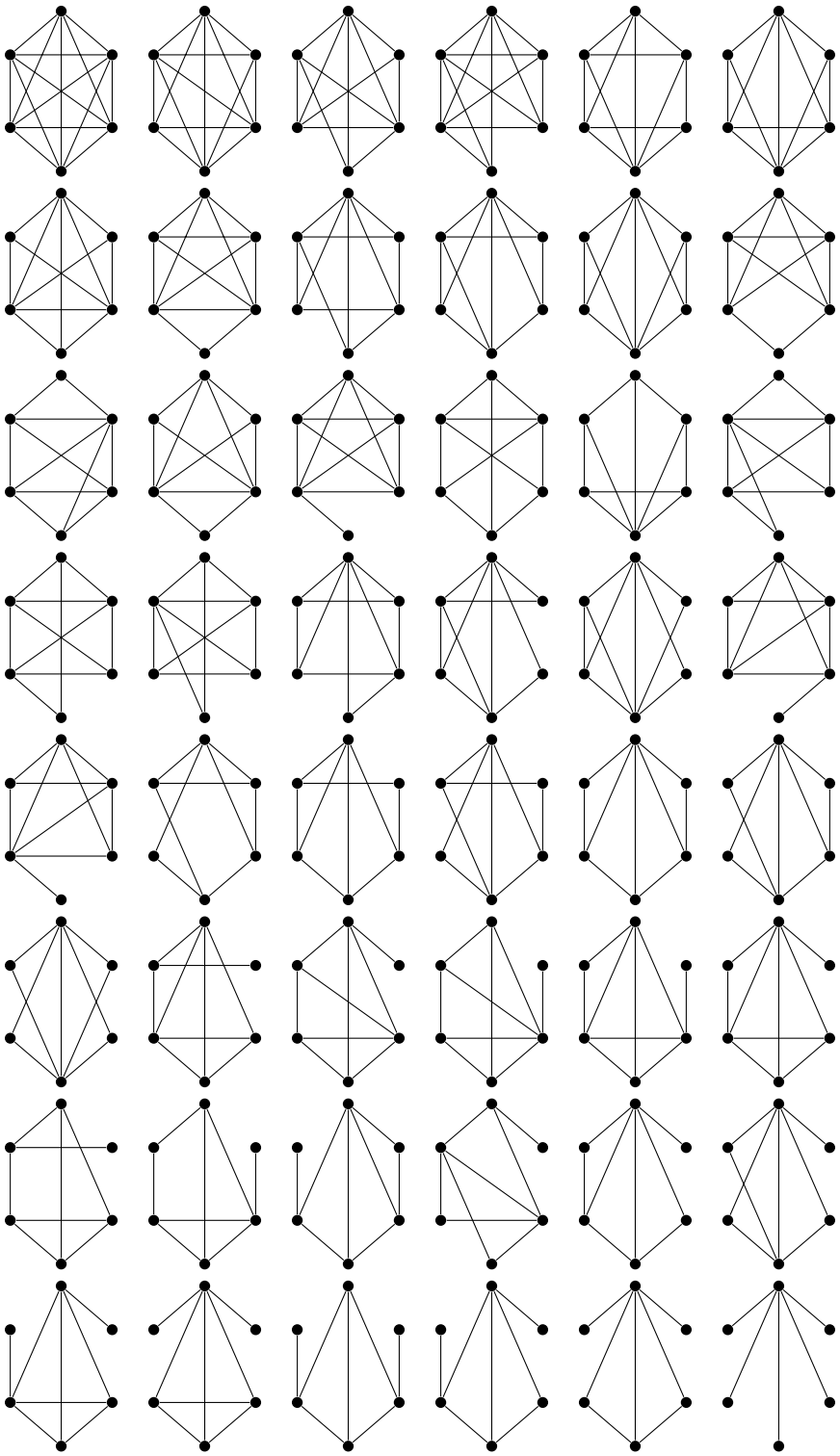

Figure B.1: Every connected graph on 6 vertices which is indecomposable

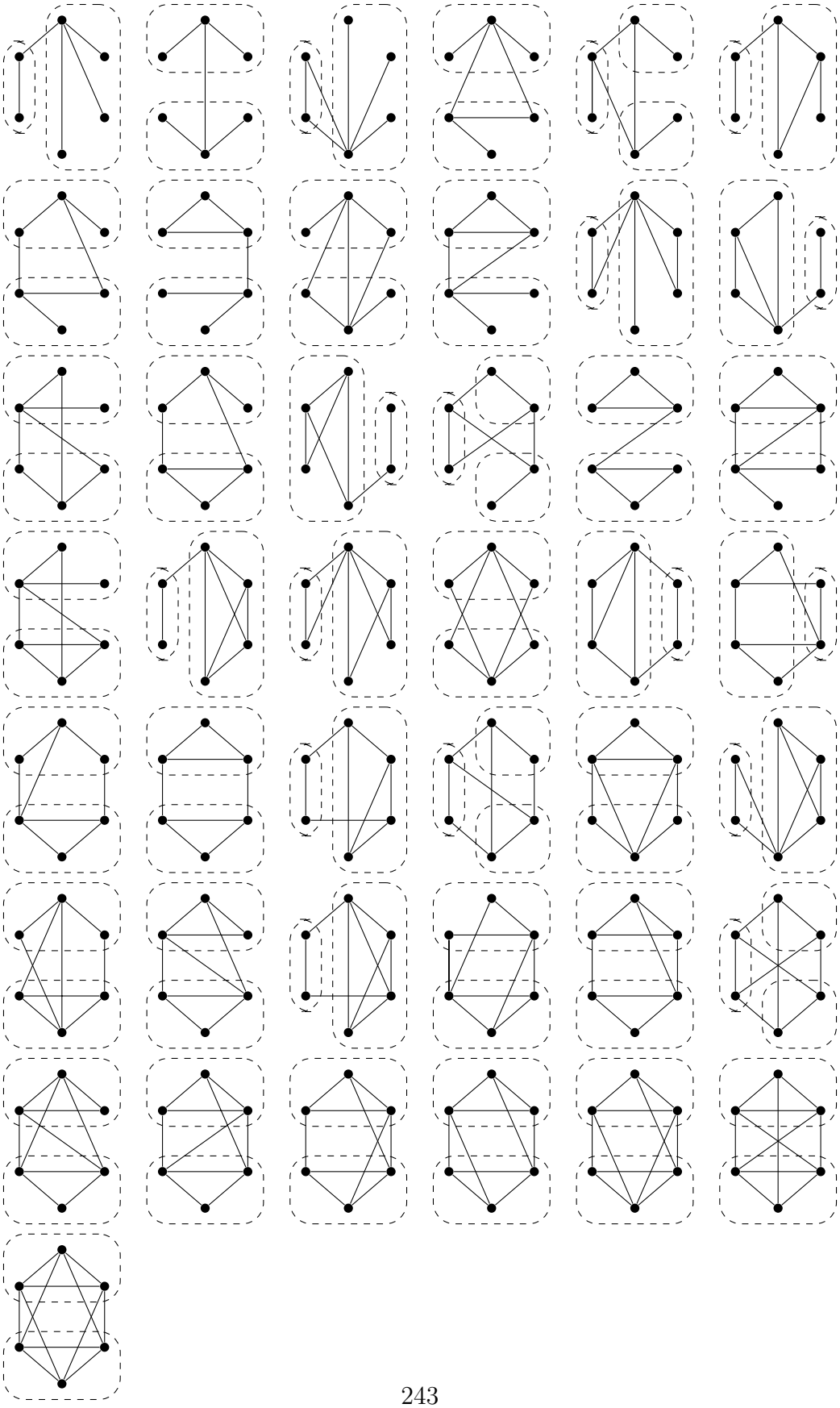

Figure B.2: All the decomposable connected graphs of order 6 with unique non-trivial equilibria

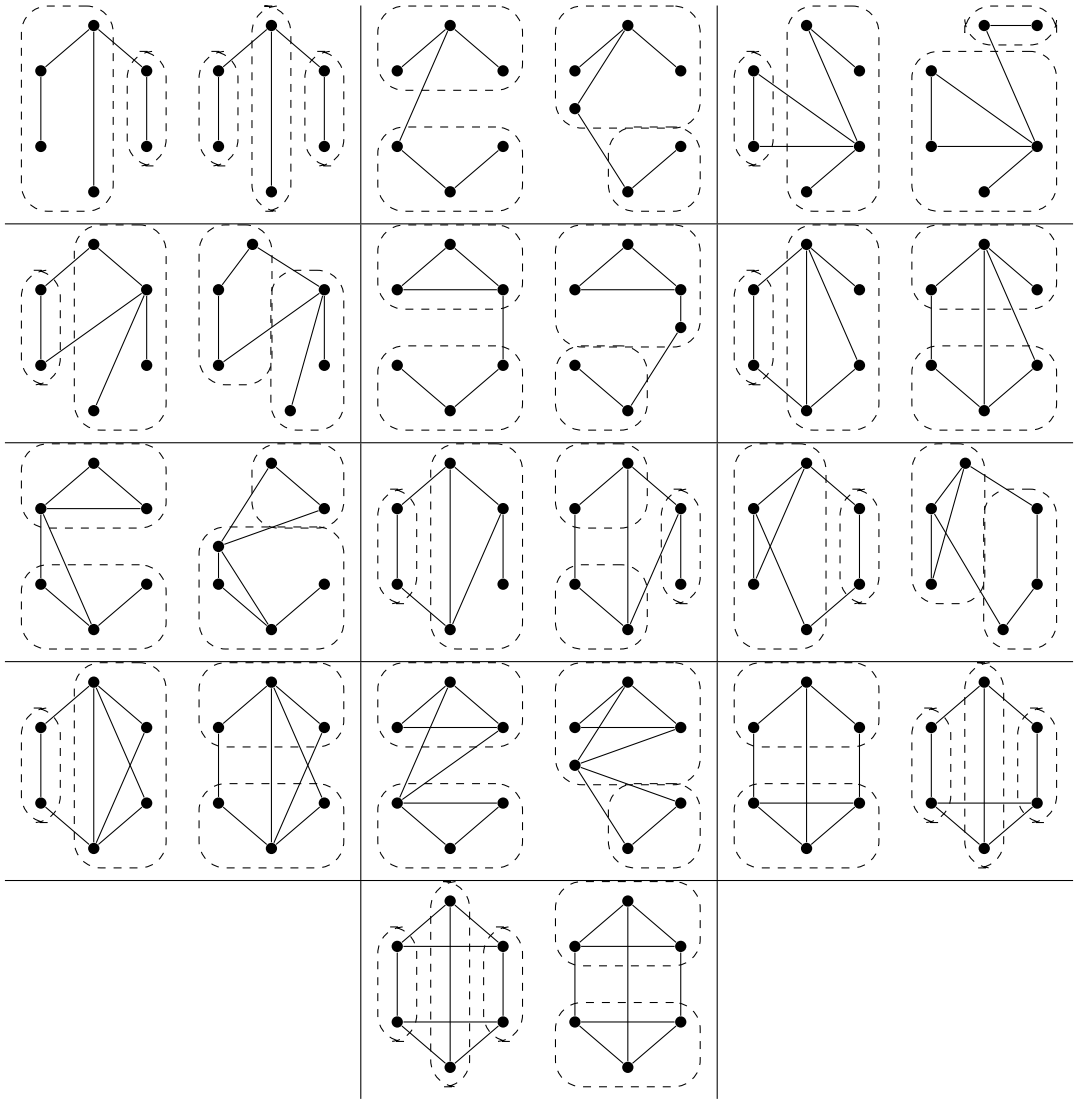

Figure B.3: Every decomposable connected graph of order 6 with exactly two non-trivial equilibrium partitions

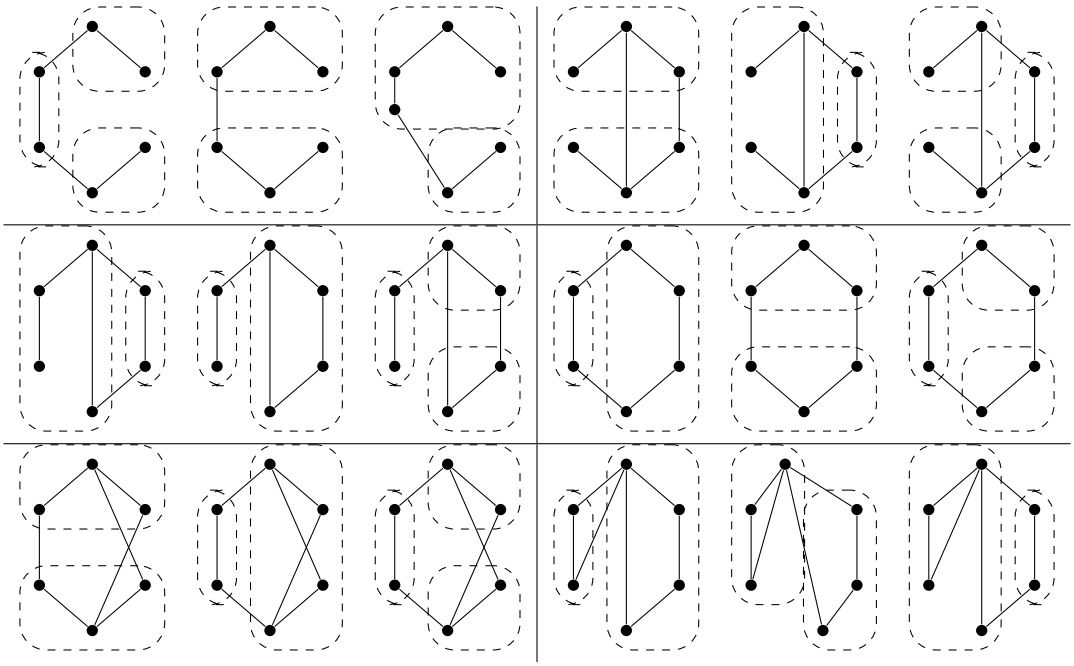

Figure B.4: Every decomposable graph of order 6 with exactly three non-trivial equilibrium partitions

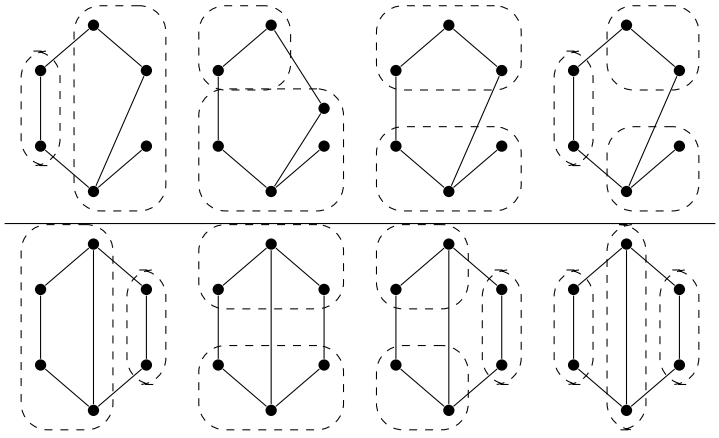

Figure B.5: All of the decomposable graphs of order 6 with exactly 4 non-trivial equilibrium partitions.

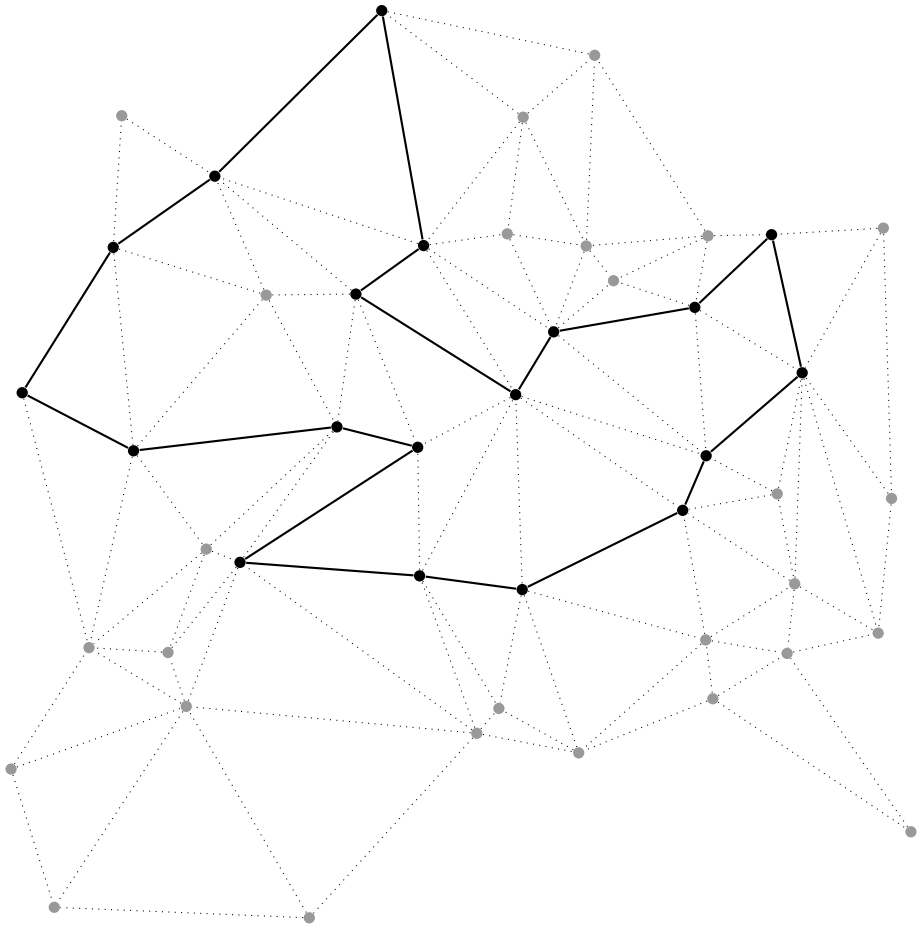

Figure C.1: An initial subgraph (in the solid lines) from the cycle space of the graph shown in the dotted lines

C Cycle Shortening Flow Example

The following several figures are a sequence of subgraphs from the cycle space of the graph G which are obeying cycle shortening flow from chapter 3. At each time step, for each face f, C_f (the cycle of edges incident to f) is either added or not added to the subgraph depending on the present number of edges adjacent to f. If there are more edges than non-edges of f included in the subgraph then C_f is added. Otherwise, it is not. From this, the cycle shortening flow is very simple.

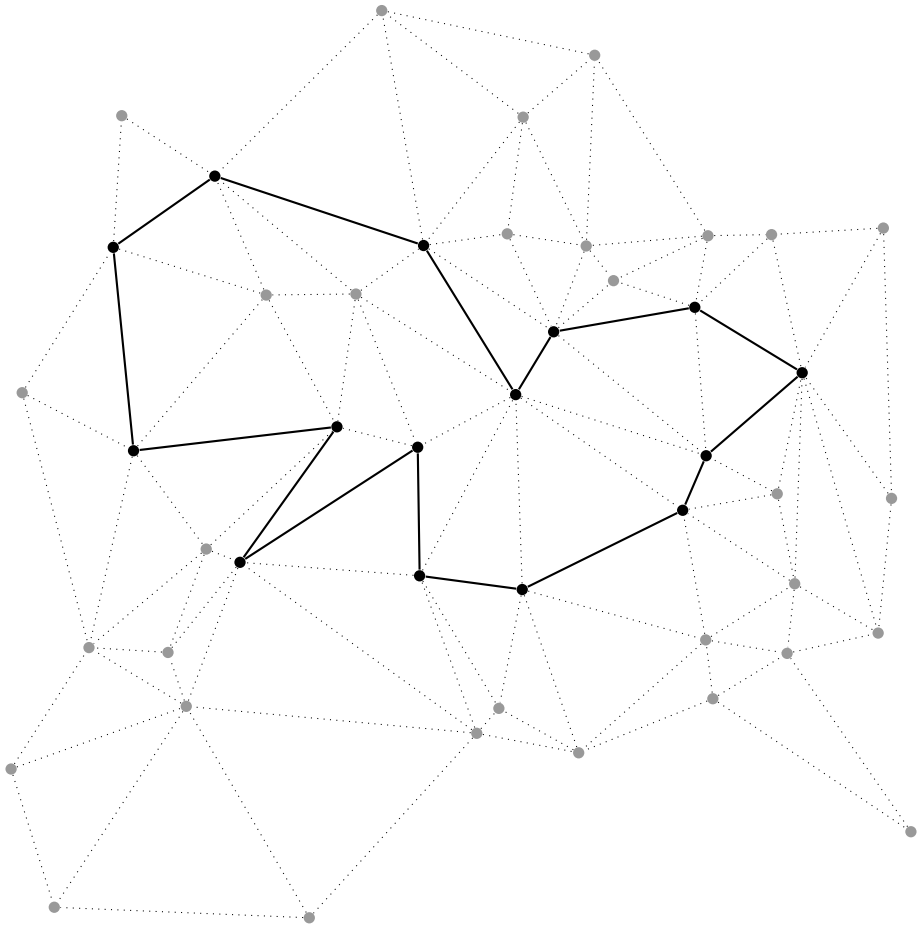

Figure C.2: After the first step of the cycle shortening flow, for every face f of G with more edges than non-edges in the subgraph, the cycle C_f is added to the subgraph.

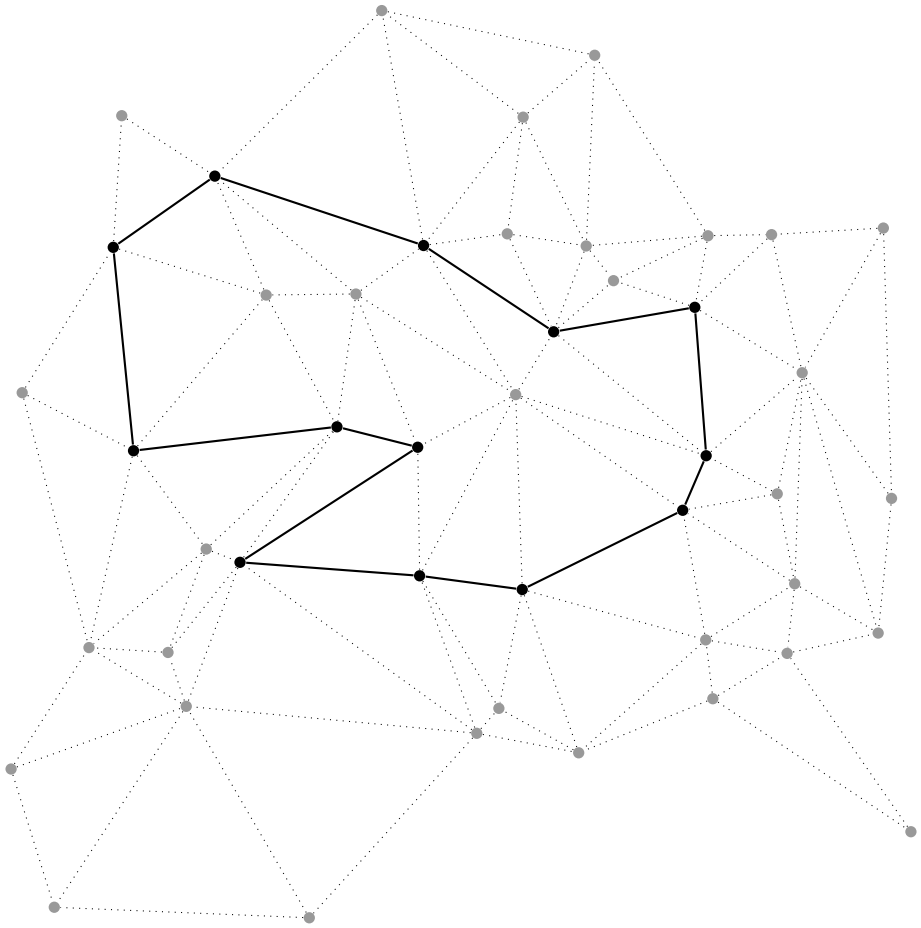

Figure C.3: After the second step of the cycle shortening flow, for every face f of G with more edges than non-edges in the subgraph, the cycle C_f is added to the subgraph.

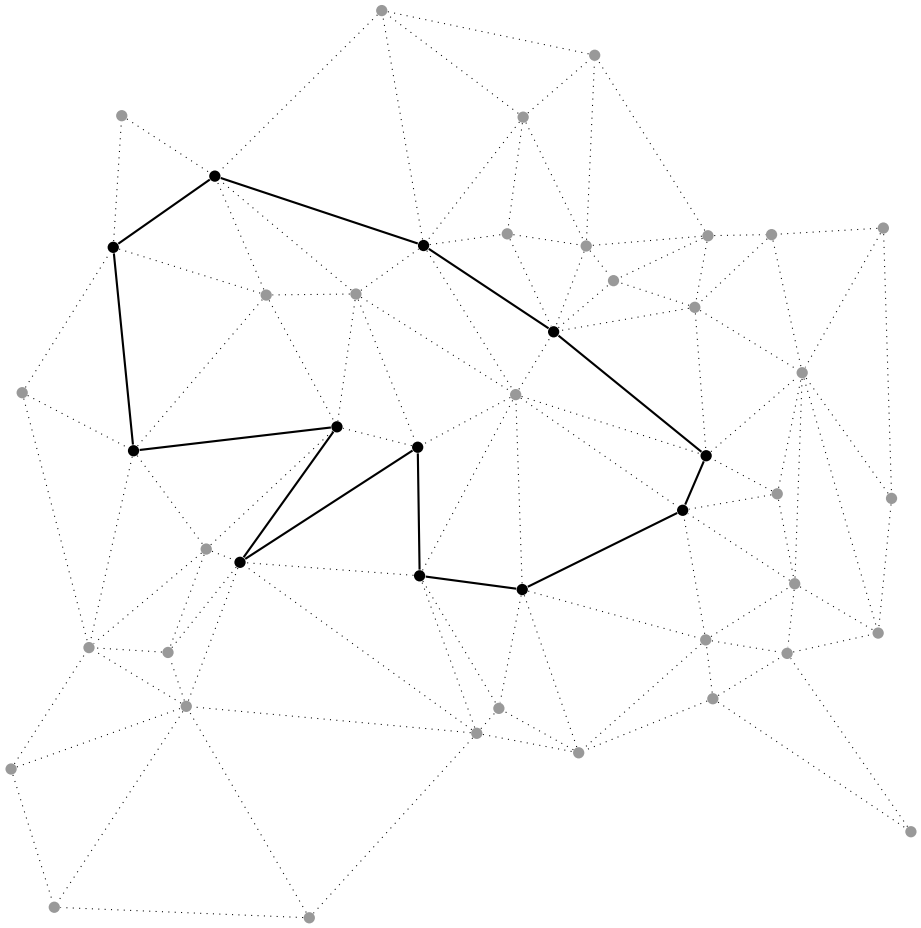

Figure C.4: After the third step of the cycle shortening flow, for every face f of G with more edges than non-edges in the subgraph, the cycle C_f is added to the subgraph.

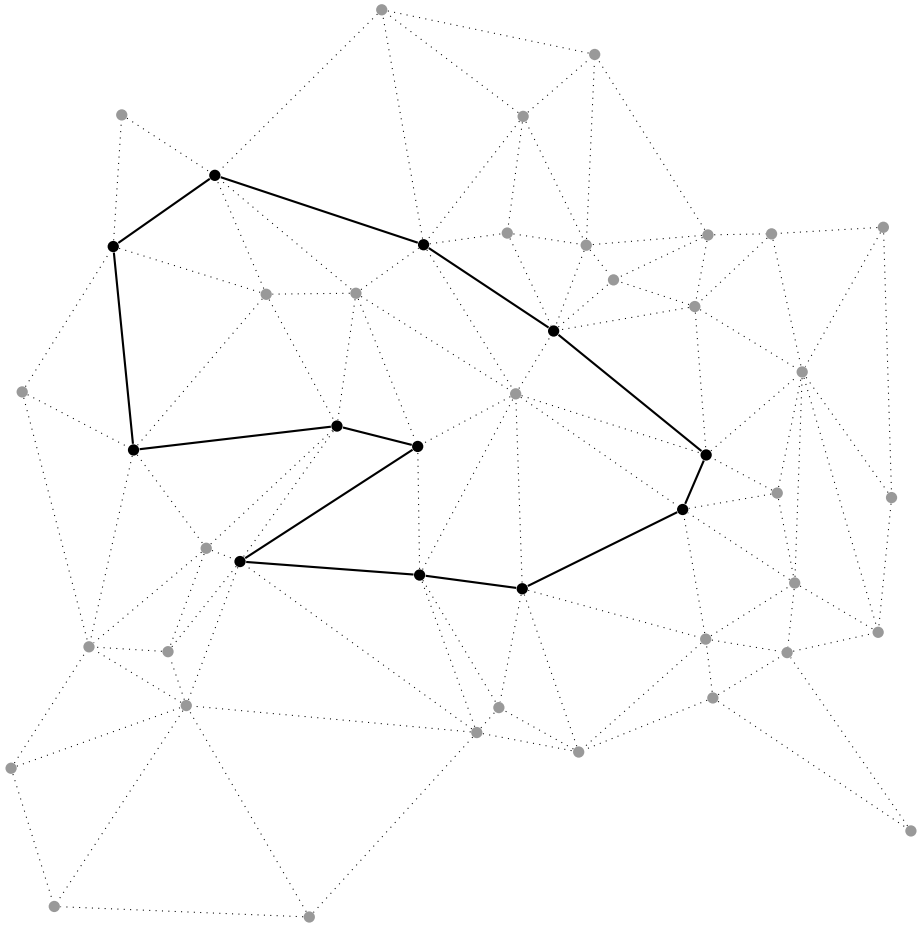

Figure C.5: After the fourth step of the cycle shortening flow, the subgraph is close to a local minimum. This is not a proper local minimum but the only shortening step is back to frame C.4. This means that the flow ends in a 2-cycle and neither strategy profile is a Nash equilibrium. In the mixed strategy case, a Nash equilibrium may be found between these two strategy profiles.

Vita

John McAlister grew up in the suburbs outside of Cincinnati Ohio with his parents Lori and Lawrence; his sister, Anne; and his twin brother Ryan. After attending Lakota East High School he sought an undergraduate degree in Zoology from The Ohio State University. It wasn't long after he began his zoology degree that he realized the elements of zoology and ecology that he enjoyed were the relationships between organisms and the mathematical models that were used to understand them. After this realization, John began to pursue a dual degree in Zoology and Mathematics with a mathematical biology concentration which eventually prompted him to pursue an PhD in Applied Math at the University of Tennessee - Knoxville. Under the direction of Nina H. Fefferman and Tadele A. Mengesha, he studied game theoretic modeling for collective behaviors through a wide variety of modeling techniques. After graduating with his PhD he joined the research group of Dr. Simon Levin at Princeton University to continue studying spatial models in ecology and evolution.